Prediction and Optimization of Machining Parameters for Minimizing Surface Roughness and Power Consumption during Turning of AISI 1045 Steel

THESIS

Submitted in partial fulfilment
of the requirements for the degree of

DOCTOR OF PHILOSOPHY

by

GIRISH KANT

Under the Supervision of

Prof. KULDIP SINGH SANGWAN

BITS Pilani
Pilani | Dubai | Goa | Hyderabad

BIRLA INSTITUTE OF TECHNOLOGY & SCIENCE, PILANI

2016

Prediction and Optimization of Machining Parameters for Minimizing Surface Roughness and Power Consumption during Turning of AISI 1045 Steel

THESIS

Submitted in partial fulfilment
of the requirements for the degree of

DOCTOR OF PHILOSOPHY

by

GIRISH KANT
(2006PHXF421P)

Under the Supervision of

Prof. KULDIP SINGH SANGWAN

BITS Pilani
Pilani | Dubai | Goa | Hyderabad

BIRLA INSTITUTE OF TECHNOLOGY & SCIENCE, PILANI

2016

BIRLA INSTITUTE OF TECHNOLOGY AND SCIENCE
PILANI – 333 031 (RAJASTHAN) INDIA

CERTIFICATE

This is to certify that the thesis entitled **"Prediction and Optimization of Machining Parameters for Minimizing Surface Roughness and Power Consumption during Turning of AISI 1045 Steel"** submitted by **Girish Kant**, ID.No. **2006PHXF421P** for award of PhD Degree of the institute embodies original work done by him under my supervision.

Signature in full of the Supervisor _____

Name in capital block letters **Prof. KULDIP SINGH SANGWAN**

Designation Professor

Department of Mechanical Engineering

BITS-Pilani, Pilani Campus

Date _____

Acknowledgements

My supervisor, Dr. Kuldip Singh Sangwan, has been a great mentor, support and guide throughout my studies at BITS Pilani. I would like to thank him for believing in me and encouraging me in my academic efforts as well as in my personal endeavors. It has been a privilege for me to work under his guidance.

I wish to thank Prof. V. S. Rao (Acting Vice-Chancellor, BITS Pilani) and Prof. A.K. Sarkar, (Director, Pilani Campus), for providing me the opportunity to pursue my doctoral thesis by providing necessary facilities. I am also grateful to Prof. S. K. Verma (Dean, Academic Research Division) and Prof. Hemant R. Jadhav (Associate Dean, Academic Research Division, Pilani Campus) for their constant support and encouragement. I feel obliged to Prof. Ravi Prakash (Director, Amity School of Engineering and Technology and former Dean, Research and Consultancy Division, BITS Pilani) for their support.

I put on record my gratitude to Prof. M. S. Dasgupta and Dr. R. P. Mishra for providing me constant encouragement and critic reviews as Doctoral Advisory Committee (DAC) members. I also wish to thank Prof. Srikanta Routroy, Convener, Doctoral Research Committee (DRC) for constant encouragement during research. I also express my gratitude to Prof. B.K. Rout, Head, Department of Mechanical Engineering for his constant encouragement and emotional support.

I deeply acknowledge the unabated support and counseling during difficult times, provided by my colleagues Dr. Sharad Srivastava, Dr. J.S. Rathore and Dr. Sachin U. Belgamwar. I also highly appreciate the technical cooperation given by them.

I also express my gratitude to all staff members of BITS Pilani Workshop, especially Mr. C.R Rao, Mr. Naresh Kumar Rohil and Mr. Vinod Naruka for their efforts in assisting me in the experimental work.

I would like to thank Mr. Santosh Kumar Saini (ARC Division) for his help in compilation of the thesis.

Finally, I feel indebted to my family for their support, understanding and sacrifices throughout all these years and standing by my side with never ending trust and encouragement.

Girish Kant

Abstract

After well known formula relating tool life to cutting speed given by Taylor in 1907, a lot of research on the modelling and optimization of machining parameters for surface roughness, tool wear, forces, etc. has been done during last 100 years. However, a little research has been done to optimize the energy efficiency of machine tools. The energy efficiency of machines tools is generally very low particularly during the discrete part manufacturing. Reduction in power consumption, in addition to economical benefits, will also improve the environmental impact of machine tools and manufacturing processes. However, sustainability performance may be reduced artificially by increasing the surface roughness as lower surface finish requires lesser power and resources to finish the machining. But this may lead to more rejects, rework and time. Therefore, an optimum combination of power and surface finish is desired for sustainability performance of the machining processes. There is a close interdependence among productivity, quality and power consumption of a machine tool. The surface roughness is widely used index of product quality in terms of various parameters such as aesthetics, corrosion resistance, subsequent processing advantages, tribological considerations, fatigue life improvement, precision fit of critical mating surfaces, etc. But the achievement of a predefined surface roughness below certain limit generally increases power consumption exponentially and decreases the productivity. The capability of a machine tool to produce a desired surface roughness with minimum power consumption depends on machining parameters, cutting phenomenon, workpiece properties, cutting tool properties, *etc*. The first step towards reducing the power consumption and surface roughness in machining is to analyze the impact of machining parameters on power consumption and surface roughness.

This study focuses on development of predictive and optimization models to analyze the influence of machining parameters on power consumption and surface roughness and to

obtain the optimal machining parameters leading to minimum surface roughness and power consumption during turning of AISI 1045 steel using tungsten carbide tools. Predictive models for surface roughness and power consumption are developed using response surface methodology, support vector regression and artificial neural networks. The developed models have been compared using relative error and validated using hypothesis testing. Optimization models have been developed using response surface methodology and genetic algorithms. The results have been validated using the confirmation experimental tests. A multi-objective predictive and optimization model is developed to obtain the machining parameters leading to minimum power consumption and surface roughness simultaneously.

The results reveal that the developed predictive models provide a close relation between the predicted values and the experimental values for surface roughness and power consumption. The optimal machining parameters indicate that feed is the most significant machining parameter followed by depth of cut and cutting speed to reduce power consumption and surface roughness simultaneously. The optimization of machining parameters for minimum power requirement and surface roughness is expected to lead to the application of lower rated motors, drives and auxiliary equipments and hence save consumption of power not only during machining but as well as during build-up to machining, post machining and idling conditions.

Table of Contents

List of Figures

List of Tables

List of Abbreviations

3D	Three Dimensional
ABC	Artificial Bee Colony
ACO	Ant Colony Optimization
AISI	American Iron and Steel Institute
ANN	Artificial Neural Network
ANOVA	Analysis of Variance
CIRP	International Academy for Production Engineering
BP	Back Propagation
CNC	Computer Numerical Control
DOE	Design of Experiment
DOF	Degree of Freedom
FEM	Finite Element Method
GA	Genetic Algorithm
GFRP	Glass Fibre Reinforced Polymer
GRA	Grey Relational Analysis
HRC	Rockwell Hardness
HSS	High Speed Steel
ISO	International Organization for Standardization
KKT	Karush Kuhn Tucker
MAE	Mean Absolute Error
MAPE	Mean Absolute Percentage Error
MP_f	Machining Performance
MP_r	Machining Process
MQL	Minimum Quantity Lubrication

MS	Mean Square
MSE	Mean Square Error
OEM	Original Equipment Manufacturer
PCA	Principal Component Analysis
PCBN	Polycrystalline Cubic Boron Nitride
PCD	Polycrystalline Diamond
PEEK	Poly Ether Ether Keytone
PSO	Particle Swarm Optimization
PT	Predictive Technique
PVD	Physical Vapor Deposition
RA	Regression Analysis
RBF	Radial Basis Function
RMSE	Root Mean Square Error
RSM	Response Surface Methodology
SA	Simulated Annealing
SAE	Society of Automotive Engineers
S/N	Signal-to-Noise
SS	Sum of Square
SSE	Sum Square Error
SVM	Support Vector Machine
SVR	Support Vector Regression
USD	United States Dollar

List of Symbols

B	Fibre orientation angle
C	Regularization parameter
ce	Cutting environment
cfr	Cutting fluid ratio
CF	Cutting fluid
D	Drilling
d	Depth of cut (mm)
d_a	Axial depth of cut (mm)
d_r	Radial depth of cut (mm)
f	Feed (mm/rev)
f_t	Feed/tooth (mm)
f^*	Feed (mm/min)
F_c	Cutting force (N)
F_f	Feed force (N)
F_r	Radial force (N)
F_t	Thrust force (N)
F_{rf}	Resultant force (N)
h	Workpiece hardness
K	Approach Angle
l_t	Lubricant temperature (^oC)
m_t	Machining tolerance (mm)
MRR	Material removal rate (g/min)
n	Spindle speed (rpm)
P	Power consumption (kW)
r	Tool nose radius (mm)
r_d	Drill diameter (mm)
R_a	Surface roughness (µm)
R_{max}	Surface roughness maximum (µm)
R_q	Root mean square roughness (µm)

R_t	Maximum peak to valley height roughness (µm)
R_z	Surafce roughness parameter (µm)
SCEA	Side cutting edge anagle
T	Turning
Temp	Temperature (^oC)
T_l	Tool life (min)
t	Time (min)
M	Milling
v	Cutting speed (m/min)
VB	Flank wear
Vy	Cutting tool vibration in radial cutting force direction (m/s2)
Vz	Cutting tool vibration in main cutting force direction (m/s2)
Fx, Fy,	Forces in x, y, z directions (N)
Fz	Rake angle
γ	Roundness (mm)
ϕ	Insensitive loss function
ε	

Chapter 1

Introduction

1.1 Introduction

The 1980s have witnessed a fundamental change in the way governments and development agencies think about environment and development. The two are no longer regarded as mutually exclusive. It has been recognized that a healthy environment is essential for a healthy economy. Energy and materials are the two primary inputs required for the growth of any economy and these are obtained by exploiting the natural resources like fossil fuels and material ores. The industrial sector accounts for about one-half of the world's total energy consumption and the consumption of energy by this sector has almost doubled over the last 60 years (Fang et al., 2011). The consumption of critical raw materials (steel, aluminum, copper, nickel, zinc, wood, *etc*.) for industrial use has increased worldwide. The rapid growth in manufacturing has created many economic, environmental and social problems from global warming to local waste disposal (Sangwan, 2011). There is a strong need, particularly, in emerging and developing economies to improve manufacturing performance so that there is less industrial pollution, and less material & energy consumption. Energy efficiency and product quality have become important benchmarks for assessing any industry. Manufacturing operations account for 37% of global energy demand (Diaz-Elsayed et al., 2015). U.S. manufacturing industry annually consumes 21.1 quadrillion BTU energy (about 21% of total U.S. energy consumption) and generates more than 1.4 billion metric tons of CO_2 emissions (about 26% of total U.S. CO_2 emissions) (Yuan et al., 2012). Machine tools have less than 30% efficiency (He et al., 2012) and more than 99% of the

environmental impacts are due to the consumption of electrical energy used by the machine tools in discrete part manufacturing machining processes like turning and milling (Li et al., 2011). Worldwide, machine tool manufacturing is a USD 68.6 billion industry and very few energy assessments have been conducted for discrete manufacturing facilities (Diaz-Elsayed et al., 2015). Sustainability performance of machining processes can be achieved by reducing the power consumption (Camposeco-Negrete, 2013). If the energy consumption is reduced, the environmental impact generated from power production is diminished (Pusavec et al., 2010). Sustainability performance may be reduced artificially by increasing the surface roughness as lower surface finish requires lesser power and resources to finish the machining. However, this may lead to more rejects, rework and time. Therefore, an optimum combination of power and surface finish is desired for sustainability performance of the machining processes. There is a close interdependence among productivity, quality and power consumption of a machine tool. The surface roughness is widely used index of product quality in terms of various parameters such as aesthetics, corrosion resistance, subsequent processing advantages, tribological considerations, fatigue life improvement, precision fit of critical mating surfaces, *etc*. But the achievement of a predefined surface roughness below certain limit generally increases power consumption exponentially and decreases the productivity. The capability of a machine tool to produce a desired surface roughness with minimum power consumption depends on machining parameters, cutting phenomenon, workpiece properties, cutting tool properties, *etc*. The first step towards reducing the power consumption and surface roughness in machining is to analyze the impact of machining parameters on power consumption and surface roughness.

1.2 Research Motivation

After well known formula relating tool life to cutting speed given by Taylor in 1907, a lot of research on the modelling and optimization of machining parameters for surface roughness, tool wear, forces, *etc*. has been done during last 100 years. However, a little research has been done to optimize the energy efficiency of machine tools. Moreover, in the past, metal cutting operations have been mainly optimized on the basis of economical and technological considerations without the environmental dimension (Yan and Li, 2013). Reduction in power consumption improves the environmental impact of machine tools and manufacturing processes. Machine tools require power during machining, build-up to machining, post machining and idling condition to drive motors and auxiliary equipment. However, the design of a machine tool is based on the peak power requirement during machining of material which is very high as compared to non-peak power requirement of the machine tool. This leads to higher inefficiency of energy in machine tools. The optimization of machining parameters for minimum power requirement is expected to lead not only to the application of lower rated motors, drives and auxiliary equipment, but also power saving during machining, build-up to machining, post machining and idling condition. In addition to the machining parameters, the power requirement during machining also depends upon workpiece properties and cutting tool properties. In this study, the workpiece material is steel and cutting tool material is uncoated tungsten carbide. This combination is the most widely used combination in the industry and any reduction in power consumption is expected to lead to high saving of power in absolute numbers. No doubt, steel is one of the widely researched materials in machining for more than last half a century, but there is a renewed interest in application of steel because of its sustainability – 100% recyclable and almost indefinite life cycle. Energy requirement for steel recycling is less than one

third of aluminum recycling. AISI 1045 steel is widely used in different industries (construction, transport, automotive, power, *etc*.).

Process models have often targeted the prediction of fundamental variables such as stresses, strains, strain rate, temperature, *etc*.; but to be useful for industry, these variables must be correlated to performance measures and product quality (accuracy, dimensional tolerances, finish, *etc*.) (Arrazola et al., 2013). Recent review papers on machining show that the most widely machining performances considered by the researchers are surface roughness followed by machining/production cost and material removal rate (Yusup et al., 2012). Recently, the researchers have started to analyze and optimize the power consumption in machining (Aggarwal et al., 2008; Camposeco-Negrete, 2013; Hanafi et al., 2012). Energy savings upto 6-40% can be obtained based on the optimum choice of cutting parameters, tools and the optimum tool path design (Newman et al., 2012). The process planners as well as operators use their experience with the help of data from machining handbooks and tool catalogs to achieve the best possible machining performance. Due to inadequate knowledge and complexity of factors affecting the machining performance, an improper decision may cause energy inefficiency, low product quality and high production cost. These issues motivated for analyzing and improving the performance of machining process for enhancing product quality and minimizing power consumption. This thesis aims at optimizing the surface roughness and power consumption simultaneously during turning of AISI 1045 steel. Optimization of machining parameters through experimentation is not only tedious but costly also, therefore, this thesis presents a predictive mathematical model to optimize the power consumption and surface roughness simultaneously. Predictive modelling can be used as an effective and an alternative method for the experimental studies in machining.

1.3 Objective and Scope of the Study

The objective of this study is to develop predictive and optimization models for analyzing the influence of machining parameters on (i) surface roughness, (ii) power consumption, and (iii) finally on surface roughness and power consumption simultaneously. The effect of cutting speed, feed and depth of cut will be studied during the turning of AISI 1045 steel using carbide cutting tools. This objective is achieved by:

- Development of predictive and optimization models to determine the optimum machining parameters leading to minimum surface roughness,
- Development of predictive and optimization models to determine the optimum machining parameters leading to minimum power consumption, and
- Development of a multi-objective predictive and optimization model to determine the machining parameters leading to minimum power consumption and surface roughness simultaneously.

Response Surface Methodology (RSM), Support Vector Regression (SVR) and Artificial Neural Networks (ANN) will be used to develop the predictive models. RSM and Genetic Algorithms (GA) will be used to develop optimization models.

1.4 Methodology

The following methodology has been used to achieve the objectives of the study:

- Development of the experimental setup to get the surface roughness and power consumption data: the process parameters and response variables have been selected for the AISI 1045 steel during turning by carbide cutting tools. Experiments have been designed using Design of Experiments (DOE).
- Development of the predictive models for surface roughness using RSM, SVR and ANN. The developed models have been compared using relative error and

validated using hypothesis testing. A mathematical formulation has been developed by using RSM and an optimization model has been developed using GA. The results have been validated using the confirmation experimental tests.

- Development of the predictive models for power consumption using RSM, SVR and ANN. The developed models have been compared using relative error and validated using hypothesis testing. A mathematical formulation has been developed by using RSM and an optimization model has been developed using GA. The results have been validated using the confirmation experimental tests.
- Development of a multi-objective predictive and optimization model to determine the machining parameters leading to minimum surface roughness and power consumption simultaneously. Grey Relational Analysis (GRA) coupled with Principal Component Analysis (PCA) and RSM have been used to determine the best machining parameters for surface roughness and power minimization simultaneously.

1.5 Significance of the Study

The efficient use of energy and other resources is important to meet the increasing concern about economy and environment. Machine tool is a major consumer of energy and thus it is a potential sector for energy saving. Machining parameters such as cutting speed, feed and depth of cut play a vital role in machining the given workpiece to the required shape and finish. These parameters have a major effect on the tool-life/tool wear, part accuracy, surface roughness, power consumption, *etc*. in addition to time and cost. The judicious selection of these parameters is significant. The selected machining parameters should give the desired quality on the machined surface with the minimum environmental impact. Traditionally, the selection of machining parameters is carried out on the basis of the experience of the machinist or the process planner and reference to the available catalogues and handbooks. Manual selection of machining parameters

highlights the problem of variability in experience and judgment among the process planners. In addition to this, the induction of cost intensive Computer Numerical Control (CNC) machines emphasizes effective utilization of these resources using the optimal machining parameters.

This study focuses on development of predictive and optimization models, which eliminate the necessity of extensive experimentation process currently used in industry to understand relationship between machining parameters and performance characteristics. Development of predictive and optimization models is cost effective and accurate prediction of optimum machining parameters leads to minimum surface roughness and power consumption. The predictive capability could also be used for automatic monitoring. With the known boundaries of surface roughness, power consumption and machining conditions, machining could be done with a relatively high rate of success leading to better surface finish and lower power consumption. Process planning and production scheduling, which link product design and manufacturing, are two of the most important functions in modern manufacturing processes and both impact the performance of the modern manufacturing system, especially in energy consumption and production of waste emissions (Jin et al., 2015). In recent decades, many research publications have dealt with these functions. However, only Kant and Sangwan (2014) and Shrouf et al. (2014) simultaneously considered low fossil-carbon and sustainability (Jin et al., 2015).

1.6 Organization of the Thesis

This study presents an experimental work which leads to the development of predictive and optimization models for machining performance (surface roughness and power

consumption) in terms of machining parameters during turning of AISI 1045 steel. The organization of the thesis is as:

- A review of relevant research publications in predictive modelling and optimization of machining operations is presented in chapter 2. Available predictive and optimization models are studied to find the research gap in this chapter. The need for developing new predictive and optimization models for turning of AISI 1045 steel has been justified.
- Chapter 3 describes the experimental setup and plan, which is carried out to establish a relationship between machining performance (surface roughness and power consumption) and machining parameters (cutting speed, feed and depth of cut).
- In chapter 4, the relationship between machining parameters and surface roughness is obtained by using RSM, SVR and ANN. Optimum machining parameters leading to minimum surface roughness are achieved by using RSM and GA. Confirmation experiments are conducted to verify the results.
- In chapter 5, the relationship between machining parameters and power consumption is obtained by using RSM, SVR and ANN. Optimum machining parameters leading to minimum power consumption are achieved by using RSM and GA. Confirmation experiments are conducted to verify the results.
- In chapter 6, a multi-objective predictive and optimization model has been developed to simultaneously integrate the effects of the surface roughness and power consumption. The conformation experiments are conducted to verify the results.
- Chapter 7 summarizes the modelling and optimization research work completed in this investigation and future research directions are discussed.

References

Aggarwal, A., Singh, H., Kumar, P., Singh, M., 2008. Optimizing power consumption for CNC turned parts using response surface methodology and Taguchi's technique—A comparative analysis. J. Mater. Process. Technol. 200, 373–384.

Arrazola, P.J., Umbrello, D., Davies, M., Jawahir, I.S., 2013. Recent advances in modelling of metal machining processes. CIRP Ann. - Manuf. Technol. 62, 695–718.

Camposeco-Negrete, C., 2013. Optimization of cutting parameters for minimizing energy consumption in turning of AISI 6061 T6 using Taguchi methodology and ANOVA. J. Clean. Prod. 53, 195–203.

Diaz-Elsayed, N., Dornfeld, D., Horvath, A., 2015. A comparative analysis of the environmental impacts of machine tool manufacturing facilities. J. Clean. Prod. 95, 223–231.

Fang, K., Uhan, N., Zhao, F., Sutherland, J.W., 2011. A new approach to scheduling in manufacturing for power consumption and carbon footprint reduction. J. Manuf. Syst. 30, 234–240.

Hanafi, I., Khamlichi, A., Cabrera, F.M., Almansa, E., Jabbouri, A., 2012. Optimization of cutting conditions for sustainable machining of PEEK-CF30 using TiN tools. J. Clean. Prod. 33, 1–9.

He, Y., Liu, B., Zhang, X., Gao, H., Liu, X., 2012. A modeling method of task-oriented energy consumption for machining manufacturing system. J. Clean. Prod. 23, 167–174.

Jin, M., Tang, R., Huisingh, D., 2015. Call for papers for a special volume on Advanced Manufacturing for Sustainability and Low Fossil Carbon Emissions. J. Clean. Prod. 87, 7–10.

Li, W., Zein, A., Kara, S., Herrmann, C., 2011. An Investigation into Fixed Energy Consumption of Machine Tools, in: Hesselbach, J., Herrmann, C. (Eds.), Glocalized Solutions for Sustainability in Manufacturing: Proceedings of the 18th CIRP International Conference on Life Cycle Engineering. Springer Berlin Heidelberg,

Berlin, Heidelberg, pp. 268–275.

Newman, S.T., Nassehi, A., Imani-Asrai, R., Dhokia, V., 2012. Energy efficient process planning for CNC machining. CIRP J. Manuf. Sci. Technol. 5, 127–136.

Pusavec, F., Krajnik, P., Kopac, J., 2010. Transitioning to sustainable production – Part I: application on machining technologies. J. Clean. Prod. 18, 174–184.

Sangwan Kuldeep Singh, 2011. Development of a multi criteria decision model for justification of green manufacturing systems. Int. J. Green Econ. 5, 285–305.

Taylor F.W, 1907. On the art of cutting metals. Trans. ASME 28, 31–350.

Yan, J., Li, L., 2013. Multi-objective optimization of milling parameters e the trade-offs between energy , production rate and cutting quality. J. Clean. Prod. 52, 462–471.

Yuan, C., Zhai, Q., Dornfeld, D., 2012. A three dimensional system approach for environmentally sustainable manufacturing. CIRP Ann. - Manuf. Technol. 61, 39–42.

Yusup, N., Mohd, A., Zaiton, S., Hashim, M., 2012. Expert Systems with Applications Evolutionary techniques in optimizing machining parameters : Review and recent applications (2007 – 2011). Expert Syst. Appl. 39, 9909–9927.

Chapter 2

Literature Review

This chapter sets the background for this study. It is an assessment of the present state of the art of the wide and complex field of modelling and optimization of machining operations and their application in conventional machining processes.

2.1 Introduction

Merchant (1974) reported that in conventional machining, the machined components take only about 6% to 10% of the total available production time on machines being used. It has been estimated that this percentage would increase to 65% – 80% in modern computer-based manufacturing (Armarego, 1996) due to advent of computer-based and automated machining systems. An CIRP (International Institution for Production Engineering Research) working paper (Armarego, 1996) quotes the findings of a survey by a leading cutting tool manufacturer as, "In the USA the correct cutting tool is selected less than 50% of the time, the tool is used at the rated cutting speed only 58% of the time, and only 38% of the tools are used up to their full tool-life capability". Similarly, an earlier survey for machining aluminum alloy components in the U.S aircraft industry has shown that the selected cutting speeds were far below the optimal economic speeds (Finnie, 1956). One of the reasons for this poor performance is the lack of predictive models. The difficulties in realizing true predictive models for machining arise from the extreme physical phenomenon inherent in the system. Machining generates a highly inhomogeneous plastic flow where local stresses generate high rates of plastic deformation (up to $10^6 s^{-1}$) that gives rise to inhomogeneous thermal fields, high temperatures (1200ºC in machining steel), and high pressures (10 MPa) (Ivester et al., 2000). This type of complex plastic flow is difficult to predict even with sophisticated numerical softwares and the

basic data on material behavior under such conditions is non-existent for most materials of practical interest (Ivester et al., 2000). This has inhibited the widespread use of the numerical modeling techniques. Thus, the development of empirical modeling and optimization is gaining importance in the field of machining.

According to van Luttervelt et al. (1998) predictive modelling and optimization of machining operations is carried out in three phases: (i) fundamental modelling (ii) applied modelling and (iii) determination of optimal or near-optimal cutting conditions as shown in Figure 2.1. Modelling of input–output relationship is considered as an abstract representation of a process linking causes and effects or transforming process inputs into outputs (Markos et al., 1998). The resulting model provides the basic mathematical input required for formulation of the process objective function. An optimization technique provides optimal or near-optimal solution to the overall optimization problem.

2.2 Predictive Modelling of Machining Operations

Predictive modelling of machining operations is the first and the most important step for process control and optimization. A predictive model is an accurate relationship between the independent input variables and dependent output performance measures (Kardekar, 2005). The primary goal of modelling of machining operations is to be able to quantitatively predict the performance of machining operations accurately. Modelling can facilitate effective planning of machining operations to achieve optimum productivity, quality and cost. According to an major CIRP study by van Luttervelt et al. (1998), the major obstacle in the modelling of machining operations is attributed to the lack of fundamental understanding of basic mechanisms due to the interactions of cutting tools and the work material and great variety and complexity of real machining operations.

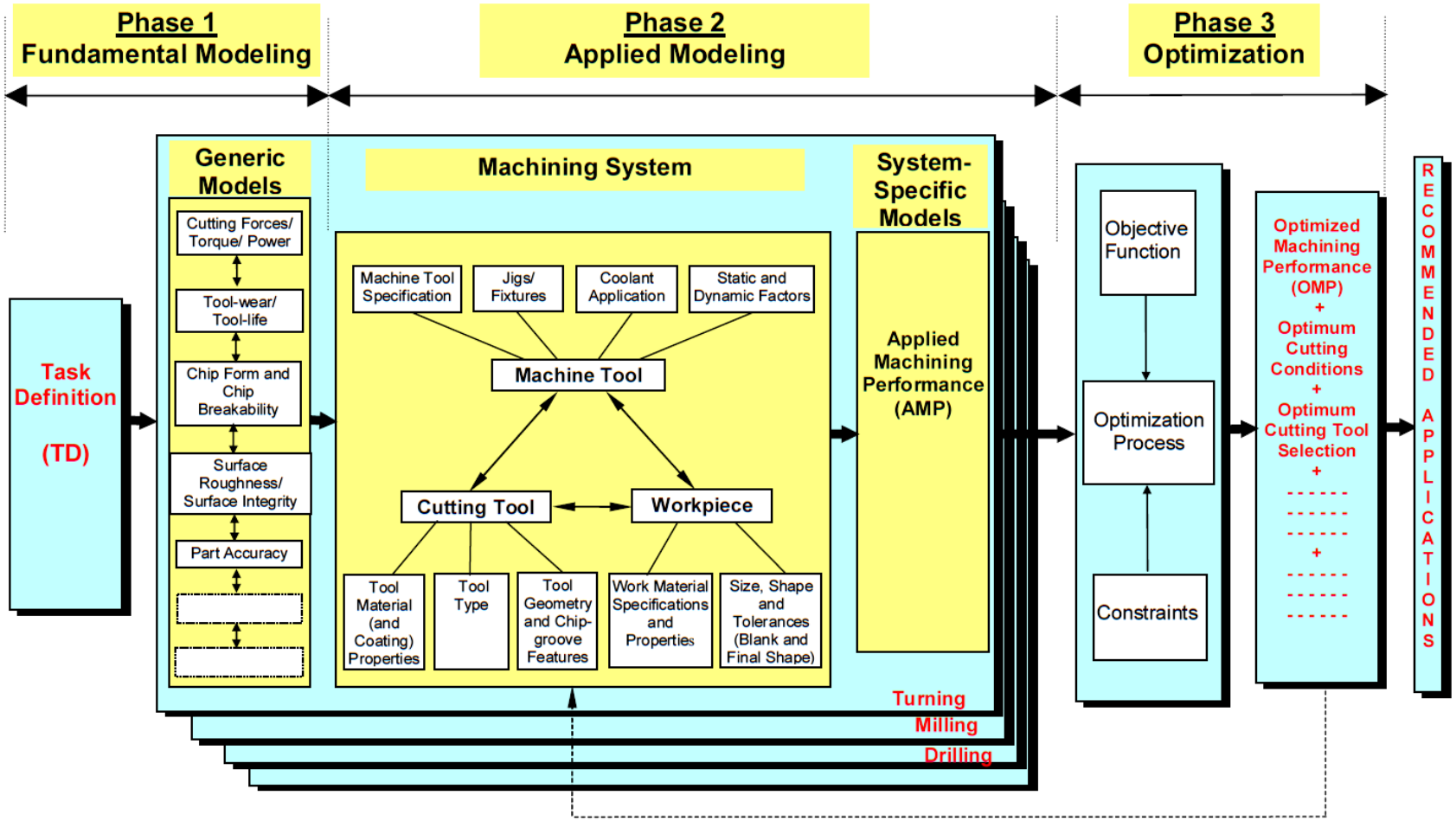

Figure 2.1: Phases in predictive modelling and optimization of machining operations for practical applications (van Luttervelt et al., 1998)

Predictive modelling of machining operations for practical applications consists of two phases as shown in Figure 2.1 (phase 1 and phase 2). The first phase is development of predictive models for machining variables and the second is development of models for machining performance. The typical input conditions include cutting conditions, tool geometry, tool and workpiece properties, machine tool dynamics, *etc*. In phase 1, basic phenomena in the chip formation process such as the strains, strain rates, temperatures, friction, tool-chip contact length, chip flow, *etc*. are predicted. In phase 2, machining performance measures such as, cutting forces, torque, power, tool-wear/tool-life, chip-form/chip breakability, surface roughness/integrity, part accuracy, *etc*. required for the practical application are predicted. The major challenge is the transformation of the outputs from phase 1 to phase 2. Arrazola et al. (2013) have also emphasized that the phase 1 variables must be correlated to performance measures and product quality of phase 2.

The machining performance can be classified as 'technological' and 'commercial' (van Luttervelt et al., 1998). The technological machining performance measures, directly or indirectly, affect the commercial machining performance measures. The technological machining performance is limited by a large number of variables involved in machining processes as shown in Figure 2.2. The major technological performance measures (tool life/tool wear, part accuracy, surface roughness, cutting force/power consumption, chip form/chip breakability) are attributed to the interaction between cutting tool and workpiece caused by the relative motion provided by the machine tool in a machining process. The workpiece material properties, shape and size affect the machining performance. Cutting tool material, type, geometry, and chip breakers also affect the machining performance. Machining performance is also affected by the

machine tool and process such as static and dynamic properties; application of coolants; cutting conditions of speed, feed and depth of cut; and operational features.

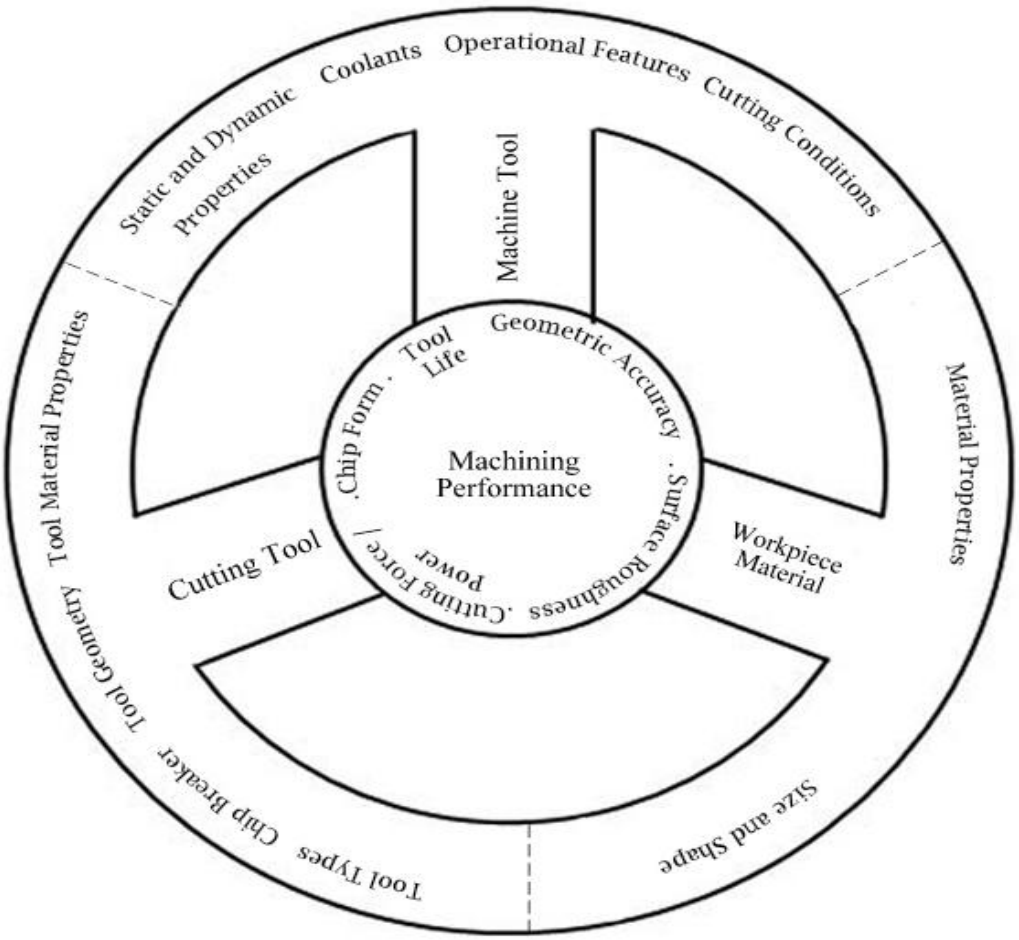

Figure 2.2: Factors influencing technological machining performance

There are many methodologies which can be used to establish the relationships among process inputs and outputs and there is no single methodology which can perform the above defined task reliably due to highly non-linear nature of metal cutting operations (Yigit, 2007). Modelling of machining has evolved through three main stages over the years, namely analytical modelling, numerical modelling and empirical modelling. According to van Luttervelt et al. (1998), 43% of research groups were active in the empirical modelling, 32% in analytical modelling and 18% in numerical modelling.

2.2.1 Analytical modelling

The input-output relationships can be made by purely analytical models that are based solely on the fundamental theoretical physics of the machining process. Analytical modelling or science based modelling began to emerge in the 1940s. Geometric, analytical or mechanistic modelling methods form the basis of this approach. Analytical modelling was initiated largely by Merchant's physics-based modelling and analysis of the basic force system acting among the cutting tool, chip and workpiece in a machining process. In this approach predictions are made from the basic physical properties of the tool and workpiece materials together with the kinematics and dynamics of the process. Thus after the appropriate physical data is determined, the effect of changes in cutting conditions (e.g., tool geometry, cutting parameters, *etc*.) on machining performance (e.g., wear rate, geometric conformance, surface quality, *etc*.) can be predicted.

The usual approach in analytical studies was to propose a model of chip formation from experimental observations and then to develop an approximate machining theory. The best known model of this kind is the shear plane model (Ernst and Merchant, 1941). The model was of the following form:

$$2\varphi + \beta - \alpha = 90° \tag{2.1}$$

where α, φ and β are the rake, shear angle and friction angle respectively. However, the comparison of this model with experimental results proved unsuccessful. In a later attempt by Merchant (Merchant, 1945), the effect of compressive (or hydrostatic) stress on the shear stress of the metal cut was considered and a second model, represented by Eq. (2.2), was suggested.

$$2\varphi + \beta - \alpha = c \tag{2.2}$$

where c is a constant which takes different values for different workpiece materials. This

model appeared to offer a degree of approximation to the experimental results obtained in the case of SAE 4340 steel. However, this result was only brought into agreement with theoretical relations by assuming that the value of the yield stress is a function of the hydrostatic stress on the shear plane. This hypothesis is true for rupture, but generally regarded as inadmissible at ordinary metal working levels (Bridgman, 1952; Finnie, 1963). Lee and Shaffer (1949) analyzed the machining process by applying slip-line field analysis. The model is given as:

$$2\varphi + \beta - \alpha = 45° \tag{2.3}$$

On the other hand, for certain reasonable values of friction and rake angles (for example, $\alpha = 0°$ and $\beta = 50°$), the model in Eq. (2.3) produces a negative value for the shear angle φ, whereas φ is greater than zero in practice. Some other analytical models includes Kobayashi and Thomsen (1962) model using the limit-load theorem; Kudo (1965) proposed several new slip-line field solutions; Childs (1980) incorporated the elastic effects in slip-line field modelling; and Oxley and Young (1989) developed theory on a shear zone model. If robust predictive models can be developed, this approach would substantially reduce the cost of gathering experimental data and would provide a platform for a *priori* optimization of machining process parameters based upon the physics of the system (Ivester et al., 2000).

Analytical models provide useful insight into the cutting process. However, they are based on over simplistic assumptions (Komvopoulos and Erpenbeck, 1991; Lin and Lin, 1992). The assumptions have rendered these models inadequate in predicting accurate chip flow (Dirikolu and Childs, 2000). Apart from the limitations of the simple geometrical and kinematical configurations of classical orthogonal and oblique cutting theories applied to the more complex practical operations, difficulties have been met in developing predictive models for various performance measures such as the cutting

forces, power, surface roughness, and tool temperatures. However, due to many unexpected and unaccounted events occurring during the process and the amount of assumptions, a researcher needs to be sure that the problem is solvable. Results of analytical models are not reliable enough to make them worthy (Ulutan, 2013).

2.2.2 Numerical modelling

Numerical modelling also known as computer based modelling began to emerge in the 1970s and was the watershed event in the advent of digital computer technology. Amongst the numerical modelling techniques, the finite-element methods (FEMs) are the most frequently used (van Luttervelt et al., 1998). The main objective of finite element studies is to derive a computational model for predicting machining performance measures like cutting force, temperature, temperature distribution, chip geometry, *etc.* under different cutting conditions. Finite element techniques use small mesh representations of the material and cutting tool which are based on continuity principles (Ceretti et al., 2000; Guo and Liu, 2002; Ohbuchi and Obikawa, 2003; Özel and Altan, 2000). When material model, tool-friction conditions, and thermal properties of the workpiece and tool are defined properly, finite element analysis provides the information about the process. Machining process with finite element analysis can be modeled as; rigid-plastic or elastic-plastic; Eulerian (fixed mesh) or Lagrangian (mesh flow with the material); adaptive meshing or non-adaptive meshing. Cutting edge of the tool poses difficulties in terms of generating meshes in Lagrangian approach. In order to correct highly distorted elements around the cutting edge, techniques such as mesh rezoning and dynamic remeshing are utilized.

Since 1970s finite element analysis has been increasingly employed in machining problems. One of the first FE models of machining was developed by Klamecki (1973).

This was an updated-Lagrangian, elastic-plastic, three-dimensional model. However, it was limited to only the initial stages of chip formation. The first two-dimensional (or orthogonal) FE machining simulation was proposed by Shirakashi and Usui (1974). They used the elastic-plastic material model and assumed the chip shape and the material stream lines. They developed a special method of computation, called the "Iterative Convergence Method", in order to obtain solutions for a steady state of cutting and for quickening the convergence of computations in comparison with the real transient process. The main limitation of this model is the treatment of chip separation by a small crack at the cutting edge that contradicts the plastic deformation nature of the machining process at steady-state conditions.

Tay et al. (1974) used the finite element method to compute the temperature field in the tool, the chip, and the workpiece during orthogonal cutting process. Their approach was to develop a model based on the knowledge of the strain-rate field from experimental data. They were able to obtain an acceptable two dimensional temperature distribution. More simplified version of this finite element method was described by Tay et al. (1976) to reduce the computer run time and to eliminate the need for an experimental strain rate field for each set of conditions.

Muraka et al. (1979) used the finite element method to investigate the effect of the cutting speed, flank wear rate, and coolant on the temperature distribution on the tool flank and rake faces. The rate of heat generation was calculated from the experimentally measured strain rates in the primary and secondary shear zones.

Stevenson et al. (1983) presented a further development of Tay's finite element model and extended its range of application. Modifications were applied to the procedures for calculating the strain rate field, the mesh and the flow stress. The resulting procedure

avoided the need for the flow field as an input and was able to accommodate a wide range of shear angles and tool-chip contact lengths.

Iwata et al. (1984) developed a method of numerical modelling for plane strain orthogonal cutting in steady state on the basis of the rigid-plastic material model. However, the temperature effects were neglected.

Carroll and Strenkowski (1988) described computer models dealing with orthogonal metal cutting using the FE methods. The models are based on a specially modified version of a large deformation updated Lagrangian code called NIKE2D, which employed either elastic-plastic or visco-elastic material models and either simple Coulomb's Law or friction elements for simulating friction between the chip and the cutting tool. Chip separation was allowed to occur when the effective plastic strain at a node adjacent to the cutting edge reached a critical value. The temperatures in the deforming zone were determined with this model.

Childs and Maekawa (1990) developed an elastic-plastic and thermal FE analysis of chip flow and stresses, tool temperatures and wear in metal cutting. The computer model was based on a simplified version of a supercomputer program (Usui et al., 1981). The flank and crater wear rates of the steel-cutting carbide tools were determined by using an empirical relation which depends on temperature and contact stress. Additionally, empirical relations provided the flow stress and friction characteristics. FE analysis gives good predictions of tool cutting forces but provides error in thrust forces and temperatures under the imposed friction and wear characteristics.

Lin and Lin (1992) developed a thermo elastic-plastic cutting model. The finite difference method was adapted to determine the temperature distribution within the chip and the tool. In this model, a chip separation criterion based on the strain energy density

was introduced. It was stated that this criterion was a material constant and therefore independent of cutting conditions involved. The constant friction coefficient has been used to describe chip/tool interface friction.

Shih and Yang (1993) developed a finite element simulation method for metal cutting which was based on the updated-Lagrangian formulation and which included the effects of elasticity, visco-plasticity, temperature, strain rate, and large strain on the stress-strain relationship as well as the effect of frictional force on the tool-chip interface. An element separation criterion based on the distance between the tool tip and the nodal point connecting the four elements ahead of the cutting tool was assumed. A friction model was proposed which assumed a constant friction coefficient in the sticking region and a linearly decaying (to zero) friction coefficient in the sliding region.

Wu et al. (1996) developed a thermo visco-plastic finite element cutting model. In this model, the chip-tool friction conditions are characterized by a temperature-dependent friction model. The temperature effect was incorporated into this model by assuming that the friction stress is directly related to the local value of the effective stress that had already been considered to vary with temperature.

Kim and Sins (1996) developed a thermo-viscoplastic cutting model by using finite element method to analyze the mechanics of steady-state orthogonal cutting process. The authors assumed that the workpiece is a thermo-viscoplastic material and the flow stress is a function of strain, strain rate and temperature. In the temperature analysis, the authors applied the full upwind scheme to overcome the spurious oscillations in the solution arising from the standard discretization of the heat transfer equation involving both diffusion and convection. The experimental data comparison included the cutting

force and the temperature analyze. Validation of the cutting temperature was performed by comparing the simulated temperature distributions, maximum temperature and the location of maximum temperature with Tay et al. (1974, 1976) results and was found in good agreement.

Ceretti et al. (1996) proposed a finite element model to simulate the orthogonal cutting process with continuous and segmented chip flow. Despite the simplifying assumptions related to friction conditions, properties of the workpiece material, limited work hardening, strain rate, and temperature effects, the results were in good agreement with the experiments in terms of estimating chip geometry, tool workpiece contact length, and chip and tool temperatures.

Ng et al. (1999) presented an FE model to simulate cutting forces and temperature distributions during orthogonal turning of a hardened hot work die steel, AISI H13 (52HRC), with polycrystalline cubic boron nitride (PCBN) tooling. Experimental data from infrared chip surface temperature measurements and cutting force output were used to validate the model. Good correlation was obtained between experimental and modelled results for temperature. However, the FE analysis underestimated feed force results due to a lack of adequate workpiece property data and simplistic tool/chip friction assumptions.

Shet and Deng (2000) analyzed the metal cutting process with the finite element method using plain strain conditions and found that the finite element simulations were able to re-produce experimentally observed phenomena in orthogonal metal cutting, such as the existence of the primary and secondary shear zones. Also, the finite element solutions obtained in this study show that friction along the tool-chip interface strongly affects the distribution of the thermo-mechanical fields.

Bil et al. (2004) revealed the effects of friction, chip formation model and material data in the simulation of orthogonal cutting. The results showed that friction parameter affects the simulation results drastically but this parameter yields good agreement only for some variables in the range. A smaller friction parameter leads to good results for cutting force, whereas other variables such as thrust force and shear angle are computed more accurately with larger friction parameters. Therefore, the accuracy of the simulation must be assessed by examining all predictable process parameters. It was observed that none of the well known shear angle relationships are material dependent, hence material behavior can only be seen in the parameters such as temperature, forces and contact length.

Fang and Fang (2007) used experimentally validated FE model to graphically depict the distributions of strain, strain rate, stress, and temperature. The results show that a large strain primarily exists in the secondary deformation region along the tool-chip interface and the machined surface. A large strain rate also exists in the primary and tertiary deformation regions. A large stress exists in the primary deformation region and on the round tool edge. The maximum temperature occurs on the round tool edge.

Although finite element methods are capable of predicting cutting forces without assuming shear zone geometry or use of empirical coefficients, their accuracy is a strong function of the underlying material model, incorporation of dynamic effects and the available computational power (Kapoor et al., 1998). This approach is criticized as being not based on physics of machining. Computation time, sensitivity to material constitutive model and friction definitions, and instability problems with meshing are some of the drawbacks of finite element modelling.

2.2.3 Empirical modelling

Empirical modelling emerged as an organized process in the late 1890s to early 1900s. It originated with F. W. Taylor's pioneering engineering research and development of empirical methodology for estimating reasonably economic machining conditions. Taylor, who has been acknowledged as the father of metal cutting science, adopted the empirical approach in proposing his well known Taylor's equation, $vT^n = C$ where v is cutting speed, T is tool life, and n and C are constants (Taylor F.W, 1907). This equation has since been extended to include other cutting conditions like feed and depth of cut. The Taylor equation and its extended versions are extensively used even today in assessing machinability and machining economics. The machining databases that the industry uses are dominated by Taylor parameters. The power-law form of the extended Taylor equation has subsequently been applied to include simple work material properties and tool geometry parameters (Colding, 1991; Colding, 1958; Kronenberg, 1966). Rubenstein (1976) has provided a rationale for the extended Taylor equation by utilizing a power-law expression for cutting temperature while modelling crater wear and flank wear based on the assumption of adhesion and diffusion wear effects. The American Society of Metal Handbook and Metcut Research Associates Machining Data Handbook provide tabulated data for a wide range of potential work materials and their values of n and C. Armarego and Zhao (1996) created a comprehensive data on machining parameters based on practical machining operations from which average forces and torque trends were curve fitted using multivariable regression analysis.

The popularity of the empirical approach stems from the simplicity involved in building the model and the resulting prediction accuracy maintained over a range of cutting conditions. In contrast, other methods such as slip-line field solutions and shear plane

angle solutions become less effective when applied to realistic oblique machining processes (Bayoumi et al., 1994).

Empirical models are simple, easy to apply and allow a wide range of problems to be addressed (Trent and Wright, 2000). Relationships between outputs and inputs can be obtained by using design of experiment principles. Process outputs such as surface roughness and residual stresses can be modeled by empirical modelling since they are influenced by hard-to-model factors (Chou et al., 2003; Feng and Wang, 2003; Özel and Karpat, 2005; Wang and Feng, 2002). In order to obtain reliable models, large numbers of experiments should be performed. Regression and neural network based models are usually employed to establish the relationships between inputs and outputs. Benardos and Vosniakos (2003) made an extensive literature review on predicting surface roughness and found the neural network approach to be effective.

The empirical approach is considered as a practical method and it is the most suited approach for industrial applications (Kardekar, 2005). Large amount of experimentation is required to establish the empirical relationships among various influencing independent operation variables and the technological performance measures. Once the experimental work has been done to establish the exponents and constants in the equations, they can be used by production personnel to set up and operate their machines. In some studies, tools such as design of experiments and curve fitting are used to obtain the empirical relationship from experimental data. The advantage of this approach lies in the fact that, depending on the level of understanding of the participating phenomena, it can produce very good results. It must be pointed out that it is not easy to produce the expected results from a set of experiments because there are too many

factors to be considered regarding the explained phenomenon and the equipments used (Benardos and Vosniakos, 2003). Moreover, the obtained conclusions have very specific applications and little or no general applicability. Extensive new experimentation is needed each time a new cutting variable is added to the power-law relationship and the entire process needs to be repeated afresh each time a new tool-work material combination is encountered.

The classification of different empirical modelling techniques is shown in Figure 2.3.

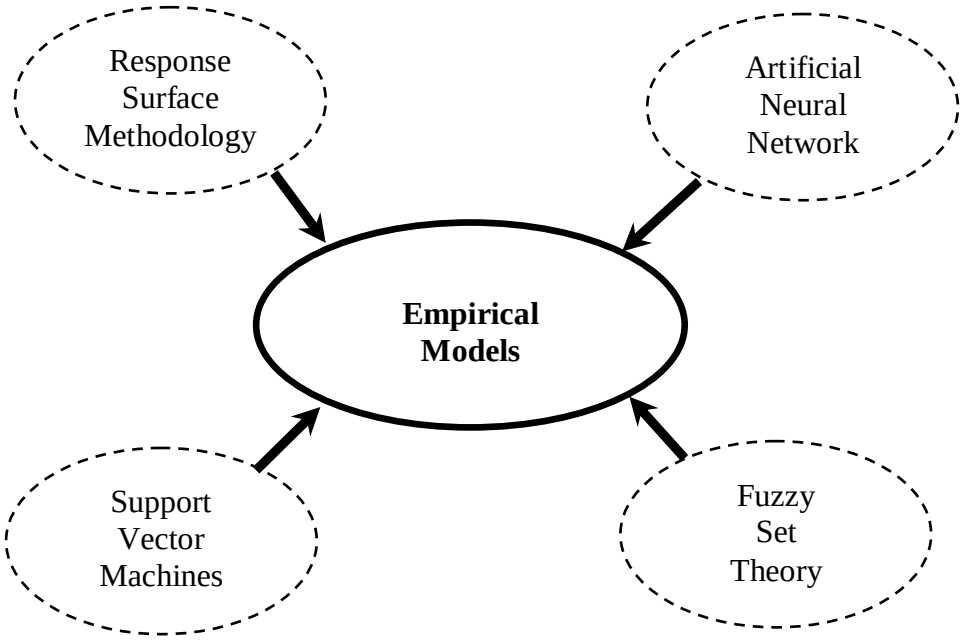

Figure 2.3: Different empirical modelling techniques (adapted from Mukherjee and Ray, 2006)

Szecsi (1999) proposed an approach for modelling cutting forces with the help of artificial neural networks. Feed-forward, multi-layer neural networks trained by back propagation algorithm were used. The training of the networks was performed with experimental machining data. A three layer feed-forward neural network with 7-8 neurons in the hidden layer for predicting the three cutting force components was proposed for better results.

Davim (2001) applied regression analysis to establish a correlation between cutting parameters (cutting velocity, feed and depth of cut) and responses (average surface roughness and maximum peak-to-valley height) during turning of free machining steel with cemented carbide tool. The results showed that cutting speed was the most significant variable followed by the feed; and depth of cut had no significant effect on the roughness. The results gained through the developed model shows a maximum error of 10%, while the results obtained by the geometric theoretical model shows a minimum error of 16%.

Suresh et al. (2002) developed a surface roughness prediction model for machining mild steel using RSM. The experimentation was carried out with TiN-coated tungsten carbide cutting tools for machining mild steel work-pieces covering a wide range of machining conditions. A second order mathematical model in terms of machining parameters was developed for surface roughness prediction.

Davim (2003) examined the influence of cutting conditions (cutting speed and feed) and cutting time on turning metal matrix composites. ANOVA was applied to investigate the characteristics of composite using PCD cutting tools. A correlation was developed between cutting speed, feed and the cutting time with the tool wear, power required to perform the machining operation, and surface roughness using the regression analysis. The confirmation experiments were performed to compare the experimental and predicted results.

Feng and Wang (2003) developed an empirical model for surface roughness prediction during finish turning of steel 8620 with coated carbide insert. The model considers the work-piece hardness, feed, cutter nose radius, spindle speed, and depth of cut as input parameters. Two modelling techniques – non-linear regression analysis and

computational neural networks – were applied in developing the empirical models. The values of surface roughness predicted by these models were compared with representative models in the literature. Metal cutting experiments and hypothesis testing demonstrated that the developed models have a satisfactory goodness of fit.

Noordin et al. (2004) presented an experimental investigation into the effect of feed rate, side cutting edge angle and cutting speed on the surface roughness and tangential force during turning of AISI 1045 steel with chemical vapor deposition coated carbide inserts. The ANOVA revealed that feed is the most significant factor influencing the response variables. The quadratic effects of side cutting edge angle and the feed and side cutting edge angle interaction factor provided secondary contribution to the responses. Additionally, the cutting speed also provided secondary contribution to the tangential force. The quadratic models developed using RSM were reasonably accurate and can be used for prediction within the limits of the factors investigated.

Öktem et al. (2005) utilized RSM to create a mathematical model for surface roughness in terms of cutting parameters (feed, cutting speed, axial depth of cut, radial depth of cut and machining tolerance) for predicting surface roughness values in milling mold surfaces made of Aluminum (7075-T6). The accuracy of the RSM model was verified with the experimental measurements. The prediction error was found to be 2.05%.

Oktem et al. (2006) used ANN for prediction of surface roughness during end milling of Aluminum (7075-T6). A feed forward neural network model was developed exploiting experimental measurements. The neural network model was trained and tested using MATLAB. The results predicted from ANN model were compared with experimental measurements and a good correlation was obtained between ANN predictions and experimental measurements.

Sahin and Motorcu (2005) used RSM to develop surface roughness prediction models during turning of mild steel (AISI 1040) with coated carbide inserts. The first-order and second order prediction models were developed in terms of feed, cutting speed and depth of cut. They concluded that surface roughness increases with increasing feed rate but decreases with increasing cutting speed and the depth of cut. The predicted results were found to be close to the experimental values.

Singh and Rao (2006) established surface roughness prediction model using RSM during hard turning of bearing steel (AISI 52100) with mixed ceramic inserts. Results indicated that the feed is the dominant factor affecting the surface roughness, followed by the nose radius, cutting velocity and effective rake angle.

Al-Ahmari (2007) developed empirical models for tool life, surface roughness and cutting force during turning of austenitic AISI 302. Process parameters of cutting speed, feed rate, depth of cut, and tool nose radius were used as inputs to the models. Predictive modelling techniques of response surface methodology and neural networks were used. Regression Analysis (RA), RSM and ANN modelling techniques were compared and evaluated using descriptive statistics and hypothesis testing. It was found that the ANN models are better than RA and RSM models. Also, RSM models are better than RA models for predicting tool life and cutting force.

Aslan et al. (2007) investigated the effects of three cutting parameters, namely cutting speed, feed rate and depth of cut on flank wear and surface roughness using ANOVA. A relationship between the parameters and the performance measures were determined using linear regression. Average percentage errors for developed models were found as 45% for flank wear and 28% for surface roughness which were quite high. It was observed that cutting speed is the only statistically significant factor influencing the tool

wear. The tool wear decreased as the cutting speed was increased. An analysis of the interaction plots revealed that in order to minimize the surface roughness, the highest level of the cutting speed, the lowest level of axial depth of cut and the medium level of feed rate should be preferred.

Palanikumar (2007) developed a mathematical model using RSM for surface roughness to correlate the machining parameters during machining of GFRP composites. The four input variables considered were cutting speed, fiber orientation angle, depth of cut, and feed rate. The influences of these parameters on surface roughness were analyzed based on the developed mathematical model. It was found that the surface roughness decreases with the increase of cutting speed and depth of cut while surface roughness increases with the increase of feed rate and fiber orientation angle.

Aggarwal et al. (2008) used RSM to develop the empirical models for prediction of power consumption during turning of AISI P-20 tool steel with coated inserts. The percentage error between the actual and predicted values for power was from 3.9 to 4.4%. It can be said that the developed empirical models were reasonably accurate. All the actual values for the confirmation run were within the 95% prediction interval.

Davim et al. (2008) developed the surface roughness prediction model using artificial neural network (ANN) to investigate the effects of cutting conditions during the turning of free machining steel with cemented carbide tool. The ANN model of surface roughness parameters was developed with feed rate, cutting speed and depth of cut as the process parameters. 3D surface plots were generated to study the interaction effects of cutting conditions on surface roughness parameters. The analysis reveals that the cutting speed and the feed rate have significant effects in reducing the surface roughness while the depth of cut has the least effect.

Lalwani et al. (2008) investigated the effect of cutting parameters (cutting speed, feed rate and depth of cut) on cutting forces (feed force, thrust force and cutting force) and surface roughness during finish hard turning of MDN250 steel using coated ceramic tool. The machining experiments were conducted and a mathematical model was developed using RSM. It was found that a linear model best fits the variation of cutting forces with feed rate and depth of cut and a non-linear quadratic model best describes the variation of surface roughness with major contribution of feed rate and secondary contributions of interaction effect between feed rate and depth of cut.

Tsao and Hocheng (2008) presented the prediction of thrust force and surface roughness during drilling of composite materials using regression analysis and the artificial neural network. The experimental results indicated that the feed rate and the drill diameter were the most significant factors affecting the thrust force, while the feed rate and spindle speed contributed most to the surface roughness. A correlation among the feed rate, spindle speed and drill diameter with the induced thrust force and surface roughness was obtained by multi-variable regression analysis. The experimental results indicated the neural network was more effective than multi-variable regression analysis.

Cakir et al. (2009) examined the effects of cutting parameters (cutting speed, feed rate and depth of cut) on the surface roughness through the mathematical model developed using regression analysis and the exponential method from the data gathered through a series of turning experiments. The experiments were repeated for two carbide inserts having same geometry and substrate but different coating layers. The total average error of the model was found to be 4.2% and 5.2% for the two inserts.

Karayel (2009) presented a neural network approach for the prediction of surface roughness during turning on a Computer Numerical Control (CNC) lathe. The cutting parameters used in the experiment were depth of cut, cutting speed and feed rate. A feed forward multilayered neural network was developed and the network model was trained using the back propagation algorithm. R_a, R_z and R_{max} were modelled and evaluated individually. One hidden layer was used for all the models while the numbers of neurons in the hidden layer of the R_a model were five and the numbers of neurons in the hidden layers of the R_z and R_{max} models were ten. The results of the neural network approach were compared with actual values and found to be satisfactory.

Abhang and Hameedullah (2010) developed a predictive model, using RSM, for turning of EN-31 steel with a tungsten carbide tool. The results show that feed rate has the most significant effect on power consumption, followed by depth of cut, tool nose radius and cutting speed. It was shown that the second order model is more precise than the first order model in predicting the power consumption during machining.

Gupta (2010) developed empirical models for predicting surface roughness, tool wear and power required during turning operations. These response parameters were mainly dependent upon cutting speed, feed and cutting time. Three modelling techniques – response surface methodology, artificial neural networks and support vector regression – were applied in developing the empirical models. The data of 27 experiments was used to generate, compare and evaluate the proposed models of tool wear, power required and surface roughness. Results demonstrated that the developed models were suitable for predicting the response parameters with a satisfactory goodness of fit. It was found that ANN and SVR models are much better than regression and RSM models for predicting the three response parameters.

Kini and Chincholkar (2010) investigated the effect of varying machining parameters on surface roughness and material removal rate during turning of glass fiber reinforced polymers (GFRP) using coated tungsten carbide inserts under dry cutting conditions. They developed a second order predictive model using regression analysis by utilizing factorial experiments covering speed, feed, depth of cut, and tool nose radius at 95% confidence interval. Contour plots of the surface roughness and material removal rate for different machining conditions were generated from the empirical equations. It was found that feed rate is the main influencing factor on the roughness followed by the depth of cut and depth of the cut is the main influencing factor on the roughness followed by the tool nose radius.

Zain et al. (2010a) presented an ANN model for predicting the surface roughness during machining of titanium alloy (Ti-6Al-4V). Feed forward back propagation was selected as the algorithm with traingdx, learngdx, MSE, logsig as the training, learning, performance, and transfer functions respectively. It was found that a 3-1-1 network structure provides the best ANN model in predicting the surface roughness value. The recommended combination of cutting conditions to obtain the best surface roughness value was: high speed with low feed rate and radial rake angle.

Zain et al. (2010b) investigated the effect of the radial rake angle of the tool, cutting speed and feed rate on the surface roughness. A machining experiment was referred as a case study and the regression model was developed to formulate the fitness function of the GA. The results revealed that the regression model provides good prediction in estimating the surface roughness.

Cetin et al. (2011) evaluated the performance of vegetable based cutting fluids and cutting parameters (spindle speed, feed rate and depth of cut) for reducing the surface

roughness, cutting and feed forces during turning of AISI 304L austenitic stainless steel with carbide insert tools. Results indicate that the effects of feed rate and depth of cut were more effective than cutting fluids and spindle speed on reducing the forces and improving the surface finish. Regression analysis was performed to indicate the fitness of experimental measurements. Regression models obtained from the surface roughness, cutting force and feed force measurements matched well with the experimental data.

Correia and Davim (2011) examined the influence of the wiper inserts on the surface roughness during turning. Experimental studies were carried out on the AISI 1045 carbon steel because of its large application in manufacturing industry. Surface roughness was represented by different amplitude parameters. It was found that wiper inserts and high feed rate lead to better surface roughness.

Kilickap et al. (2011) develop a mathematical prediction model of the surface roughness using RSM during drilling of AISI 1045 steel with TiN coated high speed steel tools. The effects of drilling parameters on the surface roughness were evaluated. The predicted and measured values were quite close, indicating that the developed model can be effectively used to predict the surface roughness.

Korkut et al. (2011) presented ANN and RA models for the tool–chip interface temperature prediction during the turning of AISI 1117 steel with cemented carbide inserts. The temperature values predicted by the ANN and RA models were found close to experimental values.

Neşeli et al. (2011) applied RSM during turning of AISI 1040 steel with Al_2O_3 coated insert tools. A quadratic model was developed for the surface roughness to investigate the influence of cutting insert geometry. The results indicated that the tool nose radius was the dominant factor on the surface roughness with 51.45% contribution. Approach

angle and rake angle are significant factors on surface roughness with 18.24% and 17.74% contributions respectively in the total variability of the model. A good agreement between the predicted and measured surface roughness values was observed. The quadratic effect of tool nose radius provided little contribution to the model.

Mahdavinejad and Saeedy (2011) used regression analysis to analyze the influence of cutting parameters on tool life and surface finish during turning of AISI 304 stainless steel. Experiments were performed at different feed rates and cutting speeds with and without cutting fluid. ANOVA was used to determine the effects of each parameter on the tool wear and the surface roughness. It was found that cutting speed has the main influence on the flank wear. The feed rate has the most important influence on the surface roughness. The application of cutting fluid results in longer tool life and better surface finish.

Mandal et al. (2011) applied regression analysis to assess machinability of AISI 4340 steel with ceramic inserts. ANOVA was used to find the significance and percentage contribution of each parameter. It was observed that depth of cut has maximum contribution on tool wear. The mathematical model of flank wear was developed using regression analysis as a function of machining parameters. The predicted value from the developed model and the experimental values were found close to each other.

Aouici et al. (2012) investigated the effects of cutting speed, feed rate, work piece hardness, and depth of cut on surface roughness and cutting force components during the hard turning of AISI H11 steel with cubic boron nitride inserts. Mathematical models for surface roughness and cutting force components were developed using RSM. Results revealed that the cutting force components were influenced by depth of cut and work piece hardness. Feed rate and work piece hardness had statistical significant effect on surface roughness.

Comparison of experimental and predicted values of the cutting force components and the surface roughness were close to each other.

Asiltürk and Neşeli (2012) developed a mathematic model for predicting surface roughness during CNC turning of AISI 304 austenitic stainless steel with coated carbide inserts. The model for the surface roughness as a function of cutting parameters was obtained using RSM. The adequacy of the developed mathematical model was proved by ANOVA. The influence of cutting speed, feed rate and depth of cut on the surface roughness was examined. The results indicated that the feed rate was the dominant factor affecting surface roughness.

Pontes et al. (2012) applied radial base function neural networks for prediction of surface roughness during the turning of SAE 52100 hardened steel with the use of Taguchi's orthogonal arrays. Artificial neural networks models proved to be capable to predict surface roughness in accurately and precisely.

Zain et al. (2012) used ANN to predict the value of surface roughness as function of cutting speed, feed and radial rake angle during milling of titanium alloy with coated and uncoated carbide tools. After comparing a number of network structures it was found that the 3-7-7-1 network structure provides better prediction of surface roughness.

Chinchanikar and Choudhury (2013) investigated the performance of coated carbide tools considering the effect of work material hardness and cutting parameters during turning of hardened AISI 4340 steel at different levels of hardness. The correlations between the cutting parameters and performance measures of cutting forces, surface roughness and tool life were established by linear regression models. Significance of parameters was determined by performing an ANOVA. It was observed that higher cutting forces were required for machining harder work material.

Hessainia et al. (2013) developed a surface roughness model using RSM during hard turning of 42CrMo4 hardened steel with Al_2O_3/TiC mixed ceramic cutting tools. The combined effects of cutting parameters and tool vibration on surface roughness were investigated using ANOVA. The results indicated that the feed rate is the dominant factor affecting the surface roughness. A good agreement was observed between the predicted and the experimental surface roughness.

Makadia and Nanavati (2013) developed a mathematical prediction model of the surface roughness using RSM during tuning of AISI 410 steel with ceramic inserts. The developed prediction equation reveals that the feed is the main factor followed by the tool nose radius. The surface roughness was found to increase with the increase in the feed and it decreases with the increase in the tool nose radius. The verification experiments carried out to check the validity of the developed model predicted surface roughness within 6% error.

Yalcin et al. (2013) investigated the effect of cutting parameters on the cutting force, surface roughness and temperature during milling of AISI 1050 steel using artificial neural networks which were trained by using experimental results obtained from Taguchi's L_8 orthogonal array. A feed forward back propagation artificial neural network was employed for the training, simulation and prediction. The results demonstrated that the artificial neural network is an effective tool for prediction of cutting force, surface roughness and temperature.

Wang et al. (2013) applied the response surface methodology to investigate the effect of cutting speed, feed rate, depth of cut, and rake angle on the machining force components during turning of Fe-based amorphous alloy with physical vapor deposition coated tools. It was found that depth of cut is the dominant cutting parameter affecting the machining force

components. Rake angle and interaction of feed rate and depth of cut provided secondary significance to machining forces. Cutting speed has insignificant influence on machining force components. ANOVA results indicated that a linear model best fits the radial force prediction while a quadratic model best describes the axial force and cutting force predictions.

Bartarya and Choudhury (2014) analyzed the forces and surface finish produced during turning of hardened EN31 steel using uncoated cubic boron nitride inserts. ANOVA was applied to measure the goodness of fit of the measured data. The regression models developed for prediction of forces and surface roughness were found statistically significant. The most significant parameter affecting the forces was the depth of cut followed by feed.

Bhardwaj et al. (2014) developed a surface roughness prediction model using RSM during turning of AISI 1019 steel with coated carbide inserts. A quadratic model was developed in terms of feed, speed, depth of cut, and nose radius. A prediction model was developed by improving the normality, linearity and homogeneity of the data using a Box–Cox transformation. Confirmation experiments showed that the Box–Cox transformation has a strong potential to improve the prediction capability of empirical models. The results showed that the feed was the main influencing factor on the surface roughness while the depth of cut had no significant influence.

Sarıkaya and Güllü (2014) developed mathematical models using RSM to study the effect of cooling condition, cutting speed, feed rate, and depth of cut on average surface roughness (R_a) and average maximum height of the profile (R_z) during turning of AISI 1050 steel with physical vapor deposition coated inserts. ANOVA results showed that the feed rate and the cooling condition have the highest influence on machined surface roughness. Feed rate was the most influencing factor with a contribution of 68.68%

followed by cooling conditions with a contribution of 16.98% on R_a. R_z was influenced by feed rate with a contribution of 77.50%. Confirmation experiments showed that the percentage deviation between the actual and experimental data is between 2.72% and 7.14%.

2.3 Optimization Techniques used in Machining

A large number of optimization techniques have been developed by researchers to determine optimal cutting conditions for machining operations. Broadly, these may be classified as: (i) conventional optimization techniques and (ii) non-conventional optimization techniques as shown in Figure 2.4.

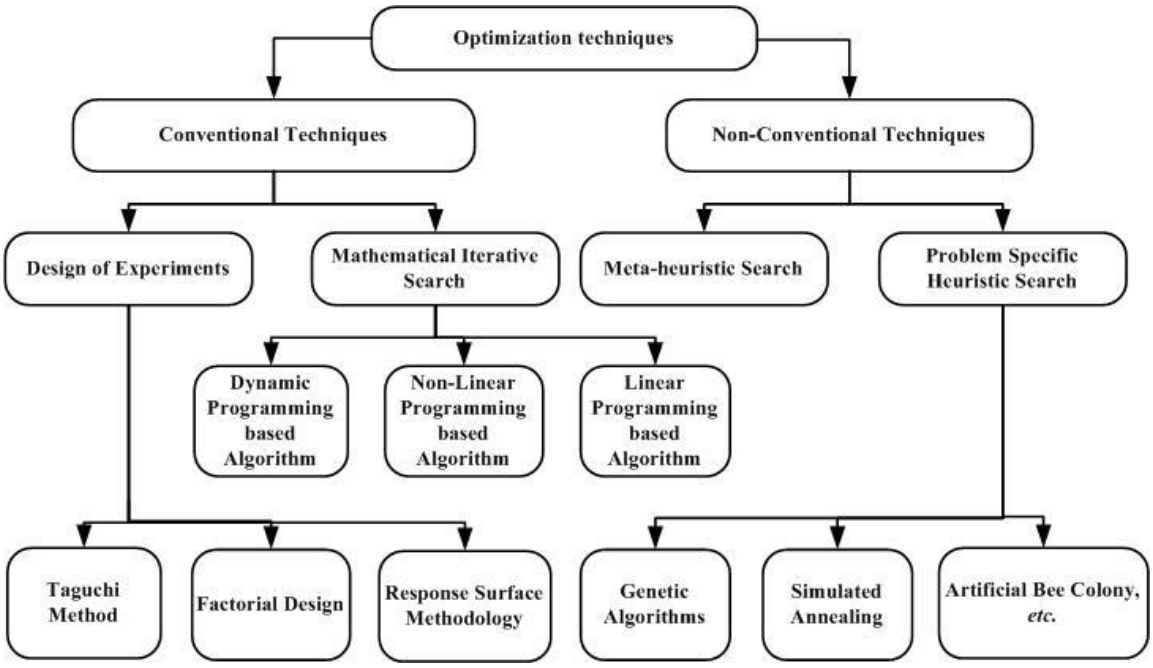

Figure 2.4: Conventional and non-conventional optimization techniques (adapted from Mukherjee and Ray, 2006)

2.3.1 Conventional optimization techniques

These techniques are based on deterministic algorithms with specific rules for moving from one solution to the other. These algorithms have been successfully applied to many engineering design problems. Traditional mathematical

programming techniques such as linear programming, integer programming, dynamic programming, geometric programming, *etc*. have been used to solve machining optimization problems. Gilbert (1950) studied the optimization of machining parameters during turning with respect to maximum production rate and minimum production cost. Linear programming was used in the early stage of machining process optimization by Ermer and Patel (1974). Geometric Programming (GP) has also been widely adopted by Ermer (1971), Eskicioglu et al. (1985), and Gopalakrishnan and Al-Khayyal (1991). Its major disadvantage is its requirement that the objective function and constraints must be in the polynomial form. Agapiou (1992) used a dynamic programming model to determine the optimum value of the objective function (weighted sum of production cost and time) and the number of passes. Successive quadratic programming (Wen et al., 1992) and iterative Newton's method (Xiao et al., 1992) have been used to optimize grinding processes. Jha and Hornik (1995) applied the generalized reduced gradient method to optimize tool geometry and cutting condition in plain milling processes. Da et al. (1997) used non-linear programming technique for turning operations. Extensive literature exists on optimization of machining processes largely focusing on maximum production rate and minimum cost.

Ghani et al. (2004) applied Taguchi optimization methodology to optimize cutting parameters during end milling of AISI H13 hardened steel with TiN coated P10 carbide insert tool under semi-finishing and finishing conditions of high speed cutting. The milling parameters evaluated were cutting speed, feed rate and depth of cut. An orthogonal array, Signal-to-Noise (S/N) ratio and Pareto analysis of variance were employed to analyze the effect on milling parameters. Results showed that the optimal

combination for low resultant cutting force and surface roughness were high cutting speed, low feed rate and low depth of cut.

Nalbant et al. (2007) used Taguchi method to find the optimal cutting parameters for surface roughness during turning. The orthogonal array, the signal-to-noise ratio and analysis of variance were employed to study the performance characteristics during turning of AISI 1030 steel bars using TiN coated tools. Three cutting parameters namely, insert radius, feed rate and depth of cut were optimized with considerations of surface roughness. The experimental results demonstrated that the insert radius and feed rate are the main parameters among the three controllable factors that influence the surface roughness during turning of AISI 1030 carbon steel.

Aggarwal et al. (2008) used RSM and Taguchi's technique to investigate the effect of cutting speed, feed, depth of cut, nose radius, and cutting environment during turning of AISI P20 tool steel on the power consumption. Results show that the cutting speed is the most significant factor followed by depth of cut and feed. The analysis of the results for power consumption shows that the RSM and Taguchi methodology provide similar results. It was concluded that RSM technique can model the response in terms of significant parameters, their interactions and square terms which cannot be done by Taguchi's technique. 3D surface plots generated by RSM can help in visualizing the effect of parameters on response in the entire range specified whereas Taguchi's technique gives the average value of response at the given level of parameters.

Bhattacharya et al. (2009) investigated the effects of cutting parameters on surface finish and power consumption by employing Taguchi technique. The investigation was carried during high speed machining of AISI 1045 using coated carbide tools. A combined technique using orthogonal array and analysis of variance was employed to investigate

the contribution and effects of cutting speed, feed rate and depth of cut on surface roughness and power consumption. The results showed a significant effect of cutting speed on the surface roughness and power consumption while the other parameters did not substantially affect the responses.

Kilickap (2010) presented an application of the Taguchi method for investigating the effects of cutting parameters and point angle on the delamination factor in dry drilling of GFRP composites. The analysis of experimental results was carried out using Taguchi's orthogonal array and ANOVA. The results of ANOVA revealed that feed rate is the main cutting parameter influencing delamination factor. Low feed rates provided minimum damage. Optimal parameters based on the S/N ratio for the minimum entrance and exit damage were the cutting speed at Level 1 (5 m/min) and the feed rate at Level 1 (0.1 mm/rev).

Asiltürk and Akkuş (2011) used Taguchi method for optimizing turning parameters to minimize surface roughness. The statistical methods of signal to noise ratio and the analysis of variance were applied to investigate effects of cutting speed, feed rate and depth of cut on surface roughness. Results indicated that the feed rate was the most significant factor effecting surface roughness.

Fratila and Caizar (2011) applied Taguchi methodology to optimize the cutting conditions during face milling of $AlMg_3$ with High Speed Steel (HSS) tool under semi finishing conditions to get the best surface roughness and the minimum power consumption. The appropriate orthogonal array, signal to noise ratio and Pareto analysis of variance were employed to analyze the effect of the mentioned parameters on the surface roughness. The results indicated that the optimum cutting conditions to minimize power consumption were minimum depth of cut, minimum feed rate, minimum cutting speed, and maximum

lubricant flow rate. It was found that the feed rate has significant effect on surface roughness. Depths of cut and cutting speed have the significant influence on power.

Neşeli et al. (2011) applied response surface optimization during turning of AISI 1040 steel with Al_2O_3 coated insert tools. The results revealed the optimal combination of tool nose radius, approach angle and rake angle for better surface roughness.

Mandal et al. (2011) used Taguchi method to determine the optimal cutting parameters during machining of AISI 4340 steel with ceramic inserts. Based on the mean response and signal to noise ratio, the best optimal cutting conditions were cutting speed of 280 m/min, depth of cut of 0.5 mm and feed rate of 0.12 mm/rev. A confirmation run was carried out to verify the optimized results and it was found that the values obtained were within the prescribed limits.

Abhang and Hameedullah (2012) used Taguchi method for optimization of machining parameters during turning of steel. The experimental work was carried out by turning EN-31 steel alloy using tungsten carbide inserts. The optimal process parameters were obtained based on signal to noise ratio. The significance of each parameter was determined by ANOVA analysis. The cutting parameters namely feed rate, depth of cut, and lubricant temperature were varied to observe the effects on surface roughness. It was found that better surface finish can be obtained by applying cooled lubricant.

Aouici et al. (2012) used desirability function analysis in RSM to determine the optimum values of cutting speed, feed rate, workpiece hardness, and depth of cut during the hard turning of AISI H11 steel with cubic boron nitride inserts. Results revealed that the best surface roughness is achieved at the lower feed rate and the higher cutting speed.

Asiltürk and Neşeli (2012) determined multi-objective optimal cutting conditions using Taguchi method and RSM. The RSM was found to be more effective for the identification and development of significant relationships among cutting parameters. It was concluded that RSM technique can model the responses in terms of all parameters, their interactions and square terms. The optimal parameters for R_a was cutting speed of 50 m/min, feed rate of 0.15 mm/rev and depth of cut of 1.5 mm, while for R_z cutting speed of 150 m/min, feed rate of 0.15 mm/rev and depth of cut as 1 mm were found to be optimal parameters.

Bhushan (2013) used RSM to determine the optimal machining parameters during machining of Al 7075 alloy using tungsten carbide cutting tool to get minimum power consumption and maximum tool life. The study revealed that cutting speed is the most significant parameter followed by depth of cut, feed and nose radius. Confirmation test was conducted to validate the test results. The application of desirability function analysis in RSM proved to be an effective tool for optimizing the machining parameters.

Hessainia et al. (2013) used the quadratic model of RSM associated with response optimization technique and composite desirability to find optimum values of cutting parameters and tool vibration during hard turning of 42CrMo4 hardened steel with Al_2O_3/TiC mixed ceramic cutting tools. Optimal cutting condition and tool vibration leading to the minimum surface roughness were highlighted.

Makadia and Nanavati (2013) used response surface contours for determining the optimum conditions for a required surface roughness during tuning of AISI 410 steel with ceramic inserts. Response surface optimization showed that the optimal combination of machining

parameters of 255.75 m/min, 0.1 mm/rev, 0.3 mm, 1.2 mm for cutting speed, feed rate, depth of cut, and tool nose radius respectively.

Camposeco-Negrete (2013) applied Taguchi methodology to optimize the cutting parameters during turning of AISI 6061 T6 under roughing condition to achieve minimum energy consumption and minimum surface roughness. The results of this research showed that the feed rate was the most significant factor followed by the depth of cut and the cutting speed for minimizing energy consumption. However, the objective function was not multi-objective and the power consumption and surface roughness were considered in isolation to each other.

Chinchanikar and Choudhury (2013) used desirability function approach in RSM to determine optimum cutting conditions. It was found that the use of lower feed value, lower depth of cut and by limiting the cutting speed while turning 35 and 45 HRC AISI 4340 steel ensures minimum cutting forces, minimum surface roughness and better tool life.

Yalcin et al. (2013) used Taguchi method to determine the optimum machining parameters leading to minimum cutting force, surface roughness and temperature during milling of AISI 1050 steel. According to the signal to noise ratio a depth of cut of 1.25 mm, feed rate of 0.05 mm/teeth, cutting speed of 130 m/min, and wet cutting were the best parameters that minimize the cutting force, surface roughness and temperature values.

Campatelli et al. (2014) utilized RSM to analyze the effect of cutting speed, feed rate, radial and axial depth of cut on energy consumption during milling of carbon steel. The optimal values of the radial engagement and feed to minimize the specific energy related to the efficiency of the cutting were 1 mm and 0.12 mm/tooth respectively.

Emami et al. (2014) used Taguchi method to investigate the performance of four lubricants to reduce the cutting force, specific energy and surface roughness during near dry grinding of Al_2O_3 engineering ceramic. Taguchi's L_{16} orthogonal array was used for experimental design. The optimal lubricant and grinding parameters of depth of cut, feed rate and abrasive grain size for minimum cutting force, specific energy and surface roughness were obtained. The feed rate was found to be the most significant machining parameter to minimize specific energy.

Sarıkaya and Güllü (2014) used Taguchi method and desirability function analysis in RSM to determine the optimal values of machining parameters leading to minimum surface roughness characteristics. Based on signal to noise ratio of Taguchi method, the optimized surface roughness values were obtained for optimal combination of parameters. Based on the desirability function analysis method of RSM, the optimal turning parameters of AISI 1050 steel were found to be as: cooling condition of MQL at 120 mL/h flow rate, cutting speed of 200 m/min, feed rate of 0.07 mm/rev, and depth of cut of 1.2 mm. It was concluded that RSM can predict the effect of parameters better and desirability function analysis in the RSM is a better method for optimization.

Optimization methods have been widely used in the manufacturing industries for continual improvement of machining processes and the output quality of the machined products. However, the optimization problems related to manufacturing are usually complex in nature and characterized by mixed continuous–discrete variables and discontinuous and non-convex design spaces (Rao, 2011). Determination of optimal cutting conditions through cost-effective mathematical models is complex in nature and the techniques of optimization have undergone substantial development and expansion (Mukherjee and Ray, 2006). Hence, the conventional optimization methods fail to give global optimum solutions as they are usually trapped at the local optimum (Rao, 2011). These techniques are usually slow in convergence.

Conventional optimization techniques are mostly gradient-based and they pose many limitations in application to complex machining models (Rao, 2011). To overcome these problems, researchers have proposed non-conventional techniques.

2.3.2 Non-conventional optimization techniques

These algorithms are stochastic in nature with probabilistic transition rules. These methods are mainly based on biological, molecular or neurological phenomena that mimic the metaphor of natural biological evolution and/or the social behavior of species. To mimic the efficient behavior of these species, various researchers have developed computational systems that seek fast and robust solutions to complex optimization problems. Hence, many new algorithms based on random search techniques are being used in solving machining optimization problems (Rao, 2011). Examples of these algorithms include Simulated Annealing (SA), Genetic Algorithm (GA), Particle Swarm Optimization (PSO), Artificial Bee Colony (ABC), Ant Colony Optimization (ACO), *etc*.

Suresh et al. (2002) optimized the surface roughness using GA. The GA provided the minimum and maximum values of surface roughness and their respective optimal machining conditions.

Öktem et al. (2005) coupled the RSM model with an GA to find the optimum cutting conditions leading to the least surface roughness value. The predicted optimum cutting conditions were validated with an experimental measurement. It was found that optimum parameters prediction by GA correlates very well with the experimental data. It was also found that coupled RSM and GA model is effective and can be utilized in other machining problems such as tool life optimization, dimensional errors minimization, *etc*.

Oktem et al. (2006) presented an approach for determination of the best cutting parameters leading to minimum surface roughness during end milling by coupling neural network and genetic algorithms.

Palanisamy et al. (2007) used GA to determine optimal cutting parameters for milling operations. The machining time was considered as the objective function and constraints were tool life, limits of feed rate, depth of cut, cutting speed, surface roughness, cutting force, and amplitude of vibrations while maintaining a constant material removal rate. The good agreement between the optimized cutting forces and measured cutting forces clearly demonstrated the accuracy and effectiveness of the model. The obtained results indicated that the optimized parameters were capable of machining the workpiece more efficiently with better surface finish.

Lu et al. (2009) investigated optimal design of the cutting parameters for rough cutting processes during high-speed end milling of SKD61 tool steel. The major characteristic indices selected to evaluate the processes were tool life and metal removal rate, and the corresponding cutting parameters were type of milling, spindle speed, feed per tooth, radial depth of cut, and axial depth of cut. Grey relational analysis was used to determine the optimal combination of cutting parameters. The principal component analysis was applied to evaluate the weights corresponding to various performance characteristics. The results of confirmation experiments reveal that grey relational analysis coupled with principal component analysis can effectively predict the optimal combination of cutting parameters.

Tzeng et al. (2009) investigated the optimization of CNC turning parameters for machining SKD11 tool steel using the grey relational analysis method. Nine experimental runs, based on an orthogonal array of Taguchi method, were performed. The surface properties of average roughness and maximum roughness as well as the

roundness were selected as the quality targets. An optimal parameter combination of the turning operation was obtained using grey relational analysis. The depth of cut was identified as the most influential factor on the roughness average; and cutting speed was the most influential factor for the maximum roughness and the roundness.

Zain et al. (2010b) used a genetic algorithm for estimating the optimal cutting conditions for minimum surface roughness. A regression model was used to formulate the objective function. High cutting speed, low feed rate and high radial rake angle lead to lower surface roughness.

Kilickap et al. (2011) used the quadratic model developed by using RSM as the objective function to determine minimum surface roughness using GA during drilling of AISI 1045 steel with TiN coated high speed steel tool. It was found that the results of GA were close to the experimental results.

Fu et al. (2012) optimized the cutting parameters during high-speed milling of NAK80 mold steel. An experiment based on Taguchi's technique was performed. The optimum cutting parameters were obtained using grey relational analysis. The principal component analysis was applied to evaluate the weights so that their relative significance can be described. The results showed that grey relational analysis coupled with principal component analysis can effectively predict the optimal combination of cutting parameters and the proposed approach can be a useful tool to reduce the cutting force.

Hanafi et al. (2012) applied grey relational theory coupled with Taguchi methodology to optimize the cutting parameters during machining of PEEK-CF30 using TiN tools under dry conditions. The objective of optimization was to achieve the minimum power and best surface quality simultaneously. The obtained results revealed that depth of cut was the most influential parameters followed by cutting speed and feed rate. The optimal parameters for achieving the best surface roughness and power consumption

were low cutting speed, low feed rate and low depth of cut. This corresponds to the cutting speed of 100 m/min, feed rate of 0.05 mm/rev and depth of cut of 0.25 mm.

Zain et al. (2012) used ANN coupled with GA to search for a set of optimal cutting condition points that lead to the minimum value of surface roughness. Three machining cutting conditions considered in this study were speed (v), feed (f) and radial rake angle (γ). The used approach reduced the surface roughness value compared to the experimental, regression, ANN, and response surface methods.

Yan and Li (2013) presented a multi-objective optimization method based on weighted grey relational analysis and RSM to optimize the cutting parameters during milling of medium carbon steel with carbide tools to achieve the minimum cutting energy, maximum material removal rate and minimum surface roughness. The results indicated that width of cut was the most influencing parameter followed by depth of cut, feed rate and spindle speed. The experimental results indicated that GRA coupled with RSM is very useful tool for multi-objective optimization of cutting parameters.

Table 2.1 presents the review of 72 research papers from year 2000 onwards in terms of machining process involved, workpiece material, cutting tool material, machining parameters, machining performance, predictive technique, and optimization technique. The review focused on conventional machining processes and does not include the relatively newer machining processes such as water jet machining, electric discharge machining, electrochemical machining, *etc*.

The literature review reveals that researchers have focused on various predictive modelling and optimization techniques to determine optimal or near-optimal cutting conditions. Statistical regression analysis and artificial neural networks have been widely used modelling techniques in development of predictive models for machining. However, RSM is most widely used as it offers enormous information from even small

number of experiment and even it is possible to analyze the influence of independent parameters on performance characteristics. The various authors have used Taguchi method, RSM, genetic algorithm, grey relation analysis, *etc.* as optimization techniques. Table 2.1 suggests that turning is the most commonly used machining process. The various machining parameters used for modelling and optimization are cutting speed, feed rate, depth of cut, nose radius, rake angle, and approach angle, but the most widely optimized parameters are cutting speed, feed rate and depth of cut. It may be due to the fact that these are the most critical parameters in any machining operation and these are easily controllable during the machining process. It has been observed that most of the researchers have used steel as workpiece material. Steel is one of the widely researched materials in machining for more than last half a century, but there is a renewed interest in application of steel because of its sustainability – 100% recyclable and almost indefinite life cycle (Kant and Sangwan, 2014). AISI 1045 steel is one of the steel grades widely used in different industries (construction, transport, automotive, power, *etc*.).

Table 2.1: Review of literature on machining parameters, workpiece/cutting tool material, machining process and performance, and predictive and optimization techniques

S.No.	Author	MP_r	Machining Parameters	Workpiece Material/ Cutting Tool Material	MP_f	PT	OT	Remarks
1.	Davim (2001)	T	*v* (71,143, 283) *f* (0.1,0.16,0.25) *d* (0.5,0.75,1)	Free machining steel/Cemented carbide	R_a R_t	RA	-	RA model hasss an associated error lower than geometric model.
2.	Benardos and Vosniakos (2002)	M	*v* 300,500,700) f_t (0.08,0.14,0.2) *d* (0.25,0.75,1.2)	Aluminum alloy/ Not provided	R_a F_c F_f F_t	ANN	Taguchi	ANN is a powerful tool to predict surface roughness.
3.	Suresh et al. (2002)	T	*v* (95,170, 280) *f* (0.1,0.2,0.3) *d* (0.5,1,1.5)	Mild steel/TiN-coated tungsten carbide	R_a	RSM	GA	Provided the optimum machining conditions for maximum and minimum values of surface roughness.
4.	Davim (2003)	T	*v* (250,350,500) *f* (0.05,0.1,0.2) *t* (1,5,10)	Metal matrix composite/PCD cutting tool	VB P R_a	RA	-	The influence of cutting parameters on responses has been studied during turning of composites.
5.	Feng and Wang (2003)	T	*h* (steel 8620, HRB 86, AL 6061 T, HRB 52) *v* (80,120) *f* (0.102,0.254) *d* (0.508,1.016) *r* (0.794,6.320)	Steel 8620, HRB 86, AL 6061 T, HRB 52/ Carbide insert	R_a	RA, ANN	-	RA and ANN provided satisfactory results.
6.	Ghani et al. (2004)	M	*v* (0.4,0.8,1.2) *f* (0.15,0.25,0.35) d_r (0.5,1.5,2.5)	AISI H13 hardened steel/TiN coated carbide	R_a F_{rf}	-	Taguchi	Optimum values of cutting parameters found to obtain better surface finish.

MP_r – Machining process, MP_f – Machining performance, PT – Predictive technique, OT – Optimization technique

S.No.	Author	MP_r	Machining Parameters	Workpiece Material/ Cutting Tool Material	MP_f	PT	OT	Remarks
7.	Noordin et al. (2004)	T	*v* (240,300,375) *f* (0.18,0.23,0.28) *SCEA* (-3,0,-5)	AISI 1045 Steel/CVD coated carbide insert	R_a F_c	RSM	-	RSM was reasonably accurate in prediction of surface roughness and cutting force.
8.	Wang and Chang (2004)	M	*v* (20,40,60,80,100) f_t (0.02,0.04,0.06,0.08,1.0) d_a (0.1,0.5,0.9,1.3,1.7) *coolant* (wet, dry)	AL2014-T6/ Not provided	R_a	RSM	-	RSM can model efficiently using experimental results.
9.	Öktem et al. (2005)	M	f_t (0.08,0.105,0.13) *v* (100,200,300) d_a (0.3,0.5,0.7) d_r (1,1.5,2) m_t (0.001,0.0055,0.01)	Aluminum (7075-T6)/PVD AlTiN coated with solid carbide	R_a	RSM	GA	GA coupled with response surface methodology used to find optimum cutting conditions leading to minimum surface roughness.
10.	Reddy and Rao (2005)	M	*v* (150,200,250) *f* *(200,300,400) d_a (20) *r* (0.4,0.8,1.2)	AISI 1045 steel/ Solid coated (TiAlN) carbide	R_a	RSM	GA	The optimization methodology provided the best possible surface quality.
11.	Sahin and Motorcu (2005)	T	*v* (181,208,240, 276, 317) *f* (0.1,0.13,0.15, 0.18, 0.21) *d* (0.36,0.43,0.50, 0.58, 0.66)	AISI 1040 mild steel/ TiN-coated carbide	R_a	RSM	-	RSM and experimental results close to each other.
12.	Oktem et al. (2006)	M	f_t (0.08-0.13) *v* (100–300) d_a (0.3–0.7) d_r (1–2) m_t (0.001–0.01)	Aluminum (7075-T6)/PVD AlTiN coated with solid carbide	R_a	ANN	GA	ANN coupled with GA used to get optimum machining parameters for minimum surface roughness.
13.	Ozcelik and Bayramoglu (2006)	M	*n* (4000,5500,7000,8500, 10000) *f* *(640,1320,2240,3400, 4800) *d* (0.1,0.3,0.5,0.7,0.9) *step over* (1,2,3,4,5)	AISI 1040 steel/ TiAlN coated solid carbide	R_a	RA	-	Statistical models developed to predict the surface roughness.

S.No.	Author	MP_r	Machining Parameters	Workpiece Material/ Cutting Tool Material	MP_f	PT	OT	Remarks
14.	Al-Ahmari (2007)	T	*v* (25,60,144) *f* (0.1,0.25,0.7) *d* (0.25,0.5,1.6) *r* (0.4,0.8,1.6)	Austenitic AISI 302/ Carbide	T_l F_c R_a	RA, RSM, ANN	-	ANN models are better as compared to RSM and RA.
15.	Aslan et al. (2007)	T	*v* (100,175,250) *f* (0.05,0.1,0.2) *d* (0.25,0.5,1)	AISI 4140 steel/Al2O3 + TiCN mixed ceramic	VB R_a	RA	-	Influences of machining parameters on responses have been studied.
16.	Korkut and Donertas (2007)	M	*v* (44,56,71,88,111) *f* * (20,63,100) *d* (2,3)	AISI 1020 and AISI 1040 steels/Carbide	R_a F_c, F_f, F_t	-	-	AISI 1020 requires more forces for machining than AISI 1040.
17.	Nalbant et al. (2007)	T	*r* (0.4,0.8,1.2) *f* (0.15,0.25,0.35) *d* (0.5,1.5,2.5)	AISI 1030 carbon steel/ TiN coated	R_a	-	Taguchi	Optimal values of machining parameters have been found.
18.	Palanisamy et al. (2007)	M	*v* (20-40) f_t (0.05-0.3) *d* (0.5-3)	Mild steel/High speed steel	R_a F_c T_l vibration	-	GA	GA based optimization approach can increase the machine efficiency by providing optimal values of cutting parameters.
19.	Palanikumar (2007)	T	*v* (50,75,125,175,200) *B* (15,30,60,90,120) *d* (0.25,0.5,1,1.5,1.75) *f* (0.05,0.1,0.25,0.5,0.75)	Fibre resin composite/Coated cermet	R_a	RSM	-	Influence of cutting speed, feed rate, fiber orientation angle, depth of cut, and fibre resin on surface roughness.
20.	Singh and Rao (2007)	T	*v* (100,150,200) *f* (0.1,0.2,0.32) *d* (0.4,0.8,1.2) γ (6, 16, 26)	AISI 52100 steel /Ceramic	R_a	RSM	-	RSM used to develop mathematical model for prediction of surface roughness.

S.No.	Author	MP_r	Machining Parameters	Workpiece Material/ Cutting Tool Material	MP_f	PT	OT	Remarks
21.	Zhang et al. (2007)	M	*n* (1500,2500,3500) *f* (20,30,40) inch per minute *d* (0.06,0.08,0.1) inches	Aluminum/Coated carbide	R_a	-	Taguchi	Taguchi method used for determining the optimal cutting parameters.
22.	Aggarwal et al. (2008)	T	*v* (120,160,200) *f* (0.10,0.12,0.14) *d* (0.20,0.35,0.50) *r* (0.4,0.8,1.2) *ce* (dry,wet,cryo)	AISI P-20 tool steel/TiN coated	P	RSM	RSM and Taguchi	RSM and Taguchi methodology have given similar results.
23.	Davim et al. (2008)	T	*v* (71,141,283) *f* (0.10,0.16,0.25) *d* (0.5,0.75,1)	Free machining steel/Cemented carbide	R_a R_t	ANN	-	ANN models can predict the responses for cutting parameters with high accuracy.
24.	Kadirgama et al. (2008)	M	*v* (100,140,180) *f* (0.1,0.15,0.2) d_a (0.1,0.15,0.2) d_r (2,3.5,5)	Aluminium alloys (AA6061-T6)/Carbide	R_a	RSM, ANN	GA	ANN predicted surface roughness more accurately as compared to RSM.
25.	Lalwani et al. (2008)	T	*v* (44.5,83,144.5) *f* (0.039,0.104,0.210,0.216) *d* (0.2)	MDN250 steel/Coated ceramic	F_c F_f F_r R_a	RSM	-	Experimental investigation of the effect of cutting parameters on response parameters has been studied.
26.	Tsao and Hocheng (2008)	D	*f* (0.01,0.03,0.05) *n* (800,1000,1200) r_d (6,8,10)	Composite material/High speed steel	F_t R_a	ANN, RA	-	ANN is more effective as compare to RA for prediction of responses.
27.	Bhattacharya et al. (2009)	T	*v* (58,96,151,240) *f* (0.045,0.1,0.125,0.16) *d* (1,1.2,1.5,2)	AISI 1045 Steel/ Coated carbide	R_a, R_q, R_t, P	-	Taguchi	Influence of machining parameters on response has been studied.

S.No.	Author	MP_r	Machining Parameters	Workpiece Material/ Cutting Tool Material	MP_f	PT	OT	Remarks
28.	Cakir et al. (2009)	T	*v* (120,160,200) *f* (0.12,0.18,0.22) *d* (1,1.5,2)	Cold-worked tool steel AISI P20/Carbide coated	R_a	RA, RSM, Exp.	-	RSM is the most appropriate methodology.
29.	Karayel (2009)	T	*v* (100,150,200,250) *f* (0.1,0.15,0.2,0.3) *d* (0.5,1.0,1.5,2.0)	St 50.2 steel/Tungsten carbide	R_a R_{max} R_z	ANN	-	The results of ANN were close to the experimental.
30.	Lu et al. (2009)	M	*Milling type* (down, up) *n* (12000,16000,20000) f_t (0.04,0.07,0.1) d_a (0.6,0.8,1.0) d_r (0.6,0.8,1.0)	SKD tool steel/ Tungsten carbide	VB MRR	-	GRA coupled with PCA	The technique has effectively acquired the optimal set of cutting conditions.
31.	Sun and Guo (2009)	M	*v* (50,65,80,95,110) f_t (0.08,0.06,0.1,0.12,0.14) d_a (1.5) d_r (2,3,4,5,6)	Ti–6Al–4V alloy/ carbide end mill with TiAlN coating	R_a Residual stresses	-	-	Surface roughness increases with feed and radial depth of cut but has much less variation in the cutting speed range.
32.	Tzeng et al. (2009)	T	*v* (125,155,185) *f* (0.12,0.16,0.2) *d* (0.5,0.65,0.8) *cfr* (4,8,12)	SKD 11 tool steel/Carbide coated with TiN	R_a R_t ϕ	-	GRA and Taguchi	Gray relational analysis coupled with Taguchi is effective for multi objective optimization.
33.	Yang et al. (2009)	M	*v* (160,240) *f* (0.1,0.2) d_a (1.5,4.5)	High-purity graphite / carbide	R_a	RA	-	Feed rate effect on surface finish studied.
34.	Gupta (2010)	T	*v* (250,350,500) *f* (0.05,0.1,0.2) *t* (1,5,10)	Metal matrix composite/ Polycrystalline diamond	VB P R_a	RA, RSM, ANN, SVR	-	ANN and SVR models are better than regression and RSM models.

S.No.	Author	MP_r	Machining Parameters	Workpiece Material/ Cutting Tool Material	MP_f	PT	OT	Remarks
35.	Kilickap (2010)	D	*v* (5,10,15,20) *f* (0.1,0.2,0.3,0.4) *Point angle* (118,135)	GFRP composite/High speed steel	Delamin-ation factor	-	Taguchi	Optimal values of machining parameters were found.
36.	Kini and Chincholkar (2010)	T	*v* (59.94,92.072,133.204) *f* (0.1,0.25,0.4) *d* (0.1,0.15,0.2 *r* (0.4,0.8,1.2)	Glass fiber reinforced polymer /Tungsten carbide	R_a MRR	RSM	-	Provides influence of machining parameters on surface roughness.
37.	Moshat et al. (2010)	M	*n* (300,450,600) *f* *(30,50,70) *d* (0.2,0.5,0.8)	Aluminium/CVD coated carbide	R_a MRR	-	Taguchi	Taguchi method found to be efficient for solving multi-attribute decision problems.
38.	Munoz-Escalona and Maropoulos (2010)	M	*v* (800,900,1000) f_t (0.1,0.2,0.3) d_a (1.0,1.5,2.0)	Martensitic 416 stainless steel/ PVD-TiAlN coated carbide	R_a T_1 MRR	-	Taguchi	Results showed that a longer tool life can be achieved by using low values of cutting speed, feed and axial depth of cut.
39.	Zain et al. (2010a)	M	*v* (124.53,130,144.22,160,167.03) *f* (0.025,0.03,0.046,0.07,0.083) γ (6.2,7,9.5,13,14.8)	Ti-6Al-4V/Uncoated and coated solid carbide	R_a	ANN	-	ANN is capable to get accurate prediction values by using a small number of training data.
40.	Zain et al. (2010b)	M	*v* (124.53,130,144.22,160,167) *f* (0.025,0.03,0.046,0.07,0.083) γ (6.2,7,9.5,13,14.8)	Titanium alloy/Uncoated and coated carbide	R_a	RSM	GA	GA outperforms RSM for prediction of cutting parameters leading to minimum surface roughness.
41.	Asiltürk and Akkuş (2011)	T	*v* (90,120,150) *f* (0.18,0.27,0.36) *d* (0.2,0.4,0.6)	Hardened AISI 4140 /Coated carbide cutting	R_a	-	Taguchi	Optimum cutting parameters have been found.
42.	Correia and Davim (2011)	T	*v* (345,410,470) *f* (0.075,0.15,0.25) *r* (0.4,0.8) *Insert type* (conventional,wiper)	AISI 1045 steel /Cemented carbide	R_a R_q R_t	-	-	Wiper inserts provide better surface finish.

S.No.	Author	MP_r	Machining Parameters	Workpiece Material/ Cutting Tool Material	MP_f	PT	OT	Remarks
43.	Gupta et al. (2011)	M	v (60,70,80) f_t (0.2,0.25,0.3) d_a (0.5,0.75,1.0)	GS-563 series steel/ Carbide	R_a T_l	RSM	GA	The regression model coupled with GA is effective for optimizing the machining parameters.
44.	Kilickap et al. (2011)	D	v (5,10,15) f (0.1,0.2,0.3) *ce* (MQL,compressed air,dry)	AISI 1045/TiN coated high speed steel	R_a	RSM	GA	Integrated RSM and GA approach provides an effective methodology for modelling and optimization.
45.	Korkut et al. (2011)	T	v, f, d, F_c, F_f, F_r	AISI 1117 steel/Cemented Carbide	Temp.	ANN, RA	-	Temperature values predicted using ANN and RA.
46.	Mahdavinej and Saeedy (2011)	T	v (100,125,150,175,200) f (0.2,0.3,0.4) *CF* (dry,wet)	AISI 304 stainless steel/ Tungsten carbide	VB R_a	RA	-	The influence of cutting parameters on response analyzed.
47.	Mandal et al. (2011)	T	v (140,280,480) f (0.5,1.0,1.5) d (0.24,0.18,0.12)	AISI 4340 steel/ Ceramic	VB	RA	Taguchi	Coupled Taguchi and RA used to determine optimal values of cutting parameters.
48.	Neşeli et al. (2011)	T	r (0.4,1.8,1.2) K (60,75,90) γ (-9,-6,-3)	AISI 1040 steel/Al_2O_3 coated	R_a	RSM	RSM	Optimum cutting insert geometry parameters were found.
49.	Abhang and Hameedullah (2012)	T	f (0.05,0.10,0.15) d (0.2,0.4,0.6) l_t (10,30,50)	EN 31 Steel/Tungsten carbide	R_a	-	Taguchi	The optimal values of cutting parameters have been found.
50.	Aouici et al. (2012)	T	v (120,180,240) f (0.08,0.12,0.16) d (0.15,0.3,0.45) h (40,45,50)	AISI H11 steel/CBN	R_a F_c F_f F_r	RSM	RSM	Experimental and predicted values are in good agreement with each other.

S.No.	Author	MP_r	Machining Parameters	Workpiece Material/ Cutting Tool Material	MP_f	PT	OT	Remarks
51.	Asiltürk and Neşeli (2012)	T	*v* (50,100,150) *f* (0.15,0.2,0.25) *d* (1,1.5,2)	AISI 304 austenitic stainless steel/Coated carbide	R_a R_z	RSM	RSM and Taguchi	A coupled Taguchi and RSM model used to determine optimum cutting parameters.
52.	Fu et al. (2012)	M	*n* (2000, 2400, 2800) f_t (0.1,0.14,0.18) *d* (0.2,0.35,0.5)	Plastic mold steel/ Tungsten carbide	F_c F_f F_r	-	GRA coupled with PCA and Taguchi	Optimum machining parameters have been found.
53.	Hanafi et al. (2012)	T	*v* (100,200,300) *f* (0.05,0.15,0.2) *d* (0.25,0.75,1.25)	PEEKCF30/TiN coated	P R_a	-	GRA and Taguchi	Multi-objective optimization to determine the optimum machining parameters.
54.	Pontes et al. (2012)	T	*v* (200,240) *f* (0.05,1) *d* (0.15,0.3)	52100 hardened steel/Mixed ceramic	R_a	ANN	Taguchi	Taguchi can be used to identify optimum network structure to predict surface roughness.
55.	Vakondios et al. (2012)	M	*v* (60) *f* (0.2–0.6) d_a (0.3–0.6) d_r (0.3–0.6)	Al7075-T6/Coated carbide	R_a	RA	-	Model developed for the determination of the expected surface quality.
56.	Zain et al. (2012)	M	*v* (124.53, 130, 144.22, 160, 167.03) *f* (0.025,0.03,0.046,0.07,0.083) γ (6.2,7,9.5,13,14.8)	Ti-6Al-4V/Uncoated and coated solid carbide	R_a	ANN	GA	Integrated ANN-GA approach used to predict and optimize the machining parameters to achieve minimum surface roughness.
57.	Bhushan (2013)	T	*v* (90,150,210) *f* (0.15,0.2,0.25) *d* (0.2,0.4,0.6) *r* (0.4,0.8,1.2)	7075 Al alloy SiC composites /Tungsten carbide	P T_l	RSM	RSM	RSM used for multi-objective optimization to achieve maximum tool life and minimum power consumption.

S.No.	Author	MP_r	Machining Parameters	Workpiece Material/ Cutting Tool Material	MP_f	PT	OT	Remarks
58.	Camposeco-Negrete (2013)	T	*v* (150,200,250) *f* (0.1,0.2,0.3) *d* (1,2,3)	AISI 6061 T6/Carbide	P R_a	-	Taguchi	Optimum machining parameters have been found to minimize power consumption.
59.	Chinchanikar and Choudhury (2013)	T	*v* (100,200,300) for 35 HRC *v* (100,150,200) for 45 HRC *f* (0.1,0.2,0.3) *d* (0.5,1.5,2.5)	AISI 4340 steel/Coated tungsten based cemented carbide	F_c F_f F_r R_a	RSM	RSM	Optimum cutting parameters determined to minimize surface roughness.
60.	Hessainia et al. (2013)	T	*v* (90,120,180) *f* (0.08,0.12,0.16) *d* (0.15,0.3,0.45)	Hardened steel/ Ceramic cutting	R_a, R_t, V_y, V_z	RSM	RSM	The optimal values of cutting parameters have been found.
61.	Maiyar et al. (2013)	M	*v* (25,50,75) f_t (0.06,0.09,0.12) d_a (0.2,0.4,0.6)	Inconel 718/Uncoated tungsten carbide	R_a	-	GRA and Taguchi	GRA coupled with Taguchi used effectively for optimization of machining parameters.
62.	Makadia and Nanavati (2013)	T	*v* (220,250,280) *f* (0.1,0.15,0.2) *d* (0.3,0.6,0.9) *r* (0.4,0.8,1.2)	AISI 410 steel/Ceramic	R_a	RA	RSM	Optimal values of machining parameters were found.
63.	Pratyusha et al. (2013)	M	*n* (1000,1250,1500) *f* * (100,150,200) *d* (0.25,0.5,0.75)	Hardened EN31 alloy steel/Carbide	R_a MRR	-	Taguchi	Taguchi method provides a systematic and efficient methodology for searching optimal milling parameters.
64.	Rawangwong et al. (2013)	M	*n* (2400,3000,3600) *f* *(1000,1200,1500) *d* (0.5)	Aluminum semi-solid 2024/Carbide	R_a	RA	-	Higher cutting speed and lower feed tend to decrease the surface roughness.

S.No.	Author	MP_r	Machining Parameters	Workpiece Material/ Cutting Tool Material	MP_f	PT	OT	Remarks
65.	Subramanian et al. (2013)	M	v (100,130,160,190,220) f_t (0.06,0.07,0.08,0.09,0.1) d_a (0.5,1.0,1.5,2.0,2.5)	Aluminium 7075-T6/Carbide	F_c F_f F_t	RSM	GA	Response surface methodology and genetic algorithm have been utilized for establishing optimum machining parameters.
66.	Vijay and Krishnaraj (2013)	M	v (30,40,50,60) f_t (0.01,0.015,0.02,0.025) d_a (2.0,2.5,3.0,3.5)	TI-6Al-4V/ Solid carbide	R_a F_r	-	Taguchi	Optimal cutting parameters have been found.
67.	Wang et al. (2013)	T	v (60,70,80) f (0.06,0.09,0.12) d (0.1,0.2,0.3) γ (5, 10, 15)	Fe-based amorphous alloy/PVD coated	F_c F_f F_r	RSM	RSM	The optimal values of cutting parameters have been found.
68.	Wang et al. (2013)	M	v (100,400) f_t (0.02,0.1) d_a (0.1,0.2)	Aluminum matrix composites/ Polycrystalline diamond	R_a	-	-	Cutting speed has the highest influence on surface roughness followed by interaction of cutting speed and feed rate followed by the feed rate.
69.	Yalcin et al. (2013)	M	v (100,130) f (0.05,0.1) d (1.25, 2) *coolant* (wet, dry)	AISI 1050 steel/Not provided	R_a F_c Temp.	ANN	Taguchi	ANN and Taguchi has been used to determine optimum values of machining parameters.
70.	Bartarya and Choudhury (2014)	T	v (100, 150, 200,250) f (0.1, 0.15, 0.2, 0.3) d (0.5, 1.0, 1.5, 2.0)	EN 31 steel/CBN	F_c F_f F_r R_a	RA	-	The prediction through regression model showed coherence with the measured value.
71.	Bhardwaj et al. (2014)	T	v (50,90.54,150,209.46, 250) f (0.02,0.1,0.21,0.32,0.4) d (0.10,0.28,0.55,0.82,1.0) r (0.4,0.8)	AISI 1019 steel/ Coated carbide insert	R_a	RSM	-	The predictive results are close to experimental results.

S.No.	Author	MP_r	Machining Parameters	Workpiece Material/ Cutting Tool Material	MP_f	PT	OT	Remarks
72.	Kivak (2014)	M	*v* (90,120,150) *f* (0.09,0.12,0.15) *d* (0.5)	Hadfield steel/PVD coated & CVD coated	R_a VB (mm)	RA	Taguchi	CVD coated carbide inserts exhibited better performance than PVD coated carbide inserts.

v – cutting speed (m/min), f – feed (mm/rev), f*– feed (mm/min), f_t – feed/tooth (mm), d – depth of cut (mm), d_a – axial depth of cut (mm), d_r – radial depth of cut (mm), r – tool nose radius (mm), K – approach angle (Degree), γ – rake angle, B – fiber orientation angle, F_c – cutting force (N), F_f – feed force (N), F_r – radial force (N), F_t – thrust force (N), F_{rf} – resultant force (N), h – work piece hardness, m_t – machining tolerance (mm), MRR – material removal rate (g/min), R_a – surface roughness (µm), R_t – maximum peak to valley height roughness (µm), R_q – root mean square roughness (µm), R_z – surface roughness parameter (µm), R_{max} – surface roughness maximum (µm), temp. – temperature (^{o}C), $SCEA$ – side cutting edge angle (degree), T_l – tool life (min), P – power consumption (W), t – time (min), VB – flank wear (mm), n – spindle speed (rpm), r_d – drill diameter (mm), V_y – cutting tool vibration in radial cutting force direction (m/s^2), V_z – cutting tool vibration in main cutting force direction (m/s^2), ce – cutting environment, l_t – lubricant temperature (^{o}C), cfr – cutting fluid ratio, ϕ – roundness (µm), CF – cutting fluid.

2.4 Gaps in Existing Literature

A lot of research has been done in last 100 years; since well known Taylor's formula relating tool life to cutting speed (Taylor F.W, 1907); on the modelling and optimization of machining parameters for forces, tool wear, temperature, *etc*. but a little research has been done to optimize the energy efficiency of machine tools. Moreover, in the past, metal cutting operations have been mainly optimized based on economical and technological considerations without the environmental dimension (Yan and Li, 2013). The few works available for optimization of power consumption and surface roughness for different materials show contrasting results – few authors observed that cutting speed is the most significant factor followed by depth of cut to reduce the power consumption (Aggarwal et al., 2008; Bhattacharya et al., 2009; Bhushan, 2013). Other authors (Fratila and Caizar, 2011; Hanafi et al., 2012) observed that depth of cut is the significant factor followed by cutting speed to reduce the power consumption. Some authors (Abhang and Hameedullah, 2010; Camposeco-Negrete, 2013) observed that feed rate is the significant factor followed by depth of cut to reduce the power consumption. Therefore, more studies need to be carried out to observe the influence of machining parameters on performance characteristics. A generalized relationship between the cutting parameters and the process performance is hard to model accurately mainly due to the nature of the complicated stochastic process mechanisms in machining. This work is an attempt to fill this gap in the research. Machining is still an open field of research after more than last 100 years of research mainly because of the changes in machining technology, materials and the advancement in the modelling and optimization techniques as well as the advancements in computational technology.

References

Abhang, L.B., Hameedullah, M., 2010. Power prediction model for turning EN-31 steel Using response surface methodology. J. Eng. Sci. Technol. Rev. 3, 116–122.

Abhang, L.B., Hameedullah, M., 2012. Optimization of machining parameters in steel turning operation by taguchi method. Procedia Eng. 38, 40–48.

Agapiou, J.S., 1992. The optimization of machining operations based on a combined criterion, part 1: the use of combined objectives in single-pass operations. J. Manuf. Sci. Eng. 114, 500–507.

Aggarwal, A., Singh, H., Kumar, P., Singh, M., 2008. Optimizing power consumption for CNC turned parts using response surface methodology and Taguchi's technique—A comparative analysis. J. Mater. Process. Technol. 200, 373–384.

Al-Ahmari, A.M.A., 2007. Predictive machinability models for a selected hard material in turning operations. J. Mater. Process. Technol. 190, 305–311.

Aouici, H., Yallese, M.A., Chaoui, K., Mabrouki, T., Rigal, J.-F., 2012. Analysis of surface roughness and cutting force components in hard turning with CBN tool: Prediction model and cutting conditions optimization. Measurement 45, 344–353.

Armarego, E.J.A., 1996. Predictive modeling of machining operations—a means of bridging the gap between the theory and practice—a keynote paper, in: The 13th Symposium on Engineering Applications of Mechanics, CMSE, Hamilton, Ontario, Canada. pp. 7–9.

Armarego, E.J.A., Zhao, H., 1996. Predictive force models for point-thinned and circular centre edge twist drill designs. CIRP Ann. Technol. 45, 65–70.

Arrazola, P.J., Umbrello, D., Davies, M., Jawahir, I.S., 2013. Recent advances in modelling of metal machining processes. CIRP Ann. - Manuf. Technol. 62, 695–718.

Asiltürk, İ., Akkuş, H., 2011. Determining the effect of cutting parameters on surface roughness in hard turning using the Taguchi method. Measurement 44, 1697–1704.

Asiltürk, İ., Neşeli, S., 2012. Multi response optimisation of CNC turning parameters via Taguchi method-based response surface analysis. Measurement 45, 785–794.

Aslan, E., Camuşcu, N., Birgören, B., 2007. Design optimization of cutting parameters when turning hardened AISI 4140 steel (63 HRC) with Al2O3+TiCN mixed ceramic tool. Mater. Des. 28, 1618–1622.

Bartarya, G., Choudhury, S.K., 2014. Influence of machining parameters on forces and surface roughness during finish hard turning of EN 31 steel. Proc. Inst. Mech. Eng. Part B J. Eng. Manuf. 228, 1068–1080.

Benardos, P.G., Vosniakos, G., 2003. Predicting surface roughness in machining : a review. Int. J. Mach. Tools Manuf. 43, 833–844.

Benardos, P.G., Vosniakos, G.C., 2002. Prediction of surface roughness in CNC face milling using neural networks and Taguchi ' s design of experiments. Robot. Comput. Integr. Manuf. 18, 343–354.

Bhardwaj, B., Kumar, R., Singh, P.K., 2014. Surface roughness (Ra) prediction model for turning of AISI 1019 steel using response surface methodology and Box-Cox transformation. Proc. Inst. Mech. Eng. Part B J. Eng. Manuf. 228, 223–232.

Bhattacharya, A., Das, S., Majumder, P., Batish, A., 2009. Estimating the effect of cutting parameters on surface finish and power consumption during high speed machining of AISI 1045 steel using Taguchi design and ANOVA. Prod. Eng. 3, 31–40.

Bhushan, R.K., 2013. Optimization of cutting parameters for minimizing power consumption and maximizing tool life during machining of Al alloy SiC particle composites. J. Clean. Prod. 39, 242–254.

Bil, H., Kiliç, S.E., Tekkaya, a. E., 2004. A comparison of orthogonal cutting data from experiments with three different finite element models. Int. J. Mach. Tools Manuf. 44, 933–944.

Bridgman, P.W., 1952. Studies in large plastic flow and fracture with special emphasis on the effects of hydrostatic pressure. McGraw-Hill.

Cakir, M.C., Ensarioglu, C., Demirayak, I., 2009. Mathematical modeling of surface roughness for evaluating the effects of cutting parameters and coating material. J. Mater. Process. Technol. 209, 102–109.

Campatelli, G., Lorenzini, L., Scippa, A., 2014. Optimization of process parameters using a Response Surface Method for minimizing power consumption in the milling of carbon steel. J. Clean. Prod. 66, 309–316.

Camposeco-Negrete, C., 2013. Optimization of cutting parameters for minimizing energy consumption in turning of AISI 6061 T6 using Taguchi methodology and ANOVA. J. Clean. Prod. 53, 195–203.

Carroll, J.T., Strenkowski, J.S., 1988. Finite element models of orthogonal cutting with application to single point diamond turning. Int. J. Mech. Sci. 30, 899–920.

Ceretti, E., Fallböhmer, P., Wu, W.T., Altan, T., 1996. Application of 2D FEM to chip formation in orthogonal cutting. J. Mater. Process. Technol. 59, 169–180.

Ceretti, E., Lazzaroni, C., Menegardo, L., Altan, T., 2000. Turning simulations using a three-dimensional FEM code. J. Mater. Process. Technol. 98, 99–103.

Cetin, M.H., Ozcelik, B., Kuram, E., Demirbas, E., 2011. Evaluation of vegetable based cutting fluids with extreme pressure and cutting parameters in turning of AISI 304L by Taguchi method. J. Clean. Prod. 19, 2049–2056.

Chandrakanth Shet, X.D., 2000. Finite Element Simulation of the Orthogonal Metal Cutting Process. J. Mater. Process. Technol. 105, 95–109.

Childs, T.H.C., 1980. Elastic effects in metal cutting chip formation. Int. J. Mech. Sci. 22, 457–466.

Childs, T.H.C., Maekawa, K., 1990. Computer-aided simulation and experimental studies of chip flow and tool wear in the turning of low alloy steels by cemented carbide tools. Wear 139, 235–250.

Chinchanikar, S., Choudhury, S.K., 2013. Effect of work material hardness and cutting parameters on performance of coated carbide tool when turning hardened steel: An optimization approach. Measurement 46, 1572–1584.

Chou, Y.K., Evans, C.J., Barash, M.M., 2003. Experimental investigation on cubic boron nitride turning of hardened AISI 52100 steel. J. Mater. Process. Technol. 134, 1–9.

Colding, B.N., 1958. A Three-dimensional, Tool-life Equation: Machining Economics. J. Eng. Ind. 81, 239–250.

Colding, B.N., 1991. A tool-temperature/tool-life relationship covering a wide range of cutting data. CIRP Ann. Technol. 40, 35–40.

Correia A.E., Davim, J.P., 2011. Surface roughness measurement in turning carbon steel AISI 1045 using wiper inserts. Measurement 44, 1000–1005.

Da, Z., 1997. Optimization of finish turning operations based on a hybrid model. Ph.D., Mechanical Engineering. Lexington, KY, University of Kentucky.

Davim, J.P., 2001. A note on the determination of optimal cutting conditions for surface finish obtained in turning using design of experiments. J. Mater. Process. Technol. 116, 3–6.

Davim, J.P., 2003. Design of optimisation of cutting parameters for turning metal matrix composites based on the orthogonal arrays. J. Mater. Process. Technol. 132, 340–344.

Davim, J.P., Gaitonde, V.N., Karnik, S.R., 2008. Investigations into the effect of cutting conditions on surface roughness in turning of free machining steel by ANN models. J. Mater. Process. Technol. 205, 16–23.

Dirikolu, M.H., Childs, T.H.C., 2000. Modelling requirements for computer simulation of metal machining. Turkish J. Eng. Environ. Sci. 24, 81–93.

Emami, M., Sadeghi, M.H., Sarhan, A.A.D., Hasani, F., 2014. Investigating the Minimum Quantity Lubrication in grinding of Al2O3 engineering ceramic. J. Clean. Prod. 66, 632–643.

Ermer, D.S., 1971. Optimization of the constrained machining economics problem by geometric programming. J. Manuf. Sci. Eng. 93, 1067–1072.

Ermer, D.S., Patel, D.C., 1974. Maximization of the production rate with constraints by linear programming and sensitivity analysis, in: Proc. NAMRC. pp. 436–449.

Ernst, H. and Merchant, M.E., 1941. Chip formation, friction and high quality machined surfaces. Surf. Treat. Met. 29, 299–378.

Eskicioglu, H., Nisli, M.S., Kilic, S.E., 1985. An application of geometric programming to single-pass turning operations, in: Twenty-Fifth International Machine Tool Design and Research Conference. pp. 149–157.

Fang, N., Fang, G., 2007. Theoretical and experimental investigations of finish machining with a rounded edge tool. J. Mater. Process. Technol. 191, 331–334.

Feng, C.-X. (Jack), Wang, X.-F. (David), 2003. Surface roughness predictive modeling: neural networks versus regression. IIE Trans. 35, 11–27.

Finnie, I., 1956. A Review of the Metal Cutting Analysis of the Past Hundred Years. Trans. Am. Soc. Mech. Eng. 78, 715–721.

Finnie, I., 1963. Comparison of stress-strain behavior in cutting with that in other materials tests. Int. Res. Prod. Eng. 76–82.

Fratila, D., Caizar, C., 2011. Application of Taguchi method to selection of optimal lubrication and cutting conditions in face milling of AlMg 3. J. Clean. Prod. 19, 640–645.

Fu, T., Zhao, J., Liu, W., 2012. Multi-objective optimization of cutting parameters in high-speed milling based on grey relational analysis coupled with principal component analysis. Front. Mech. Eng. 7, 445–452.

Ghani, J, Choudhury, I, Hassan, H, 2004. Application of Taguchi method in the optimization of end milling parameters. J. Mater. Process. Technol. 145, 84–92.

Gilbert, W.W., 1950. Economics of machining. Mach. theory Pract. 465–485.

Gopalakrishnan, B., Al-Khayyal, F., 1991. Machine parameter selection for turning with constraints: an analytical approach based on geometric programming. Int. J. Prod. Res. 29, 1897–1908.

Guo, Y.B., Liu, C.R., 2002. 3D FEA Modeling of Hard Turning. J. Manuf. Sci. Eng. 124, 189.

Gupta, A.K., 2010. Predictive modelling of turning operations using response surface methodology, artificial neural networks and support vector regression. Int. J. Prod. Res. 48, 763–778.

Gupta, A.K., Chandna, P., Tandon, P., 2011. Tool life optimization in 2.5d milling by coupling regression model and genetic algorithm. Int. J. Eng. Technol. 1, 2–8.

Hanafi, I., Khamlichi, A., Cabrera, F.M., Almansa, E., Jabbouri, A., 2012. Optimization of cutting conditions for sustainable machining of PEEK-CF30 using TiN tools. J. Clean. Prod. 33, 1–9.

Hessainia, Z., Belbah, A., Yallese, M.A., Mabrouki, T., Rigal, J.-F., 2013. On the prediction of surface roughness in the hard turning based on cutting parameters and tool vibrations. Measurement 46, 1671–1681.

Ivester, R.W., Kennedy, M., Davies, M., Stevenson, R., Thiele, J., Furness, R., Athavale, S., 2000. Assessment of Machining Models: Progress Report. Mach. Sci. Technol. 4, 511–538.

Iwata, K., Osakada, K., Terasaka, Y., 1984. Process modeling of orthogonal cutting by the rigid-plastic finite element method. J. Eng. Mater. Technol. 106, 132–138.

Jha, N.K., Hornik, K., 1995. Integrated computer-aided optimal design and finite element analysis of a plain milling cutter. Appl. Math. Model. 19, 343–353.

K.Kadirgama, M.M.Noora, N.M.Zuki.N.M, M.M. Rahmana, M.R.M. Rejaba, R. Dauda, K.A.A.-E.-H., 2008. Optimization of Surface Roughness in End Milling on Mould Aluminium Alloys (AA6061-T6) Using Response Surface Method and Radian Basis Function Network. Jordan J. Mech. Ind. Eng. 2, 209–214.

Kant, G., Sangwan, K.S., 2014. Prediction and optimization of machining parameters for minimizing power consumption and surface roughness in machining. J. Clean. Prod. 83, 151–164.

Kapoor, S.G., DeVor, R.E., Zhu, R., Gajjela, R., Parakkal, G., Smithey, D., 1998. Development of Mechanistic Models for the Prediction of Machining Performance: Model Building Methodology. Mach. Sci. Technol. 2, 213–238.

Karayel, D., 2009. Prediction and control of surface roughness in CNC lathe using artificial neural network. J. Mater. Process. Technol. 209, 3125–3137.

Kardekar, A.D., 2005. Modeling and optimization of machining performance measures in face milling of automotive aluminum alloy A380 under different lubrication/cooling conditions for sustainable manufacturing. Ph.D. Thesis, Mechanical Engineering. Lexington, KY, University of Kentucky.

Kilickap, E., 2010. Optimization of cutting parameters on delamination based on Taguchi method during drilling of GFRP composite. Expert Syst. Appl. 37, 6116–6122.

Kilickap, E., Huseyinoglu, M., Yardimeden, A., 2011. Optimization of drilling parameters on surface roughness in drilling of AISI 1045 using response surface methodology and genetic algorithm. Int. J. Adv. Manuf. Technol. 52, 79–88.

Kim, K.W., Sins, H.-C., 1996. Development of a thermo-viscoplastic cutting model using finite element method. Int. J. Mach. Tools Manuf. 36, 379–397.

Kini, M.V., Chincholkar, A. M., 2010. Effect of machining parameters on surface roughness and material removal rate in finish turning of ±30° glass fibre reinforced polymer pipes. Mater. Des. 31, 3590–3598.

Kivak, T., 2014. Optimization of surface roughness and flank wear using the Taguchi method in milling of Hadfield steel with PVD and CVD coated inserts. Measurement 50, 19–28.

Klamecki, B.E., 1973. Incipient Chip Formation in Metal Cutting - A 3D Finite Element Analysis. Ph.D., Thesis, University of Illinois, Urbana Champaign, USA.

Kobayashi, S., Thomsen, E.G., 1962. Metal-cutting analysis—I: re-evaluation and new method of presentation of theories. J. Manuf. Sci. Eng. 84, 63–70.

Komvopoulos, K., Erpenbeck, S.A., 1991. Finite element modeling of orthogonal metal cutting. J. Manuf. Sci. Eng. 113, 253–267.

Korkut, I., Acır, A., Boy, M., 2011. Application of regression and artificial neural network analysis in modelling of tool–chip interface temperature in machining. Expert Syst. Appl. 38, 11651–11656.

Korkut, I., Donertas, M. A., 2007. The influence of feed rate and cutting speed on the cutting forces, surface roughness and tool-chip contact length during face milling. Mater. Des. 28, 308–312.

Kronenberg, M., 1966. Machining science and application. Pergamon Press, London.

Kudo, H., 1965. Some new slip-line solutions for two-dimensional steady-state machining. Int. J. Mech. Sci. 7, 43–55.

Lalwani, D.I., Mehta, N.K., Jain, P.K., 2008. Experimental investigations of cutting parameters influence on cutting forces and surface roughness in finish hard turning of MDN250 steel. J. Mater. Process. Technol. 206, 167–179.

Lee, E.H., Shaffer, B.W., 1949. The theory of plasticity applied to a problem of machining. Division of Applied Mathematics, Brown.

Lin, Z.C., Lin, S.Y., 1992. A Coupled Finite Element Model of Thermo-Elastic-Plastic Large Deformation for Orthogonal Cutting. J. Eng. Mater. Technol. 114, 218–226.

Lu, H.S., Chang, C.K., Hwang, N.C., Chung, C.T., 2009. Grey relational analysis coupled with principal component analysis for optimization design of the cutting parameters in high-speed end milling. J. Mater. Process. Technol. 209, 3808–3817.

Mahdavinejad, R.A., Saeedy, S., 2011. Investigation of the influential parameters of machining of AISI 304 stainless steel. Sadhana 36, 963–970.

Maiyar, L.M., Ramanujam, R., Venkatesan, K., Jerald, J., 2013. Optimization of machining parameters for end milling of Inconel 718 super alloy using Taguchi based grey relational analysis. Procedia Eng. 64, 1276–1282.

Makadia, A.J., Nanavati, J.I., 2013. Optimisation of machining parameters for turning operations based on response surface methodology. Measurement 46, 1521–1529.

Mandal, N., Doloi, B., Mondal, B., Das, R., 2011. Optimization of flank wear using Zirconia Toughened Alumina (ZTA) cutting tool: Taguchi method and Regression analysis. Measurement 44, 2149–2155.

Merchant, M.E., 1945. Mechanics of the metal cutting process. I. Orthogonal cutting and a type 2 chip. J. Appl. Phys. 16, 267–275.

Merchant, M.E., 1974. Industry research interaction in computer-aided manufacturing, in: Int. Conf. on Prod. Tech., IE Aust., Melbourne. pp. 1–29.

Moshat, S., Datta, S., Bandyopadhyay, A., Pal, P.K., 2010. Optimization of CNC end milling process parameters using PCA-based Taguchi method. Int. J. Eng. Sci. Technol. 2, 92–102.

Mukherjee, I., Ray, P.K., 2006. A review of optimization techniques in metal cutting processes. Comput. Ind. Eng. 50, 15–34.

Munoz-Escalona, P., Maropoulos, P., 2010. Integrated optimisation of surface roughness and tool performance when face milling 416 SS. Int. J. Comput. Integr. Manuf. 3, 37–41.

Muraka, P.D., Barrow, G., Hinduja, S., 1979. Influence of the process variables on the temperature distribution in orthogonal machining using the finite element method. Int. J. Mech. Sci. 21, 445–456.

Nalbant, M., Gökkaya, H., Sur, G., 2007. Application of Taguchi method in the optimization of cutting parameters for surface roughness in turning. Mater. Des. 28, 1379–1385.

Neşeli, S., Yaldız, S., Türkeş, E., 2011. Optimization of tool geometry parameters for turning operations based on the response surface methodology. Measurement 44, 580–587.

Ng, E.-G., Aspinwall, D.K., Brazil, D., Monaghan, J., 1999. Modelling of temperature and forces when orthogonally machining hardened steel. Int. J. Mach. Tools Manuf. 39, 885–903.

Noordin, M.., Venkatesh, V.., Sharif, S., Elting, S., Abdullah, a, 2004. Application of response surface methodology in describing the performance of coated carbide tools when turning AISI 1045 steel. J. Mater. Process. Technol. 145, 46–58.

Ohbuchi, Y., Obikawa, T., 2003. Finite Element Modeling of Chip Formation in the Domain of Negative Rake Angle Cutting. J. Eng. Mater. Technol. 125, 324.

Oktem, H., Erzurumlu, T., Erzincanli, F., 2006. Prediction of minimum surface roughness in end milling mold parts using neural network and genetic algorithm. Mater. Des. 27, 735–744.

Öktem, H., Erzurumlu, T., Kurtaran, H., 2005. Application of response surface methodology in the optimization of cutting conditions for surface roughness. J. Mater. Process. Technol. 170, 11–16.

Oxley, P.L.B., Young, H.T., 1989. The mechanics of machining: an analytical approach to assessing machinability, Ellis Horwood Publisher.

Ozcelik, B., Bayramoglu, M., 2006. The statistical modeling of surface roughness in high-speed flat end milling. Int. J. Mach. Tools Manuf. 46, 1395–1402.

Özel, T., Altan, T., 2000. Determination of workpiece flow stress and friction at the chip-tool contact for high-speed cutting. Int. J. Mach. Tools Manuf. 40, 133–152.

Özel, T., Karpat, Y., 2005. Predictive modeling of surface roughness and tool wear in hard turning using regression and neural networks. Int. J. Mach. Tools Manuf. 45, 467–479.

Palanikumar, K., 2007. Modeling and analysis for surface roughness in machining glass fibre reinforced plastics using response surface methodology. Mater. Des. 28, 2611–2618.

Palanisamy, P., Rajendran, I., Shanmugasundaram, S., 2007. Optimization of machining parameters using genetic algorithm and experimental validation for end-milling operations. Int. J. Adv. Manuf. Technol. 32, 644–655.

Pontes, F.J., Paiva, A.P. De, Balestrassi, P.P., Ferreira, J.R., Silva, M.B. Da, 2012. Optimization of Radial Basis Function neural network employed for prediction of surface roughness in hard turning process using Taguchi's orthogonal arrays. Expert Syst. Appl. 39, 7776–7787.

Pratyusha, J., Ashok, U., Laxminarayana, P., 2013. Optimization of Process Parameters for Milling Using Taguchi Methods. Int. J. Adv. Trends Comput. Sci. Eng. 2, 129–135.

Rao, R., 2011. Advanced Modeling and Optimization of Manufacturing Processes, Media. Springer Verlag, Heidelberg New York.

Rawangwong, S., Chatthong, J., Boonchouytan, W., Burapa, R., 2013. An Investigation of Optimum Cutting Conditions in Face Milling Aluminum Semi Solid 2024 Using Carbide Tool. Energy Procedia 34, 854–862.

Reddy, N.S.. ., Rao, P.V.R., 2005. a Genetic Algorithmic Approach for Optimization of Surface Roughness Prediction Model in Dry Milling. Mach. Sci. Technol. 9, 63–84.

Rubenstein, C., 1976. An Analysis of Tool Life Based on Flank-Face Wear—Part 1: Theory. J. Manuf. Sci. Eng. 98, 221–226.

S. Markos, Zs. J. Viharos, L.M., 1998. Quality-oriented, comprehensive modelling of machining processes, in: Sixth ISMQC IMEKO Symposium on Metrology for Quality Control in Production. pp. 67–74.

Sahin, Y., Motorcu, A.R., 2005. Surface roughness model for machining mild steel with coated carbide tool. Mater. Des. 26, 321–326.

Sarıkaya, M., Güllü, A., 2014. Taguchi design and response surface methodology based analysis of machining parameters in CNC turning under MQL. J. Clean. Prod. 65, 604–616.

Shih, A.J., Yang, H.T.Y., 1993. Experimental and finite element predictions of residual stresses due to orthogonal metal cutting. Int. J. Numer. Methods Eng. 36, 1487–1507.

Shirakashi, T., Usui, E., 1974. Simulation analysis of orthogonal metal cutting mechanism, in: Proceedings of the First International Conference on Production Engineering, Part I. pp. 535–540.

Singh, D., Rao, P.V., 2007. A surface roughness prediction model for hard turning process. Int. J. Adv. Manuf. Technol. 32, 1115–1124.

Stevenson, M.G., Wright, P.K., Chow, J.G., 1983. Further developments in applying the finite element method to the calculation of temperature distributions in machining and comparisons with experiment. J. Manuf. Sci. Eng. 105, 149–154.

Subramanian, M., Sakthivel, M., Sooryaprakash, K., Sudhakaran, R., 2013. Optimization of cutting parameters for cutting force in shoulder milling of Al7075-T6 using response surface methodology and genetic algorithm. Procedia Eng. 64, 690–700.

Sun, J., Guo, Y.B., 2009. A comprehensive experimental study on surface integrity by end milling Ti-6Al-4V. J. Mater. Process. Technol. 209, 4036–4042.

Suresh, P.V.S., Venkateswara Rao, P., Deshmukh, S.G., 2002. A genetic algorithmic approach for optimization of surface roughness prediction model. Int. J. Mach. Tools Manuf. 42, 675–680.

Szecsi, T., 1999. Cutting force modeling using artificial neural networks 93, 344–349.

Tay, A.O., Stevenson, M.G., Davis, G.D.V., 1974. Using the finite element method to determine temperature distributions in orthogonal machining. Proc. Inst. Mech. Eng. 188, 627–638.

Tay, A.O., Stevenson, M.G., de Vahl Davis, G., Oxley, P.L.B., 1976. A numerical method for calculating temperature distributions in machining, from force and shear angle measurements. Int. J. Mach. Tool Des. Res. 16, 335–349.

Taylor F.W, 1907. On the art of cutting metals. Trans. ASME 28, 31–350.

Trent, E.M., Wright, P.K., 2000. Metal cutting. Butterworth-Heinemann.

Tsao, C.C., Hocheng, H., 2008. Evaluation of thrust force and surface roughness in drilling composite material using Taguchi analysis and neural network. J. Mater. Process. Technol. 203, 342–348.

Tzeng, C.-J., Lin, Y.-H., Yang, Y.-K., Jeng, M.-C., 2009. Optimization of turning operations with multiple performance characteristics using the Taguchi method and Grey relational analysis. J. Mater. Process. Technol. 209, 2753–2759.

Ulutan, D., 2013. Predictive modeling and multi-objective optimization of machining-induced residual stresses: Investigation of machining parameter effects. New Brunswick, New Jersey, The State University of New Jersey.

Usui, E., Maekawa, K., Shirakashi, T., 1981. Simulation Analysis of Built-Up Edge Formation in Machining of Low Carbon Steel. BULL. JAPAN SOC. Precis. ENG. 15, 237–242.

Vakondios, D., Kyratsis, P., Yaldiz, S., Antoniadis, A., 2012. Influence of milling strategy on the surface roughness in ball end milling of the aluminum alloy Al7075-T6. Measurement 45, 1480–1488.

Van Luttervelt, C.A., Childs, T.H.C., Jawahir, I.S., Klocke, F., Venuvinod, P.K., Altintas, Y., Armarego, E., Dornfeld, D., Grabec, I., Leopold, J., Lindstrom, B., Lucca, D., Obikawa, T., Sato, H., 1998. Present Situation and Future Trends in Modelling of Machining Operations Progress Report of the CIRP Working Group "Modelling of Machining Operations." CIRP Ann. - Manuf. Technol. 47, 587–626.

Vijay, S., Krishnaraj, V., 2013. Machining Parameters Optimization in End Milling of Ti-6Al-4V. Procedia Eng. 64, 1079–1088.

Wang, M., Xu, B., Dong, S., Zhang, J., Wei, S., 2013. Experimental investigations of cutting parameters influence on cutting forces in turning of Fe-based amorphous overlay for remanufacture. Int. J. Adv. Manuf. Technol. 65, 735–743.

Wang, M.-Y., Chang, H.-Y., 2004. The optimum of tool geometry on surface roughness in end milling AL2014-T6. J. Stat. Manag. Syst. 7, 283–294.

Wang, T., Xie, L.J., Wang, X.B., Jiao, L., Shen, J.W., Xu, H., Nie, F.M., 2013. Surface integrity of high speed milling of Al/SiC/65p aluminum matrix composites. Procedia CIRP 8, 475–480.

Wang, X., Feng, C.X., 2002. Development of empirical models for surface roughness prediction in finish turning. Int. J. Adv. Manuf. Technol. 20, 348–356.

Wen, X.M., Tay, A.A.O., Nee, A.Y.C., 1992. Micro-computer-based optimization of the surface grinding process. J. Mater. Process. Technol. 29, 75–90.

Wu, J.-S., Dillon, O.W., Lu, W.-Y., 1996. Thermo-viscoplastic modeling of machining process using a mixed finite element method. J. Manuf. Sci. Eng. 118, 470–482.

Xiao, G., Malkin, S., Danai, K., 1992. Intelligent control of cylindrical plunge grinding, in: American Control Conference, 1992. IEEE, pp. 391–399.

Yalcin, U., Karaoglan, A.D., Korkut, I., 2013. Optimization of Cutting Parameters in Face Milling with Neural Networks and Taguchi based on Cutting Force, Surface Roughness and Temperatures. Int. J. Prod. Res. 51, 3404–3414.

Yan, J., Li, L., 2013. Multi-objective optimization of milling parameters e the trade-offs between energy , production rate and cutting quality. J. Clean. Prod. 52, 462–471.

Yang, Y.K., Chuang, M.T., Lin, S.S., 2009. Optimization of dry machining parameters for high-purity graphite in end milling process via design of experiments methods. J. Mater. Process. Technol. 209, 4395–4400.

Yigit, K., 2007. Predictive modeling and optimization of hard turning_Investigations of effects on cutting tool micro geometry.

Zain, A.M., Haron, H., Sharif, S., 2010a. Prediction of surface roughness in the end milling machining using Artificial Neural Network. Expert Syst. Appl. 37, 1755–1768.

Zain, A.M., Haron, H., Sharif, S., 2010b. Application of GA to optimize cutting conditions for minimizing surface roughness in end milling machining process. Expert Syst. Appl. 37, 4650–4659.

Zain, A.M., Haron, H., Sharif, S., 2012. Integrated ANN – GA for estimating the minimum value for machining performance. Int. J. Prod. Res. 50, 191–213.

Zhang, J.Z., Chen, J.C., Kirby, E.D., 2007. Surface roughness optimization in an end-milling operation using the Taguchi design method. J. Mater. Process. Technol. 184, 233–239.

Chapter 3

Experimental Setup and Plan

This chapter provides the details regarding the experimental setup and the plan to obtain the two performance characteristics – power consumption and surface roughness – for the research.

3.1 Introduction

Predictive modelling and optimization require selection of appropriate sets of machining parameters of the process. This can mainly be achieved by understanding the interrelationship among the large number of parameters affecting the process and identifying the optimal machining conditions. Experiments are performed on a given machine tool in order to understand the effect of different process parameters on performance characteristics *i.e.* surface roughness and power consumption.

3.2 Material

The sample material for the research is AISI 1045 steel. There is a renewed interest in the application of this steel because of its sustainability. It is 100% recyclable and almost has indefinite life cycle. AISI 1045 steel is one of the steel grades widely used in different industries (construction, transport, automotive, power, *etc*.). Some of the commonly used components of 1045 steel are gears, shafts, axles, bolts, studs, connecting rods, spindles, rams, hydraulic pumps, *etc*. The chemical composition and mechanical properties of the AISI 1045 steel are given in Table 3.1 and Table 3.2 respectively.

Twenty seven experiments were performed according to the experimental design discussed in section 3.6. The nine workpieces were machined from solid cylindrical bar

to a final dimension of 250 mm length and 47 mm diameter as shown in Figure 3.1. The total length to be machined during each reading is 50 mm. 30 mm length on each side is provided for clamping the workpieces into three jaw chuck. Each piece was used to perform three experiments. Therefore, 10 mm steps were provided on the workpiece as shown in the figure. A pre-cut of 1.5 mm depth was performed on each workpiece prior to actual turning using a different cutting tool. This was done in order to remove the rust or hardened top layer from the surface and to minimize any effect of non-homogeneity on the experimental results.

Table 3.1: Chemical composition of AISI 1045 steel in percentage weight

Material	C%	Mn%	P%	S%	Si%
AISI 1045 Steel	0.43	0.7	0.04	0.05	0.16

Table 3.2: Mechanical properties of AISI 1045 steel

Material	Density (kg/m^3)	Elastic modulus (GPa)	Yield strength (MPa)	Tensile strength (MPa)	Hardness (HB)	Elongation (%)	Poison ratio
AISI 1045 Steel	7.8	205	505	585	170	12	0.28

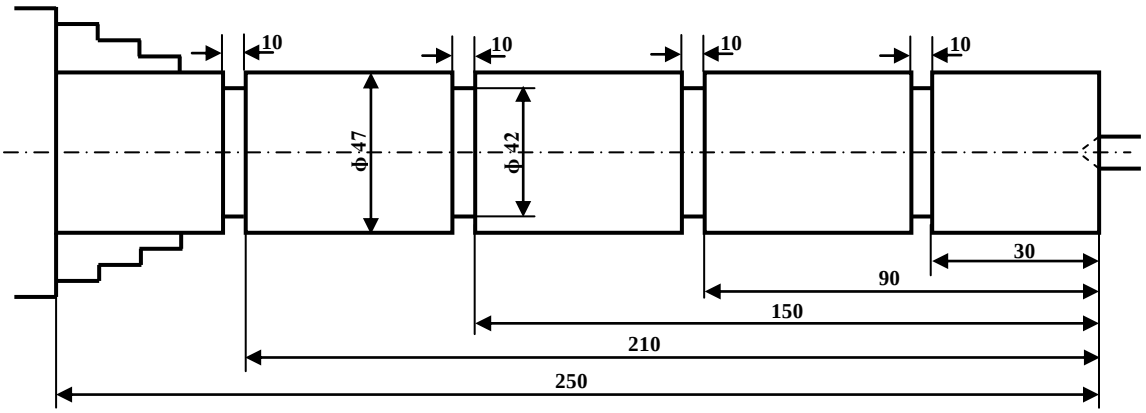

Figure 3.1: Detailed drawing of the cylindrical bar used in experimentation

(All dimensions are in mm)

3.3 Cutting Tool Inserts and Holder

Uncoated tungsten carbide tools were used for the experiments. The cutting tool used is proper for machining of AISI 1045 steel with ISO P25 quality. Sandvik inserts with the ISO TNMG 16 04 12 designation were mounted on the tool holder designated by ISO as PTGNR 2020 K16 having rake angle of 7^0, clearance angle of 6^0 and 0.4 mm nose radius. An insert mounted on the tool holder is shown in Figure 3.2.

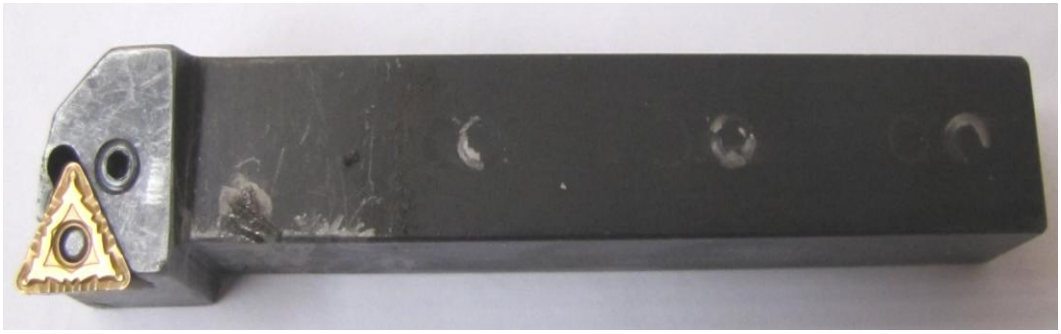

Figure 3.2: Insert mounted on the tool holder

3.4 Machine Tool

The turning experiments were carried out in dry cutting conditions using an HMT centre lathe. It has a maximum spindle speed of 2300 rpm and spindle power of 5.5 kW. Workpiece was held between chuck and tailstock; and the tool overhang was kept 20 mm to increase rigidity of the machining system as shown in Figure 3.3.

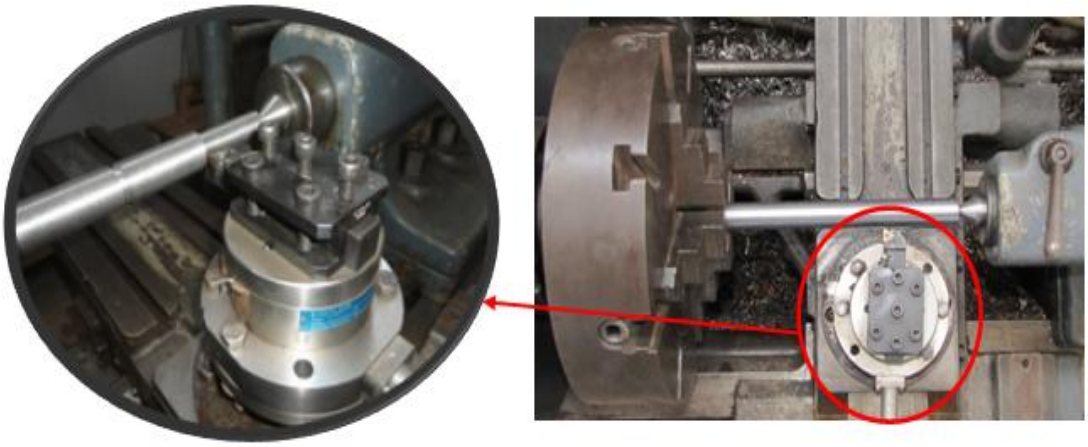

Figure 3.3: Tool overhung and workpiece clamped between chuck and tailstock

The experiments were conducted by turning the workpiece with feed direction towards the chuck of the lathe (referred to as "left feed direction") as is often the case during conventional turning. As the workpiece was comparatively long, workpiece was held in the tailstock during all experiments as shown in Figure 3.3.

3.5 Selection of Machining Parameters and their Levels

The choice of machining parameters was made by taking into account the capacity/limiting cutting conditions of the lathe, tool manufacturer's catalogue and the values taken by researchers in the literature. Cutting speed (v), feed rate (f) and depth of cut (d) are the input parameters chosen for the research. The performance characteristics chosen to investigate the effect of machining parameters were surface roughness (R_a) and power consumption (P). Table 3.3 shows the three machining parameters and the three levels for each parameter.

Table 3.3: Machining parameters and their levels

Factor	Symbol	Level 1	Level 2	Level 3
Cutting speed (m/min)	v	103.31	134.30	174.14
Feed rate (mm/rev.)	f	0.12	0.16	0.2
Depth of cut (mm)	d	0.5	1.0	1.5

3.6 Experimental Design

In any experimental investigation, the results depend to a large extent on the data collection methodology. The most preferred method of experimentation utilized by researchers is a full factorial set of experiments, where experiments are carried out for all combinations of variables. A full factorial design of experiments (DOE) measures the response of every possible combination of factors and factor levels. These responses are

analyzed to provide information about every main effect and every interaction effect. The experimental design for three turning parameters (*v, f, d*) with three levels (3^3) are organized by the Taguchi's L_{27} orthogonal array as shown in Table 3.4. L_{27} is the most suitable array which has 27 runs and 26 degrees of freedoms (DOF) which are more than the required 18 DOFs. As per Taguchi's experimental design method, the total DoFs of selected orthogonal array must be greater than or equal to the total DoFs required for the experiment and hence L_{27} orthogonal array has been selected as per Taguchi (1990). The columns chosen for the main factors are 1, 2, and 5 (Table 3.4). The first column of the table is assigned to the cutting speed (*v*), the second to the feed rate (*f*) and fifth to the depth of cut (*d*).

Table 3.4: An L_{27} Orthogonal array

Experiment No.	Column Number												
	1	**2**	**3**	**4**	**5**	**6**	**7**	**8**	**9**	**10**	**11**	**12**	**13**
1	1	1	1	1	1	1	1	1	1	1	1	1	1
2	1	1	1	1	2	2	2	2	2	2	2	2	2
3	1	1	1	1	3	3	3	3	3	3	3	3	3
4	1	2	2	2	1	1	1	2	2	2	3	3	3
5	1	2	2	2	2	2	2	3	3	3	1	1	1
6	1	2	2	2	3	3	3	1	1	1	2	2	2
7	1	3	3	3	1	1	1	3	3	3	2	2	2
8	1	3	3	3	2	2	2	1	1	1	3	3	3
9	1	3	3	3	3	3	3	2	2	2	1	1	1
10	2	1	2	3	1	2	3	1	2	3	1	2	3
11	2	1	2	3	2	3	1	2	3	1	2	3	1
12	2	1	2	3	3	1	2	3	1	2	3	1	2
13	2	2	3	1	1	2	3	2	3	1	3	1	2
14	2	2	3	1	2	3	1	3	1	2	1	2	3
15	2	2	3	1	3	1	2	1	2	3	2	3	1
16	2	3	1	2	1	2	3	3	1	2	2	3	1
17	2	3	1	2	2	3	1	1	2	3	3	1	2

Experiment No.	Column Number												
	1	**2**	**3**	**4**	**5**	**6**	**7**	**8**	**9**	**10**	**11**	**12**	**13**
18	2	3	1	2	3	1	2	2	3	1	1	2	3
19	3	1	3	2	1	3	2	1	3	2	1	3	2
20	3	1	3	2	2	1	3	2	1	3	2	1	3
21	3	1	3	2	3	2	1	3	2	1	3	2	1
22	3	2	1	3	1	3	2	2	1	3	3	2	1
23	3	2	1	3	2	1	3	3	2	1	1	3	2
24	3	2	1	3	3	2	1	1	3	2	2	1	3
25	3	3	2	1	1	3	2	3	2	1	2	1	3
26	3	3	2	1	2	1	3	1	3	2	3	2	1
27	3	3	2	1	3	2	1	2	1	3	1	3	2

3.7 Power Consumption Measurement

The power consumption has been measured through the indirect method by measuring the cutting forces. In literature there are two methods – direct method using wattmeter or power sensor (e.g. Aggarwal et al., 2008; Balogun and Mativenga, 2013; Campatelli et al., 2014; Yan and Li, 2013) and indirect method using dynamometer (e.g. Abhang and Hameedullah, 2010; Hanafi et al., 2012; He et al., 2011; Kuram et al., 2013). Both methods have their own advantages and limitations. The direct method measures exactly the power required by the machine tool "system" including auxiliary power. This research aims at developing a relationship between cutting parameters and process performance (power and surface roughness during cutting). The auxiliary power measurement does not add any value. An indirect method of power measurement by measuring the cutting forces was used to measure the power consumed during the experimentation. The schematic to measure the forces is shown in Figure 3.4. Kistler 9272 dynamometer, shown in Figure 3.5, is used to capture the force signals during the cutting process in X, Y and Z directions (feed force, thrust force and cutting force). The

dynamometer consists of three-component force sensors fitted under high preload between a base plate and a top plate. Each sensor contains three pairs of quartz plates, one sensitive to pressure in the Z direction and the other two responding to shear in the X and Y directions.

The specifications of the dynamometer are illustrated in Table 3.5. The calibration of dynamometer is done by applying known weights and collecting the measured data. The load is varied from 0 to 1500 N in the Z direction. The calibration was done for both loading and unloading conditions, so that any hysteresis in the measurement can be observed. No hysteresis was observed for the cutting force calibration. The cutting tool was mounted on the top of the dynamometer. Further, the dynamometer was connected to a multichannel charge amplifier (Type 5070A) as shown in Figure 3.6 by a highly insulated connection cable and a desktop personal computer. The amplifier amplifies the electrical charges delivered from the dynamometer and converts them into proportional forces using data acquisition system and then these forces are processed using Dynoware software. The cutting force is obtained based on the average of steady state region values of cutting operation as shown in Figure 3.7. The data collected from an unsteady state can result in inaccurate values, which can affect the analysis. Out of the three force components, cutting force is used to calculate the power required to perform the machining operation. Power is the product of cutting force and cutting speed and is a better criterion for design and selection of any machine tools. The machining parameters and the corresponding measured cutting force and calculated power values are given in Table 3.6.

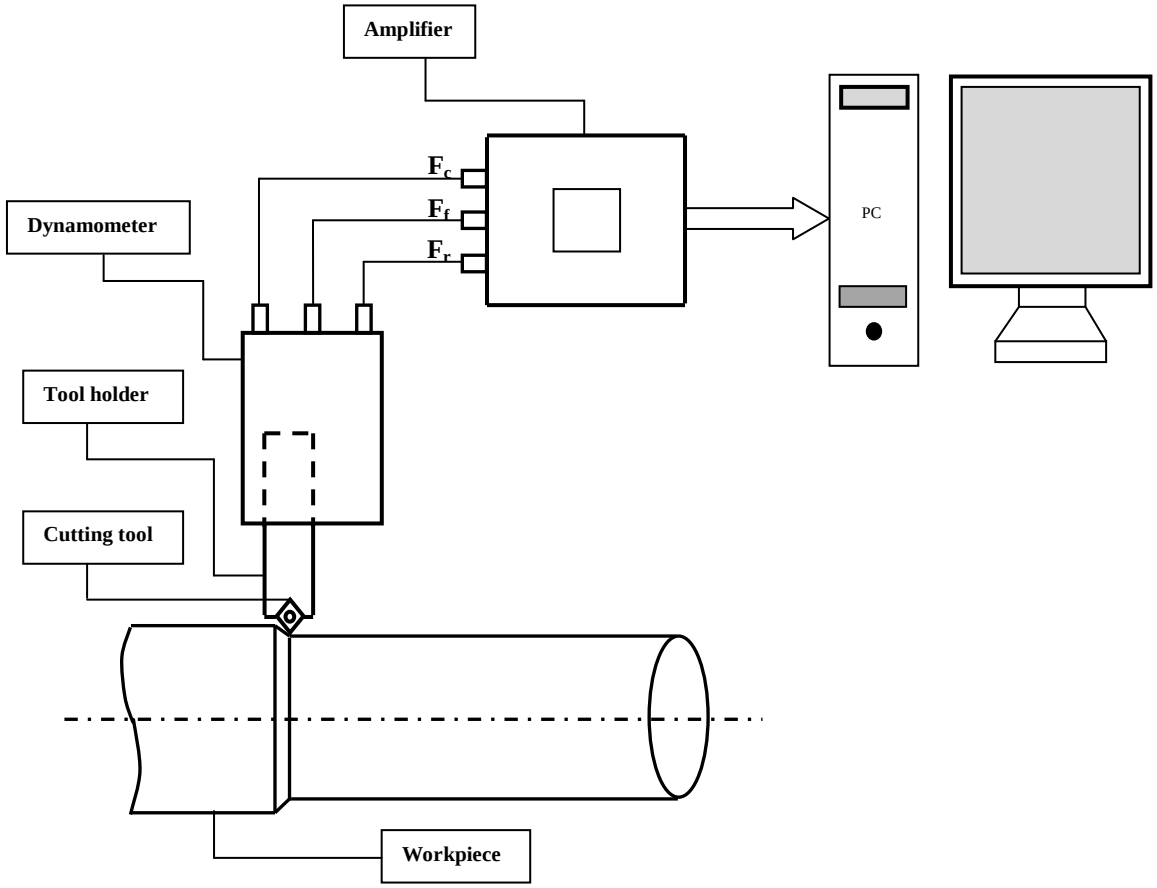

Figure 3.4: Schematic of experimental procedure to measure the forces

Figure 3.5: Kistler 9272 dynamometer

Table 3.5: Kistler 9272 dynamometer specifications

Factor		Value
Measuring range	Fx, Fy	-5 … 5 kN
	Fz	-5 … 20 kN
Calibrated measuring range	Fx, Fy	0 … 5 kN
	Fz	0… 20 kN
Overload	Fx, Fy	-6 … 6 kN
	Fz	-6 … 24 kN
Threshold	Fx, Fy	< 0.01 N
	Fz	< 0.02 N
Sensitivity	Fx, Fy	≈ -7.8 pC/N
	Fz	≈ -3.5pC/N
Linearity	All range	≤ ± 1
Hysteresis	All range	≤ 1

Figure 3.6: 5070A multi-channel amplifier connected to computer to process the force data

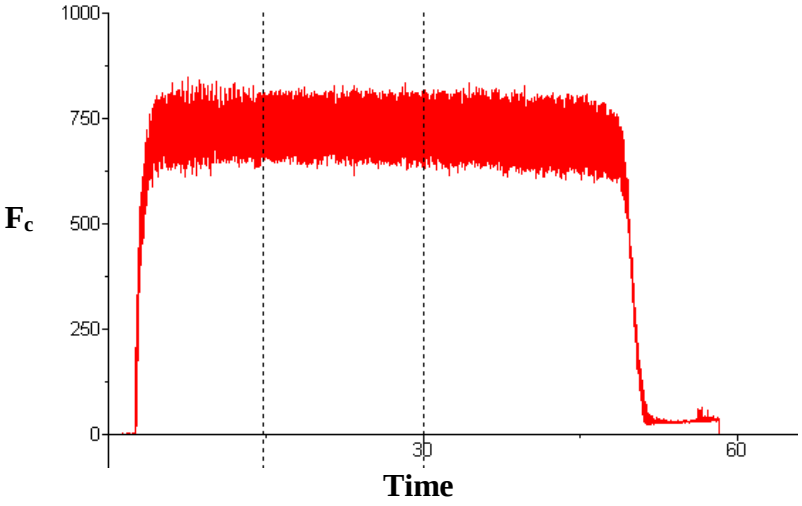

Figure 3.7: Cutting force steady state region

Table 3.6: Power consumption at L_{27} full factorial machining parameters

Experiment No.	*v* (m/min.)	*f* (mm/rev.)	*d* (mm)	F_c (N)	*P* (kW)
1	103.31	0.12	0.50	288.70	0.497
2	103.31	0.12	1.00	397.00	0.684
3	103.31	0.12	1.50	592.90	1.021
4	103.31	0.16	0.50	315.10	0.543
5	103.31	0.16	1.00	588.20	1.013
6	103.31	0.16	1.50	737.20	1.269
7	103.31	0.20	0.50	345.70	0.586
8	103.31	0.20	1.00	568.90	0.980
9	103.31	0.20	1.50	878.10	1.512
10	134.30	0.12	0.50	295.00	0.574
11	134.30	0.12	1.00	368.30	0.824
12	134.30	0.12	1.50	574.10	1.285
13	134.30	0.16	0.50	269.70	0.604
14	134.30	0.16	1.00	498.00	1.115
15	134.30	0.16	1.50	691.00	1.547
16	134.30	0.20	0.50	322.00	0.721
17	134.30	0.20	1.00	584.70	1.309
18	134.30	0.20	1.50	801.70	1.794
19	174.14	0.12	0.50	237.90	0.690
20	174.14	0.12	1.00	338.30	0.982
21	174.14	0.12	1.50	561.90	1.631
22	174.14	0.16	0.50	280.70	0.815
23	174.14	0.16	1.00	404.20	1.173
24	174.14	0.16	1.50	689.90	2.002
25	174.14	0.20	0.50	304.40	0.883
26	174.14	0.20	1.00	650.60	1.888
27	174.14	0.20	1.50	837.20	2.430

3.8 Surface Roughness Measurement

The workpiece shown in Figure 3.1 was cut into three parts each having an equal length of 50 mm for measuring the surface roughness. The final workpiece used for measuring the surface roughness is shown in Figure 3.8.

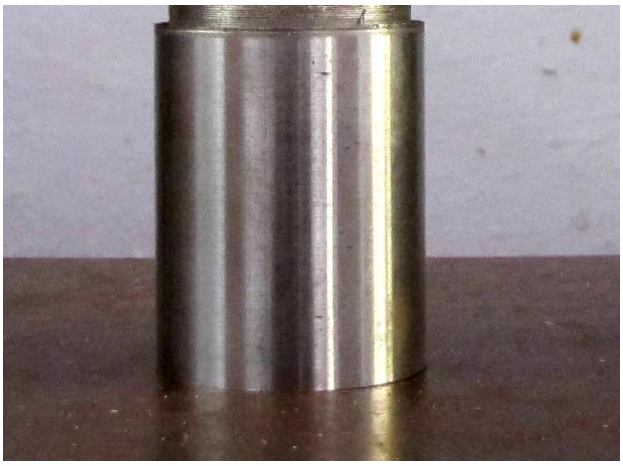

Figure 3.8: Workpiece used for measuring the surface roughness

The surface roughness of the finished surface is measured by placing the workpiece on a V-block over a cast iron surface plate after each cut (Figure 3.9). After the setup was ready, trial cuts were taken and equipment was calibrated to ensure that the part quality adhered to the quality requirements of the Original Equipment Manufacturer (OEM), and to compare the stability of the machining process to that of the OEM's. The equipment was calibrated by measuring the known diameter (12.4867 mm) of a high precision spherical ball. Figure 3.10 shows the surface roughness profile, measured on spherical ball which shows that the form error (P_t) is considerably less than the OEM specified upper limit of 0.25 μm. This confirms the stability of the experimental setup compared to the OEM's recommended specification. Once the stability of the setup was confirmed the experiments were conducted and the surface roughness was measured at three equally spaced locations around the circumference of the workpiece to obtain the statistically significant data for test and then the mean

of measurements was calculated. Thus, probable observation errors were kept relatively small. The specifications of the measuring setup are presented in the Table 3.7.

Table 3.7: Specifications of the surface roughness measurement instrument

Factor	**Specification**
Make	Taylor Hobson
Model	Form Talysurf Intra
Speed of traverse	1 mm/sec – 10 mm/sec
Nominal measuring range	1 mm
Resolution	16 nm
Pickup	Inductive type
Parameters measurable	$R_a/R_z/R_t$

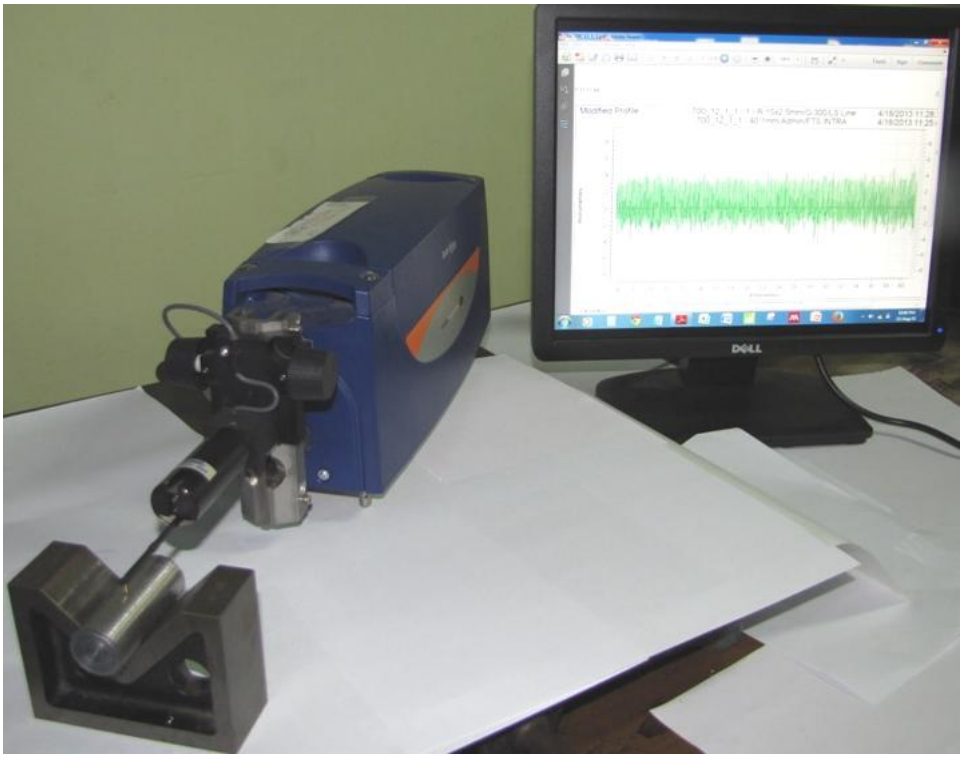

Figure 3.9: Taylor and Hobson profilometer used to measure surface roughness

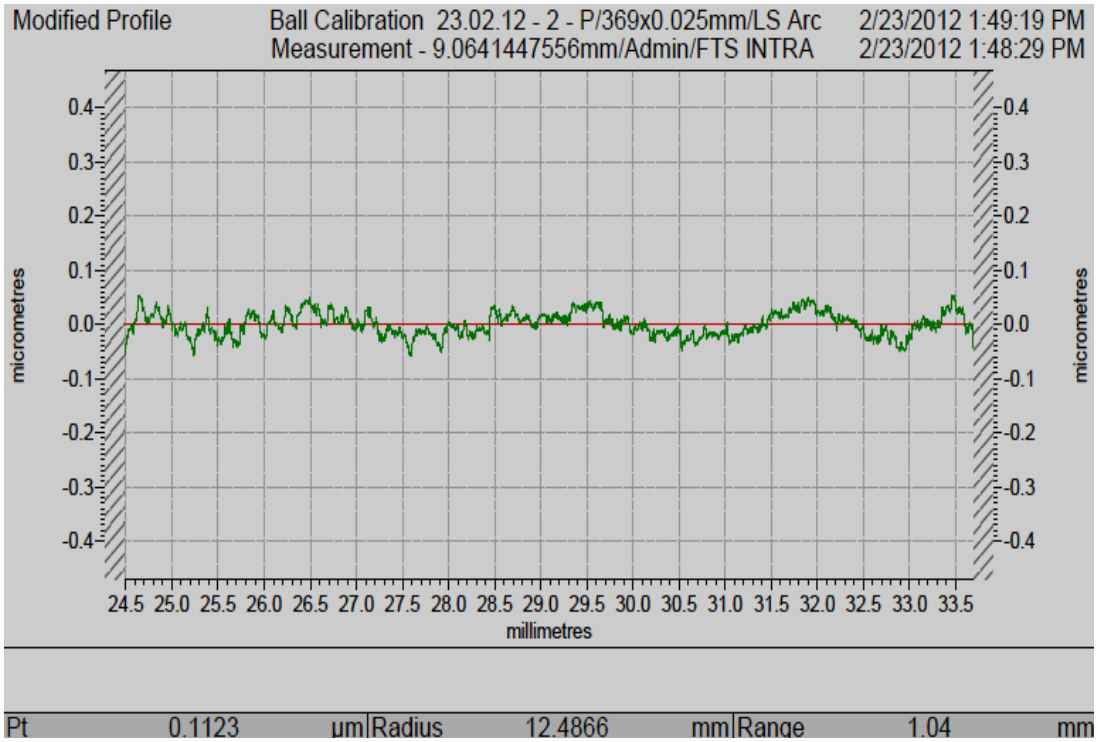

Figure 3.10: Surface roughness profile for the calibrated high precision spherical ball

There are many different surface roughness parameters, which include average variation from mean line (R_a), the highest peak to the deepest valley (R_t) and the average R_t over a given length (R_z). R_a is universally recognized and the most widely used parameter for roughness as it can be easily measured by graphical processes (Correia and Davim, 2011). Besides, R_a values are more accurate than the R_t and R_z values because it considers the averages of peaks and valleys on the surface. Hence, R_a was selected as measuring parameter for surface roughness. The observations of the surface roughness are illustrated in Figure 3.11. The machining parameters and the corresponding measured surface roughness (R_a) are given in Table 3.8.

After finalizing the experimental setup and developing the experimental procedure, the next step is to develop a predictive and optimization model based on the collected experimental data. The following chapters provide the development of predictive and optimization models using the collected experimental data of this chapter.

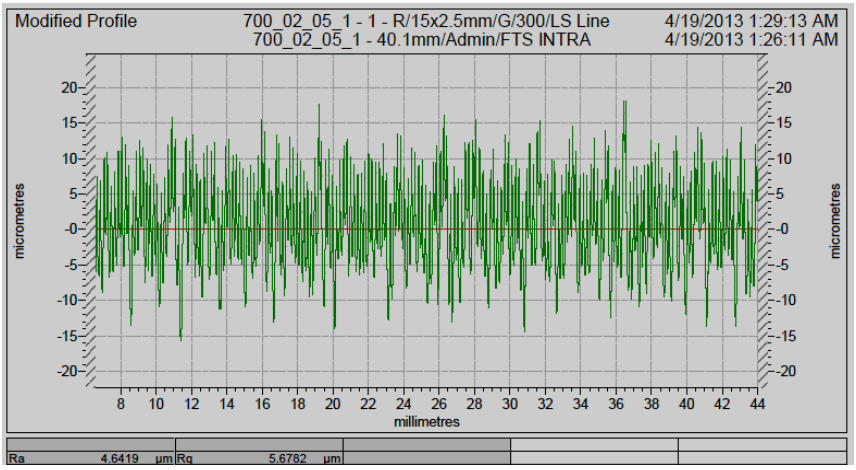

(a)

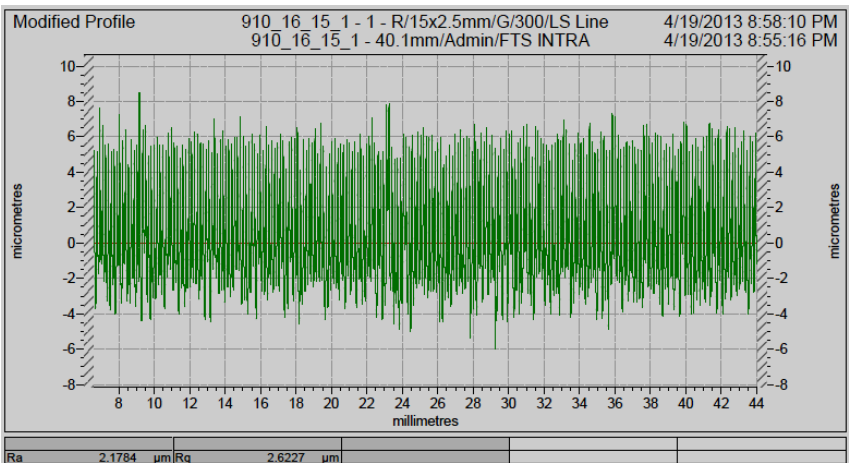

(b)

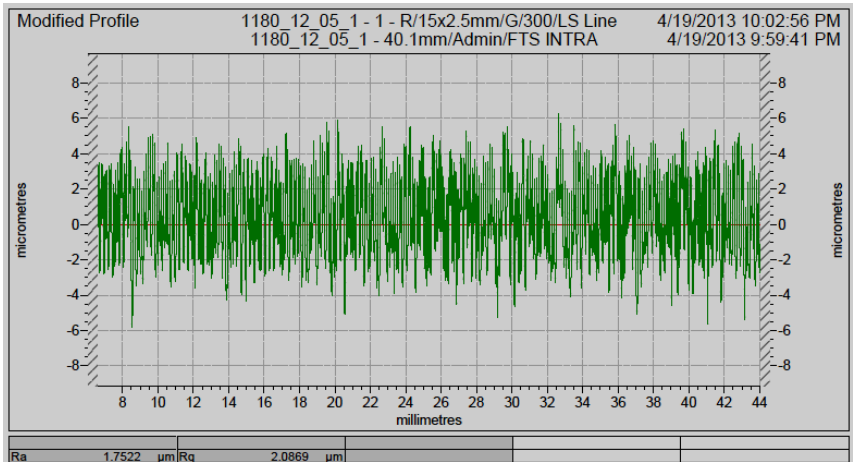

(c)

Figure 3.11: Typical surface roughness observed at different cutting conditions: (a) cutting speed = 103.31 m/min, feed rate = 0.20 mm/rev., depth of cut = 0.5 mm, (b) cutting speed = 134.30 m/min, feed rate = 0.16 mm/rev., depth of cut = 1.5 mm, (c) cutting speed = 174.14 m/min, feed rate = 0.12 mm/rev., depth of cut = 0.5 mm

Table 3.8: Measured surface roughness at L_{27} full factorial machining parameters

Experiment No.	*v* (m/min)	*f* (mm/rev)	*d* (mm)	R_a (µm)			
				Run 1	Run 2	Run 3	Average
1	103.31	0.12	0.50	1.863	2.046	1.811	1.907
2	103.31	0.12	1.00	1.489	1.526	1.481	1.499
3	103.31	0.12	1.50	1.716	1.704	1.908	1.776
4	103.31	0.16	0.50	3.201	4.446	0.403	2.684
5	103.31	0.16	1.00	2.389	2.636	3.680	2.902
6	103.31	0.16	1.50	2.747	2.769	2.792	2.769
7	103.31	0.20	0.50	4.642	3.827	2.587	3.685
8	103.31	0.20	1.00	3.869	4.200	4.486	4.185
9	103.31	0.20	1.50	4.142	3.983	3.822	3.983
10	134.30	0.12	0.50	1.327	1.338	1.186	1.284
11	134.30	0.12	1.00	1.277	1.282	1.212	1.257
12	134.30	0.12	1.50	1.539	1.528	1.485	1.517
13	134.30	0.16	0.50	2.585	2.915	2.043	2.514
14	134.30	0.16	1.00	2.534	2.419	3.698	2.884
15	134.30	0.16	1.50	2.178	2.177	2.225	2.194
16	134.30	0.20	0.50	3.653	3.683	3.726	3.687
17	134.30	0.20	1.00	3.329	3.317	3.307	3.318
18	134.30	0.20	1.50	3.433	3.442	3.467	3.447
19	174.14	0.12	0.50	1.752	1.386	1.910	1.683
20	174.14	0.12	1.00	1.487	1.434	1.528	1.483
21	174.14	0.12	1.50	1.586	1.579	1.530	1.565
22	174.14	0.16	0.50	2.070	2.061	2.077	2.069
23	174.14	0.16	1.00	2.225	2.239	2.234	2.232
24	174.14	0.16	1.50	3.316	3.350	3.293	3.320
25	174.14	0.20	0.50	3.449	3.432	3.410	3.430
26	174.14	0.20	1.00	3.399	3.391	3.352	3.381
27	174.14	0.20	1.50	3.547	3.512	3.662	3.574

References

Abhang, L.B., Hameedullah, M., 2010. Power Prediction Model for Turning EN-31 Steel Using Response Surface Methodology. J. Eng. Sci. Technol. Rev. 3, 116–122.

Aggarwal, A., Singh, H., Kumar, P., Singh, M., 2008. Optimization of multiple quality characteristics for CNC turning under cryogenic cutting environment using desirability function. J. Mater. Process. Technol. 205, 42–50.

Balogun, V.A., Mativenga, P.T., 2013. Modelling of direct energy requirements in mechanical machining processes. J. Clean. Prod. 41, 179–186.

Campatelli, G., Lorenzini, L., Scippa, A., 2014. Optimization of process parameters using a Response Surface Method for minimizing power consumption in the milling of carbon steel. J. Clean. Prod. 66, 309–316.

Correia A.E., Davim, J.P., 2011. Surface roughness measurement in turning carbon steel AISI 1045 using wiper inserts. Measurement 44, 1000–1005.

G.Taguchi, 1990. Introduction to Quality Engineering. Asian Productivity Organisation, Tokyo.

Hanafi, I., Khamlichi, A., Cabrera, F.M., Almansa, E., Jabbouri, A., 2012. Optimization of cutting conditions for sustainable machining of PEEK-CF30 using TiN tools. J. Clean. Prod. 33, 1–9.

He, Y., Liu, F., Wu, T., Zhong, F.-P., Peng, B., 2011. Analysis and estimation of energy consumption for numerical control machining. Proc. Inst. Mech. Eng. Part B J. Eng. Manuf. 226, 255–266.

Kuram, E., Ozcelik, B., Bayramoglu, M., Demirbas, E., Simsek, B.T., 2013. Optimization of cutting fluids and cutting parameters during end milling by using D-optimal design of experiments. J. Clean. Prod. 42, 159–166.

Yan, J., Li, L., 2013. Multi-objective optimization of milling parameters e the trade-offs between energy , production rate and cutting quality. J. Clean. Prod. 52, 462–471.

Chapter 4

Predictive Modelling and Optimization for Surface Roughness

In this chapter the experimental data of surface roughness is used to develop surface roughness predictive models using RSM, SVR and ANN techniques. Further, response surface methodology and genetic algorithms are used to obtain the machining parameters to optimize surface roughness.

4.1 Introduction

Designers constantly strive to design products and machinery that can run faster, last longer and operate more precisely. Modern development of high speed machines has resulted in higher loading and increased speeds of moving parts which requires that bearings, seals, shafts, machine ways, gears, etc. must be dimensionally and geometrically accurate or the surface texture of the produced parts must be precise. Unfortunately, manufacturing processes produce parts with surfaces that are either unsatisfactory from the perspective of geometrical perfection or quality of surface texture. Surface texture of produced parts demands significant attention at the design as well as manufacturing stage. Process models have often targeted the prediction of fundamental variables such as stresses, strains, strain rate, temperature, etc but to be useful for industry these variables must be correlated to performance measures and product quality (Arrazola et al., 2013). Productivity and accuracy of machine tools are important competitive aspects. A significant improvement in productivity can be obtained by optimization of machining parameters that lead to desired response in accuracy at lower cost of manufacturing. There is a close interdependence among productivity, quality and power consumption of a machine tool. Surface roughness is a widely used index of product quality in terms of various parameters such as aesthetics,

corrosion resistance, subsequent processing advantages, tribological considerations, fatigue life improvement, precision fit of critical mating surfaces, etc (Kant and Sangwan, 2014). Moreover, in practice, the machining parameters are generally chosen primarily on the basis of human judgment and experience and to some extent on the basis of handbook data. This, generally, does not lead to the optimum machining parameters and hence loss of productivity and accuracy. The loss of productivity and accuracy is more significant for the costly computerized numerical control machine tools. The capability of a manufacturing process to produce a desired surface roughness depends on machining parameters, cutting phenomenon, work piece properties, and cutting tool properties (Benardos and Vosniakos, 2003). As shown in Figure 4.1, feed rate, cutting speed, depth of cut, tool angle, and cutting fluids are important machining parameters affecting surface roughness particularly in the turning process at low speeds. Even small changes in any of these parameters may have a significant effect on the surface roughness. Therefore, it is important for the researchers to model and quantify the relationship between surface roughness and the parameters affecting it.

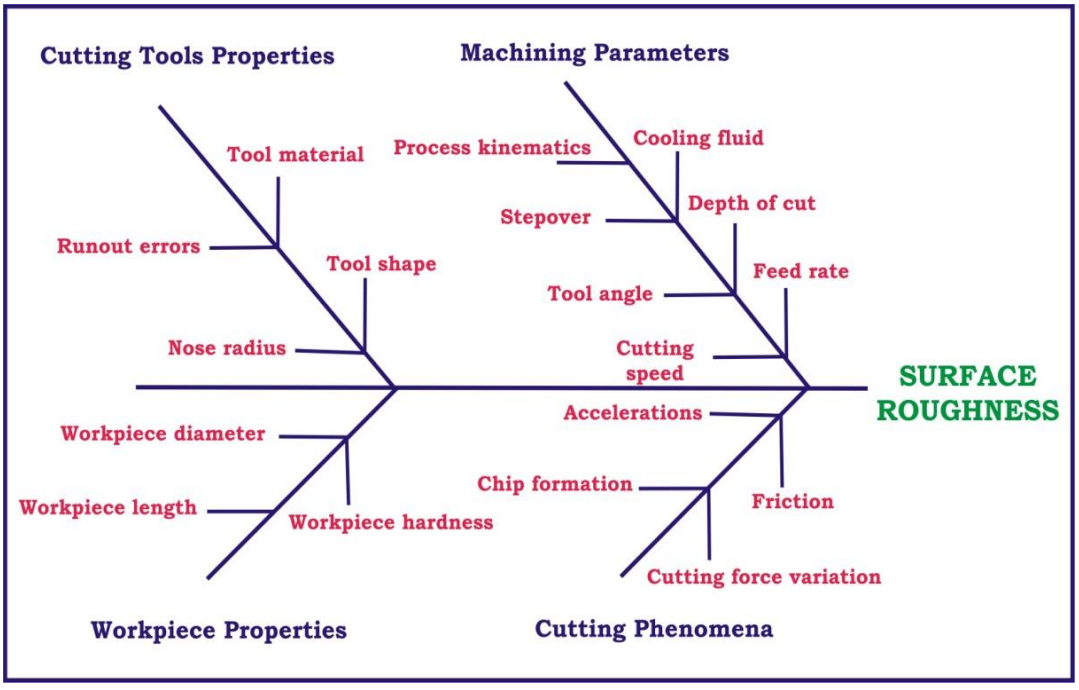

Figure 4.1: Parameters affecting surface roughness (Benardos and Vosniakos, 2003)

The purpose of metal cutting processes is not only to shape machined elements but also to manufacture them so that they can achieve functions according to geometric, dimensional and surface considerations (Karayel, 2009). But surface roughness cannot be controlled as accurately as geometric form and dimensional quality as it depends upon the complex interactions of physical factors such as machine tool, cutting tool and workpiece as well as cutting phenomenon and machining parameters. Today, there exists text book knowledge which provides approximate range of surface roughness provided by various machining processes. But as precision manufacturing requirement demands accurate and not approximate results, machining parameters are chosen based on the human judgment and experience, and theoretical models have limited applications because of the ever increasing range of materials and machining parameters, therefore the textbook knowledge is of limited practical application. Theoretical models proposed to estimate these parameters are given by Eq.(4.1) and Eq. (4.2) (Davim et al., 2008).

$$R_a = \frac{1000 f^2}{32r} \tag{4.1}$$

$$R_t = \frac{1000 f^2}{8r} \tag{4.2}$$

where f is the feed rate (mm/rev) and r is the tool nose radius (mm). However, these models do not reflect the effect of other process parameters on surface roughness. It has been shown that cutting speed and feed rate play important roles on surface quality of finished component (Davim, 2001). Theoretical models do not take into account any imperfections in the process such as tool vibration or chip adhesion on surface roughness (Diniz and Micaroni, 2002). Despite numerous studies on process optimization problems, there exists no universal input–output and in process parameter relationship model which is applicable to all kinds of machining processes (Hassan and Suliman, 1990). Luong and

Spedding (1995) emphasized the lack of basic mathematical models that can predict cutting behavior over a wide range of cutting conditions.

4.2 Surface Roughness

Figure 4.2 shows the various surface form deviations. First order deviations refer to form (flatness, circularity, etc) and second order deviation refers to waviness and these deviations are due to machine tool errors, deformation of the workpiece, erroneous setups and clamping, vibration, and workpiece material inhomogenities. Third and fourth order deviations refer to periodic grooves, and to cracks and dilapidations, which are connected to the shape and condition of the cutting edges, chip formation and process kinematics. Fifth and sixth order deviations refer to workpiece material structure, which is connected to physical–chemical mechanisms acting on a grain and lattice scale (slip, diffusion, oxidation, residual stress, etc.). Surface roughness refers to deviation from the nominal surface of the third up to sixth order (Benardos and Vosniakos, 2003). Different order deviations are superimposed and form the surface roughness profile as shown in Figure 4.2.

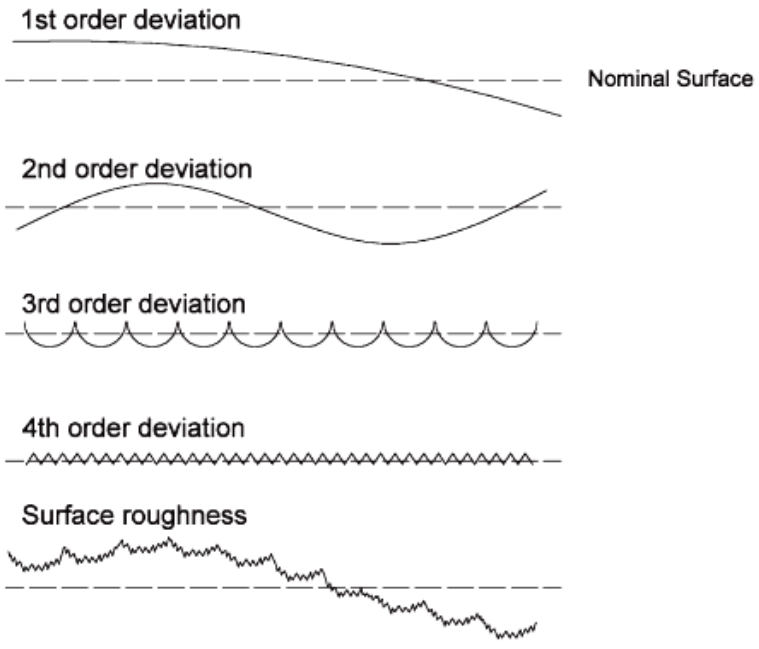

Figure 4.2: Surface form deviations (Benardos and Vosniakos, 2003)

The average surface roughness (R_a) is usually described on the basis of the ISO 4287. Roughness parameter (R_a) specifies the arithmetic mean of the absolute amounts of all variances in the roughness profile from the center line over the total as given by Eq. (4.3) (Arbizu and Pérez, 2003) and shown in Figure 4.3.

$$R_a = \frac{1}{l}\int_0^l |y(x)|dx \tag{4.3}$$

where l is the sampling length and y is the coordinate of the profile curve.

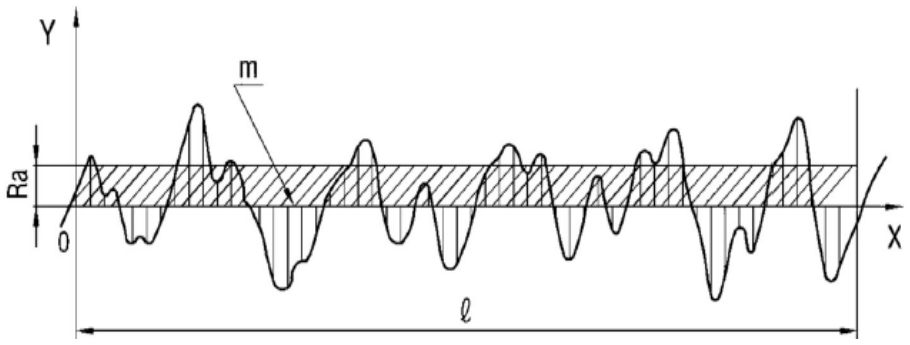

Figure 4.3: Representation of the calculation of roughness (Sarıkaya and Güllü, 2014)

4.3 Predictive Modelling for Surface Roughness using Response Surface Methodology

Engineering experiments aim at determining the conditions that can lead to optimum performances. One of methodologies for obtaining the optimum performance is Response Surface Methodology (RSM). RSM, developed by Box and Draper (1987), is a collection of mathematical and statistical techniques that are useful for the modelling and analysis of problems in which a response of interest is influenced by several variables and the objective is to optimize the response. It is a sequential experimentation strategy for empirical model building and optimization. By conducting experiments and applying regression analysis, a model of the response to independent input variables can be obtained. A near optimal point can then be deduced based on the model of the response.

RSM is often applied in the characterization and optimization of processes. In RSM, it is possible to represent independent process parameters in quantitative form as:

$$Y = f(X_1, X_2, X_3, ... X_n) \pm \varepsilon \tag{4.4}$$

where, Y is the response, f is the response function, ε is the experimental error, and X_1, X_2, X_3, ……, X_n are independent parameters. Y is plotted to get the response surface. The form of f is unknown and may be very complicated, therefore, RSM aims at approximating f by a suitable lower ordered polynomial in some region of the independent process variables. If the response can be well modeled by a linear function of the independent variables the function Eq. (4.4) can be written as:

$$Y = b_0 + b_1 x_1 + b_2 x_2 + ... + b_n x_n \pm \varepsilon \tag{4.5}$$

However, if a curvature appears in the system, then a higher order polynomial such as quadric model (Eq. (4.6)) may be used:

$$Y_u = b_0 + \sum_{\mathrm{i}=1}^{\mathrm{n}} b_i x_{\mathrm{i}} + \sum_{\mathrm{i}=1}^{\mathrm{n}} b_{ii} x_i^2 + \sum_{i<j}^{n} b_{ij} x_i x_j \tag{4.6}$$

where Y is the corresponding response and x_i (1, 2, …, n) are the independent input parameters. The terms b_0, b_1, b_2, *etc.* are the second-order regression coefficients. The second term contributes to linear effect, the third term contributes to the higher-order effects, and the fourth term contributes to the interactive effects of the input parameters. The values of the coefficients are estimated by using the responses collected (Y_1, Y_2,…, Y_n) through the design points (n) by applying the least square technique. This equation can be rewritten in terms of the three variables as:

$$Y_u = b_0 + b_1 x_1 + b_2 x_2 + b_3 x_3 + b_{11} x_1^2 + b_{22} x_2^2 + b_{33} x_3^2 + b_{12} x_1 x_2 + b_{13} x_1 x_3 + b_{23} x_2 x_3 \tag{4.7}$$

The objective of using RSM is not only to investigate the response over the entire factor space, but also to locate the region of interest where the response reaches its optimal or near optimal value. Careful study of the response surface model provides the combination

of factors giving best response. The response surface method is a sequential process and the methodology used for the modelling can be summarized as shown in Figure 4.4.

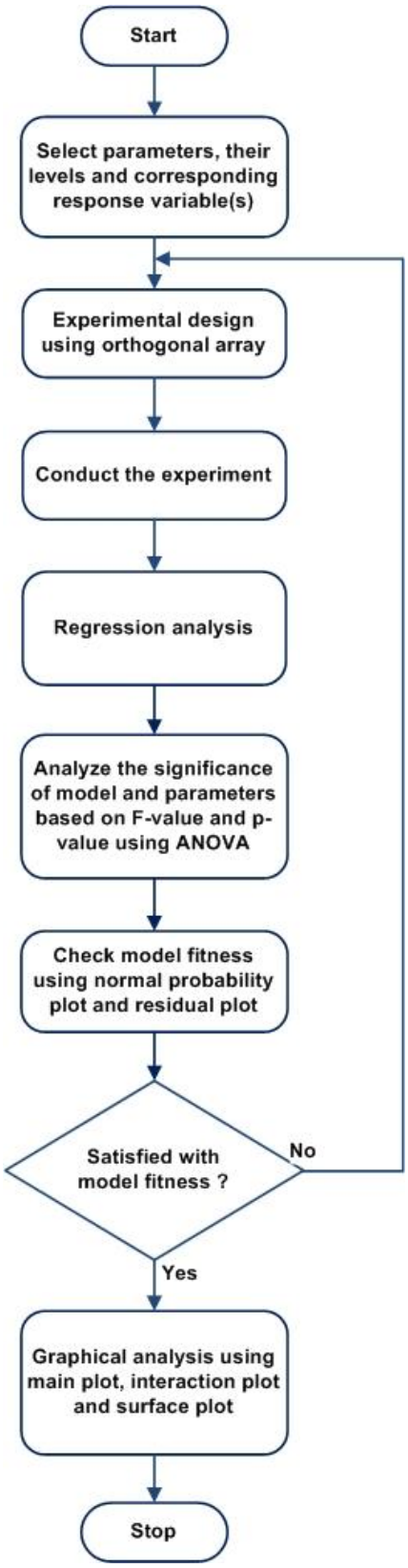

Figure 4.4: Outline of response surface methodology used

4.3.1 Mathematical model

The mathematical model for the surface roughness prediction based on the experimental results given in Chapter 3 (Table 3.8) is developed using Eq. (4.7). The developed mathematical model to predict surface roughness (R_a) is:

$$\begin{aligned} R_a &= 1.67023 - 0.0527596\,v + 38.7308\,f - 1.08526\,d \\ &\quad + 0.000191348\,v^2 - 16.5660\,f^2 + 0.179244\,d^2 \\ &\quad - 0.0606859\,vf + 0.00521919\,vd + 0.899583\,fd \end{aligned} \tag{4.8}$$

Predicted values of surface roughness from the developed mathematical model and the experimental values are shown in Figure 4.5 and Table 4.1. The comparison of predicted and measured values shows that the predicted values of the surface roughness are very close to measured values. The mean relative error between the experimental and predicted values is 7.64%.

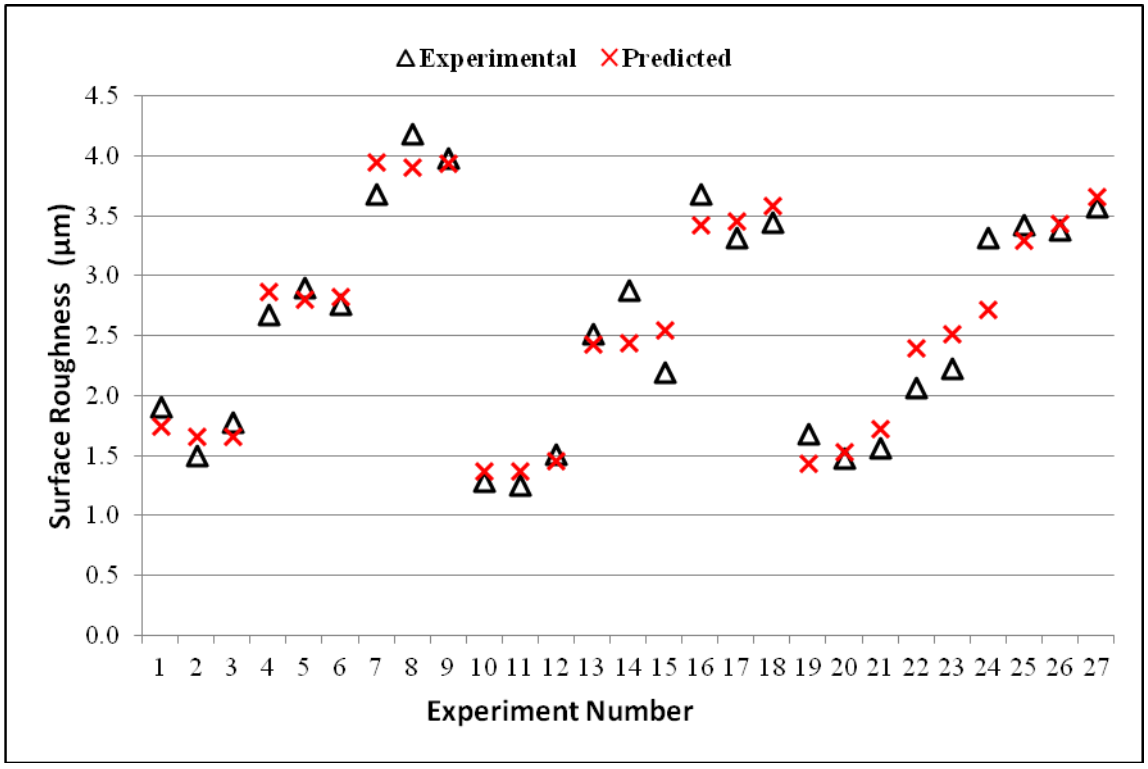

Figure 4.5: Experimentally measured and predicted values of surface roughness

Table 4.1: Experimental and predicted values of surface roughness

Experiment No.	Surface roughness (R_a) (μm)	
	Experimental	RSM
1	1.907	1.745
2	1.499	1.660
3	1.776	1.665
4	2.684	2.875
5	2.902	2.809
6	2.769	2.832
7	3.685	3.953
8	4.185	3.905
9	3.983	3.946
10	1.284	1.374
11	1.257	1.370
12	1.517	1.456
13	2.514	2.429
14	2.884	2.444
15	2.194	2.547
16	3.687	3.432
17	3.318	3.464
18	3.447	3.586
19	1.683	1.437
20	1.483	1.537
21	1.565	1.727
22	2.069	2.396
23	2.232	2.514
24	3.320	2.722
25	3.430	3.302
26	3.381	3.438
27	3.574	3.664

4.3.2 Analysis of variance

Table 4.2 shows ANOVA results for the linear [v, f, d,] quadratic [v^2, f^2, d^2] and interactive [($v \times f$), ($v \times d$), ($f \times d$)] factors. The sum of squares is used to estimate the square of deviation from the mean. Mean squares are estimated by dividing the sum of squares by degrees of freedom. F-value which is a ratio between the regression mean square and the mean square error is used to measure the significance of the model under investigation with respect to the variance of all the terms including the error term at the desired significance level. Usually, $F > 4$ means that the change of the design

parameter has a significant effect on the response variable. p-value or probability value is used to determine the statistical significance of results at a confidence level. In this study the significance level of $\alpha = 0.05$ is used, i.e. the results are valid for a confidence level of 95%. Table 4.2 shows the p-values, the significance levels associated with the F-values for each source of variation. If the p-value is less than 0.05 then the corresponding factor (source) has a statistically significant contribution to the response variable and if the p-value is more than 0.05 then it means the effect of factor on the response variable is not statistically significant at 95% confidence level. The last column of the Table 4.2 shows the percentage contribution of each source to the total variation indicating the degree of influence on the result.

Table 4.2: Analysis of variance (ANOVA) results

Source	**DOF**	**Seq. SS**	**Adj. SS**	**Adj. MS**	**F**	**p**	**% contribution**
Regression	9	20.437	20.437	2.271	27.90	0.000	93.66
Linear	3	19.892	19.766	6.589	80.96	0.000	91.16
v	1	0.342	0.391	0.391	4.80	0.043	1.57
f	1	19.469	19.285	19.285	236.98	0.000	89.22
d	1	0.080	0.090	0.090	1.10	0.309	0.37
Square	3	0.350	0.350	0.117	1.43	0.268	1.60
*v*v*	1	0.333	0.333	0.333	4.10	0.059	1.53
*f*f*	1	0.004	0.004	0.004	0.05	0.823	0.02
*d*d*	1	0.012	0.012	0.012	0.15	0.705	0.05
Interaction	3	0.196	0.196	0.065	0.80	0.509	0.90
*v*f*	1	0.089	0.089	0.089	1.10	0.310	0.41
*v*d*	1	0.103	0.103	0.103	1.27	0.276	0.47
*f*d*	1	0.004	0.004	0.004	0.05	0.830	0.02
Residual Error	17	1.384	1.384	0.081			6.34
Total	26	21.821					
$R^2 = 0.9316$			R^2(Pred.) = 0.8439				R^2(Adj.) = 0.9030

DOF: Degree of freedom, SS: Sum of square, MS: Mean square

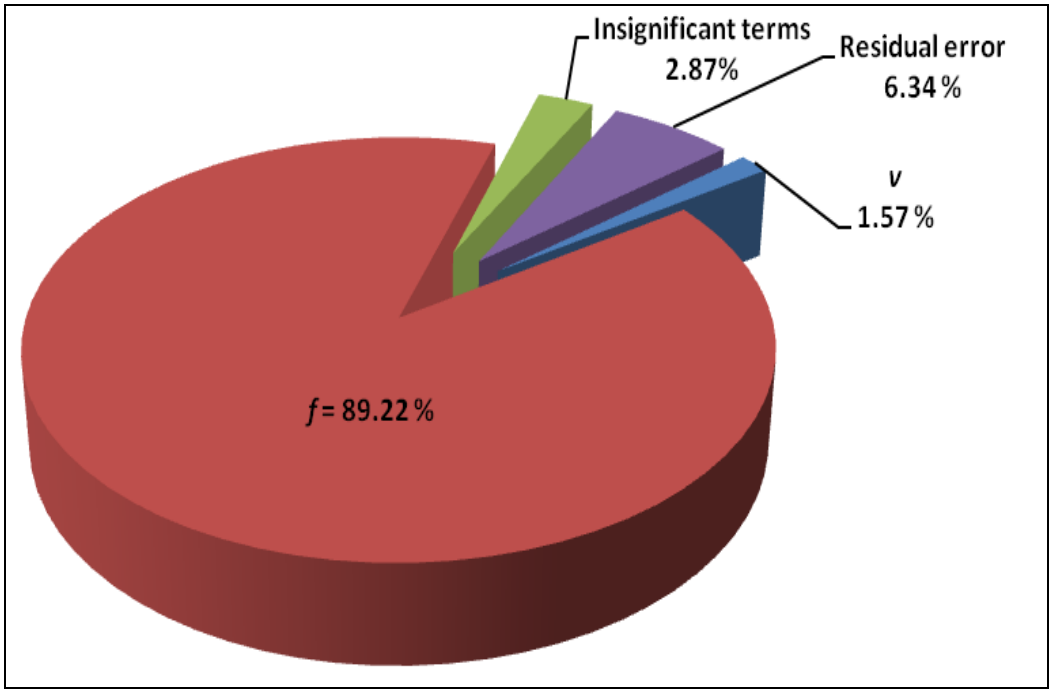

Figure 4.6: Percentage contribution of machining parameters on surface roughness

The percentage contribution of each term is also shown in Figure 4.6. feed rate (f) was found to be the most significant factor for R_a which explains 89.22% contribution of total variation. This is anticipated as it is well known that for a given tool nose radius, the theoretical surface roughness is mainly a function of feed rate (Shaw, 1984). The next contribution on R_a comes from the cutting speed with a contribution of 1.57%. The depth of cut, quadratic [v^2, f^2, d^2] and interactions [($v \times f$), ($v \times d$), ($f \times d$)] do not have statistical significance because they have much lower level of contribution and their p-value is also more than the confidence level.

The other important term is coefficient of determination R^2, which is defined as the ratio of the explained variation to the total variation and is a measure of the degree of fit. As R^2 approaches unity, the response model fitness with the actual data improves. The value of R^2 = 0.9316 which indicates that 93.16% of the total variations are explained by the model. The adjusted R^2 is a statistic used to adjust the "size" of the model, i.e. the number of factors (machining parameters). The value of the R^2 (Adj.) =

0.9030 indicating 90.30% of the total variability is explained by the model after considering the significant factors. R^2 (Pred.) = 0.8439 is in good agreement with the R^2 (Adj.) and shows that the model would be expected to explain 84.39% of the variability in new data.

4.3.3 Model fitness check

The adequacy of the modal has been investigated by the examination of residuals. The residuals, which are the differences between the respective observed response and the predicted response, are examined using normal probability plots of the residuals and the plots of the residuals versus the predicted response. If a model is adequate, the points on the normal probability plots of the residuals should form a straight line. Figure 4.7 reveals that the residuals are not showing any particular trend and the errors are distributed normally. The residual versus the predicted response plot in Figure 4.8 also shows that there is no obvious pattern and unusual structure.

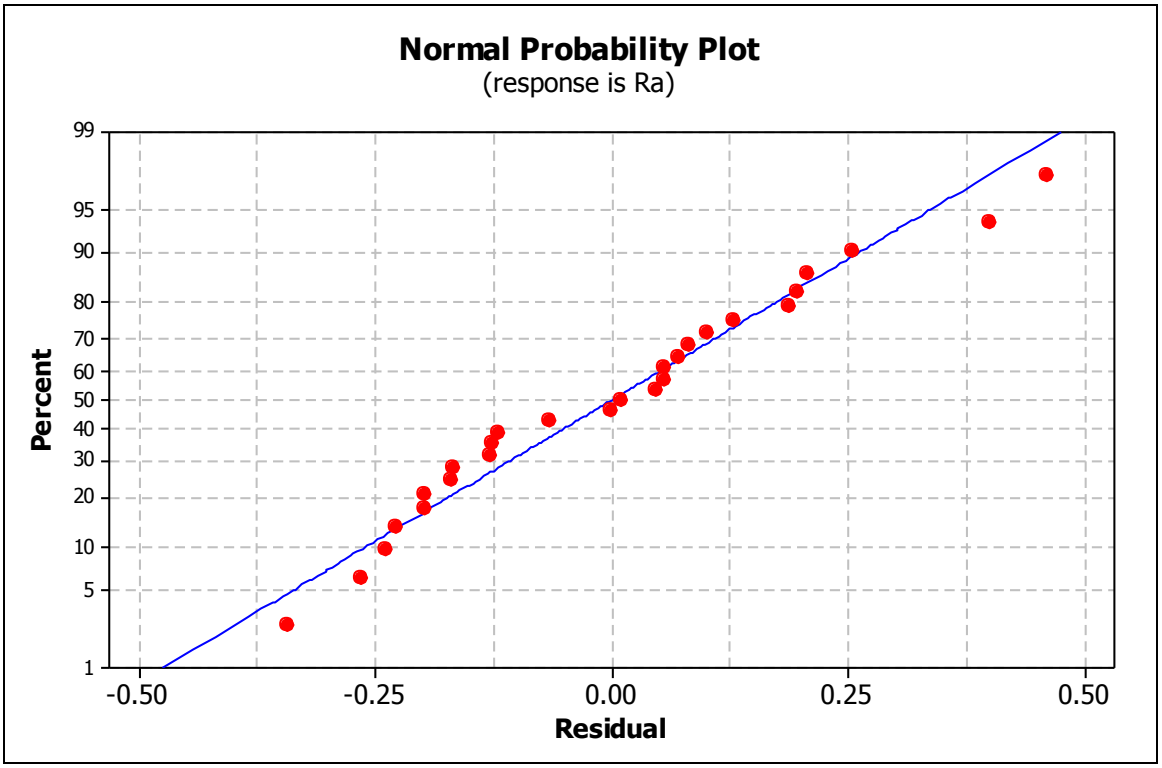

Figure 4.7: Normal probability plot of residual for surface roughness

4.3.4 Parametric influence on surface roughness

Theoretically, surface roughness is a function of feed rate and nose radius. But in practice, cutting speed, depth of cut and tool wear also affect surface roughness. Since the inserts used in the experiments have identical nose radius values, the effect of nose radius was not investigated in this study. The effect of tool wear was neglected as a new cutting edge was used for each experiment and wear did not reach high levels enough to affect the surface roughness.

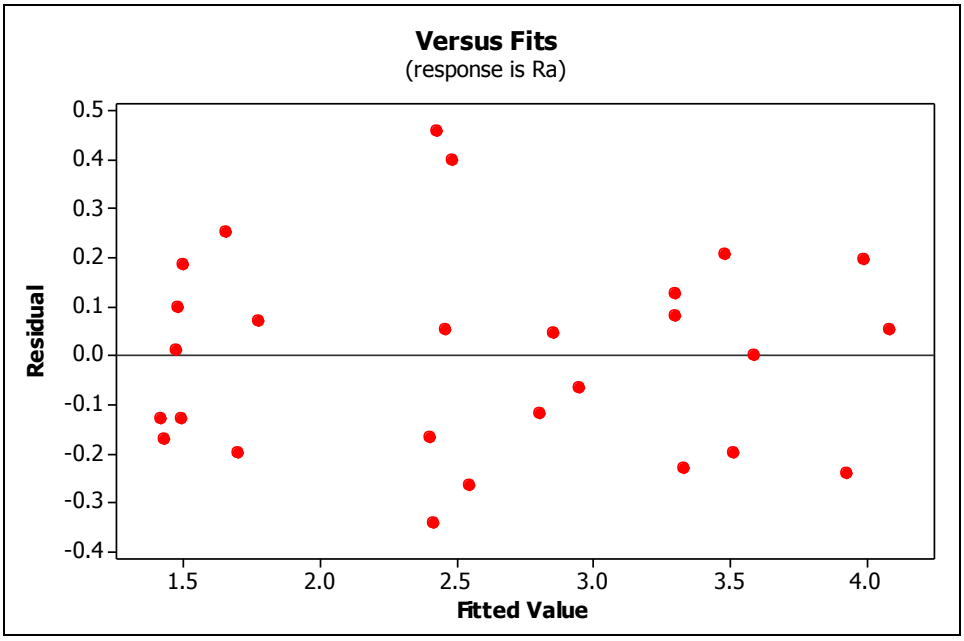

Figure 4.8: Plot of residual versus fitted surface roughness values

The main effects of machining parameters are shown in Figure 4.9. Feed rate has the greatest effect on surface roughness. The effect of cutting speed is very less and the effect of depth of cut is negligible as seen in Figure 4.9. Even after a 300% increase in cutting depth, no considerable change was noticed. The results also match with the ANOVA results in Table 4.2. An increase in cutting speed improves surface quality. This result supports the argument that high cutting speeds reduce cutting forces together with the effect of natural frequency and vibrations giving better surface finish (Sarıkaya and Güllü, 2014). The best surface quality values can be achieved at low feed rate and high cutting

speeds. Sahin and Motorcu (2005) also demonstrated that surface roughness increases with increase in feed rate and decreases with increase in cutting speed during the cutting of AISI 1040 steel with TiN coated carbide tools. However, Cetin et al. (2011) indicated that the effects of feed rate and depth of cut are more effective than cutting speed on reducing the forces and improving the surface finish.

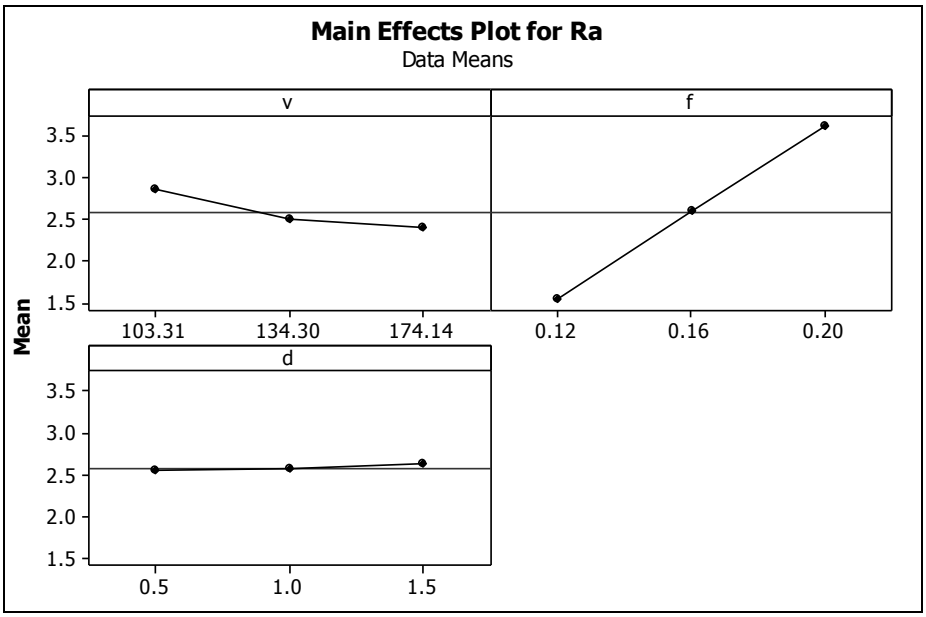

Figure 4.9: Main effect plot of surface roughness

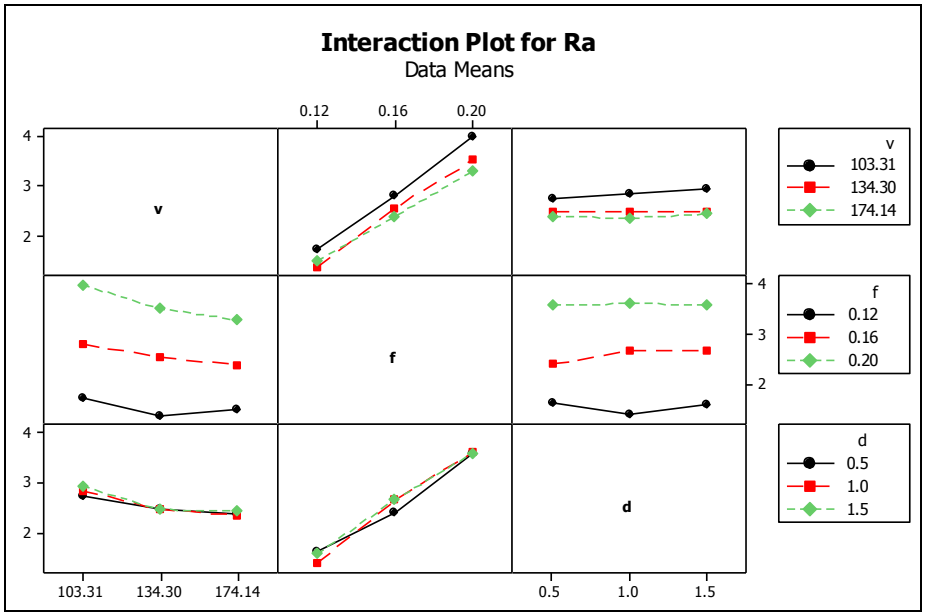

Figure 4.10: Interaction plot of surface roughness

The interaction plot for surface roughness is shown in Figure 4.10. This figure clearly shows that the surface roughness is high with variation of feed rate at any depth of cut (row 3 column 2) and at any cutting speed (row 1 column 2) as the minimum surface roughness is close to 1 µm for level 1 feed rate and all levels of depth of cut and cutting speed, and the maximum surface roughness is more than 3 µm for level 3 feed rate and all levels of depth of cut and cutting speed. The variation of depth of cut has negligible effect on surface roughness for cutting speed (row 1 column 3) as the spacing between the lines is very small. The 3D surface and contour plots for the surface roughness are shown in Figure 4.11. Figure 4.11(a) shows the surface and contour plots for surface roughness at 1 mm depth of cut. It is clear from Figure 4.11(a) that the surface roughness increases with increase in feed rate. It is observed that the surface roughness increases with increase in cutting speed at lower feed rate, while at higher feed rate the surface roughness decreases with increase in cutting speed.

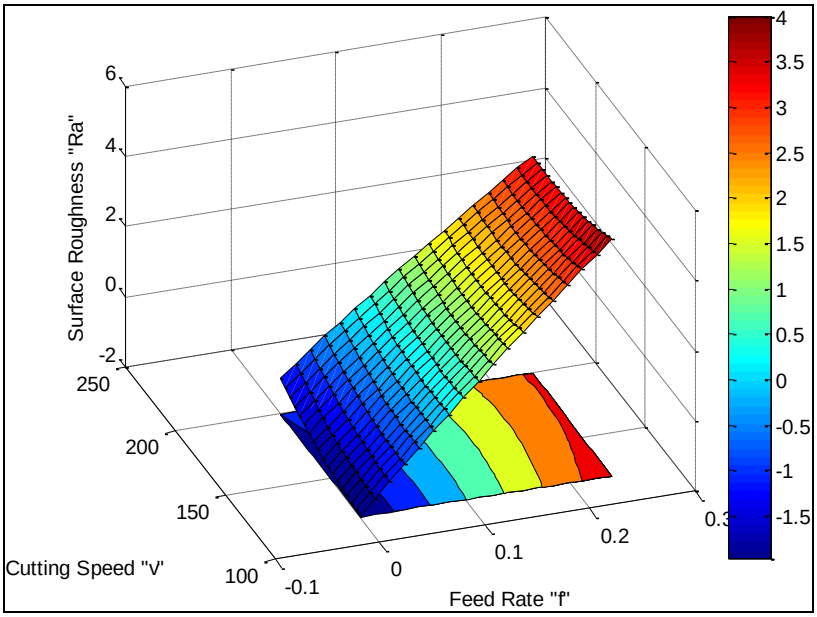

Figure 4.11(a): Surface and contour plot of R_a for varying cutting speed and feed rate at 1 mm depth of cut

Figure 4.11(b) shows the surface and contour plots for surface roughness at cutting speed of 134.30 m/min. It reveals that surface roughness increases with increase in feed rate and depth of cut has no significant effect. Figure 4.11(c) shows the surface and contour

plots for surface roughness at a feed rate of 0.16 mm. It indicates that cutting speed as well as depth of cut both have no significant effect on surface roughness as the range of change in surface roughness is very low (2.4-2.8µm).

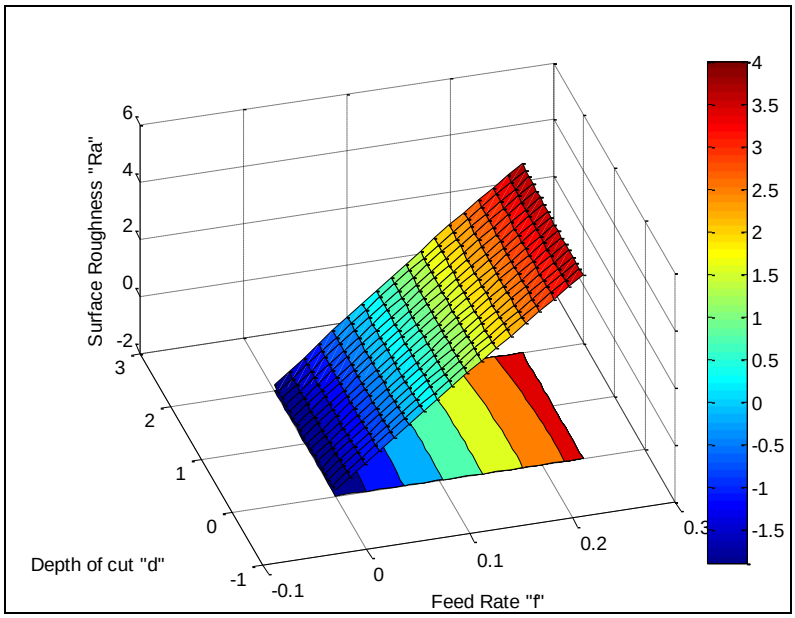

Figure 4.11(b): Surface and contour plot of R_a for varying depth of cut and feed rate at 134.30 m/min cutting speed

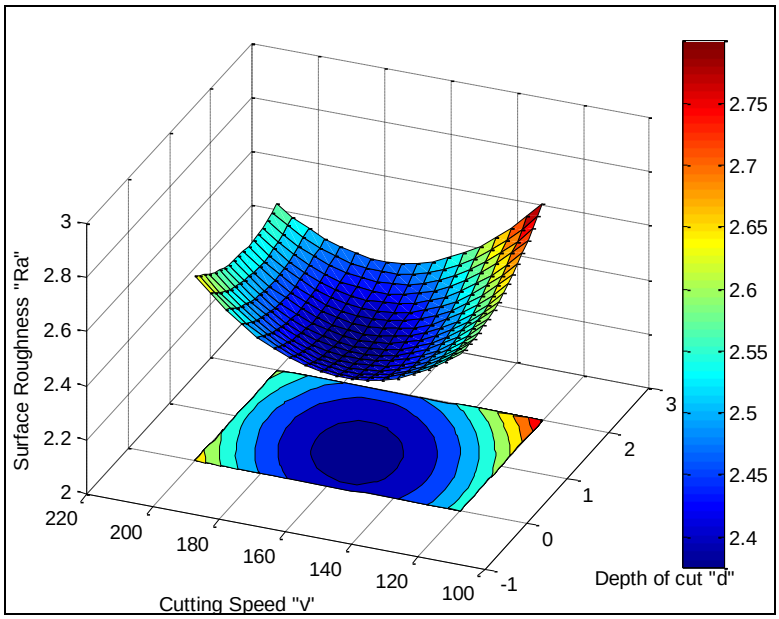

Figure 4.11(c): Surface and contour plot of R_a for varying cutting speed and depth of cut at 0.16 mm/rev. feed rate

It has been observed from Figure 4.11(c) that the surface roughness varies a little with change in depth of cut and cutting speed. However, this plot is useful to find the optimum values of cutting speed and depth of cut at a particular value of surface roughness and feed rate. These 3D surface plots can be used for estimating the surface roughness values for any suitable combination of the input parameters namely cutting speed, feed rate and depth of cut.

4.4 Predictive Modelling for Surface Roughness using Support Vector Regression

SVM (Support Vector Machines) is a very useful soft computing method based on statistical learning theory presented by Vladimir Vapnik (Çaydaş and Ekici, 2012; Salat and Osowski, 2004; Vapnik, 1998). SVM is a supervised learning model with associated learning algorithm that analyzes data and recognizes pattern. A version of SVM for regression was proposed in 1996 by Vladimir Vapnik, Harris Drucker, Chris Burges, Linda Kaufman and Alex Smola (Drucker et al., 1997). This method is called Support Vector Regression (SVR). SVR was presented as a learning technique that originated from the theoretical foundations of statistical learning theory and structural risk minimization. The SVR model depends on a subset of the training data, because the cost function for building the model ignores any training data that are close (within a threshold ε) to the model prediction (Çaydaş and Ekici, 2012).

SVR first non-linearly transforms the original input space x into a higher dimensional feature space. That is, in order to learn non-linear relations with a linear machine, it is required to select a set of non-linear features and express the data in the new representation. This transformation can be achieved by using various types of non-linear

mapping. Non-linear regression problems in an input space can become linear regression problems in a feature space.

In regression learning problem, the learning machine is given *N* training data from which it attempts to learn input–output relationship $f(x)$. A training data set is given in pairs (x_i, y_i), $i = 1, \ldots, N$ where $x_i \in R^m$ and y_i is the actual output value. SVR considers the following approximate function:

$$y = f(x) = \sum_{i=1}^{N} w_i \varphi_i(x) + b = w^T \varphi(x) + b \tag{4.9}$$

where $\varphi_i(x)$ is called feature that is non-linearly mapped from the input space *x*,

$$w = [w_1, w_2, \ldots\ldots, w_N]^T \text{ and } \varphi = [\varphi_1, \varphi_2, \ldots\ldots, \varphi_N]^T$$

Eq. (4.9) is a non-linear regression model because the resulting hyper-surface is a non-linear surface hanging over the *m*-dimensional input space. However, after the input vector *x* are mapped into vectors $\varphi(x)$ of a high dimensional kernel-induced feature space, the non-linear regression model is turned into a linear regression model in this feature space. The non-linear function is learned by a linear learning machine where the learning algorithm minimizes a convex function. The convex function is expressed as the following regularized risk function, and the support vector weight *w* and bias *b* are calculated by minimizing the risk function:

$$R(w) = \frac{1}{2} w^T w + C \sum_{i=1}^{N} |y_i - f(x)|_e \tag{4.10}$$

where, $|y_i - f(x)|_e = \begin{cases} 0, & \text{if } |y_i - f(x)| < \varepsilon \\ |y_i - f(x)| - \varepsilon, & \text{otherwise} \end{cases}$

The constant *C* is called a regularization parameter. The regularization parameter determines the trade-off between the approximation error and the weight vector norm.

An increase of the cost function *C* penalizes larger errors, which leads to a decrease of approximation error. This can also be achieved easily by increasing the weight vector norm. However, an increase in the weight vector norm does not make sure of the good generalization of the SVR model. Constants *C* and ε are user-specified parameters and $|y_i - f(x)|_e$ is called the ε-insensitive loss function (Vapnik, 2000). The loss is zero if the predicted value $f(x)$ is within an error level ε, and for all other predicted points outside the error level ε, the loss is equal to the magnitude of the difference between the predicted value and the error level ε as shown in Figure 4.12 and Figure 4.13 for linear and non-linear regressions.

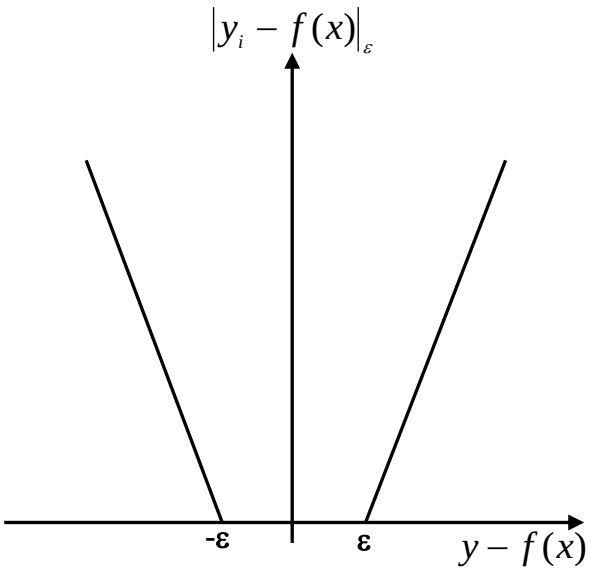

Figure 4.12: Linear ε-insensitive loss function

In SVR modelling, the data points which lie on the margin lines $(y = f(x) \pm \varepsilon)$ are the support samples or support vectors or support set, whereas the data points which lie inside the margin lines are called the remaining set and the data points which lie outside the margin lines are called the error set. Increasing the insensitivity zone ε means a reduction in requirements for the accuracy of approximation and it also decreases the number of support vectors leading to data compression. In addition,

increasing the insensitivity zone ε has smoothing effects on modelling highly noisy polluted data.

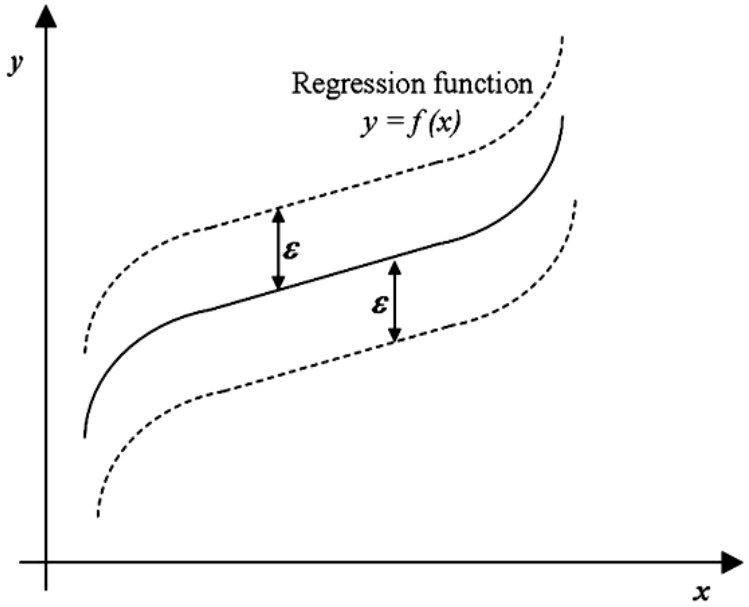

Figure 4.13: Non-linear regression with ε insensitive band in the SVR model

An online SVR toolbox for SVR modelling developed by Parrella (2007) in MATLAB has been used for predicting the surface roughness during turning. The input parameters have been normalized between 0 and 1. The training set '*x*' is a combined vector of all the three input parameters (*v*, *f*, *d*) and the training set '*y*' represents response parameter (surface roughness). Twenty seven sets of input-output pairs from experimental data have been used for training of the SVR model. SVR checks the verification of Karush–Kuhn–Tucker (KKT) conditions and simultaneously trains the data one by one by adding each sample to the function. If the KKT conditions are not verified then the sample is stabilized using the stabilization technique, else the sample is added. To optimize the values, the stabilization technique dynamically changes the SVR parameters of insensitive loss function and cost function. Training parameters for the study are ε = 0.01; C = 1000; kernel type = radial basis function (RBF); kernel parameter = 30. Figure 4.14 and Table 4.3 show the values predicted by the SVR model.

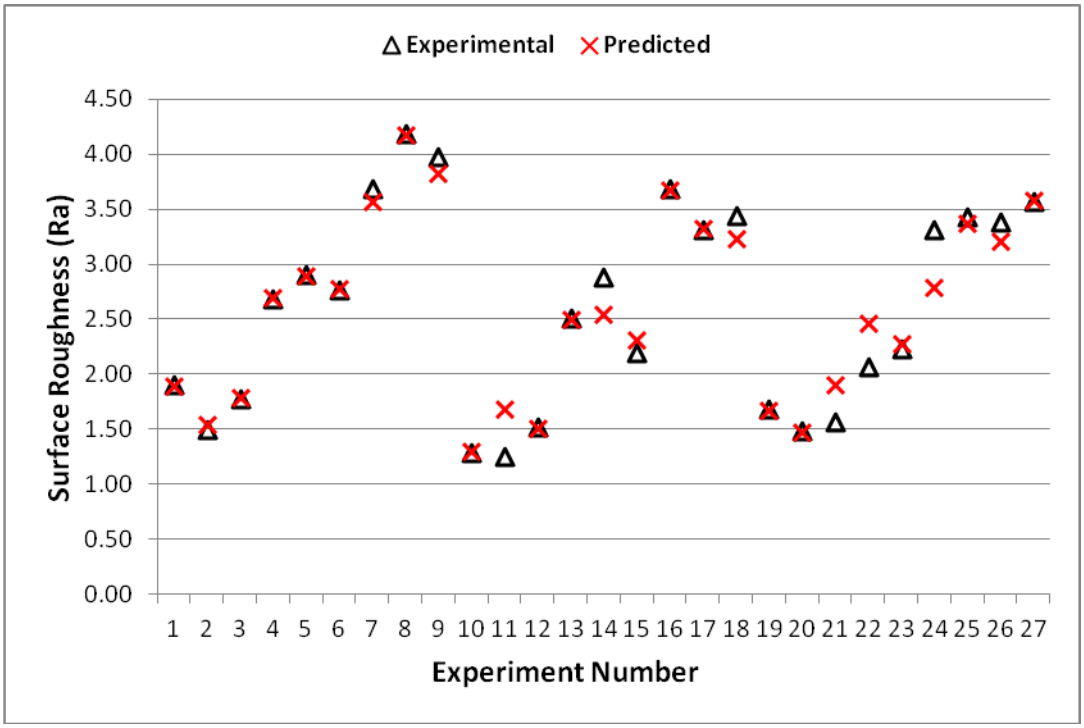

Figure 4.14: Experimentally measured and SVR predicted values of surface roughness

Table 4.3: Experimental and predicted values of surface roughness using SVR

Experiment No.	Surface roughness (R_a) (µm)	
	Experimental	SVR
1	1.907	1.897
2	1.499	1.547
3	1.776	1.786
4	2.684	2.694
5	2.902	2.892
6	2.769	2.779
7	3.685	3.576
8	4.185	4.175
9	3.983	3.832
10	1.284	1.294
11	1.257	1.688
12	1.517	1.507
13	2.514	2.504
14	2.884	2.547
15	2.194	2.312

Experiment No.	Surface roughness (R_a) (μm)	
	Experimental	SVR
16	3.687	3.677
17	3.318	3.328
18	3.447	3.235
19	1.683	1.673
20	1.483	1.473
21	1.565	1.900
22	2.069	2.470
23	2.232	2.280
24	3.320	2.791
25	3.430	3.372
26	3.381	3.208
27	3.574	3.584

4.5 Predictive Modelling for Surface Roughness using Artificial Neural Network

Neural networks, sometimes referred as artificial neural networks or parallel processing systems, are used to develop models in the same way in which the human brain processes information. The human brain is extremely effective in solving problems involving large amount of uncertain and noisy data. The neural networks attempt to mimic the functioning of biological neurons and therefore generate intelligent decisions. The fundamental processing unit in a neural network is called a neuron, which can posses a local memory and carry out localized information processing operations. They are interconnected with unidirectional signal channels (called connections) into multilevel networks. Each neuron has a single output, which branches into as many collateral connections as desired. Each neuron carries the same signal – the neuron output signal. This signal can be of any mathematical type. The processing that takes place within each neuron must be completely local – it must depend only upon the current values of the input signal arriving at the neuron through impinging connections

and upon the values stored in the neuron's local memory. Generally, a neural network has an input layer to receive data from the outside world and an output layer to send information to users or external devices. Layers that lie between the input and output are called hidden layers and have no direct contact with the environment. Neural networks may or may not have hidden layers. The structure of a neural network could be characterized by the interconnection architecture among neurons, the activation function for conversion of inputs into outputs, and the learning algorithm. Many kinds of neural network architectures including the ART models, Hopfield models, Back-Propagation models, Kohonen's models, *etc*. have been developed. The basic principles of neural networks are given in Zurada (1992) and Lippmann (1987).

A multi layer feed forward network consisting of an input layer, one or more hidden layers and an output layer is shown in Figure 4.15.

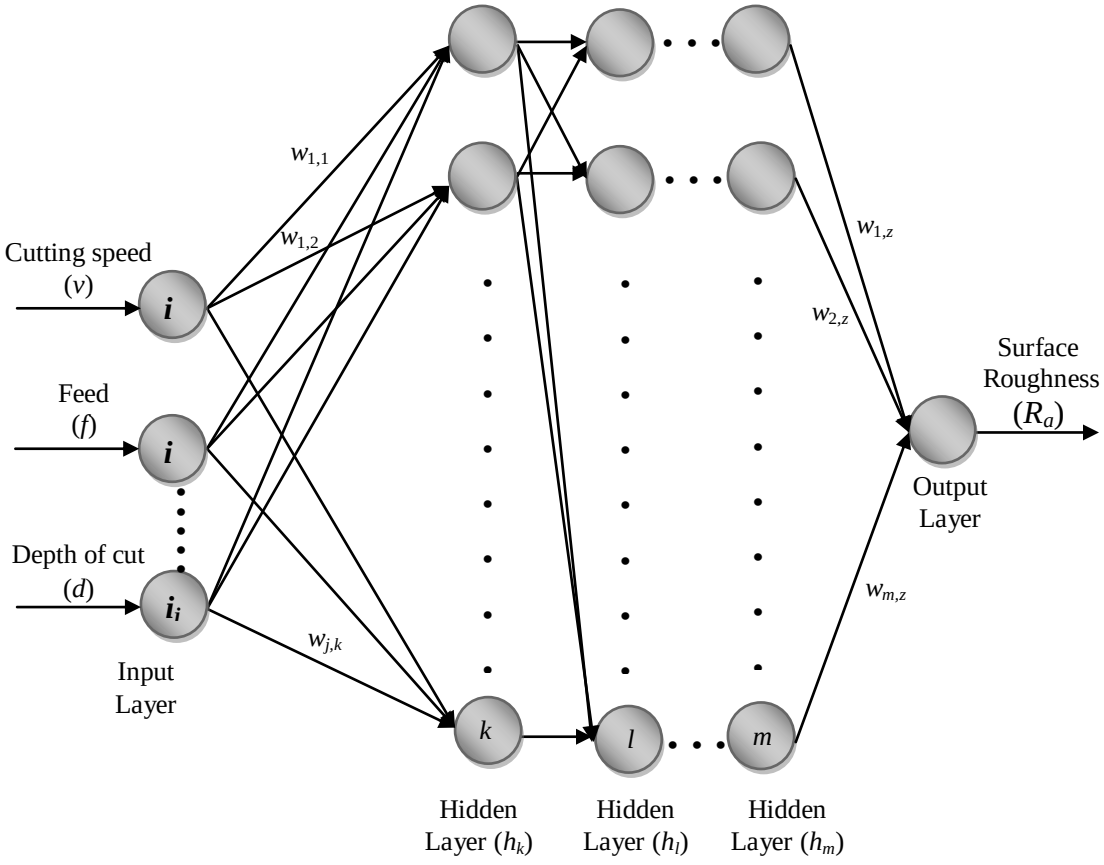

Figure 4.15: A generalized neural network structure for the study

The different layers are fully interconnected such that each neuron in one layer is connected to all neurons in the next layer. The input layer performs no information processing. Each of its neurons has only one input and it simply transmits the value at its input to its output. Actual information processing is performed by the neurons in the hidden and output layers. Signals are transmitted unidirectionally from the input layer through the hidden layers to the output layer. Information is stored in the inter-neuron connections. Learning consists of adapting the strengths (or weights) of the connections so that the network produces desired output patterns corresponding to given input patterns. In other words, a neural network can be trained to perform a particular function by adjusting the values of the connections (weights) between neurons. As each input is applied to the network, the network output is compared to the target. The error is calculated as the difference between the target output and the network output. Each hidden or output neuron receives a number of weighted input signals from each of the units of the preceding layer and generates only one output value. The diagram for a network with a single neuron is shown in Figure 4.16. Here, the scalar input (i_j) is transmitted through a connection that multiplies its strength by the scalar weight (w) to form the product (w_i), again a scalar. The inputs to the neuron can be from the actual environment or from the other neurons.

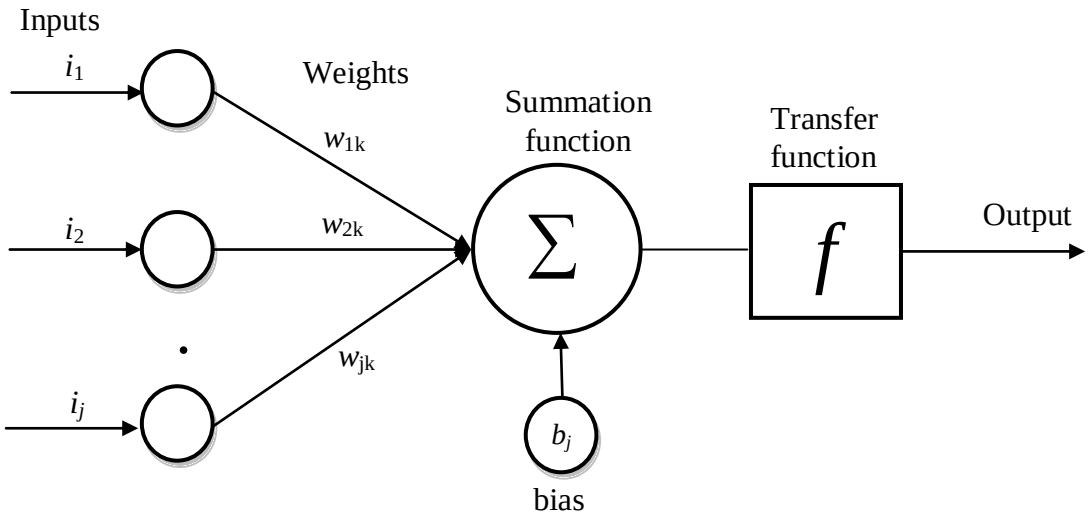

Figure 4.16: Mathematical principle of a neuron functioning

Its output can be fed into other neurons or directly into the environment. Also, this neuron has a scalar bias (b_j). The output is produced by a summation function and activation function. Summation function calculates the net input from the processing elements. Activation function (transfer function) determines the output of the neuron by the net input provided by the summation function. A transfer function generally consists of algebraic equations of linear and non-linear form. The use of non-linear transfer function makes a network capable of storing non-linear relationships between the input and the output. Output accepts the results of the transfer function and presents them either to the relevant processing element or to the outside of the network. The network is trained by adjusting weights.

4.5.1 Selection of factors influencing ANN model

ANN has been widely used by the researchers for the modelling purposes in different areas including machining. However, ANN model depends upon many factors like network structure, training and testing data, network algorithm, transfer function, network training function, learning function, and performance function. A review of ANN models used by various researchers in machining was done to get a feel of the suitable factors influencing ANN model as well as the abilities of ANN modelling for the machining processes. Table 4.4 provides the review of factors influencing ANN models.

Some of the abilities and limitations of ANN modelling in machining are (Zain et al., 2010a):

- ANN is able to handle non-linear form of modelling that learns the mapping of inputs to outputs.
- ANN is more successful, when compared to conventional approaches, in terms of speed, simplicity and capacity to learn, and also does not require much experimental data.

- An ANN model does not need any preliminary assumption to the underlying mechanisms in the modelled process.
- Improvements in the behavior of the experimental results are easy to understand in a short time from the neuron model.
- The performance of an ANN prediction model could be further improved by defining more levels for the input process parameters that can be achieved by trial and error methods and repeated training simulations.
- There are many ANN toolbox software packages such as MATLAB which can easily be used for training and testing the machining data.
- An ANN allows for simple complementing of the model by new input parameters without modifying the existing model structures.
- Researchers have the choice to use and compare different training algorithms such as back propagation and radial basis in ANN to obtain more accurate results of the prediction model.

The limitations of ANN in the machining process modelling are:

- Empirical experience is necessary in creating a realistic network.
- It is costly and time consuming for further improvement by defining more levels for the input process parameters that can be achieved by the trial and error method and repeated training simulation.
- Repeatability of training for an improved model is not assured.

The performance of the neural network is strongly influenced by the selection of following factors:

- Network structure
- Network algorithm
- Amount of training and testing data
- Transfer function, training function, learning function, and performance function

Table 4.4: Factors influencing ANN model

Author	Network structure	Training/ testing data	Network algorithm	Transfer function	Training function	Learning function	Performance function
Oktem et al. (2006)	5-42-42-1	236/7	Feedforward BP	tansig tansig	traingda	learngd	MSE
Basheer et al. (2008)	5-8-1	-	Feedforward BP	tansig tansig	trainbr and trainlm	learngd	MAE
Erzurumlu and Oktem (2007)	5-42-42-1	243/7	Feedforward BP	tansig tansig	traingda	learngd	MSE
Davim et al. (2008)	3-16-2	27/3	Feedforward BP	-	traingdx	learngdm	MSE
Nalbant et al. (2009)	3-9-1	55/5	Feedforward BP	logsig logsig	traingda and trainlm	learng and learngd	RMSE
Al-Ahmari (2007)	4-73-45-3	28/-	Feedforward BP	tansig purelin	trainscg	learngd	SSE
Sanjay et al. (2006)	4-1-1, 4-5-1, 4-10-1, 4-15-1, 4-20-1	-	Feedforward BP	logsig logsig	traingda	learngd	-
Cus and Zuperl (2006)	3-3-6-1	20/10	Feedforward BP and RB	tansig tansig	traingda	learngd	MAE
Kohli and Dixit (2005)	4-3-1	21/10	Feedforward BP	logsig logsig	traingda	learngd	RMSE
Ezugwu et al. (2005)	4-10-10-1, 4-15-15-15-1, 4-10,15-1, 4-15-10,1	-	Feedforward BP	tansig purelin	trainbr and trainlm	learngd	-
Grzesik and Brol (2003)	7-72-72-72-7	-	Feedforward BP	logsig logsig	traingdx	learngd	MSE
Zuperl and Cus (2003)	3-3-6-1	20/20	Feedforward BP and RB	logsig logsig	traingdx	learngd	MAE
Tansel et al. (2006)	-	81/-	Feedforward BP	logsig logsig	traingdx	-	-
Gupta (2010)	3-10-3	24/3	Feedforward BP	tansig purelin	trainlm	-	-

Network structure

An ANN network structure principally consists of layers and nodes. Nodes are also known as neurons. An illustration of an ANN network with layers and nodes is shown in Figure 4.15. The ANN network structure consists of three layers which are the input layer, hidden layer and output layer. The network structure has three nodes in the input layer, *k* nodes in the first hidden layer, *l* nodes in the second hidden layer, *m* nodes in the h_m hidden layer and one node in the output layer. Three nodes for the input layer stand for cutting speed (*v*), feed rate (*f*) and depth of cut (*d*). One node for the output layer stands for the predicted machining performance measure (surface roughness). When considering that a multilayer feedforward network is applied at the h_m hidden layer with *k*, *l* and *m* nodes for each hidden layer, the network shown in Figure 4.15 could be defined as a 3–*k*–*l*–*m*–1 structure. Table 4.4 shows that the researchers have applied different structures to develop ANN models. Sanjay and Jyothi (2006) applied five different structures and found that the 4–1–1 network structure to be more accurate and reliable for the prediction of the surface roughness performance measure. It could be summarized that researchers have tried different model structures to get the best prediction. In other words, an ANN model is designed on a trial and error basis to obtain the best results. The process of trial and error is carried out by adjusting the number of layers and the number of nodes of hidden layer(s) of the network structure. Researchers are free to test with any number of hidden layers with any number of nodes for each hidden layer. However, the number of hidden layers and the nodes in each hidden layer are subject to the complexity of the mapping, computer memory, computation time, and the desired data control effect. Higher nodes result in computer memory and computation time wastage, while few nodes may not provide the desired data control (Al-Ahmari, 2007).

Zhang et al. (1998) suggested that the recommended approximate number of nodes for the hidden layer providing best results are: ‘‘*n*/2”, ‘‘1*n*”, ‘‘2*n*”, and ‘‘2*n* + 1” where *n* is the number of input nodes. If the number of input variables are three, the recommended number of nodes in the hidden layer can be 2, 3, 6 or 7.

Amount of training and testing data

An increase in the amount of training data will increase the chance of getting a more accurate model. In machining, data used for training is taken from the actual experimental trials. Many constraints such as the cost and time in conducting the actual experiments might be a problem for researchers to get more data for the modelling purpose. It can be observed from Table 4.4 that several studies have used a small amount of modelling samples (less than 30 when training and testing are combined). Cus and Zuperl (2006) have obtained accurate results for predicting surface roughness with a small amount of training and testing data. Therefore, a total experimental sample size of 27 is sufficient and ANN model is expected to give accurate predictive results for surface roughness.

Ratio of training and testing data

The testing data used by researchers is smaller than the training data. The issue here is to separate the available experimental samples into training and testing. A suggested solution is to follow the guidelines given by Zhang et al. (1998) where the recommended ratio of training and testing samples could be given as percent, such as 90%:10%, 85%:15% and 80%:20%. To fit in with the available experimental sample size of 27, the selected preferred ratio was 80%:20%. 22 sample sets were chosen for training and five sample sets were used for testing the network.

Network Algorithm

Many different ANN network algorithms have been proposed by researchers for the modelling purpose – feedforward Back Propagation (BP), Elman BP, Time-delay BP, Perceptron, Radial Basis, and Self-Organizing map. Table 4.4 shows that the feedforward BP network algorithm is the most widely used by researchers in modelling of machining processes. Zuperl and Cus (2003) have used feedforward BP and radial basis network algorithm during machining of cast steel using HSS tool. It was found that the feedforward BP gives more accurate results but it requires more time for training and testing. The radial basis network is very fast and reliable but poor in term of the accuracy of the predicted results. A back propagation algorithm was used for this study. A feedforward network based on BP is a multilayered architecture made up of one or more hidden layers placed between the input and output layers. Each layer consists of units which recover their input from units directly below and send their output to units directly above the unit. Figure 4.15 illustrates an example of a multilayer feedforward BP ANN structure.

Transfer function, training function, learning function, and performance function

The net input to unit 'k' in the hidden layer provided by a multilayer feedforward training network with one hidden layer is given as:

$$\text{Net\_hidden} = \sum_{j=1}^{J} W_{j,k} i_j + b_k \tag{4.11}$$

where $W_{j,k}$ is the weight between the input and hidden neurons, i_j is the value of input which consists of cutting speed, feed rate and depth of cut of the experimental data and b_k is the bias on the hidden nodes. The weights and bias between the input and hidden layers used in this study are shown in Table 4.5.

Table 4.5: The weight and bias between input and hidden neurons used in the study

W_{jk}, j=3, k=7	W_{1k}	W_{2k}	W_{3k}	Bias (b_k)
1	2.924	0.014	4.534	-5.241
2	3.582	0.831	-4.220	-4.490
3	-2.837	4.284	1.151	3.088
4	3.467	-4.160	3.723	-0.839
5	-1.004	5.115	2.841	1.423
6	-5.034	2.821	1.429	-7.357
7	-3.223	-4.798	5.559	-3.962

The net input to the unit 'z' in the output layer is given as:

$$\text{Net\_output} = \sum_{k=1}^{K} W_{k,z} h_k + b_z \tag{4.12}$$

where $W_{k,z}$ is the weight between the hidden and output neurons, h_k is the value of output for hidden nodes and b_z is the bias on the output nodes. The weights between the hidden and output layer used in this study are shown in Table 4.6.

Table 4.6: The weight between hidden neurons and output neuron used in the study

$W_{k,z}$ k=7, z=1	W_{1k}
1	0.755
2	0.291
3	0.566
4	-0.346
5	0.643
6	1.633
7	-0.656

The bias between the hidden and output layer used in this study is 0.887.

From Eqs. (4.11) and (4.12), the output for hidden nodes can be given as Eq. (4.13) and the output for output nodes can be given as Eq. (4.14)

$$h_k = f\left(\text{net\_hidden}\right) \tag{4.13}$$

$$O_z = f\left(\text{net\_ouput}\right) = \hat{R}_a \tag{4.14}$$

where *f* is the transfer function.

Log-sigmoid transfer function (logsig), linear transfer function (purelin), hyperbolic tangent sigmoid transfer function (tansig), and hard limit transfer function (hardlim) are some of the popular transfer functions used in ANN modelling. According to the User's Guide for Neural Network Toolbox 6 written by Beale et al. (2014), three transfer functions viz. logsig, tansig and linear are most commonly used with the feedforward BP algorithm. Nalbant et al. (2009) concluded that the determination of transfer function depends upon the nature of the problem. The use of a non-linear transfer function makes a network capable of a non-linear relationship between the input and the output. Sigmoid function is self-limiting and has a simple derivative. An advantage of the sigmoid function is that the output cannot grow infinitely large or small. Kohli and Dixit (2005) have applied two different transfer functions, logsig and tansig, and it was observed that both these transfer functions produced almost the same performance. Logsig transfer function is applied in this study to determine the output for hidden nodes and tansig transfer function to determine the output for output nodes.

The logsig (log-sigmoid) transfer function is written as:

$$f = \frac{1}{1 + \mathrm{e}^{-\text{net}}} \tag{4.15}$$

where *net* is the net of hidden nodes by Eq. (4.11). Therefore, the output for hidden nodes with the log-sigmoid function could be written as:

$$h_k = f\left(\text{net\_hidden}\right) = \frac{1}{1+\text{e}^{-\sum_{j=1}^{J} W_{j,k} i_j + b_k}} \tag{4.16}$$

The tansig transfer function is written as:

$$f = \frac{1-\text{e}^{-\text{net}}}{1+\text{e}^{-\text{net}}} \tag{4.17}$$

where *net* is the net of output nodes of Eq. (4.12).

The output for output nodes with the tansig function could be written as:

$$O_z = f\left(\text{net\_output}\right) = \frac{1-\text{e}^{-\sum_{k=1}^{K} W_{k,z} h_k + b_z + b_k}}{1+\text{e}^{-\sum_{k=1}^{K} W_{k,z} h_k + b_z + b_k}} = \hat{R}_a \tag{4.18}$$

The $\hat{R}_a$ value obtained using Eq. (4.18) contains the error. The error value is obtained using following equation:

$$\text{error} = ERR = \frac{1}{2}\left(R_a - \hat{R}_a\right)^2 \tag{4.19}$$

where R_a is the experimental surface roughness value and $\hat{R}_a$ is the predicted value from the ANN model. The error must be reduced by applying the BP algorithm. The error given by Eq. (4.19) is determined by MATLAB software using performance function. Some of the commonly applied performance functions for predicting surface roughness are mean absolute error (MAE), sum square error (SSE), root mean squared error (RMSE), and mean absolute percentage error (MAPE). Since most of the previous studies applied the MSE performance function, therefore this performance function was applied for determining the error in predicting the surface roughness value. The BP algorithm is applied in the multilayer feedforward network structure to reduce the error. In an BP algorithm the input are presented to the network and the error is calculated.

The sensitivities are propagated from output layer to the first layer and then weights and biases are updated. The weights of the connections between input and hidden nodes $(W_{j,k})$ and bias on the hidden nodes (b_k) are updated using Eqs. (4.20) and (4.21) respectively.

$$\Delta W_{j,k} = -\eta \frac{\partial ERR}{\Delta \partial W_{j,k}} \tag{4.20}$$

$$\Delta b_k = -\eta \frac{\partial ERR}{\Delta \partial b_k} \tag{4.21}$$

The weights of the connections between hidden and output nodes ($W_{k,z}$) and bias on the output nodes (b_z) are updated using Eqs. (4.22) and (4.23) respectively.

$$\Delta W_{k,z} = -\eta \frac{\partial ERR}{\Delta \partial W_{k,z}} \tag{4.22}$$

$$\Delta b_z = -\eta \frac{\partial ERR}{\Delta \partial b_z} \tag{4.23}$$

In Eqs. (4.20) – (4.23), η is the learning rate which should be selected to be as small as possible for a true approximation and at the same time as large as possible to speed up the convergence. Smaller learning rates tend to slow the learning process while larger learning rates may cause oscillation in the weight space. A momentum parameter α can be used to allow for larger learning rates resulting in faster convergence while minimizing the tendency for oscillation. The effect of momentum factor for the updated weights is given by Eqs. (4.24) and (4.25).

$$\Delta W_{j,k} = -\eta \frac{\partial ERR}{\Delta \partial W_{j,k}} + \alpha \Delta W_{j,k} \tag{4.24}$$

$$\Delta W_{k,z} = -\eta \frac{\partial ERR}{\Delta \partial W_{k,z}} + \alpha \Delta W_{k,z} \tag{4.25}$$

To reduce the value of error algorithm during training and learning, the training function and the learning function are used. Various training functions applied by the researchers are: trainbr (Bayesian regularization), traingd (gradient descent BP), traingda (gradient

descent with adaptive learning rule BP), traingdm (gradient descent with momentum BP), traingdx (gradient descent with momentum and adaptive learning rule BP), and trainlm (Levenberg–Marquardt BP). Examples of learning functions are: learngd (gradient descent weight/bias learning function), learngdm (gradient descent with momentum weight/bias learning function). Since, most previous studies applied the traingdx training function and learngd learning function (Table 4.4), therefore, these two functions were used in this study. To get a successful model, the values of learning rate η and momentum factor α will be determined during the training process by the assistance of the Matlab ANN tool box.

4.5.2 Selected ANN parameters

Section 4.5.1 provides the required knowledge to start trial and error, with better ANN parameters for the study, to get accurate results in the minimum time and cost. The selected parameters after trial and error are shown in Table 4.7.

Table 4.7: Selected ANN parameters for surface roughness prediction

Selected ANN parameter	Value
Network structure	3-7-1
Training/testing data	22/5
Network algorithm	Feedforward back propagation
Transfer function	logsig, tansig
Training function	traingdx
Learning function	learngd
Performance function	MSE
Learning rate	0.14
Momentum rate	0.05

4.5.3 Results and discussion

The neural network described in the previous section was trained using the selected parameters. The mean square error decreased with the increasing iteration numbers until 250 iterations and after this point it remained constant as shown in Figure 4.17.

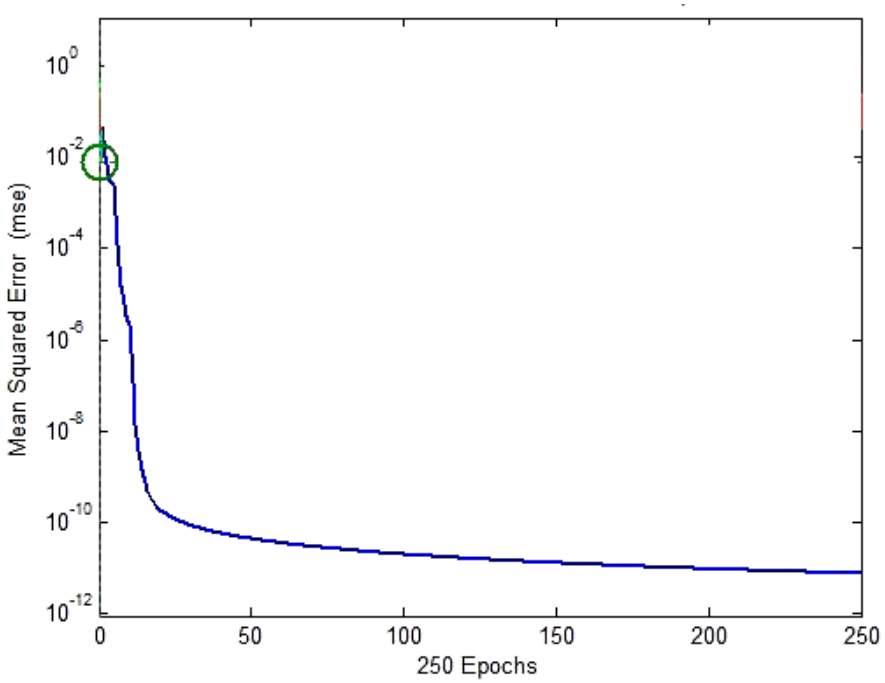

Figure 4.17: Iteration number versus mean square error

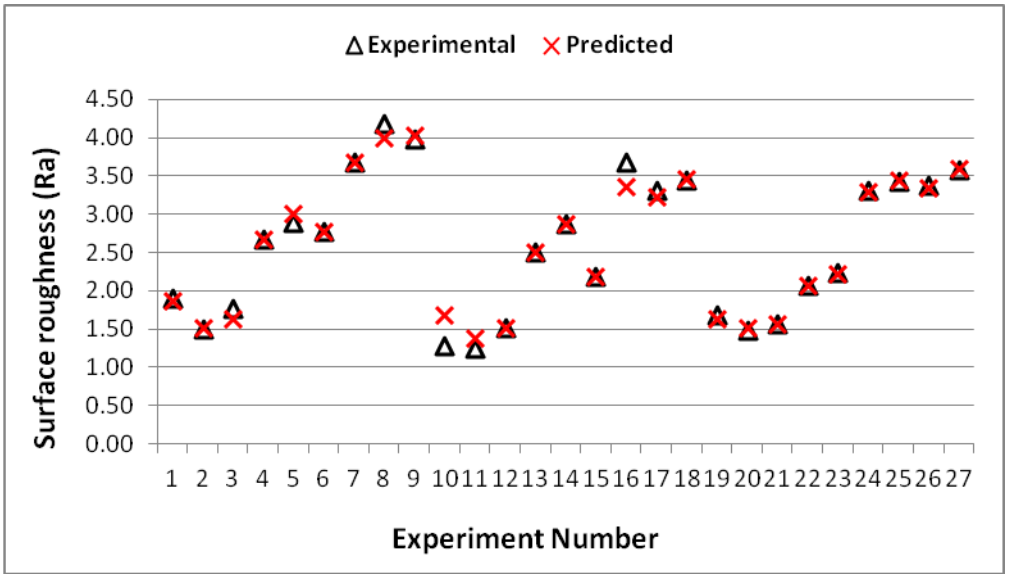

Figure 4.18: Experimentally measured and ANN predicted values of surface roughness

Therefore, the training of the algorithm was stopped at 250 iterations. After that, the ANN was tested for accuracy using the random test values selected from the experimental results which had not been used for the learning process. The predicted results of the data set are shown in Figure 4.18 and Table 4.8. It can be seen that in most cases the neural network prediction is very close to the experimental value. The mean relative error between the experimental and predicted values is 3.07%.

Table 4.8: Experimental and predicted values of surface roughness using ANN

Experiment No.	Surface roughness (R_a) (μm)	
	Experimental	ANN
1	1.907	1.879
2	1.499	1.515
3	1.776	1.643
4	2.684	2.680
5	2.902	3.006
6	2.769	2.775
7	3.685	3.686
8	4.185	3.996
9	3.983	4.027
10	1.284	1.686
11	1.257	1.388
12	1.517	1.519
13	2.514	2.515
14	2.884	2.873
15	2.194	2.182
16	3.687	3.361
17	3.318	3.225
18	3.447	3.457
19	1.683	1.641
20	1.483	1.518
21	1.565	1.568
22	2.069	2.072
23	2.232	2.225
24	3.320	3.297
25	3.430	3.451
26	3.381	3.351
27	3.574	3.600

4.6 Comparison and Validation of the Proposed Predictive Models

The results obtained from the proposed predictive modelling techniques of RSM, SVR and ANN are shown in Table 4.9 for comparison with each other.

Table 4.9: Predicted values and relative errors for modelling techniques (RSM, SVR and ANN) for surface roughness

Experiment No.	Surface roughness (μm)				Relative Error (%)		
	Experimental	RSM	SVR	ANN	RSM	SVR	ANN
1	1.907	1.745	1.897	1.879	8.506	0.509	1.479
2	1.499	1.660	1.547	1.515	10.755	3.221	1.108
3	1.776	1.665	1.786	1.643	6.247	0.574	7.473
4	2.684	2.875	2.694	2.680	7.148	0.388	0.138
5	2.902	2.809	2.892	3.006	3.209	0.341	3.598
6	2.769	2.832	2.779	2.775	2.256	0.350	0.220
7	3.685	3.953	3.576	3.686	7.276	2.959	0.019
8	4.185	3.905	4.175	3.996	6.700	0.241	4.530
9	3.983	3.946	3.832	4.027	0.928	3.791	1.122
10	1.284	1.374	1.294	1.686	7.014	0.810	31.380
11	1.257	1.370	1.688	1.388	8.997	34.302	10.407
12	1.517	1.456	1.507	1.519	4.058	0.679	0.105
13	2.514	2.429	2.504	2.515	3.384	0.414	0.036
14	2.884	2.444	2.547	2.873	15.269	11.699	0.371
15	2.194	2.547	2.312	2.182	16.134	5.394	0.547
16	3.687	3.432	3.677	3.361	6.919	0.274	8.852
17	3.318	3.464	3.328	3.225	4.413	0.307	2.809
18	3.447	3.586	3.235	3.457	4.025	6.153	0.273
19	1.683	1.437	1.673	1.641	14.598	0.565	2.467
20	1.483	1.537	1.473	1.518	3.642	0.681	2.353
21	1.565	1.727	1.900	1.568	10.356	21.439	0.204
22	2.069	2.396	2.470	2.072	15.775	19.358	0.106
23	2.232	2.514	2.280	2.225	12.622	2.130	0.336
24	3.320	2.722	2.791	3.297	18.008	15.922	0.693
25	3.430	3.302	3.372	3.451	3.743	1.690	0.609
26	3.381	3.438	3.208	3.351	1.701	5.102	0.879
27	3.574	3.664	3.584	3.600	2.522	0.288	0.730

The relative percentage error between the fitted values predicted by the three methods and the experimental values of the surface roughness are computed using the following equation.

$$\text{Relative Error (\%)} = \frac{|\text{Predicted value - Experimental value}|}{\text{Experimental Value}} \text{X } 100 \qquad (4.25)$$

Table 4.9 and Figure 4.19 show the relative errors for the modelling techniques.

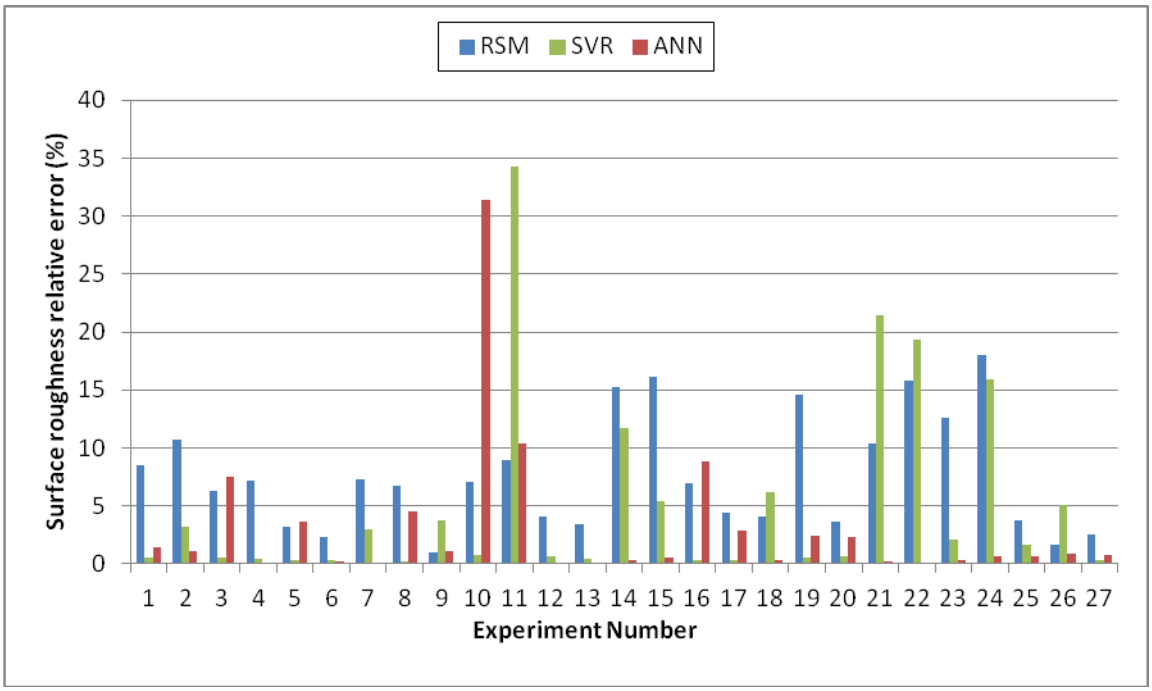

Figure 4.19: Deviation of surface roughness predicted values from the experimental values

The mean relative error by RSM, SVR and ANN models is 7.64%, 5.17% and 3.07% respectively. Mean relative error illustrates that the ANN performs better as compared to SVR and RSM. It shows that the well trained network model can take an optimal performance and has greater accuracy in predicting surface roughness as compared to RSM and SVR. All the methods are suitable for predicting the surface roughness in an acceptable range. But, the model generation and training procedure of ANN took more time as compared to SVR.

To compare the goodness of fit of the RSM, SVR and ANN models, some representative hypothesis tests were conducted and results are shown in Table 4.10. These tests are *t*-test to test the means, *f*-test and Levene's test for variance. In all these tests, the *p*-values are greater than 0.05, which means that the null hypothesis cannot be rejected. The *p*-values in the Table 4.10 also indicate that there is no significant evidence to conclude that the experimental data and the data predicted by RSM, SVR and ANN models differ. Therefore, all predictive models have statistically satisfactory goodness of fit from the modelling point of view.

Table 4.10: Hypothesis testing to compare the models at 95% confidence level using p-value (surface roughness)

Tests	***p*-value**		
	RSM	**SVR**	**ANN**
Mean paired *t*-test	1.000	0.840	0.882
Variance *F*-test	0.869	0.624	0.802
Levene's test	0.666	0.386	0.784

It is evident that ANN and SVR models provide good prediction capabilities in comparison to RSM because they generally offer the ability to model more complex non-linearity and interactions. Further, the developed predictive models were integrated with the optimization methods – response surface methodology and genetic algorithm – to determine the cutting conditions for minimum surface roughness.

4.7 Surface Roughness Optimization

After developing predictive models to predict the surface roughness, the next logical step is surface roughness optimization with respect to cutting conditions. Selection of optimum cutting conditions has always been a challenge in the machining. Low surface

roughness values can be achieved by adjusting cutting conditions with the help of appropriate optimization methods. Therefore, the process parameters are defined in the standard optimization format to be solved by optimization algorithms. The optimization of the performance measures is carried out by using response surface methodology and genetic algorithms.

Problem formulation

The surface roughness optimization problem is formulated using RSM as:

$$\text{Minimize } 1.67023 - 0.0527596\,v + 38.7308\,f - 1.08526\,d + 0.000191348\,v^2 - 16.5660\,f^2 + 0.179244\,d^2 - 0.0606859\,vf + 0.00521919\,vd + 0.899583\,fd$$

Subject to:

$$103.31 \text{ m/min} \le v \le 174.14 \text{ m/min}$$

$$0.12 \text{ mm/rev.} \le f \le 0.16 \text{ mm/rev.}$$

$$0.5 \text{ mm} \le d \le 1.5 \text{ mm}$$

4.7.1 Surface roughness optimization using response surface methodology

The method of desirability function analysis associated in RSM was proposed by Derringer and Suich in 1980. This method is based on the reduced gradient algorithm, which starts with multiple solutions and finally obtains the maximum value of the desirability to determine the optimal solution (Maji et al., 2013). The desirability function is based on the idea that the quality of a product or process that has many features is completely unacceptable if one of them is outside the "desirable" limit (Candioti et al., 2014). Several researchers have used desirability function analysis to optimize surface roughness (Bhushan, 2013; Hessainia et al., 2013; Naveen Sait et al., 2009; Sarıkaya and Güllü, 2014). In the single objective minimization problem, the first step of the desirability function analysis is to calculate the desirability index (d) using Eq. (4.26). The scale of the desirability function ranges between 0 and 1. If d = 0 or approaches 0 then the response is

completely unacceptable and if d = 1 or approaches to 1 then the response is perfectly on the target value. There are three types of individual desirability functions: a) the larger the better, b) the smaller the better and c) the nominal the better. In this study, the desirability function was selected as the smaller the better because minimum surface roughness is to be achieved with optimization of machining parameters. The desirability function for the single objective minimization problem is given below:

$$\begin{aligned} d &= 1 \text{ if } y \le y_{\min} \\ d &= \left(\frac{y - y_{\max}}{y_{\min} - y_{\max}} \right)^r, y_{\min} \le y \le y_{\max} \\ d &= 0 \text{ if } y \ge y_{\max} \end{aligned} \tag{4.26}$$

where the y is the value of the output during optimization processes, y_{min} and y_{max} are the lower tolerance limit and the upper tolerance limit in the response parameter experimental data.

The individual response optimization analysis has been performed for achieving the minimum surface roughness based on the predicted mathematical model given by Eq. (4.8). Desirability function analysis optimization results for surface parameters are shown in Figure 4.20 and Table 4.11. Optimal machining parameters obtained are – cutting speed of 149.09 m/min at feed rate of 0.12 mm/rev and 0.56 mm depth of cut. The optimized surface roughness obtained is (R_a) 1.387 μm. The desirability value is 0.976, which is very close to 1.0.

Table 4.11: Response optimization for surface roughness

Response	Goal	Optimum Combination			Lower	Target	Upper	Predicted	Desirability
		v	*f*	*d*					
R_a	Min.	149.09	0.12	0.56	1.257	1.257	4.185	1.387	0.976

Figure 4.20 shows the surface roughness optimization plots for parameters *v*, *f* and *d*. Each column of the graph corresponds to a factor. Each row of the graph corresponds to the response. Each cell of the graph shows how the response changes as a function of one of the factors, while all other factors remain fixed. The numbers displayed at the top of a column show the current factor level settings and the high and low settings of factor in the experimental design.

The current optimal parameter settings are: cutting speed of 149.09 m/min, feed rate of 0.12 mm/rev. and depth of cut of 0.56 mm for achieving the minimum surface roughness. The composite desirability (D) is displayed in the upper left corner of the graph. The label above composite desirability refers to the current setting and changes interactively with the factor settings. The optimal response plot is generated using MINITAB software. The vertical lines inside the graph represent current optimal parametric settings. The horizontal dotted lines represent the current response values.

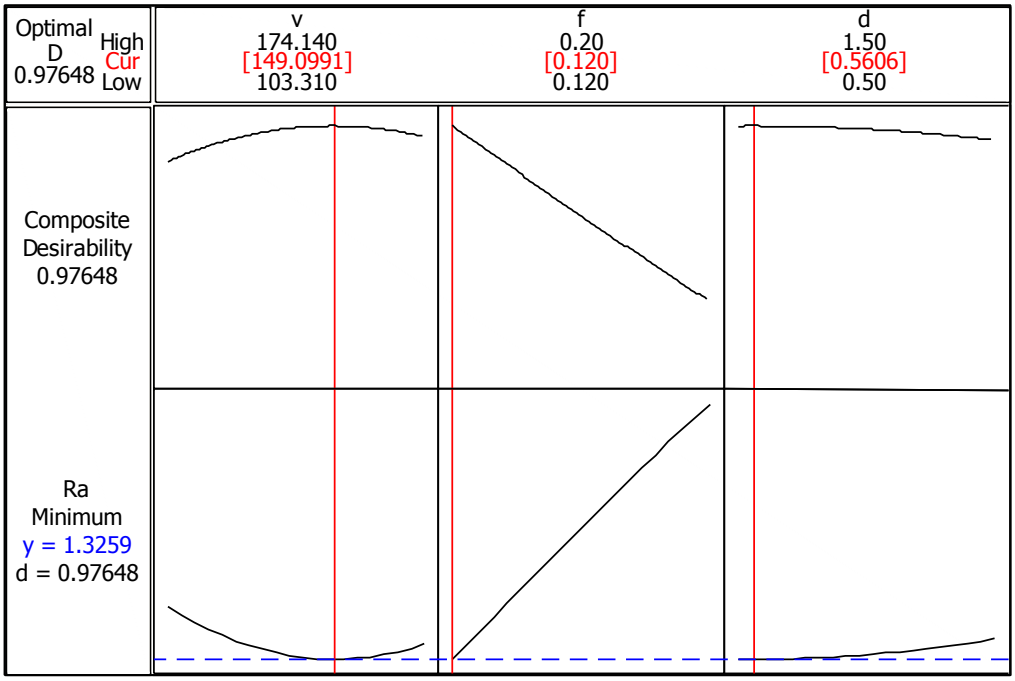

Figure 4.20: Response optimization plot for surface roughness

4.7.2 Surface roughness optimization using Genetic Algorithm

A genetic algorithm has been developed to solve the formulated problem. Genetic algorithms are random probabilistic search techniques. They emulate the natural process of evolution and hereditary by processing towards the optimum (Al-Sultan et al., 1996). The process of evolution and adaptation of individuals in nature is based on the Darwin's 'survival of fittest' principle wherein the *stronger (fitter)* individuals are more likely to survive in their environment than the *weaker* individuals. As a result, they can live longer and reproduce more often, generating new generations even stronger than themselves. Holland (1975) showed that a computer simulation of this process of natural adaptation could be employed for solving optimization problems. Goldberg (1989) gives detailed insight into different aspects of the genetic algorithms. In genetic algorithms the population, selection policy, genetic operators, and termination criteria play important role in providing efficient solutions.

Population

The search technique consists of generating an initial population at random. The population is a subset of the total solution space at any instant of the solution process. Any feasible solution of the problem called chromosome is an element of the population. Chromosomes (strings) are combinations of symbols, known as genes, which represent the individual characteristics of the chromosome. The successive generations (children) of the population are generated from the current population (parents) by a process known as *selection*.

Selection for reproduction

Reproduction is the first operator applied on a population. In this process individual strings are copied into a separate string called the 'mating pool' according to their fitness

values, i.e. the strings with a better value have a higher probability of contributing one or more offspring in the next generation.

Genetic operators

Two classical operators most commonly used are crossover and mutation operators. The exploration of search space is critically dependent on the genetic operators (Suresh et al., 1995). The crossover operator operates on two chromosomes and generates the offspring. Crossover is the exchange of sub strings between selected parents. Since it is an inheritance mechanism, the offspring inherits some characteristics of the parents (Islier, 1998). The standard crossover operators usually applied are the simple crossover, the partially matched crossover (PMX), the order crossover (OX), and the cyclic crossover (CX) (Goldberg, 1989). Other types of crossover can be used depending on the specific applications. Mutation operator makes random changes to one or more elements in a solution string. According to Goldberg (1989), when sparingly used with reproduction and crossover, it is an insurance against premature loss of important notions. Austin (1990) suggested some advanced strategies to increase the efficiency of genetic algorithms. One of these strategies - elitism is employed to prevent destruction of the good solutions by genetic operators. Elitism ensures that the best solution of each population is copied to the next generation.

Termination criteria

To get an optimal solution, the generated population is evaluated by employing a certain fitness criterion. Some conditions for obtaining the best fitness function are (Zain et al., 2010):

- The algorithm stops when the number of generations reaches the value of generations.
- The algorithm stops after running for an amount of time equal to the time limit.

- The algorithm stops when the value of the fitness function for the best point in the current population is less than or equal to the fitness limit.
- The algorithm stops when the average relative change in the fitness function value over stall generations is less than function tolerance.
- The algorithm stops if there is no improvement in the objective function during an interval of time equal to stall time limit.

The solution of an optimization problem with GA algorithm begins with a set of potential solutions known as chromosomes. The entire sets of these chromosomes comprise populations which are randomly selected. The chromosomes evolve during several iterations or generations. New generations known as offsprings are generated by utilizing the crossover and mutation techniques. The genetic algorithm repeatedly modifies a population of individual solutions. At each step, the genetic algorithm selects individuals from the current population to be parents and uses them to produce the children for the next generation. Over successive generations, the population evolves toward an optimal solution.

GA methodology for the proposed model

The GA methodology used to optimize the machining parameters is shown in Figure 4.21. In this study a set of *v*, *f* and *d* corresponds to a chromosome. Values of *v*, *f* and *d* are the three genes of a chromosome. In first step, a population comprising of *n* sets of *v*, *f* and *d* is generated randomly. This population is the current generation. The set of *v*, *f* and *d* that gives smaller surface roughness by Eq. (4.8) is considered as better or "fitter" than others. Using members of the current population, GA generates another population of *n* sets of *v*, *f* and *d* using three operators, *viz.* selection, cross-over and mutation. This is analogous to next generation being obtained from current generation in biological evolution. Selection operator chooses chromosomes from the population for reproduction.

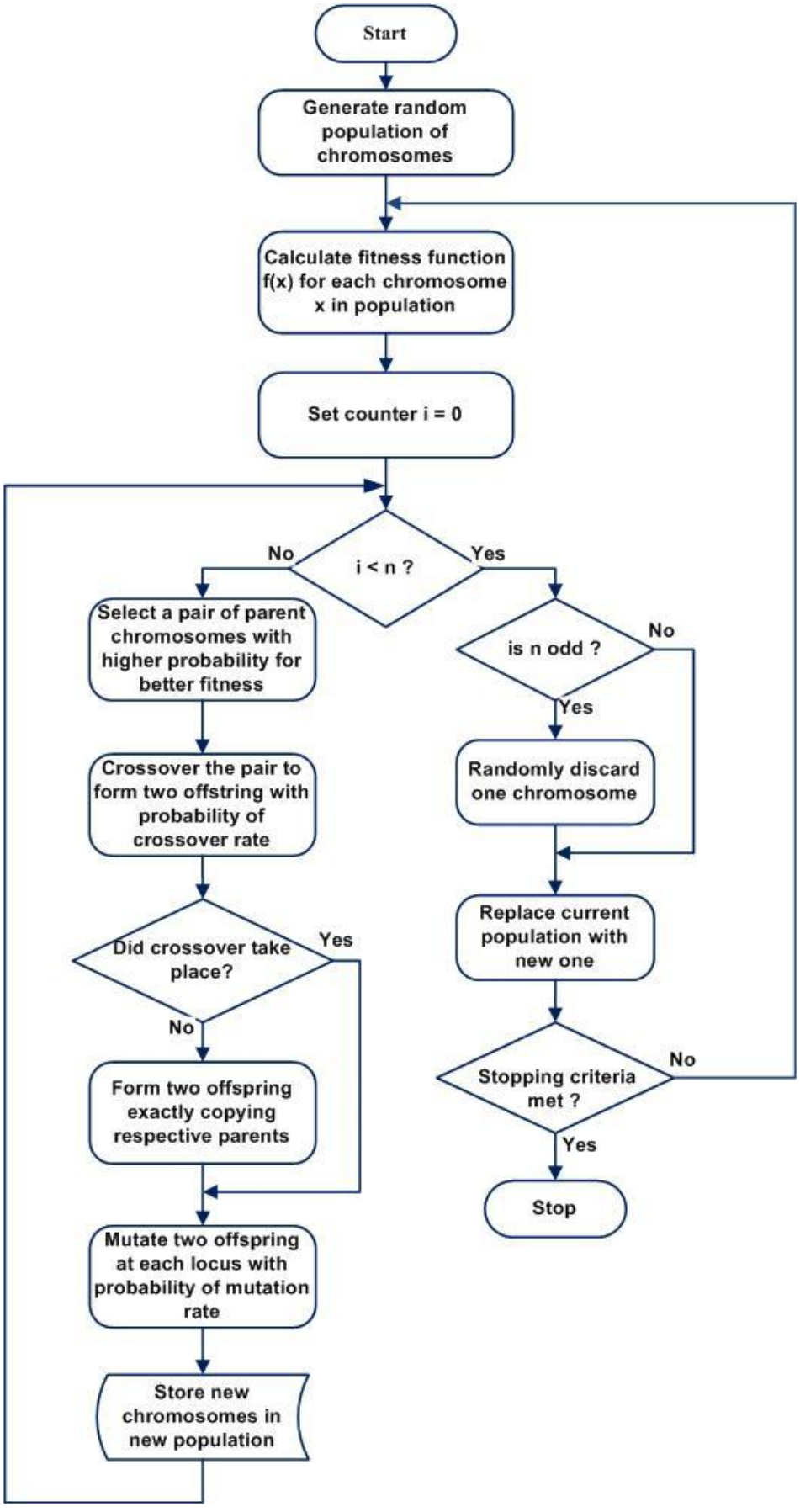

Figure 4.21: Genetic algorithm methodology for the proposed model

The fitter the chromosome, the more times it is likely to be selected to reproduce. Thus, selection is "with replacement", i.e. same chromosome can be selected as a parent more than once. Crossover operator is used to randomly choose a locus from a bit string and exchange the sub-sequences before and after the locus between the parent chromosomes to create offspring. For instance, 01001001 and 11111111 could be crossed over after the fifth locus in each to produce two offspring 01001111 and 11111001. Mutation operator randomly flips some of the bits in a chromosome from current population to generate a new set so that the algorithm does not get trapped in local optima. In addition to cross-over and mutation, a fraction of the current population that is elite, i.e. "fitter" than others is passed on without any change to the next generation. Because all the members of next generation are obtained from the fitter members of current population the overall fitness of population in successive generation improves. After some number of iterations, if the improvement in fitness falls below a set tolerance limit then the algorithm is stopped.

Optimization toolbox of MATLAB was used for implementing GA. After several number of trials using the MATLAB optimization toolbox, the best combination of the parameters that lead to the minimum values of the fitness function are: A population size of 200 and initial population range covering the entire range of values for *v, f* and *d* were used to avoid trapping in local minima. The cross over rate used was 0.8 and mutation function was "uniform". The scaling function and selection function were "rank" and "uniform" respectively.

The optimal response variable and machining parameters obtained by GA are shown in Figure 4.22. It is indicated that the optimal solution is obtained at the 29^{th} generation (iteration) of the algorithm. Based on the result of Figure 4.22, it is observed that the

criterion used by the GA algorithm to stop the optimal solution is the average relative change in the fitness function value over stall generations, which is less than function tolerance. It can be observed that the results of GA and desirability function analysis are similar to each other.

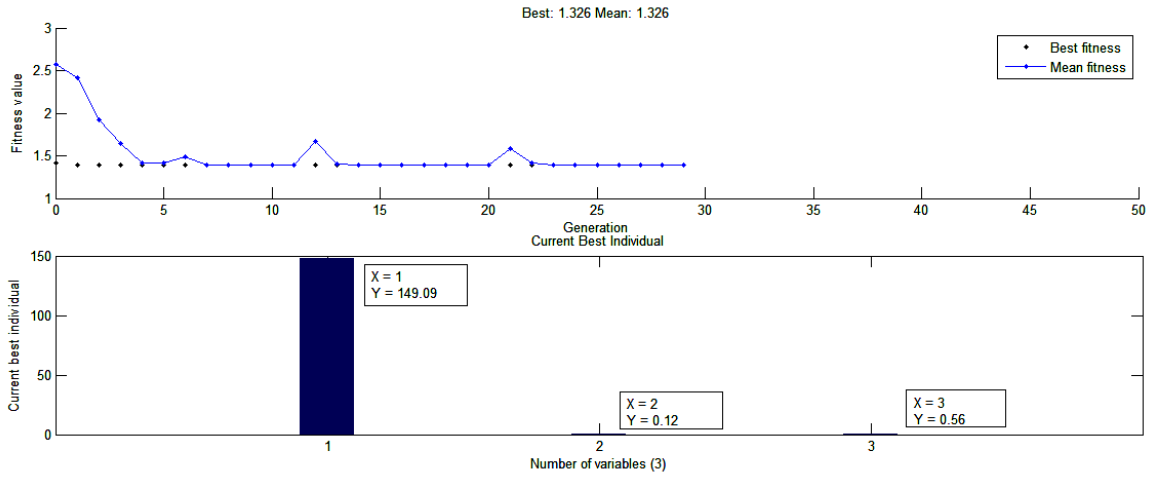

Figure 4.22: Variation of best fitness with generations and the corresponding optimal machining parameters

4.8 Experimental Confirmation

The confirmation experiments were performed to facilitate the verification of the obtained feasible optimal machining parameters (v = 149.09 m/min, f = 0.12 mm/rev and d = 0.56 mm) for the surface roughness. The results of the confirmation runs for the response R_a are listed in Table 4.12. The error between the predicted and the confirmation results is 4.67%.

Table 4.12 Confirmation results for surface roughness

Optimum cutting parameters			Surface roughness (µm)						Validation error (%)
			Experimental				RSM	GA	
v (m/min)	f (mm/rev.)	d (mm)	Run 1	Run 2	Run 3	Average			
149.09	0.12	0.56	1.387	1.392	1.393	1.390	1.326	1.326	4.67

4.9 Conclusions

In this chapter, predictive and optimization models have been presented to determine the machining parameters leading to minimum surface roughness. Three empirical models for prediction of surface roughness have been developed using RSM, SVR and ANN. The optimization models have been developed using RSM and GA to find the values of machining parameters leading to minimum surface roughness. Further the confirmation experiments are carried out to validate that the developed predictive and optimization models match with the experimental results for machining of AISI 1045 steel. The following conclusions are drawn from the study:

- The results of ANOVA reveal that the developed mathematical model using RSM allows prediction of surface roughness within 7.64% error. Feed rate is the main influencing factor on the surface roughness with 89.22% contribution, followed by the cutting speed with 1.57% contribution in the total variability of model. The depth of cut, quadratic and interaction effects of machining parameters do not have statistical significance on surface roughness. The 3D surface plots can be used for estimating the surface roughness values for any combination of the machining parameters within the suitable range. This is very useful in practice for the operator or the part programmer. These plots can also be used by the machine tool designers during the design of machine tools to estimate the suitable range of parameters to be provided.
- SVR is capable of accurately predicting the surface roughness during turning operations. The mean relative error between the predicted and experimental values was found to be 5.17%.
- The predictive model developed using the ANN shows that the surface roughness values could be obtained with the selected ANN parameters. ANN has provided a close relation between the predicted values and the experimental values. The mean

relative error between the predicted and the experimental values using ANN is 3.07%. It has been found that the model developed using ANN is capable of predicting accurately using a small number of training samples.

- The developed predictive models are compared using relative error and validated using hypothesis testing. It has been found that ANN and SVR models are better than RSM for predicting surface roughness. The mean relative errors for ANN and RSM models are 3.07% and 7.64% respectively. Also, among ANN and SVR, ANN performs better as compared to SVR.
- Low feed rate and high cutting speed were found to provide better surface finish within the specific test range using the desirability function analysis and genetic algorithms. Moreover, desirability function analysis and GA provided similar results.
- Confirmations experiments carried out using the optimum machining parameters show that the developed predictive and optimization model can be used for turning of AISI-1045 steel within 4.67% error.

References

Al-Ahmari, A.M.A., 2007. Predictive machinability models for a selected hard material in turning operations. J. Mater. Process. Technol. 190, 305–311.

Al-Sultan, K.S., Hussain, M.F., Nizami, J.S., 1996. A genetic algorithm for the set covering problem. J. Oper. Res. Soc. 702–709.

Arrazola, P.J., Umbrello, D., Davies, M., Jawahir, I.S., 2013. Recent advances in modelling of metal machining processes. CIRP Ann. - Manuf. Technol. 62, 695–718.

Austin, S., 1990. An introduction to genetic algorithms. AI Expert 5, 48–53.

Basheer, A.C., Dabade, U. A., Joshi, S.S., Bhanuprasad, V.V., Gadre, V.M., 2008. Modeling of surface roughness in precision machining of metal matrix composites using ANN. J. Mater. Process. Technol. 197, 439–444.

Beale, M.H., Hagan, M.T., Demuth, H.B., 2014. Neural Network Toolbox™ User's Guide R 2014a.

Benardos, P.G., Vosniakos, G., 2003. Predicting surface roughness in machining : a review. Int. J. Mach. Tools Manuf. 43, 833–844.

Bhushan, R.K., 2013. Optimization of cutting parameters for minimizing power consumption and maximizing tool life during machining of Al alloy SiC particle composites. J. Clean. Prod. 39, 242–254.

Box, G., Draper, N., 1987. Empirical model-building and response surface, Empirical model-building and. John Wiley & Sons, New York.

Candioti, L.V., De Zan, M.M., Cámara, M.S., Goicoechea, H.C., 2014. Experimental design and multiple response optimization. Using the desirability function in analytical methods development. Talanta 124, 123–38.

Çaydaş, U., Ekici, S., 2012. Support vector machines models for surface roughness prediction in CNC turning of AISI 304 austenitic stainless steel. J. Intell. Manuf. 23, 639–650.

Cetin, M.H., Ozcelik, B., Kuram, E., Demirbas, E., 2011. Evaluation of vegetable based cutting fluids with extreme pressure and cutting parameters in turning of AISI 304L by Taguchi method. J. Clean. Prod. 19, 2049–2056.

Cus, F., Zuperl, U., 2006. Approach to optimization of cutting conditions by using artificial neural networks. J. Mater. Process. Technol. 173, 281–290.

Davim, J.P., 2001. A note on the determination of optimal cutting conditions for surface finish obtained in turning using design of experiments. J. Mater. Process. Technol. 116, 3–6.

Davim, J.P., Gaitonde, V.N., Karnik, S.R., 2008. Investigations into the effect of cutting conditions on surface roughness in turning of free machining steel by ANN models. J. Mater. Process. Technol. 205, 16–23.

Diniz, A.E., Micaroni, R., 2002. Cutting conditions for finish turning process aiming: the use of dry cutting. Int. J. Mach. Tools Manuf. 42, 899–904.

Drucker, H., Burges, C. J. C., Kaufman, L., Smola, A., & Vapnik, V., 1997. Drucker. Adv. Neural Inf. Process. Syst. 9, NIPS 1996 155–161.

Erzurumlu, T., Oktem, H., 2007. Comparison of response surface model with neural network in determining the surface quality of moulded parts. Mater. Des. 28, 459–465.

Ezugwu, E.O., Fadare, D. A., Bonney, J., Da Silva, R.B., Sales, W.F., 2005. Modelling the correlation between cutting and process parameters in high-speed machining of Inconel 718 alloy using an artificial neural network. Int. J. Mach. Tools Manuf. 45, 1375–1385.

Goldberg, D.E., 1989. Genetic Algorithms in Search, Optimization, and Machine Learning, NN Schraudolph and J. Addison-Wesley, MA.

Grzesik, W., Brol, S., 2003. Hybrid approach to surface roughness evaluation in multistage machining processes. J. Mater. Process. Technol. 134, 265–272.

Gupta, A.K., 2010. Predictive modelling of turning operations using response surface methodology, artificial neural networks and support vector regression. Int. J. Prod. Res. 48, 763–778.

Hassan, G.A., Suliman, S.M.A., 1990. Experimental modelling and optimization of turning medium carbon steel. Int. J. Prod. Res. 28, 1057–1065.

Hessainia, Z., Belbah, A., Yallese, M.A., Mabrouki, T., Rigal, J.-F., 2013. On the prediction of surface roughness in the hard turning based on cutting parameters and tool vibrations. Measurement 46, 1671–1681.

Holland, J.H., 1975. Adaptation in natural and artificial systems: An introductory analysis with applications to biology, control, and artificial intelligence. U Michigan Press.

Islier, A. A., 1998. A genetic algorithm approach for multiple criteria facility layout design. Int. J. Prod. Res. 36, 1549–1569.

Jacek M. Zurada, 1992. Introduction to Artificial Neural Sustems. WEST Publishing Company, New York.

Kant, G., Sangwan, K.S., 2014. Prediction and optimization of machining parameters for minimizing power consumption and surface roughness in machining. J. Clean. Prod. 83, 151–164.

Karayel, D., 2009. Prediction and control of surface roughness in CNC lathe using artificial neural network. J. Mater. Process. Technol. 209, 3125–3137.

Kohli, A., Dixit, U.S., 2005. A neural-network-based methodology for the prediction of surface roughness in a turning process. Int. J. Adv. Manuf. Technol. 25, 118–129.

Lippmann, R.P., 1987. An introduction to computing with neural nets. IEEE Mag. Acoust. Signal Speech Process. 4–22.

Luong, L.H.S., Spedding, T. A., 1995. A neural-network system for predicting machining behaviour. J. Mater. Process. Technol. 52, 585–591.

Maji, K., Pratihar, D.K., Nath, A. K., 2013. Experimental investigations and statistical analysis of pulsed laser bending of AISI 304 stainless steel sheet. Opt. Laser Technol. 49, 18–27.

Nalbant, M., Gökkaya, H., Toktaş, İ., Sur, G., 2009. The experimental investigation of the effects of uncoated, PVD- and CVD-coated cemented carbide inserts and cutting parameters on surface roughness in CNC turning and its prediction using artificial neural networks. Robot. Comput. Integr. Manuf. 25, 211–223.

Naveen Sait, A., Aravindan, S., Noorul Haq, A., 2009. Optimisation of machining parameters of glass-fibre-reinforced plastic (GFRP) pipes by desirability function analysis using Taguchi technique. Int. J. Adv. Manuf. Technol. 43, 581–589.

Oktem, H., Erzurumlu, T., Erzincanli, F., 2006. Prediction of minimum surface roughness in end milling mold parts using neural network and genetic algorithm. Mater. Des. 27, 735–744.

Parrella, F., 2007. Online Support Vector Regression Online Support Vector Machines for Regression.

Puertas Arbizu, I., Luis Pérez, C.J., 2003. Surface roughness prediction by factorial design of experiments in turning processes. J. Mater. Process. Technol. 143-144, 390–396.

Sahin, Y., Motorcu, A.R., 2005. Surface roughness model for machining mild steel with coated carbide tool. Mater. Des. 26, 321–326.

Salat, R., Osowski, S., 2004. Accurate Fault Location in the Power Transmission Line Using Support Vector Machine Approach. IEEE Trans. Power Syst. 19, 979–986.

Sanjay, C., Jyothi, C., 2006. A study of surface roughness in drilling using mathematical analysis and neural networks. Int. J. Adv. Manuf. Technol. 29, 846–852.

Sanjay, C., Jyothi, C., Chin, C.W., 2006. A study of surface roughness in drilling using mathematical analysis and neural networks. Int. J. Adv. Manuf. Technol. 30, 906–906.

Sarıkaya, M., Güllü, A., 2014. Taguchi design and response surface methodology based analysis of machining parameters in CNC turning under MQL. J. Clean. Prod. 65, 604–616.

Shaw, M.., 1984. Metal Cutting Principles. Oxford University Press, Oxford, New York.

Suresh, G., Vinod, V. V, Sahu, S., 1995. A genetic algorithm for facility layout. Int. J. Prod. Res. 33, 3411–3423.

Tansel, I.N., Ozcelik, B., Bao, W.Y., Chen, P., Rincon, D., Yang, S.Y., Yenilmez, A., 2006. Selection of optimal cutting conditions by using GONNS. Int. J. Mach. Tools Manuf. 46, 26–35.

Vapnik, V., 1998. The support vector method of function estimation, in: Nonlinear Modeling. Springer, pp. 55–85.

Vapnik, V., 2000. The nature of statistical learning theory. springer, New York.

Zain, A.M., Haron, H., Sharif, S., 2010a. Prediction of surface roughness in the end milling machining using Artificial Neural Network. Expert Syst. Appl. 37, 1755–1768.

Zain, A.M., Haron, H., Sharif, S., 2010b. Application of GA to optimize cutting conditions for minimizing surface roughness in end milling machining process. Expert Syst. Appl. 37, 4650–4659.

Zhang, G., Patuwo, B.E., Hu, M.Y., 1998. Forecasting with artificial neural networks : The state of the art 14, 35–62.

Zuperl, U., Cus, F., 2003. Optimization of cutting conditions during cutting by using neural networks. Robot. Comput. Integr. Manuf. 19, 189–199.

Chapter 5

Predictive Modelling and Optimization for Power Consumption

In this chapter the experimental data of power consumption as a performance characteristic is used to develop power consumption predictive models using RSM, SVR and ANN techniques. Further, RSM and GA are used to obtain the machining parameters to optimize power consumption.

5.1 Introduction

The Indian economy has experienced unprecedented economic growth over the last decade (Green India Energy Summit, 2014). Today, India is the ninth largest economy in the world. This high order of sustained economic growth is placing enormous demand on its energy resources. India is the fourth-largest energy consumer in the world, trailing only the United States, China, and Russia (EIA, 2013). The New Policies Scenario (NPS) projects that India's share in world energy demand will increases from 5.5% in 2009 to 8.6% in 2035 (Ahn and Graczyk, 2012). India is largely dependent on fossil fuel imports to meet its energy demand which makes it politically vulnerable. In the year 2013, India's energy import was 42.9% of total primary energy consumption and it is expected to exceed 53% of the country's total energy consumption by 2030 (www.theenergyreport.com). The gross electricity generation (utilities) has increased from meager 4073 KWH in 1947 to 963722 GWH at the end of March, 2013. The electricity consumption (utilities and non-utilities) has increased from meager 4182 GWH in 1947 to 852903 GWH at the end of March, 2013. The growth of demand has overtaken the power supply and our country has been facing power shortage in spite of manifold growth over the years. Of the total electricity consumption in 2012-13, industry

sector accounted for the largest share (44.87%). As per the 18th Electric power survey, the electrical energy consumption is forecasted to be increased to 1098995 MU and 1611808 MU by the year 2016- 2017 and 2021- 2022 respectively. The demand and supply imbalance in energy is pervasive across all sources requiring serious efforts by Government of India to augment energy supplies. Global energy demand is expected to grow by 53% between 2008 and 2035 (Diaz et al., 2011).

Complex manufacturing facilities consume a significant amount of the electrical energy in industrial sectors to power motors, compressors and machine tools. The industrial sector accounts for about one-half of the world's total energy consumption and the consumption of energy by this sector has almost doubled over the last 60 years (Fang et al., 2011). Manufacturing sector has the largest share in energy consumed in the industrial sector. Machine tools consume high energy in the manufacturing plants and hence energy efficiency of machine tools is needed to be studied meticulously to achieve sustainability (Zhang, 2014). Energy and environmental issues have also become pertinent to all industries throughout the globe because of sustainable development issues. The global environmental problems caused by the consumption of natural resources and the pollution resulting during product life cycle (manufacture, use, end-of-life) have led to increasing political pressure and stronger regulations for the producers and users. Balogun and Mativenga (2013) reported that the use of carbon rich electricity generation sources is a global concern. Higher the consumption of electricity in manufacturing industries, higher the carbon footprints related to the manufactured products. The adoption of sustainable development in production offers industry a cost effective route to improve economic, environmental, and social performance (Pusavec et al., 2010a). With the implementation of sustainability principles in machining technologies, end-users have the potential to save money and improve their

environmental performance even if their production stays in the same range or decreases (Pusavec et al., 2010a). In machining processes, money saving and sustainability performance can be improved by reducing energy consumption (Pusavec et al., 2010b). On the production level, more focus needs to be devoted to the design and the management of machining technologies.

5.2 Power Consumption in Machine Tools

Machine tool is one of the typical production equipments widely used in the manufacturing industry. Machine tools have efficiency less than 30% (He et al., 2012) and more than 99% of the environmental impacts are due to the consumption of electrical energy used by the machine tools in discrete part manufacturing machining processes like turning and milling (Li et al., 2011). The cost of energy used over a ten-year period is about 100 times higher than the initial purchase cost of the machine tools used to manufacture products, and therefore, if energy consumption is reduced, the operating cost and the environment impact generated from power production are diminished (Pusavec et al., 2010b). According to Liow (2009) machine tool selection also plays an important role in reducing the energy footprint of a machined product. The replacement of machine tools may not be a viable alternative because of capital investment involved but the energy consumption during machining can be easily controlled by operating the machine tool at conditions requiring minimum energy. A survey of recent literature shows that current research has focused on power consumption models for machine tool components or machining processes (Li et al., 2014). Machine tools are the primary elements of a manufacturing system, which consume a significant amount of energy for machining. The energy is primarily analyzed by considering energy characteristics of energy-consuming components of machine tools. Machine tools require power during machining, build-up to machining,

post machining and in idling condition to drive motors and auxiliary equipments (Kant and Sangwan, 2014). However, the design of a machine tool is based on the peak power requirement during machining of material which is very high as compared to non-peak power requirement of the machine tools. This leads to higher inefficiency of energy in machine tools. The optimization of machining parameters for minimum power requirement is expected to lead to the application of lower rated motors, drives and auxiliary equipments and hence save power not only during machining but as well as during build-up to machining, post machining and idling condition. In addition to the machining parameters, the power requirement during machining also depends upon workpiece properties and cutting tool properties. In this study, the work material is steel and cutting tool material is uncoated tungsten carbide. This combination is the most widely used combination in the industry and any reduction in power consumption is expected to lead to high saving of power in absolute numbers.

Process models have often targeted the prediction of fundamental variables such as stresses, strains, strain rate, temperature, *etc*. but to be useful for industry these variables must be correlated to performance measures and product quality (accuracy, dimensional tolerances, finish, *etc*.) (Arrazola et al., 2013). Recent review papers on machining show that the most widely machining performances considered by the researchers are surface roughness followed by machining/production cost and material removal rate (Yusup et al., 2012). Recently, the researchers have started to analyze and optimize the power consumption in machining (Aggarwal et al., 2008; Camposeco-Negrete, 2013; Hanafi et al., 2012). Energy savings up to 6-40% can be obtained based on the optimum choice of cutting parameters, tools and the optimum tool path design (Newman et al., 2012).

5.3 Predictive Modelling for Power Consumption using Response Surface Methodology

5.3.1 Mathematical model

A mathematical model for the power consumption prediction based on the experimental results given in chapter 3 (Table 3.6) is developed using Eq. (4.7) given in chapter 4. The developed mathematical model to predict power consumption (P) is:

$$\begin{aligned} P = {} & 2.19766 - 0.0162660\,v - 10.0766\,f - 1.14194\,d \\ & + 0.0000226904\,v^2 + 4.47917\,f^2 + 0.104\,d^2 \\ & + 0.0610014\,vf + 0.007094506\,vd + 5.70833\,fd \end{aligned} \tag{5.1}$$

Predicted values of power consumption from the developed mathematical model and the experimental values are shown in Figure 5.1 and Table 5.1.

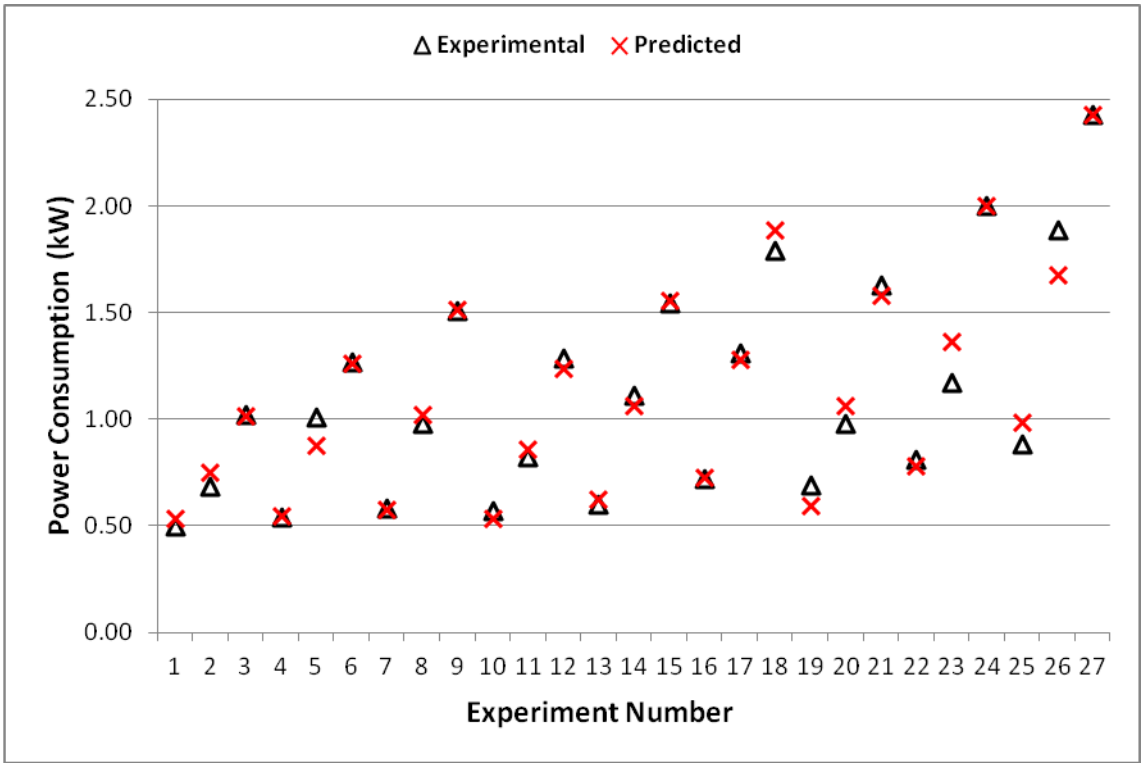

Figure 5.1: Experimentally measured and predicted values of power consumption

The comparison of predicted and experimental values shows that the predicted values of the power consumption are close to the experimental values. The mean relative error between the experimental and predicted values is 5.1%.

Table 5.1: Experimental and predicted values of power consumption

Experiment No.	Power consumption (P) (kW)	
	Experimental	RSM
1	0.497	0.535
2	0.684	0.751
3	1.021	1.019
4	0.543	0.548
5	1.013	0.878
6	1.269	1.261
7	0.586	0.576
8	0.980	1.020
9	1.512	1.517
10	0.574	0.535
11	0.824	0.861
12	1.285	1.239
13	0.604	0.624
14	1.115	1.064
15	1.547	1.556
16	0.721	0.727
17	1.309	1.281
18	1.794	1.887
19	0.690	0.598
20	0.982	1.066
21	1.631	1.585
22	0.815	0.785
23	1.173	1.366
24	2.002	2.000
25	0.883	0.985
26	1.888	1.681
27	2.430	2.428

5.3.2 Analysis of variance

Table 5.2 shows the ANOVA results for the linear [v, f, d,] quadratic [v^2, f^2, d^2] and interactive [($v \times f$), ($v \times d$), ($f \times d$)] factors. The last column of the Table 5.2 shows the percentage contribution of each source to the total variation indicating the degree of

influence on the results. Regression F-value of 80.08 indicates that the model is significant. The percentage contribution of each term is also shown in Figure 5.2.

Table 5.2: Analysis of variance (ANOVA) results

Source	**DOF**	**Seq. SS**	**Adj. SS**	**Adj. MS**	**F**	**p**	**% Contribution**
Regression	9	6.4714	6.4714	0.7191	80.08	0.000	97.69
Linear	3	6.0254	6.1153	2.0384	227.01	0.000	90.96
v	1	1.0860	1.0702	1.0702	119.18	0.000	16.40
f	1	0.8515	0.8777	0.8777	97.74	0.000	12.85
d	1	4.0879	4.1674	4.1674	464.10	0.000	61.71
Square	3	0.0091	0.0091	0.0030	0.34	0.800	0.14
*v*v*	1	0.0047	0.0047	0.0047	0.52	0.480	0.07
*f*f*	1	0.0003	0.0003	0.0003	0.03	0.855	0.00
*d*d*	1	0.0041	0.0041	0.0041	0.45	0.511	0.06
Interaction	3	0.4369	0.4369	0.1456	16.22	0.000	6.60
*v*f*	1	0.0901	0.0901	0.0901	10.03	0.006	1.36
*v*d*	1	0.1904	0.1904	0.1904	21.21	0.000	2.87
*f*d*	1	0.1564	0.1564	0.1564	17.42	0.001	2.36
Residual Error	17	0.1527	0.1527	0.0090			2.31
Total	26	6.6241					
R^2 = 0.9770		R^2(Pred.) = 0.9439		R^2(Adj.) = 0.9648			

DOF: Degree of freedom, SS: Sum of square, MS: Mean square

Depth of cut (*d*) was found to be the most significant factor on the power consumption which explains 61.71% contribution of total variation. The next contributions on the power consumption come from the cutting speed and feed rate having contribution of 16.40% and 12.85% respectively. The quadratic terms [v^2, f^2, d^2] do not have statistical significance on

power consumption because they have much lower level of contribution and their p-value is also more than the confidence level. Interactions [(v×f), (v×d) and (f×d)] have 1.36%, 2.87% and 2.36% contributions respectively. It can also be seen that residual error has only 2.31% contribution. The value of R^2 is 0.9770 which indicates that 97.70% of the total variations are explained by the model. The value of the R^2 (Adj.) = 0.9648 indicating 96.48% of the total variability is explained by the model after considering the significant factors. R^2 (Pred.) = 0.9439 which shows that the model is expected to explain 94.39% of the variability in new data.

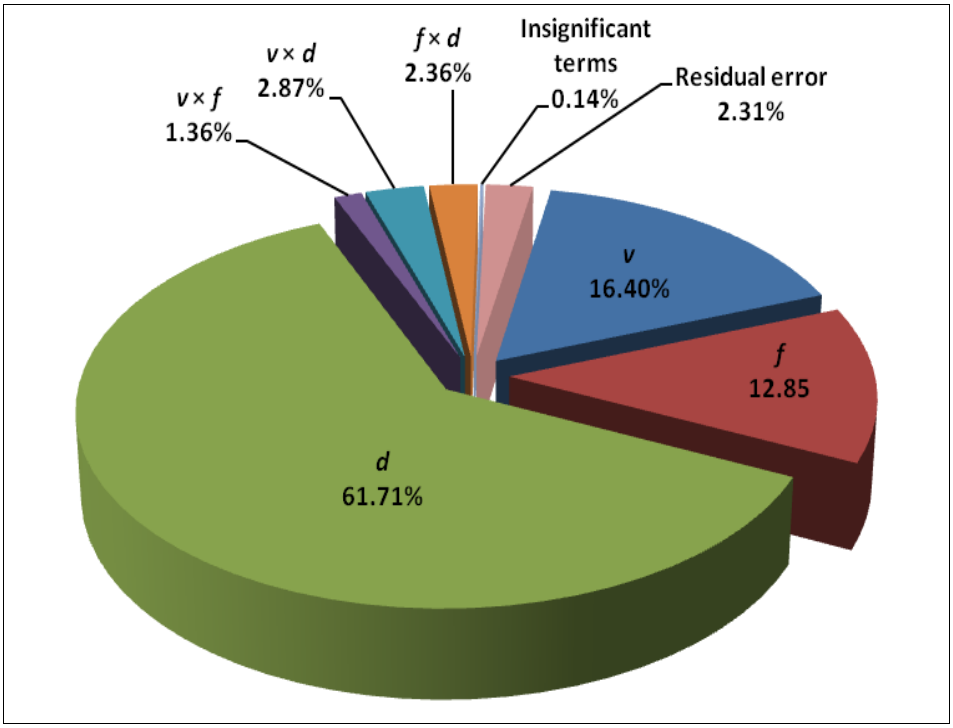

Figure 5.2: Percentage contribution of machining parameters on power consumption

5.3.3 Model fitness check

The adequacy of the modal has been investigated by the examination of residuals. Figure 5.3 reveals that the residuals are not showing any particular trend and the errors are distributed normally. The residual versus the predicted response plot in Figure 5.4 also shows that there is no obvious pattern and unusual structure.

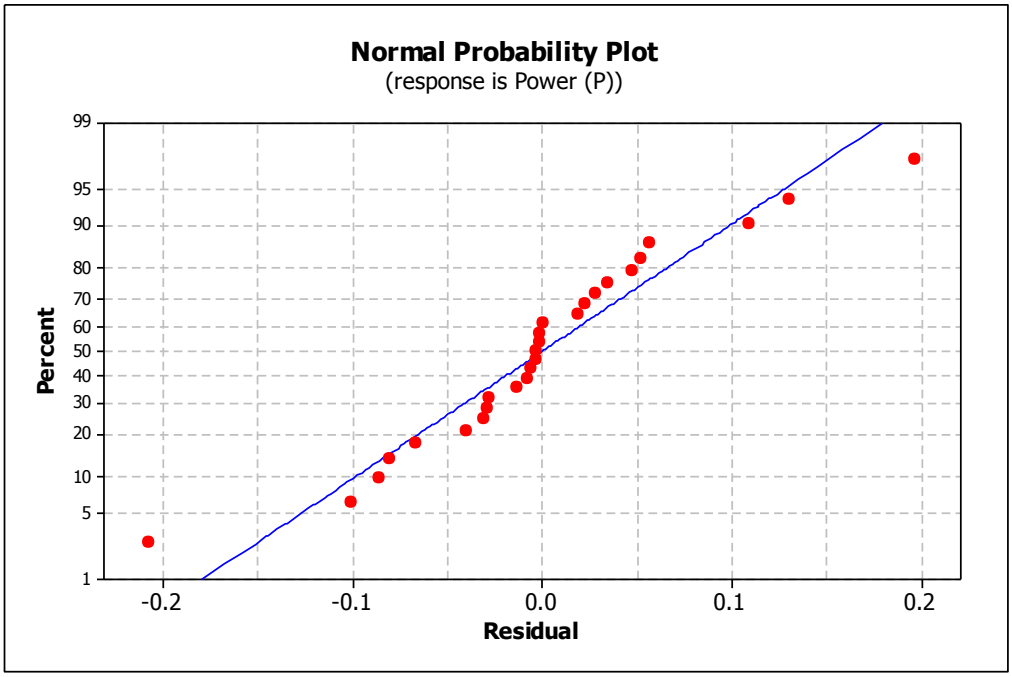

Figure 5.3: Normal probability plot of residual for power consumption data

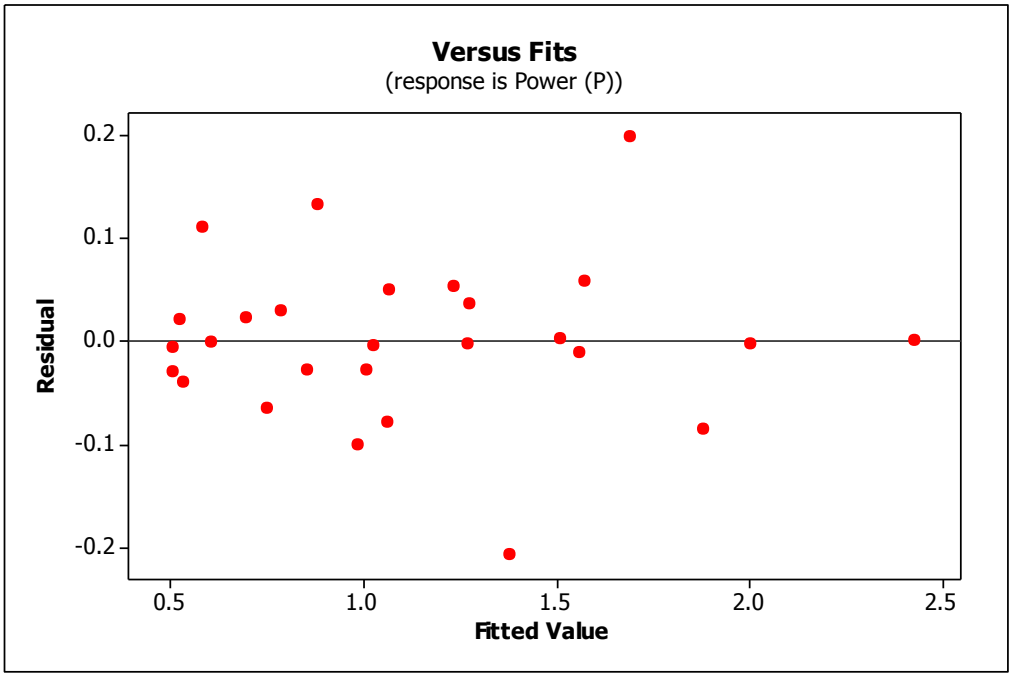

Figure 5.4: Plot of residual versus fitted power consumption values

5.3.4 Parametric influence on power consumption

The main effects of machining parameters on mean power consumption are shown in Figure 5.5. It reveals that power consumption increases with increase in cutting

parameters. The slope of depth of cut is maximum as compare to cutting speed and feed rate, which shows that depth of cut, has more impact on power consumption. This trend is also supported by the ANOVA results shown in Table 5.2. However, the results of Camposeco-Negrete (2013) while working on AISI 6061 T6 material demonstrated that feed rate is the most significant factor and cutting speed is the least significant parameter for minimizing the total power consumption. Abhang and Hameedullah (2010) demonstrated that the feed rate has the most significant effect on power consumption, followed by depth of cut, tool nose radius and cutting speed during turning of EN-31 steel with tungsten carbide tool. Bhattacharya et al. (2009) reported that cutting speed is the most significant factor followed by depth of cut to reduce the power consumption and feed rate has no significant effect on power consumption during turning of AISI 1045 steel with coated carbide tools under high speed machining. More power is consumed due to increase in material removal rate, cutting forces and temperature. Further the power is also consumed to provide the relative movement to the cutting tool with respect to workpiece (feed rate) and rotation of spindle (cutting speed). Main effect plot clearly shows that the mean power consumption was minimum, when the smaller values of cutting speed, feed rate and depth of cut was selected. The interaction plot for power consumption is shown in Figure 5.6. This figure clearly show that the power consumption is high with variation of depth of cut for cutting speed (row 1 column 3) and feed rate (row 2 column 3) as the power consumption value is more than 1.8 kW for these two cases. The power consumption is increasing with variation of cutting speed and feed rate (row 2 column 1) but the rate of change of power consumption is less as compared to variation of depth of cut and cutting speed (row 1 column 3) as well as depth of cut and feed rate (row 2, column 3).

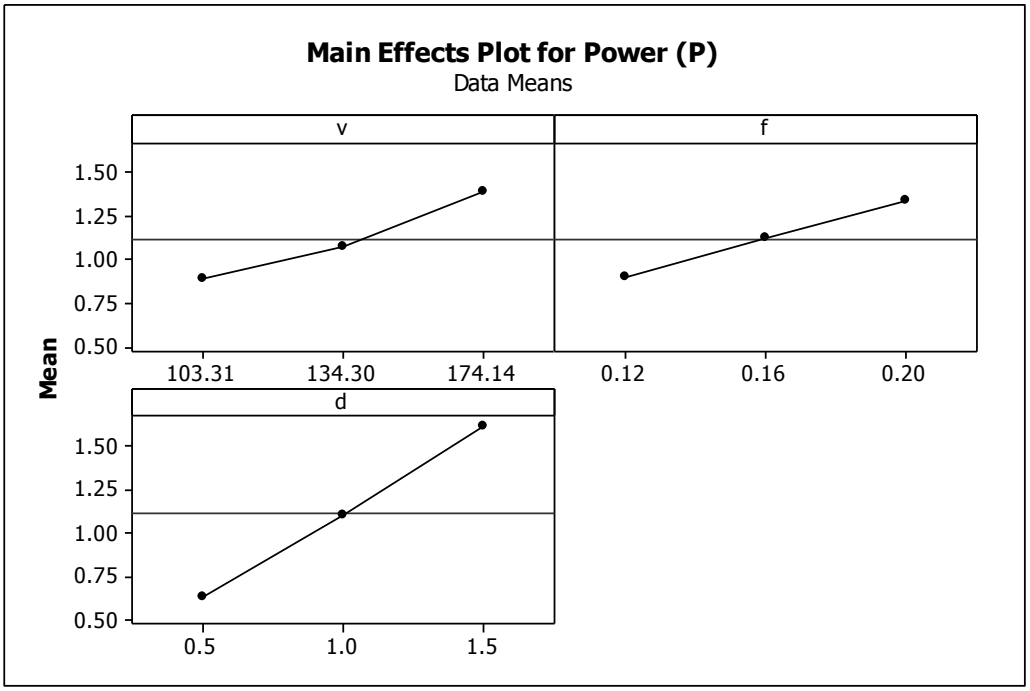

Figure 5.5: Main effect plot of power consumption

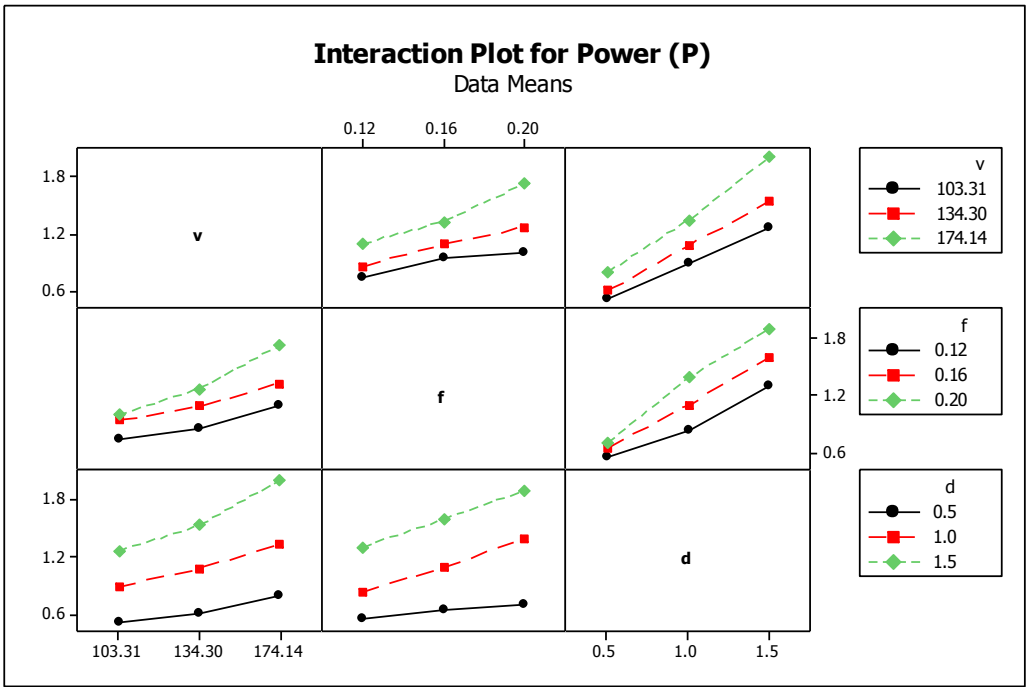

Figure 5.6: Interaction plot of power consumption

The 3D merged surface and contour plots for the power consumption are shown in Figure 5.7. Figure 5.7(a) shows the surface and contour plots for power consumption at 0.16 mm/rev. feed rate. It shows that at lower values of cutting speed and depth of cut,

the power consumption is minimum and power consumption increases drastically with increase in depth of cut even at lower value of cutting speed. It again supports this observation that depth of cut has more influence on power consumption as compared to cutting speed.

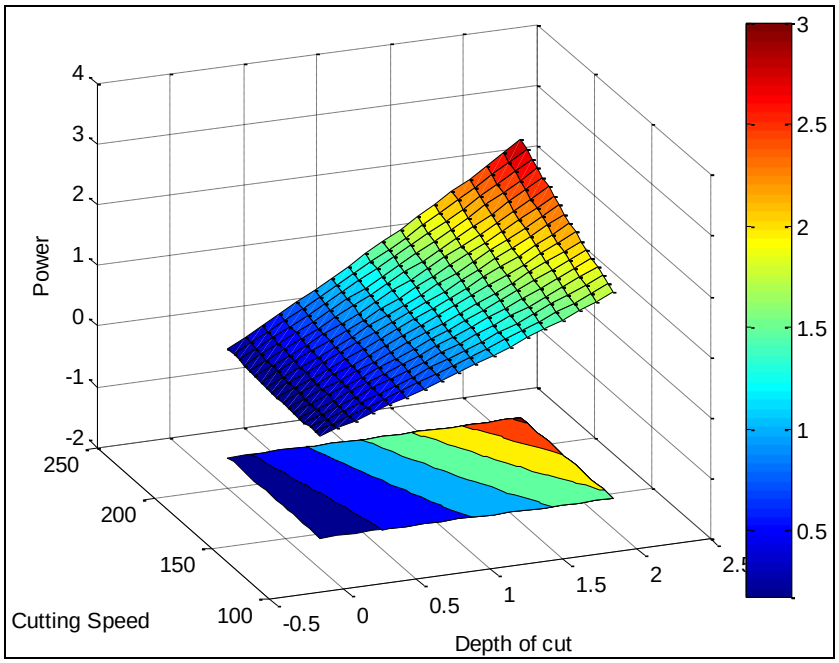

Figure 5.7(a): Surface and contour plot for power consumption for varying cutting speed and depth of cut at 0.16 mm/rev. feed rate

Figure 5.7(b) reveals that at the lower values of cutting speed and feed rate, the power consumption is minimum. Increase in cutting speed at lower values of feed rate has negligible effect on the power consumption but power consumption increases with increase in cutting speed at higher values of feed rate. Figure 5.7(c) indicates that power consumption is minimum at smaller values of depth of cut and feed rate and maximum at larger values of depth of cut and feed rate. These plots are useful to find the optimum values of cutting speed, feed rate and depth of cut for a particular value of power consumption. These 3D surface plots can be used for estimating the power consumption values for any suitable combination of the machining parameters namely cutting speed, feed rate and depth of cut. This is useful in practice for the operator or the part

programmer. These plots can also be used by the machine tool designer to estimate the suitable range of parameters during the design of machine tools.

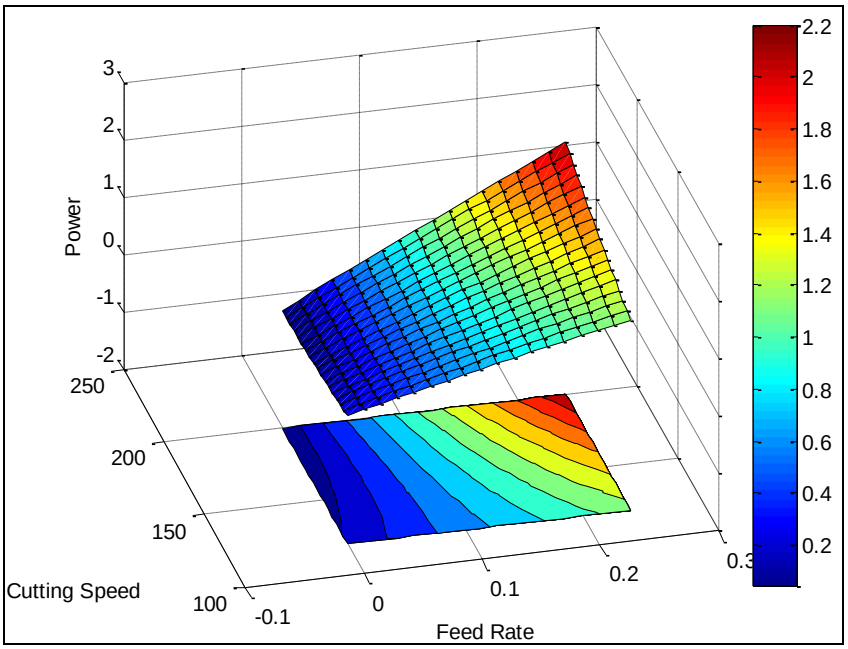

Figure 5.7(b): Surface and contour plot for power consumption for varying cutting speed and feed rate at 1 mm depth of cut

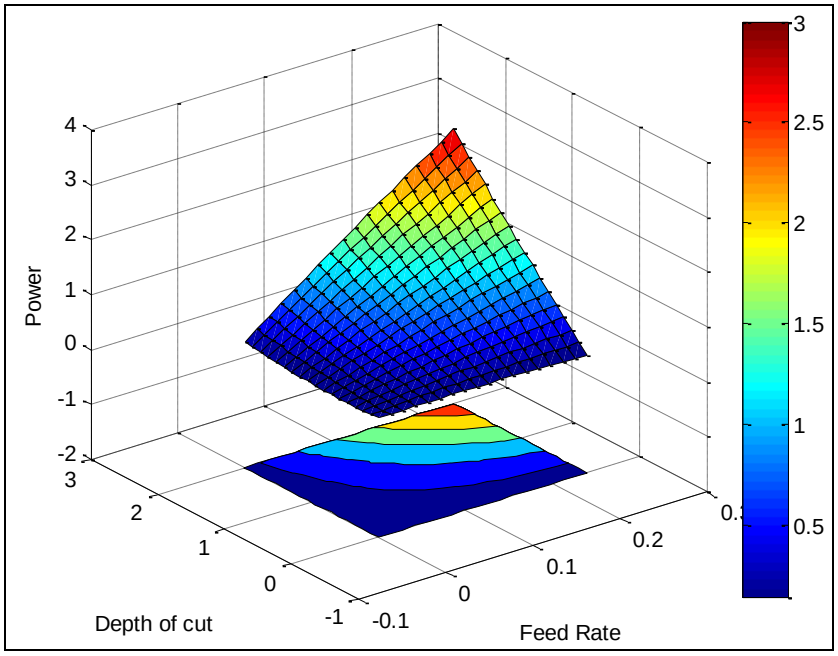

Figure 5.7(c): Surface and contour plot for power consumption for varying depth of cut and feed rate at cutting speed 134.30 m/min.

5.4 Predictive Modelling for Power Consumption using Support Vector Regression

An online SVR toolbox for SVR modelling developed by (Parrella, 2007) in MATLAB has been used for predicting the power consumption. The training set is a combined vector of all the three input parameters (*v*, *f*, *d*) and the training set *y* of power consumption. The training parameters used to develop the SVR model are given in chapter 4, section 4.4. Predicted values of power consumption from the developed SVR model and the experimental values are shown in Figure 5.8 and Table 5.3. The comparison of predicted and experimental values shows that the predicted values of the power consumption are close to experimental values. The mean relative error between the experimental and predicted values is 2.13%.

Table 5.3: Experimental and predicted values of power consumption using SVR

Experiment No.	Power consumption (P) (kW)	
	Experimental	SVR
1	0.497	0.507
2	0.684	0.694
3	1.021	1.031
4	0.543	0.533
5	1.013	0.876
6	1.269	1.273
7	0.586	0.596
8	0.980	0.990
9	1.512	1.502
10	0.574	0.571
11	0.824	0.834
12	1.285	1.295
13	0.604	0.614

Experiment No.	Power consumption (P) (kW)	
	Experimental	SVR
14	1.115	1.105
15	1.547	1.557
16	0.721	0.711
17	1.309	1.319
18	1.794	1.784
19	0.690	0.700
20	0.982	0.972
21	1.631	1.621
22	0.815	0.805
23	1.173	1.393
24	2.002	2.014
25	0.883	0.893
26	1.888	1.878
27	2.430	2.420

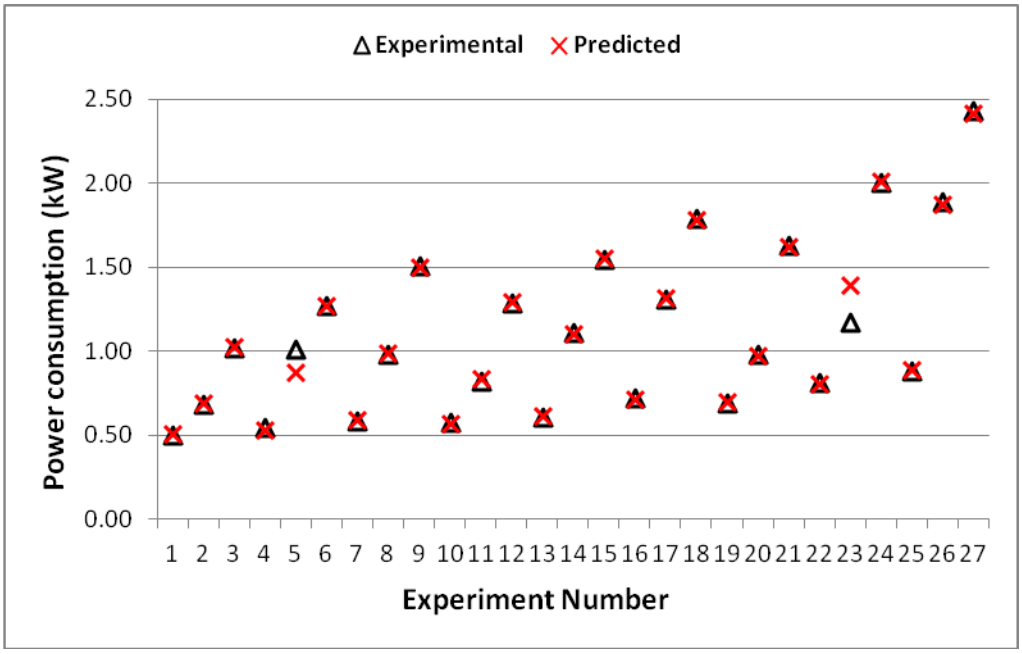

Figure 5.8: Experimentally measured and SVR predicted values of power consumption

5.5 Predictive Modelling for Power Consumption using Artificial Neural Network

The methodology for the selection of ANN parameters is given in Chapter 4, section 4.5.1. The selected parameters after trial and error are shown in Table 5.4. The weights and bias between the input and hidden layers are shown in the Table 5.5. The weights between the hidden and output layer are shown in the Table 5.6. The bias between the hidden and output layer is -0.726.

Table 5.4: Selected ANN parameters for power prediction modelling

Selected ANN parameter	Value
Network structure	3-5-1
Training/Testing data	22/5
Network algorithm	Feedforward back propagation
Transfer function	tansig, purelin
Training function	traingdx
Learning function	learngd
Performance function	MSE
Learning rate	0.14
Momentum rate	0.05

Table 5.5: The weight and bias values between input and hidden neurons

W_{jk}, j=3, k=5	W_{1k}	W_{2k}	W_{3k}	Bias (b_k)
1	0.397	0.943	-0.919	-2.524
2	-0.671	-0.525	-0.365	1.221
3	-1.874	-1.745	2.655	-1.621
4	-0.946	-2.507	-2.904	-1.349
5	-1.045	-0.803	0.102	-1.560

Table 5.6: The weight values between hidden neurons and output neuron

$W_{k,z}$ k=5, z=1	W_{1k}
1	-1.127
2	-1.097
3	0.127
4	-0.209
5	-0.158

The neural network was trained using the selected parameters mentioned in Table 5.4. The mean square error decreased with increasing iteration numbers until 432 iterations as shown in Figure 5.9. After this point it remained constant, therefore, the training of the algorithm was stopped at 432 iterations. After that, the ANN was tested for accuracy using the random test values selected from the experimental results which had not been used for the learning process. The predicted results are shown in Table 5.7 and Figure 5.10. It can be seen that in most cases the neural network prediction is close to the actual value. The mean relative error between the experimental and predicted values is 3%.

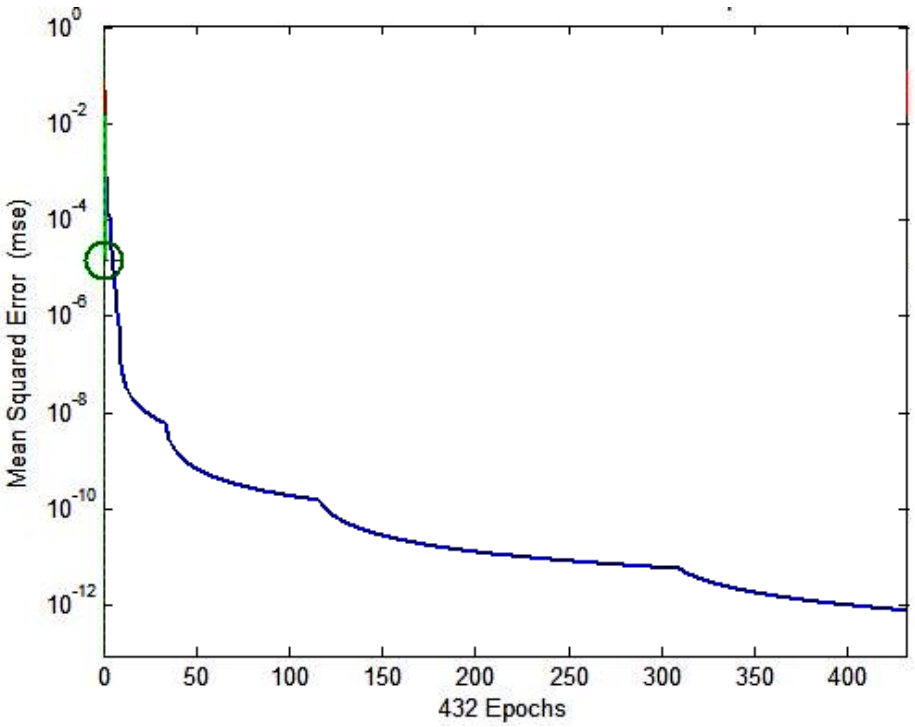

Figure 5.9: Iteration number (epochs) versus mean square error

Table 5.7: Experimental and predicted values of power consumption using ANN

Experiment No.	Power consumption (kW)	
	Experimental	ANN
1	0.497	0.493
2	0.684	0.687
3	1.021	1.026
4	0.543	0.539
5	1.013	1.012
6	1.269	1.269
7	0.586	0.635
8	0.980	1.101
9	1.512	1.467
10	0.574	0.578
11	0.824	0.797
12	1.285	1.281
13	0.604	0.615
14	1.115	1.121
15	1.547	1.509
16	0.721	0.727
17	1.309	1.307
18	1.794	1.717
19	0.690	0.697
20	0.982	0.995
21	1.631	1.634
22	0.815	0.825
23	1.173	1.516
24	2.002	1.921
25	0.883	0.872
26	1.888	1.869
27	2.430	2.399

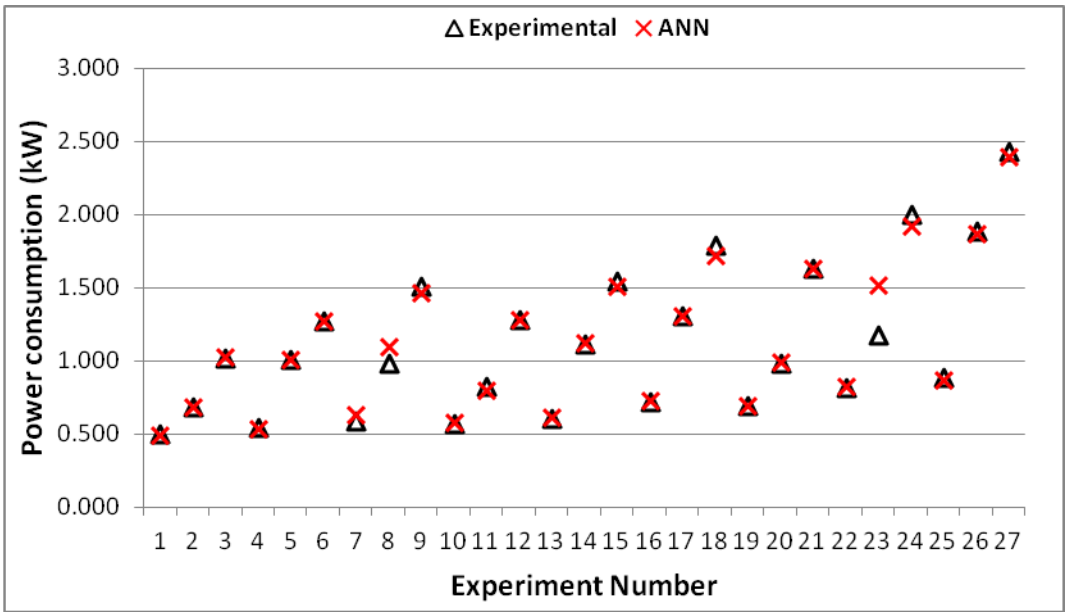

Figure 5.10: Experimentally measured and ANN predicted values of power consumption

5.6 Comparison and Validation of the Proposed Predictive Models

The results obtained from the predictive modelling techniques of RSM, SVR and ANN are shown in Table 5.8 for comparison with each other. Figure 5.11 and Table 5.8 reveal the relative errors for the modelling techniques.

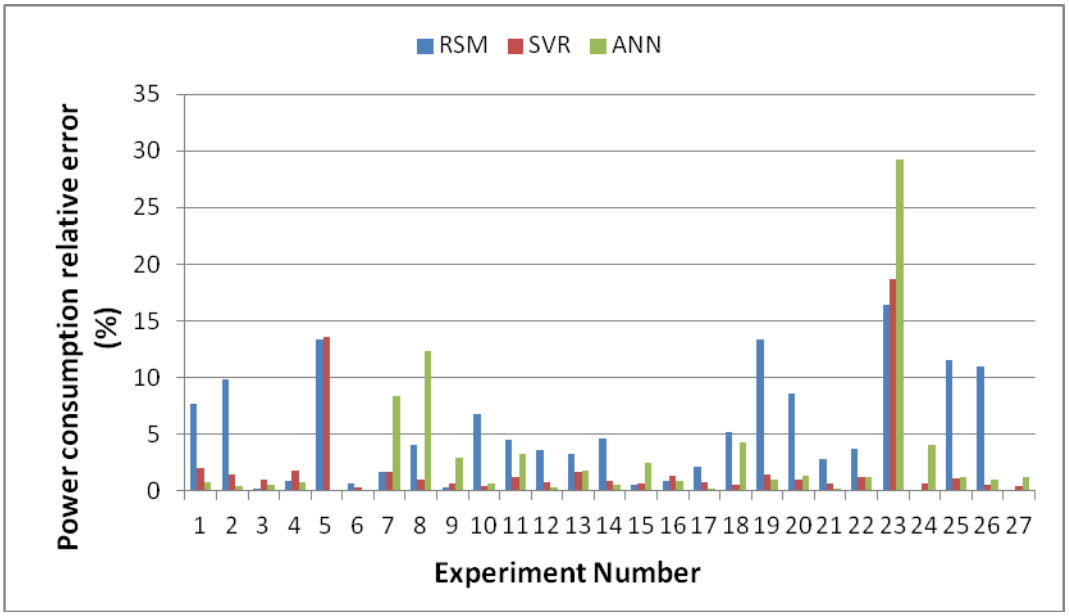

Figure 5.11: Deviation of power consumption predicted values from the experimental values

Table 5.8: Predicted values and relative errors for modelling techniques (RSM, SVR and ANN) for power consumption

Experiment No.	Power consumption (kW)				Relative Error (%)		
	Experimental	RSM	SVR	ANN	RSM	SVR	ANN
1	0.497	0.535	0.507	0.493	7.646	2.012	0.805
2	0.684	0.751	0.694	0.687	9.795	1.462	0.439
3	1.021	1.019	1.031	1.026	0.196	0.979	0.490
4	0.543	0.548	0.533	0.539	0.921	1.842	0.737
5	1.013	0.878	0.876	1.012	13.327	13.573	0.099
6	1.269	1.261	1.273	1.269	0.630	0.312	0.000
7	0.586	0.576	0.596	0.635	1.706	1.706	8.362
8	0.980	1.020	0.990	1.101	4.082	1.020	12.347
9	1.512	1.517	1.502	1.467	0.331	0.661	2.976
10	0.574	0.535	0.571	0.578	6.794	0.483	0.697
11	0.824	0.861	0.834	0.797	4.490	1.214	3.277
12	1.285	1.239	1.295	1.281	3.580	0.778	0.311
13	0.604	0.624	0.614	0.615	3.311	1.656	1.821
14	1.115	1.064	1.105	1.121	4.574	0.897	0.538
15	1.547	1.556	1.557	1.509	0.582	0.646	2.456
16	0.721	0.727	0.711	0.727	0.832	1.387	0.832
17	1.309	1.281	1.319	1.307	2.139	0.764	0.153
18	1.794	1.887	1.784	1.717	5.184	0.557	4.292
19	0.690	0.598	0.700	0.697	13.333	1.449	1.014
20	0.982	1.066	0.972	0.995	8.554	1.018	1.324
21	1.631	1.585	1.621	1.634	2.820	0.613	0.184
22	0.815	0.785	0.805	0.825	3.681	1.227	1.227
23	1.173	1.366	1.393	1.516	16.454	18.716	29.241
24	2.002	2.000	2.014	1.921	0.100	0.622	4.046
25	0.883	0.985	0.893	0.872	11.552	1.133	1.246
26	1.888	1.681	1.878	1.869	10.964	0.530	1.006
27	2.430	2.428	2.420	2.399	0.082	0.412	1.276

The mean relative error by RSM, SVR and ANN is 5.1%, 2.14% and 3% respectively. Mean relative error illustrates that the SVR performs better as compare to ANN and RSM. All the developed models are suitable for predicting the power consumption in an acceptable range. The model generation and training procedure of ANN also took more time as compared to SVR.

To compare the goodness of fit of the RSM, ANN and SVR models, representative hypothesis tests were conducted and results are shown in Table 5.9. In all these tests, the *p*-values are greater than 0.05, which means that the null hypothesis cannot be rejected. The *p*-values in Table 5.9 also indicate that there is no significant evidence to conclude that the experimental data and the data predicted by RSM, ANN and SVR models differ. Therefore, all predictive models have statistically satisfactory goodness of fit from the modelling point of view.

Table 5.9: Hypothesis testing to compare the models at 95% confidence level using *p*-value (power consumption)

Tests	***p*-value**		
	RSM	**SVR**	**ANN**
Mean paired *t*-test	0.641	0.669	0.555
Variance *F*-test	0.978	0.984	0.896
Levene's test	0.957	0.904	0.984

It is evident that ANN and SVR models provide good prediction capabilities as compared to RSM because they generally offer the ability to model more complex non-linearity and interactions. Further, the developed predictive models are integrated with the optimization methods to determine the optimum cutting conditions for power consumption.

5.7 Power Consumption Optimization

Problem formulation

The power consumption optimization problem is formulated using RSM results as:

$$\text{Minimize } 2.19766 - 0.0162660v - 10.0766f - 1.14194d + 0.0000226904v^2 + 4.47917f^2 + 0.104d^2 + 0.0610014vf + 0.007094506vd + 5.70833fd$$

Subject to:

$$103.31 \text{ m/min} \leq v \leq 174.14 \text{ m/min}$$

$$0.12 \text{ mm/rev.} \leq f \leq 0.16 \text{ mm/rev.}$$

$$0.5 \text{ mm} \leq d \leq 1.5 \text{ mm}$$

5.7.1 Power consumption optimization using RSM

The individual response optimization analysis using the desirability function analysis associated in RSM (explained in section 4.7.1) has been performed for achieving the minimum power consumption based on the developed mathematical model. Desirability function analysis optimization results for power consumption are shown in Table 5.10 and Figure 5.12. Optimal machining parameters obtained are – cutting speed of 119.05 m/min at feed rate of 0.12 mm/rev and 0.5 mm depth of cut. The optimized power consumption obtained is 0.5294 kW. The desirability value is 0.98325, which is very close to 1.0.

Table 5.10: Response optimization for power consumption

Response	Goal	Optimum Combination			Lower	Target	Upper	Predicted	Desirability
		v	*f*	*d*					
P	Min.	119.05	0.12	0.5	0.497	0.497	2.430	0.529	0.98325

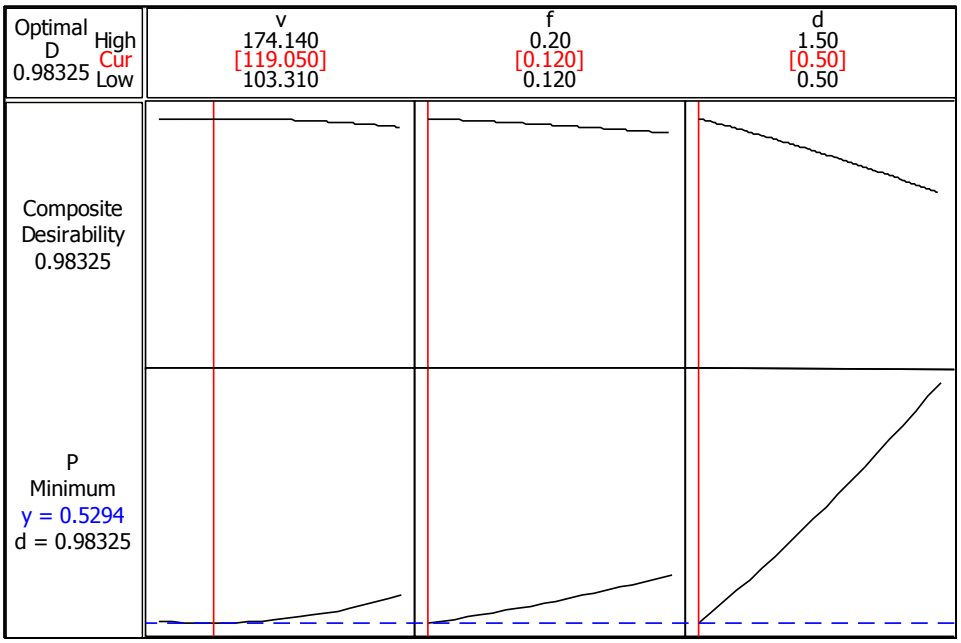

Fig. 5.12: Response optimization plot for power consumption parameters

5.7.2 Power Consumption Optimization using Genetic Algorithm

The GA methodology used to optimize the machining parameters is explained in section 4.7.2. The optimal power consumption and machining parameters obtained by GA are shown in Fig. 5.12. It is indicated that the optimal solution is obtained at the 34th generation (iteration) of the algorithm. It can be observed that the results of GA and desirability function analysis are similar to each other.

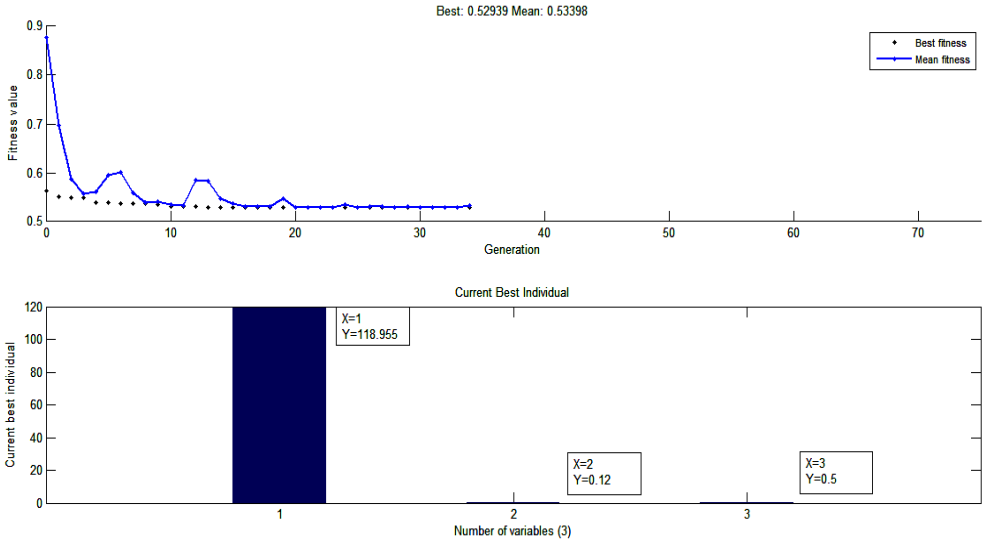

Figure 5.13: Variation of best fitness with generations and the corresponding optimal machining parameters for power consumption

5.8 Experimental Confirmation

The confirmation experiments were performed to facilitate the verification of the obtained feasible optimal machining parameters (v = 119.05 m/min, f = 0.12 mm/rev and d = 0.50 mm) for the power consumption. The results of the confirmation runs are listed in Table 5.11. The error between the predicted and the confirmation results is 3.25%.

Table 5.11: Confirmation results for power consumption

Optimum cutting parameters			Power consumption (kW)			Validation error (%)
v **(m/min)**	***f*** **(mm/rev.)**	***d*** **(mm)**	**Experimental**	**RSM**	**GA**	
119	0.12	0.5	0.547	0.529	0.529	3.29

5.9 Conclusions

In this chapter, predictive and optimization models have been presented to determine the machining parameters leading to minimum power consumption during machining. Three empirical models for prediction of power consumption have been developed using RSM, SVR and ANN. The optimization models have been developed using RSM and GA to find the values of machining parameters leading to minimum power consumption. Further, the confirmation experiments were carried out to show that the developed predictive and optimization models can be used for machining of AISI 1045 steel. The following conclusions are drawn from the study:

- The result of ANOVA reveal that the mathematical model developed using RSM allows prediction of power consumption with a 95% confidence interval. Depth of cut is the main influencing factor for the power consumption with 61.71% contribution, followed by the cutting speed with 16.41% contribution and feed rate with 12.85% contribution in the total variability of model. The quadratic effects of machining parameters do not have statistical significance on power consumption.

The interactions [(v×f), (v×d) and (f×d)] have 1.36%, 2.87% and 2.36% contributions on power consumption respectively. The 3D surface plots can be used for estimating the power consumption values for any combination of the machining parameters within the suitable range. This is very useful in practice for the operator or the part programmer. These plots can also be used by the machine tool designer to estimate the suitable range of parameters during the design of machine tools.

- SVR is capable of accurately predicting the power consumption during turning operations. The mean relative error between the predicted and experimental values was found to be 2.14%.
- The predictive model developed using the ANN shows that the power consumption values could be obtained with the selected ANN parameters. ANN model has provided a close relation between the predicted values and the experimental values. The mean relative error between the predicted and the experimental values is 3%. It has been found that the model developed using ANN is capable of predicting power consumption accurately using a small number of training samples.
- The developed predictive models have been compared using relative error and validated using hypothesis testing. It has been found that ANN and SVR models are better than RSM for predicting power consumption because they generally offer the ability to model more complex non-linearities and interaction. The mean relative errors for ANN and RSM models are 3% and 5.1% respectively. The mean relative error for SVR is 2.14%. Mean relative error illustrates that the SVR performs slightly better as compared to ANN.
- The minimum power consumption of 0.529 kW is found at cutting speed of 118.95 m/min, feed rate of 0.12 mm/rev and depth of cut as 0.5 mm using RSM and GA.
- Confirmation experiments carried out at the optimum machining parameters shows that the developed predictive and optimization models can be used for turning of AISI 1045 steel within 3.29% error.

References

Abhang, L.B., Hameedullah, M., 2010. Power Prediction Model for Turning EN-31 Steel Using Response Surface Methodology. J. Eng. Sci. Technol. Rev. 3, 116–122.

Aggarwal, A., Singh, H., Kumar, P., Singh, M., 2008. Optimizing power consumption for CNC turned parts using response surface methodology and Taguchi's technique—A comparative analysis. J. Mater. Process. Technol. 200, 373–384.

Arrazola, P.J., Umbrello, D., Davies, M., Jawahir, I.S., 2013. Recent advances in modelling of metal machining processes. CIRP Ann. - Manuf. Technol. 62, 695–718.

Balogun, V.A., Mativenga, P.T., 2013. Modelling of direct energy requirements in mechanical machining processes. J. Clean. Prod. 41, 179–186.

Bhattacharya, A., Das, S., Majumder, P., Batish, A., 2009. Estimating the effect of cutting parameters on surface finish and power consumption during high speed machining of AISI 1045 steel using Taguchi design and ANOVA. Prod. Eng. 3, 31–40.

Camposeco-Negrete, C., 2013. Optimization of cutting parameters for minimizing energy consumption in turning of AISI 6061 T6 using Taguchi methodology and ANOVA. J. Clean. Prod. 53, 195–203.

Diaz, N., Redelsheimer, E., Dornfeld, D., 2011. Energy consumption characterization and reduction strategies for milling machine tool use, in: Glocalized Solutions for Sustainability in Manufacturing. Springer, pp. 263–267.

Fang, K., Uhan, N., Zhao, F., Sutherland, J.W., 2011. A new approach to scheduling in manufacturing for power consumption and carbon footprint reduction. J. Manuf. Syst. 30, 234–240.

Green India Energy Summit, 2014. http://www.greenindiasummit.com/#!about-the-summit/cle6 (assessed 15 December 2014)

Hanafi, I., Khamlichi, A., Cabrera, F.M., Almansa, E., Jabbouri, A., 2012. Optimization of cutting conditions for sustainable machining of PEEK-CF30 using TiN tools. J. Clean. Prod. 33, 1–9.

He, Y., Liu, B., Zhang, X., Gao, H., Liu, X., 2012. A modeling method of task-oriented energy consumption for machining manufacturing system. J. Clean. Prod. 23, 167–174.

India's economic growth is driving its energy consumption, 2013 http://www.eia.gov/todayinenergy/detail.cfm?id=10611 (assessed 15 December 2014)

http://www.theenergyreport.com/pub/na/indias-widening-energy-deficit (assessed on 10 Dec 2014).

Kant, G., Sangwan, K.S., 2014. Prediction and optimization of machining parameters for minimizing power consumption and surface roughness in machining. J. Clean. Prod. 83, 151–164.

Li, W., Zein, A., Kara, S., Herrmann, C., 2011. An Investigation into Fixed Energy Consumption of Machine Tools, in: Hesselbach, J., Herrmann, C. (Eds.), Glocalized Solutions for Sustainability in Manufacturing: Proceedings of the 18th CIRP International Conference on Life Cycle Engineering. Springer Berlin Heidelberg, Berlin, Heidelberg, pp. 268–275.

Li, Y., He, Y., Wang, Y., Yan, P., Liu, X., 2014. A framework for characterising energy consumption of machining manufacturing systems. Int. J. Prod. Res. 52, 314–325.

Liow, J.L., 2009. Mechanical micromachining: A sustainable micro-device manufacturing approach. J. Clean. Prod. 17, 662–667.

Newman, S.T., Nassehi, A., Imani-Asrai, R., Dhokia, V., 2012. Energy efficient process planning for CNC machining. CIRP J. Manuf. Sci. Technol. 5, 127–136.

Parrella, F., 2007. Online Support Vector Regression Online Support Vector Machines for Regression.

Pusavec, F., Krajnik, P., Kopac, J., 2010a. Transitioning to sustainable production – Part I: application on machining technologies. J. Clean. Prod. 18, 174–184.

Pusavec, F., Kramar, D., Krajnik, P., Kopac, J., 2010b. Transitioning to sustainable production – part II: evaluation of sustainable machining technologies. J. Clean. Prod. 18, 1211–1221.

Sun-Joo Ahn and Dagmar Graczyk, 2012. Understanding Energy Challenges in India.

Yusup, N., Mohd, A., Zaiton, S., Hashim, M., 2012. Expert Systems with Applications Evolutionary techniques in optimizing machining parameters : Review and recent applications (2007 – 2011). Expert Syst. Appl. 39, 9909–9927.

Zhang, Y., 2014. Review of recent advances on energy efficiency of machine tools for sustainability. Proc. Inst. Mech. Eng. Part B J. Eng. Manuf.

Chapter 6

Multi-objective Optimization for Surface Roughness and Power Consumption

This chapter provides a multi-objective predictive model for the minimization of surface roughness and power consumption simultaneously. The optimum machining parameters minimizing the surface roughness and power consumption have been obtained by RSM.

6.1 Introduction

There is a close interdependence among productivity, quality and power consumption of a machine tool. The surface roughness is widely used index of product but the achievement of a predefined surface roughness below certain limit generally increases power consumption exponentially and decreases the productivity. The capability of a machine tool to produce a desired surface roughness with minimum power consumption depends on machining parameters, cutting phenomenon, workpiece properties, cutting tool properties, etc. Energy efficiency and product quality have become important benchmarks for assessing any industry. Machine tools have efficiency less than 30% (He et al., 2012) and more than 99% of the environmental impacts are due to the consumption of electrical energy used by the machine tools in discrete part machining processes like turning and milling (Li et al., 2011). Sustainability performance of machining processes can be achieved by reducing the power consumption (Camposeco-Negrete, 2013). If the energy consumption is reduced, the environmental impact generated from power production is diminished (Pusavec et al., 2010). However, sustainability performance may be reduced artificially by increasing the surface roughness as lower surface finish requires lesser power and resources to finish the machining. However, this may lead to more rejects, rework and time. Therefore, an

optimum combination of power and surface finish is desired for sustainability performance of the machining processes. The first step towards reducing the power consumption and surface roughness in machining is to analyze the impact of machining parameters on power consumption and surface roughness. This chapter aims at optimizing the power consumption and surface roughness simultaneously. The multi-objective predictive model has been developed using the grey relational analysis coupled with principal component analysis. The response surface methodology has been used to optimize the machining parameters to minimize the multi-objective function.

6.2 Research Methodology

The research carried out for this chapter can be broadly divided into three phases – experimental planning; multi-objective predictive model formulation; and machining parameter optimization – followed by result confirmation using experimental studies as shown in Figure 6.1. In the first phase experimental plan was developed to select the machine tool, cutting tools, machining material, machining parameters and their levels, and performance characteristics (power consumption and surface roughness) as explained in chapter 3. In the second phase, GRA coupled with principal component analysis (PCA) has been used to determine the best combination of parameters. GRA converts the multi-objective problem (power consumption and surface roughness) into a single multi-objective function (called grey relational grade); and hence simplifies the optimization procedure. Principal component analysis has been used to determine the weights of power consumption and surface roughness in the multi-objective function. Next, a mathematical model was developed to predict the relationship between machining parameters and grey relational grade using regression analysis. In the third phase, the statistical significance of the developed model was analyzed using analysis of variance (ANOVA). The fitness of developed model was checked using normal probability plot and residual plot.

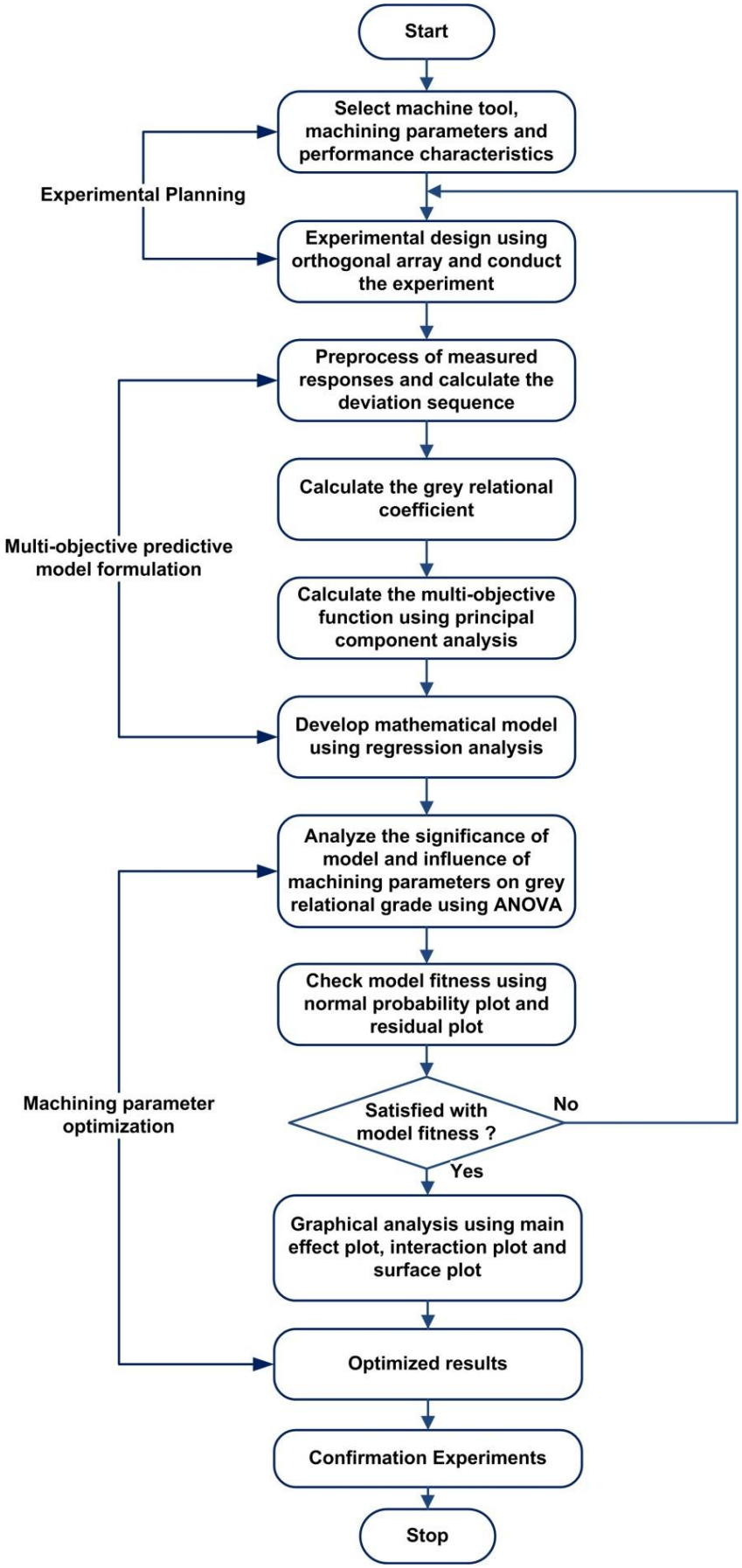

Figure 6.1: Research methodology used in this chapter

The influence of machining parameters on multi-objective function (grey relational grade) was determined using main effect and interaction plots. Response surface contours were constructed for determining a range of optimum conditions for required power consumption and surface roughness conditions. Lastly, experimental tests were carried out at the optimum machining parameters to validate the results.

6.3 Overview of Grey Relational Analysis and Principal Component Analysis Methodologies

This chapter uses the three methodologies to analyze the experimental data – response surface methodology, grey relational analysis and principal component analysis. An overview of grey relational analysis and principal component analysis methodologies is provided here. The response surface methodology is explained in section 4.3.

6.3.1 Grey relational analysis

The available experimental data may contain various kinds of uncertainties and noises either due to the existence of internal and/or external disturbances or due to the limitation of deep understanding of the subject (Liu and Lin, 2010). The grey systems theory established by Deng (1989) is a methodology that focuses on the study of uncertain systems with partially known information through generating, excavating, and extracting useful information from the available data. In grey systems theory, white indicates complete information, black unknown information and grey partially known and partially unknown information (Liu and Lin, 2010). Machining is known as one of the most complex systems due to large variety of machining operations, input and output variables, work material properties, and complex tool/work material interface (van Luttervelt et al., 1998). Therefore, grey system theory has a wide range

of applicability in machining operations. The grey relational analysis consists of following steps (Tzeng et al., 2009).

Step 1: Data preprocessing

In a multi-objective problem, various objective functions may have been measured in different units, therefore, data preprocessing is used to convert the original sequence (experimental information) to a comparable sequence (dimensionless quantity), where the original data is normalized between 0 and 1.

Let the original sequence and comparable sequence be represented as $x_i^{(o)}(k)$ and $x_i^*(k)$, i=1, 2,…., m; k=1,2,…, n, where m is the total number of experiments and n is the total number of performance characteristics. In this paper, m= 27and n = 2. Generally, three different kinds of data preprocessing methodologies are used in grey relational analysis depending upon the characteristics of original sequence (Deng, 1989). For "the-larger-the-better" characteristics such as tool life and material removal rate, the original sequence is normalized as:

$$x_i^*(k) = \frac{x_i^{(o)}(k) - \min. x_i^{(o)}(k)}{\max. x_i^{(o)}(k) - \min. x_i^{(o)}(k)} \tag{6.1}$$

For "the-smaller-the-better" characteristics such as power consumption and surface roughness, the original sequence is normalized as:

$$x_i^*(k) = \frac{\max. x_i^{(o)}(k) - x_i^{(o)}(k)}{\max. x_i^{(o)}(k) - \min. x_i^{(o)}(k)} \tag{6.2}$$

For "a specific desired value", the original sequence is normalized as:

$$x_i^*(k) = 1 - \frac{\left| x_i^{(o)}(k) - \mathrm{OD} \right|}{\max. \left\{ \max. x_i^{(o)}(k) - \mathrm{OD}, \mathrm{OD} - \min. x_i^{(o)}(k) \right\}} \tag{6.3}$$

where OD is the desired value.

Step 2: Grey relational coefficients

After data processing, a grey relational coefficient is calculated with the preprocessed sequences. The grey relational coefficient is defined as:

$$\gamma\left(x_0^*(k), x_i^*(k)\right) = \frac{\Delta_{\min.} + \zeta\,\Delta_{\max.}}{\Delta_{0i}(k) + \zeta\,\Delta_{\max.}} \tag{6.4}$$

$$0 < \gamma\left(x_0^*(k), x_i^*(k)\right) \le 1$$

where $\Delta_{0i}(k)$ is the deviational sequence of reference sequence $x_0^*(k)$ and comparability sequence $x_i^*(k)$, i.e. $\Delta_{0i}(k) = \left|x_0^*(k) - x_i^*(k)\right|$, which is the absolute value of the difference between $x_0^*(k)$ and $x_i^*(k)$.

$$\Delta_{\min} = \min_{\forall i}.\ \min_{\forall k}.\ \Delta_{0i}(k)$$

$$\Delta_{\max} = \max_{\forall i}.\ \max_{\forall k}.\ \Delta_{0i}(k)$$

ζ is the distinguish coefficient. $\zeta \in [0,1]$.

Step 3: Grey relational grades

The grey relational grade is a weighted sum of the grey relational coefficients. It is defined as :

$$\gamma\left(x_0^*, x_i^*\right) = \sum_{k=1}^{n} \beta_k \gamma\left(x_0^*(k), x_i^*(k)\right) \tag{6.5}$$

$$\sum_{k=1}^{n} \beta_k = 1$$

where β_k denotes the weighted value of the k^{th} response variable. In this study, the weights are obtained from the principal component analysis.

The grey relational grade $\gamma\left(x_0^*, x_i^*\right)$ represents the level of correlation between the reference and comparability sequence. It is a measurement of the absolute value of data

difference between the two sequences and can be used to approximate the correlation between the sequences. The value of grey relational grade is equal to one, if the two sequences are identical. It indicates the degree of influence that the comparability sequence could exert over the reference sequence.

6.3.2 Principal component analysis

Principal component analysis is the oldest and one of the best known techniques of multivariate analysis. It was first introduced by Pearson in 1901 and developed independently by Hotelling in 1933 (Jolliffe, 2002). It is a technique of dimensionality reduction, which transforms data from the high-dimensional space to space of lower dimensions. It rotates the axes of data space along lines of maximum variance. The axis of the greatest variance is called the first principal component (Sanguansat, 2012). The dimension reduction is done by using only the first few principal components as a basis set for the new space. Therefore, the subspace tends to be small and may be dropped with minimal loss of information. PCA has the following advantages (Sanguansat, 2012).

- Retains most of the useful information and reduces noise and other undesirable artifacts.
- The time and memory used in data processing are smaller.
- Provides a way to understand and visualize the structure of complex data sets.
- Helps to identify new meaningful underlying variables.

Following is the methodology to get weights of performance characteristics using PCA (Lu et al., 2009):

Step 1: Developing the original multiple quality characteristic array

$$x_i(j), i = 1,2,....., m;\ j = 1,2,....., n$$

$$x=\begin{bmatrix} x_1(1) & x_1(2) & \cdots & \cdots & x_1(n) \\ x_2(1) & x_2(2) & \cdots & \cdots & x_2(n) \\ \vdots & \vdots & \cdots & \cdots & \vdots \\ x_m(1) & x_m(2) & \cdots & \cdots & x_m(n) \end{bmatrix}$$

where m is the number of experiments, n is the number of performance characteristics and x is the grey relational coefficient of each performance characteristic. In this study m =27and n = 2.

Step 2: Computing correlation coefficient array

The correlation coefficient array is computed as:

$$R_{jl}=\left(\frac{Cov(x_i(j),x_i(l))}{\sigma x_i(j)\times\sigma x_i(l)}\right),\qquad j=1,2,.....,n,\ l=1,2,.....,n \tag{6.6}$$

where $Cov(x_i(j),x_i(l))$ is the covariance of sequences $x_i(j)$ and $x_i(l)$, $\sigma x_i(j)$ is the standard deviation of sequence $x_i(j)$, and $\sigma x_i(l)$ is the standard deviation of sequence $x_i(l)$.

Step 3: Determining the eigenvalues and eigenvectors

The eigenvalues and eigenvectors are determined from the correlation coefficient array using

$$(R-\lambda_k I_m)V_{ik}=0 \tag{6.7}$$

where λ_k is the eigenvalues and $\sum_{k=1}^{n}\lambda_k=n$, $k=1,2,.....,n$, $V_{ik}=[a_{k1}a_{k2}.....a_{km}]^T$ are the eigenvectors corresponding to the eigenvalue λ_k.

Step 4: Finding principle components

The uncorrelated principal component is formulated as:

$$Y_{mk}=\sum_{i=1}^{n}x_m(i)\cdot V_{ik} \tag{6.8}$$

where Y_{m1} is the first principal component, Y_{m2} is the second principal component and so on. The principal components are aligned in the descending order with respect to the variance. The components with an eigenvalue greater than one are chosen to replace the original responses for further analysis (Kaiser, 1960).

6.4 Formulation of A Multi-objective Predictive Mathematical Model

6.4.1 Calculating the grey relation coefficient using GRA

Experimental results for the P and R_a are shown in Table 3.6 and Table 3.8 respectively. Preprocessing sequence (Table 6.1) was computed using Eq. (6.2) as both surface roughness and power consumption fit 'the-smaller-the-better' methodology. $x_0^*(k)$ shows the value for reference sequence and $x_i^*(k)$ for comparability sequence. The deviation sequence is computed using:

$$\Delta_{01}(R_a) = \left| x_0^*(R_a) - x_i^*(R_a) \right| = |1.0000 - 0.7780| = 0.2220$$

$$\Delta_{01}(P) = \left| x_0^*(P) - x_i^*(P) \right| = |1.0000 - 1.0000| = 0.0000$$

Therefore the value of deviation sequence for comparability sequence one in Table 6.1 is: $\Delta_{01} = (0.2220, 0.0000)$

Similarly, the deviation sequences for other comparability sequences were computed and the values are shown in Table 6.1. Values of $\Delta_{\max}$ and $\Delta_{\min}$ are computed as:

$$\Delta_{\max} = \Delta_{08}(1) = \Delta_{027}(2) = 1.0000$$

$$\Delta_{\min} = \Delta_{011}(1) = \Delta_{01}(2) = 0.0000$$

The grey relational coefficient values using Eq. (6.4) are computed as:

$$\gamma\left(x_0^*(1), x_1^*(1)\right) = \frac{\Delta_{\min.} + \zeta \Delta_{\max.}}{\Delta_{01}(1) + \zeta \Delta_{\max.}} = \frac{0.0000 + 0.5 \times 1.0000}{0.2220 + 0.5 \times 1.0000} = 0.6925$$

$$\gamma\left(x_0^*(2), x_1^*(2)\right) = \frac{\Delta_{\min.} + \zeta \Delta_{\max.}}{\Delta_{01}(2) + \zeta \Delta_{\max.}} = \frac{0.0000 + 0.5 \times 1.0000}{0.0000 + 0.5 \times 1.0000} = 1.0000$$

Therefore, $\gamma\left(x_0^*(R_a), x_i^*(P)\right) = (0.6925, 1.0000)$

The same procedure was performed to get the grey relational coefficients for other comparability sequences and values as shown in Table 6.1.

Table 6.1: The calculated values of pre-processing sequences, deviational sequences, grey relational coefficient, and grey relational grade

Comparability sequence	Preprocessing sequence		Deviation sequence		Grey relational coefficient		Grey relational grade
	$x_0^*(R_a)$	$x_0^*(P)$	$\Delta_{0i}(R_a)$	$\Delta_{0i}(P)$	R_a	P	
1	0.7780	1.0000	0.2220	0.0000	0.6925	1.0000	0.8463
2	0.9173	0.9033	0.0827	0.0967	0.8581	0.8379	0.8480
3	0.8227	0.7289	0.1773	0.2711	0.7383	0.6484	0.6934
4	0.5126	0.9762	0.4874	0.0238	0.5064	0.9546	0.7305
5	0.4382	0.7331	0.5618	0.2669	0.4709	0.6519	0.5614
6	0.4836	0.6006	0.5164	0.3994	0.4919	0.5559	0.5239
7	0.1708	0.9540	0.8292	0.0460	0.3762	0.9157	0.6459
8	0.0000	0.7501	1.0000	0.2499	0.3333	0.6668	0.5001
9	0.0690	0.4749	0.9310	0.5251	0.3494	0.4878	0.4186
10	0.9908	0.9602	0.0092	0.0398	0.9819	0.9262	0.9541
11	1.0000	0.8308	0.0000	0.1692	1.0000	0.7472	0.8736
12	0.9112	0.5923	0.0888	0.4077	0.8492	0.5509	0.7000
13	0.5707	0.9446	0.4293	0.0554	0.5380	0.9003	0.7192
14	0.4443	0.6803	0.5557	0.3197	0.4736	0.6100	0.5418
15	0.6800	0.4568	0.3200	0.5432	0.6097	0.4793	0.5445
16	0.1701	0.8841	0.8299	0.1159	0.3760	0.8118	0.5939
17	0.2961	0.5799	0.7039	0.4201	0.4153	0.5434	0.4794
18	0.2520	0.3290	0.7480	0.6710	0.4007	0.4270	0.4138
19	0.8545	0.9002	0.1455	0.0998	0.7746	0.8335	0.8041
20	0.9228	0.7491	0.0772	0.2509	0.8663	0.6659	0.7661
21	0.8948	0.4133	0.1052	0.5867	0.8262	0.4601	0.6432
22	0.7227	0.8355	0.2773	0.1645	0.6432	0.7524	0.6978
23	0.6670	0.6503	0.3330	0.3497	0.6002	0.5884	0.5943
24	0.2954	0.2214	0.7046	0.7786	0.4151	0.3911	0.4031
25	0.2579	0.8003	0.7421	0.1997	0.4025	0.7146	0.5586
26	0.2746	0.2804	0.7254	0.7196	0.4080	0.4100	0.4090
27	0.2087	0.0000	0.7913	1.0000	0.3872	0.3333	0.3603

6.4.2 Computing grey relation grade

The next step is to compute grey relational grade which is a weighted sum of the grey relational coefficients using Eq. (6.5). The computation of grey relational grade also requires weights of the performance characteristics for which eigenvalues and eigenvectors are required. Grey relational coefficient values shown in Table 6.1 are further used to evaluate the corresponding coefficient matrix using Eq.(6.6). Eigenvalues, eigenvectors and corresponding principal components are computed using Eq. (6.7) and Eq. (6.8) and are given in Table 6.2 and Table 6.3.

Table 6.2: The Eigenvalues and explained variation for principle components

Principal component	**Eigenvalue**	**Explained variation (%)**
First	1.3152	65.76
Second	0.6848	34.24

Table 6.3: The Eigenvectors for principle components and contribution of performance characteristics

	Eigenvector		**Contribution**
Performance characteristic	**First principal component**	**Second principal component**	
Surface Roughness	0.7071	–0.7071	0.50
Power	–0.7071	–0.7071	0.50

The variance contribution shown in Table 6.2 for the first principal component characterizing the two performance characteristics is as high as 65.76%. The square of eigenvector can represent the contribution of corresponding performance characteristic to the principle component. Therefore, in this analysis, the square of eigenvector of first principle component was selected as the weighting values of the related performance

characteristic. Table 6.3 shows the weighting value (contribution) of Ra and P. The equal weighting values of 'Ra' and 'P' clearly show that the power consumption is as important as surface roughness for a machine tool. Therefore, the coefficients, β_1 and β_2 in Eq. (6.4) were set as 0.5 and 0.5. Based on Eq. (6.4) and the data listed in Table 1, the grey relational grade $\gamma\left(x_0^*, x_i^*\right)$ is computed as:

$$\gamma\left(x_0^*, x_i^*\right) = 0.6925 \times 0.50 + 1.0000 \times 0.50 = 0.8463$$

The grey relational grades for other 26 experimental values were calculated using above methodology. The values are given in the last column of Table 6.1. Therefore, the optimization of performance characteristics can be performed with respect to single grey relational grade rather than multiple performance characteristics. This grey relation grade is a multi-objective function integrating surface roughness and power consumption.

6.4.3 Finding best experimental run

The Taguchi method has been used to calculate the average grey relational grade for each machining parameter level. It has been done by sorting the grey relational grades corresponding to levels of the machining parameter in each column of the orthogonal array and taking an average at the same level. The average grey relation grade for $\bar{v}_1$ is computed as:

$$\bar{v}_1 = \frac{\left(0.8463 + 0.8480 + 0.6934 + 0.7305 + 0.5614 + 0.5239 + 0.6459 + 0.5001 + 0.4186\right)}{9}$$
$$= 0.6409$$

Similarly, the average grey relational grade values for *v*, *f* and *d* at the three levels are computed and given in Table 6.4.

Table 6.4: Response table for average grey relational grade

Machining parameter	Level 1	Level 2	Level 3	Max-Min
Cutting speed *(v)*	0.6409	0.6467	0.5818	0.0649
Feed *(f)*	0.7921	0.5907	0.4866	0.3055
Depth of cut *(d)*	0.7278	0.6193	0.5223	0.2055

The larger the grey relational grade, the better the corresponding performance characteristics. Accordingly, the level that gives the largest average response is best. Thus, the optimal levels of parameters are: the cutting speed at level 2 (134.3 m/min), feed at level 1 (0.12 mm/rev.) and depth of cut at level 1 (0.5 mm). Further, the Max-Min value, which is the difference between the maximum and minimum value for each cutting parameter is calculated and given in Table 6.4. The Max-Min value of feed is maximum. Depth of cut and cutting speed are at the second and third place respectively. It indicates that feed has the maximum influence on average grey relational grade while cutting speed has the minimum influence.

6.4.4 Predictive mathematical formulation

The mathematical model for the grey relational grade prediction is developed using regression analysis based on the grey relational grade values obtained. The developed predictive mathematical model for grey relational grade is:

Maximize

$$1.71831 + 0.00703258\,v - 13.0110\,f - 0.182721\,d - 0.0000256225\,v^2 + 30.3958\,f^2 + 0.0230667\,d^2 - 0.00274287\,vf - 0.000318573\,vd - 0.157500\,fd \quad (6.9)$$

Subject to:

$$103.31 \text{ m/min} \le v \le 174.14 \text{ m/min}$$

$$0.12 \text{ mm/rev.} \le f \le 0.16 \text{ mm/rev.}$$

$$0.5 \text{ mm} \le d \le 1.5 \text{ mm}$$

Figure 6.2 shows the predicted values of grey relational grade, hereafter called multi-objective function, from the developed mathematical model and the calculated values of grey relational grade obtained using GRA. Both values are in good agreement to each other. The mean relative error between the two values is 4.79%.

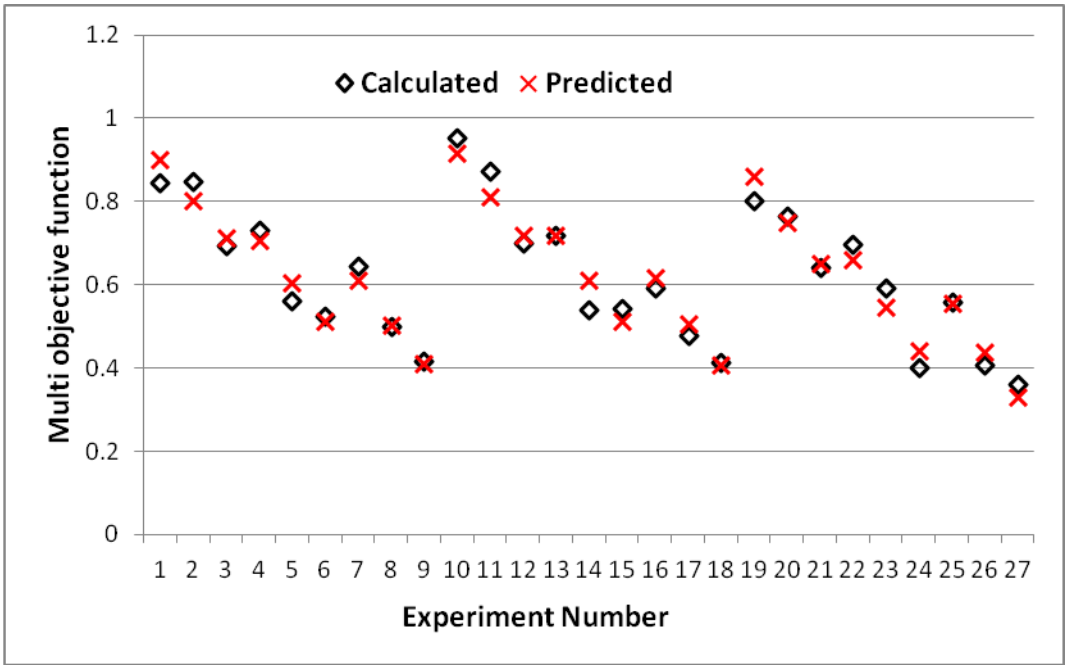

Figure 6.2: Comparison of predicted values of multi-objective function with the calculated values

6.5 Machining Parameter Optimization

6.5.1 Analysis of variance

The relative importance among the machining parameters (v, f, d) for the multiple performance characteristics (Ra and P) needs to be investigated so that the optimal parameters can be decided effectively. The analysis of variance (ANOVA) has been applied to investigate the developed model and the effect of machining parameters on the multi-objective function. Table 6.5 shows ANOVA results for the linear [v, f, d,] quadratic [v^2, f^2, d^2] and interactive [($v \times f$), ($v \times d$), ($f \times d$)] factors. F-value, which is a ratio of the regression mean square to the mean square error, is used to measure the significance of the model under investigation with respect to the variance of all the terms

including the error term at the desired significance level. Usually, F > 4 means the change of the design parameter has a significant effect on the performance characteristic. The F-value for linear terms is above 4. The p-value or probability value is used to determine the statistical significance of results at a confidence level. In this study the significance level of $\alpha = 0.05$ is used, i.e. the results are validated for a confidence level of 95%. If the *p*-value is less than 0.05 then the corresponding factor has a statistically significant contribution to the performance characteristic and if the *p*-value is more than 0.05 then it means the effect of factor on the performance characteristic is not statistically significant at 95% confidence level. The results show that all linear terms and f^2 are statistically significant at 95% level. The last column of the Table 6.5 shows the percentage contribution of each term to the total variation indicating the degree of influence on the results. The percentage contribution of each term is also shown in Figure 6.3. Feed (*f*) was found to be the most significant machining parameter due to its highest percentage contribution of 61.66% followed by the depth of cut (*d*) with 27.91% and cutting speed (*v*) with 2.53%. However, the percentage contribution of quadratic term f^2 is 2.08%. The other quadratic and interaction terms are insignificant. The other important coefficient is R^2, which is defined as the ratio of the explained variation to the total variation and is a measure of the degree of fit. As R^2 approaches unity, the response model fitness with the actual data improves. The value of R^2 obtained was 0.9518 which indicates that 95.18% of the total variations are explained by the model. The adjusted R^2 is a statistic used to adjust the "size" of the model, i.e. the number of factors (machining parameters). The value of the R^2 (Adj.) = 0.9263 indicating 92.63% of the total variability is explained by the model after considering the significant factors. R^2 (Pred.) = 87.43% is in good agreement with the R^2 (Adj.) and shows that the model would be expected to explain 87.43% of the variability in new data.

Table 6.5: Analysis of variance (ANOVA) for multi-objective function

Source	DOF	Seq. SS	Adj. SS	Adj. MS	F	p	% contribution
Regression	9	0.6482	0.6482	0.0720	37.31	0.000	95.18
Linear	3	0.6272	0.6258	0.2086	108.07	0.000	92.10
v	1	0.0172	0.0157	0.0157	8.13	0.011	2.53
f	1	0.4199	0.4197	0.4197	217.41	0.000	61.66
d	1	0.1901	0.1904	0.1904	98.65	0.000	27.91
Square	3	0.0204	0.0204	0.0068	3.52	0.038	2.99
*v*v*	1	0.0060	0.0060	0.0060	3.10	0.096	0.88
*f*f*	1	0.0142	0.0142	0.0142	7.35	0.015	2.08
*d*d*	1	0.0002	0.0002	0.0002	0.10	0.752	0.03
Interaction	3	0.0007	0.0007	0.0002	0.12	0.948	0.11
*v*f*	1	0.0002	0.0002	0.0002	0.09	0.762	0.03
*v*d*	1	0.0004	0.0004	0.0004	0.20	0.661	0.06
*f*d*	1	0.0001	0.0001	0.0001	0.06	0.807	0.02
Residual Error	17	0.0328	0.0328	0.0019			4.82
Total	26	0.681					
R^2 = 0.9518			R^2(Pred.) = 0.8743				R^2(Adj.) = 0.9263

DF: Degree of freedom, SS: Sum of square, MS: Mean square

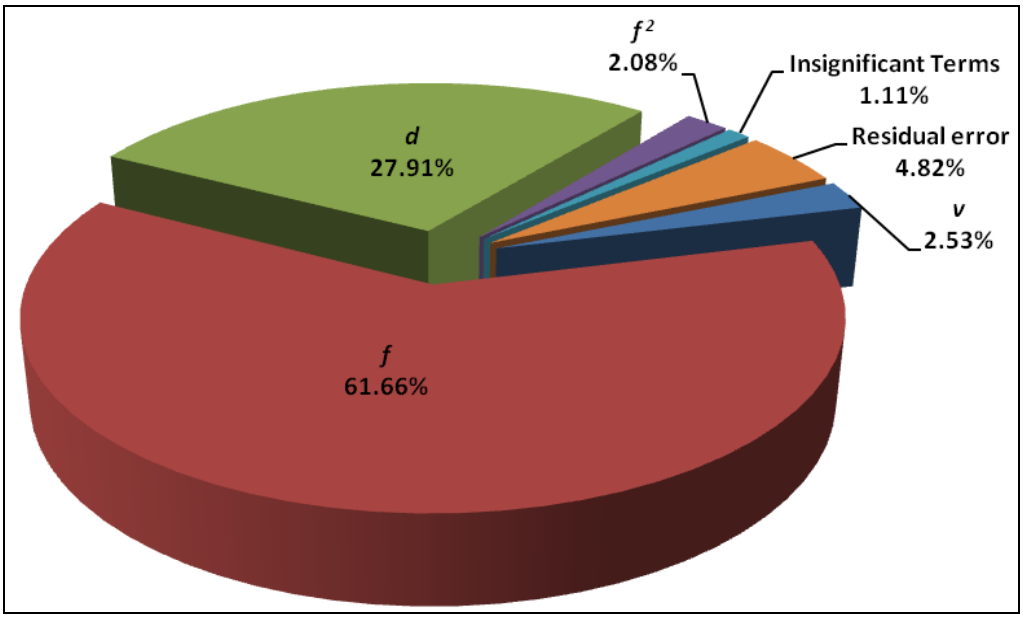

Figure 6.3: Percentage contribution of machining parameters on multi-objective function

6.5.2 Model fitness check

Figure 6.4 reveals that the residuals are not showing any particular trend and the errors are distributed normally. The residual versus the predicted response plot in Figure 6.5 also shows that there is no obvious pattern and unusual structure. This suggests the adequacy of the developed model for evaluating the multi-objective function.

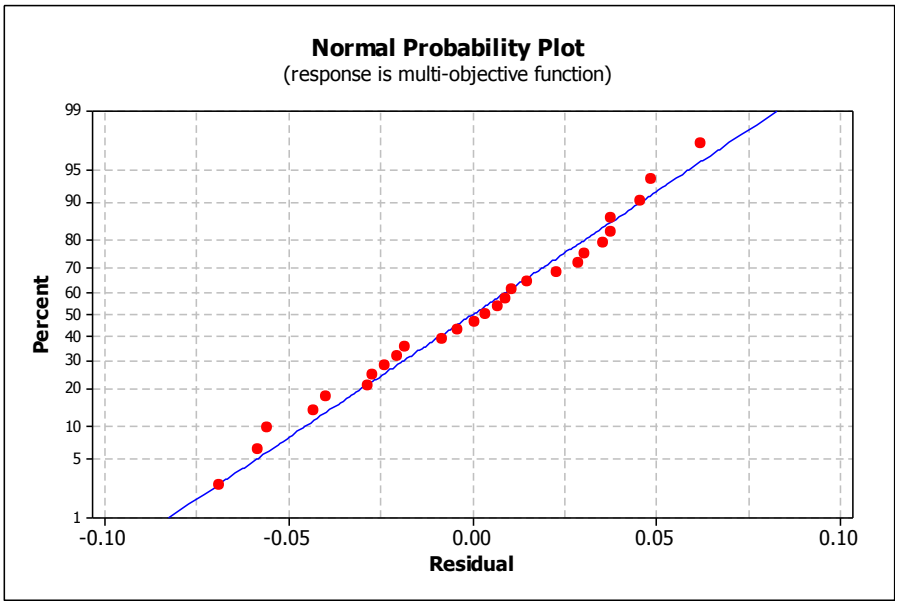

Figure 6.4: Normal probability plot of residual for multi-objective function

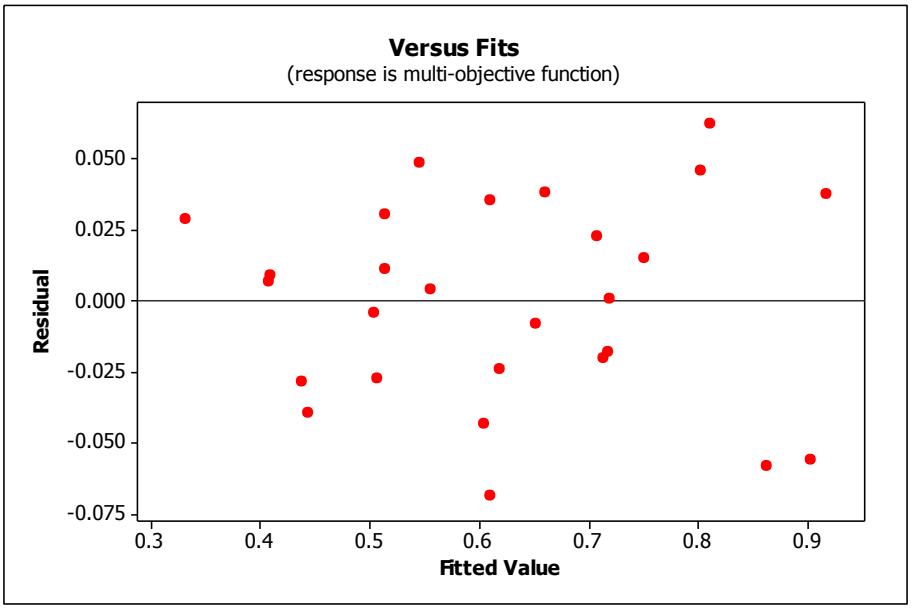

Figure 6.5: Plot of residual versus fitted values for multi-objective function

6.5.3 Parametric influence on multi-objective function

The main effects plot of machining parameters versus multi-objective function is shown in Figure 6.6.

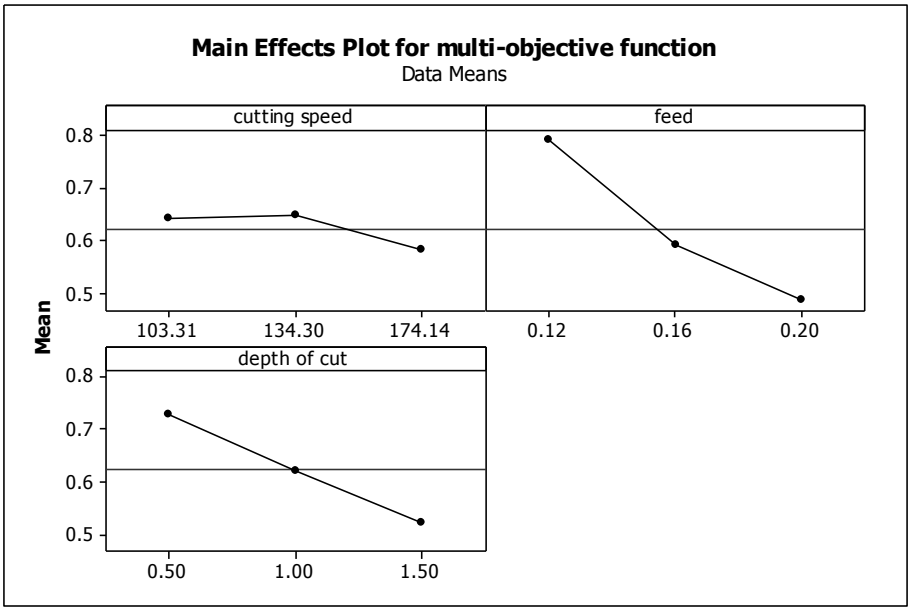

Figure 6.6: Main effect plot showing the influence of machining parameters on the multi-objective function

The slope of feed and depth of cut is large which shows that both have more impact on multi-objective function (power consumption and surface roughness). The cutting speed has almost negligible impact on multi-objective function. This trend is also supported by the percentage contribution values in the ANOVA results. Main effect plot clearly shows that the multi-objective function will be maximum when the values of feed and depth of cut are smaller. Therefore, to get the better surface finish at minimum power consumption, the recommended values are level 1 for feed and depth of cut and level 2 for cutting speed. The interaction plot for mean multi-objective function is shown in Figure 6.7. This figures clearly show that the variation of cutting speed has low effect on the multi-objective function for both feed and depth of cut variation as the spacing between the lines is small (row 1 column 2 for feed, and row 1 and column 3 for depth of cut). The variation of multi-objective function is high with variation of feed and depth of

cut (row 2 and column 3) as the multi-objective function value is approximately 0.4 for level 3 feed and level 3 depth of cut, and this value is approximately 0.9 for level 1 feed and depth of cut.

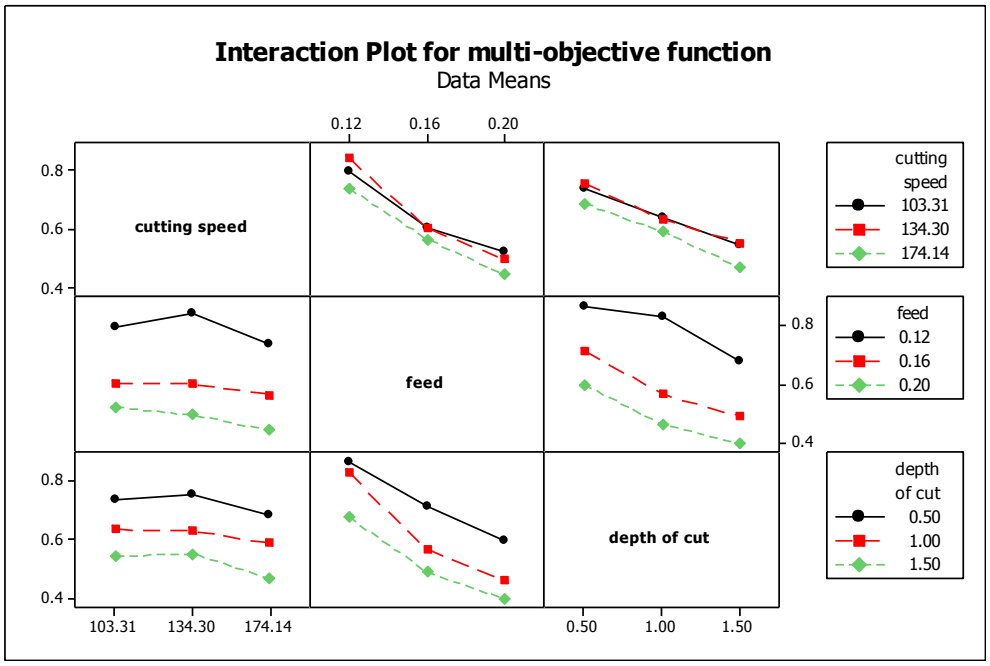

Figure 6.7: Interaction plot for multi-objective function

The 3D merged surface and contour plots for the multi-objective function are shown in Figure 6.8. Figure 6.8(a) shows the surface and contour plots for multi-objective function with respect to varying cutting speed and depth of cut at a fixed feed. It shows that at smaller values of cutting speed and depth of cut, the multi-objective function is maximum and decreases with the increase in depth of cut even at smaller value of cutting speed. It again supports this observation that depth of cut has more influence on multi-objective function as compared to the cutting speed. Figure 6.8(b) shows the surface and contour plots for multi-objective function with respect to varying cutting speed and feed at a fixed depth of cut. It reveals that at the smaller values of feed, the multi-objective function is maximum. Even with increase in cutting speed at smaller values of feed the multi-objective function is maximum and at higher values of feed it decreases. Figure 6.8(c) indicates that multi-objective function is maximum at lower values of depth of cut and feed

and minimum at higher values of depth of cut and feed. These 3D surface plots can be used for estimating the power consumption and surface roughness values for any suitable combination of the machining parameters, namely cutting speed, feed and depth of cut. This is very useful in practice for the operator or part programmer.

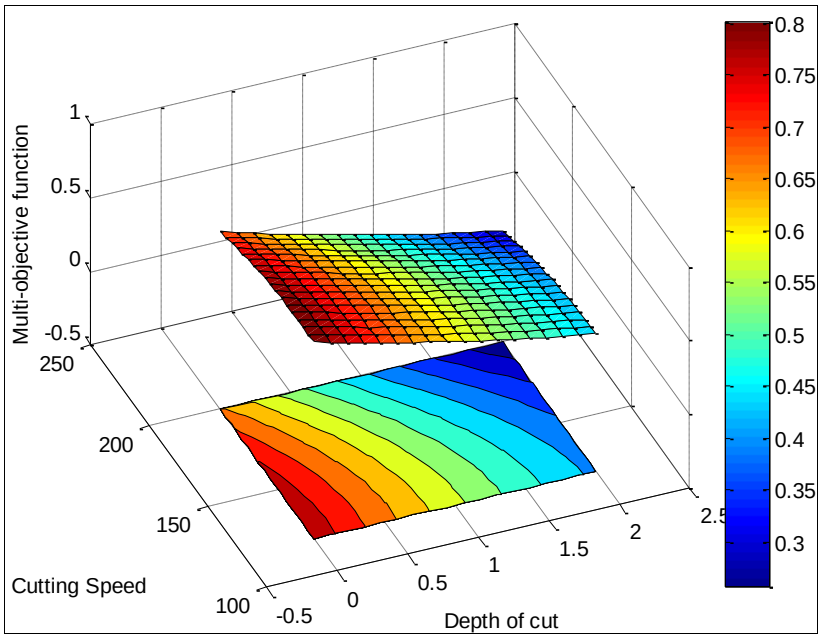

Figure 6.8(a): Surface and contour plot representing the influence of cutting speed and depth of cut on multi-objective function at 0.16 mm/rev. feed

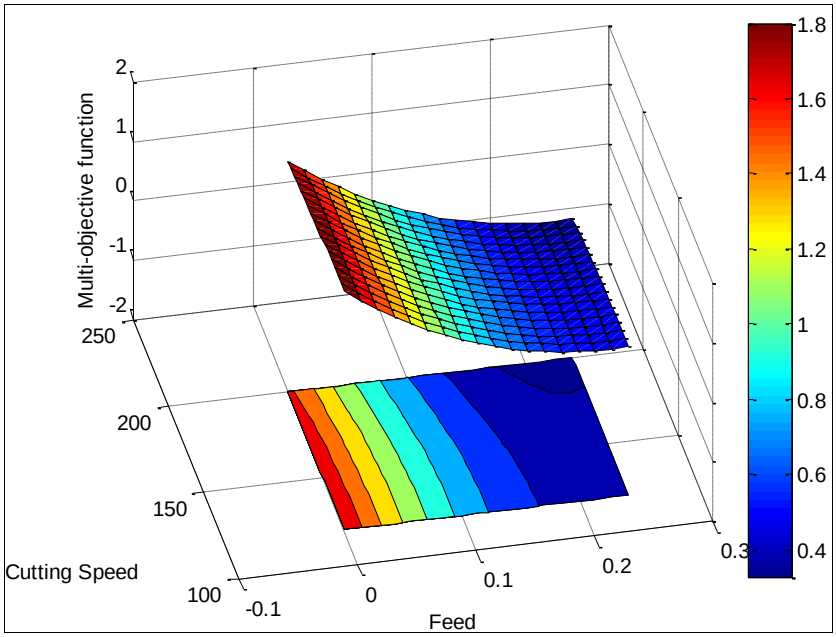

Figure 6.8(b): Surface and contour plot representing the influence of cutting speed and feed on multi-objective function at 1 mm depth of cut

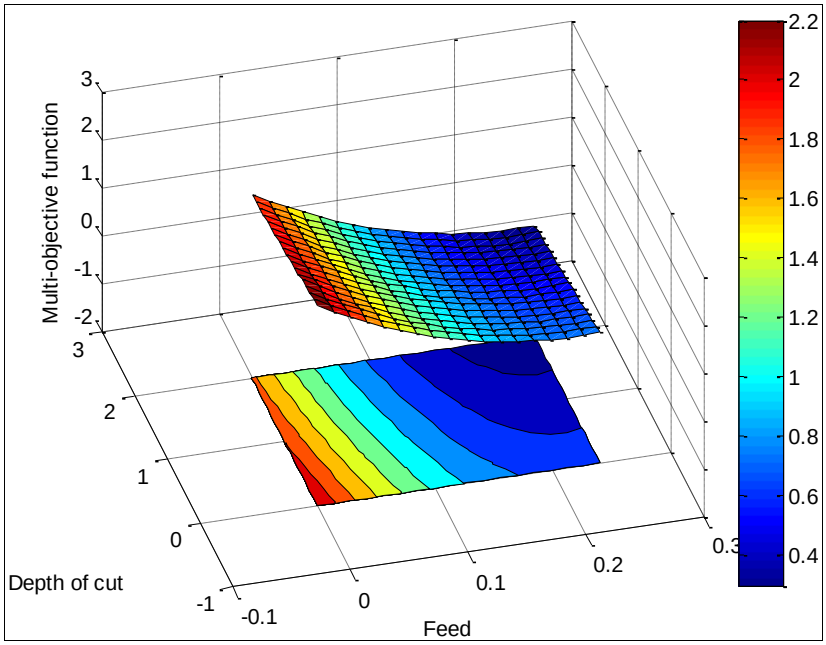

Figure 6.8(c): Surface and contour plot representing the influence of depth of cut and feed on multi-objective function at cutting speed 134.30 m/min

6.5.4 Optimum values of multi-objective function

The main objective of this research was to find the optimum values of machining parameters to achieve the minimum surface roughness and power consumption simultaneously. Desirability function analysis associated in RSM has been performed using MINITAB for obtaining the results.

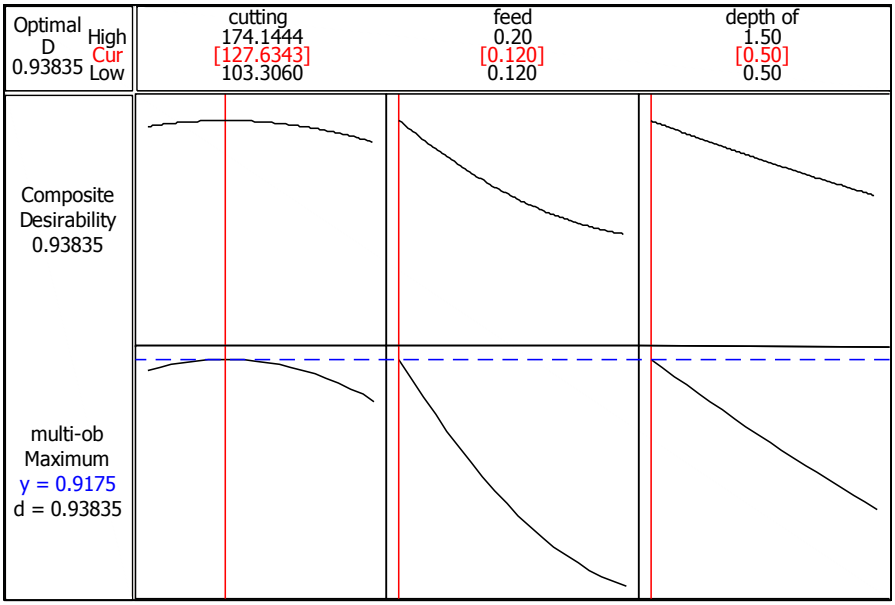

Figure 6.9: Response surface optimization plot for optimum machining parameters and multi-objective function

The desirability function analysis optimization results are shown in Figure 6.9. The optimal machining parameters for minimizing surface roughness and power consumption simultaneously are: cutting speed of 127.63 m/min at feed of 0.12 mm/rev with 0.50 mm depth of cut. The desirability value is 0.93835, which is very close to 1.0.

6.6 Confirmation Experiments

The confirmation experiments were conducted on the optimal machining parameters (v = 127.63 m/min, f = 0.12 mm/rev and d = 0.50 mm) predicted using the developed model. The results of the confirmation runs for the power consumption and surface roughness are listed in Table 6.6. It can be observed that the optimal machining parameters predicted by the developed model will lead to lower power consumption and better surface finish as shown in Table 6.6.

Table 6.6: Confirmation results for power consumption and surface roughness

Methodology	Optimum machining parameters			Power consumption (kW)	Surface roughness (μm)
	v (m/min)	*f* (mm/rev.)	*d* (mm)		
Best experimental run	134.30	0.12	0.50	0.574	1.284
Proposed model	127.63	0.12	0.50	0.536	1.250

6.7 Discussion

6.7.1 The influence of machining parameters on power consumption and surface roughness

Machine tools consume power to provide the relative movement to the cutting tool with respect to the workpiece and rotation of spindle. The three machining parameters, viz. cutting speed, feed and depth of cut determine the material removal rate. As the feed and depth of cut increases, the undeformed chip section increases and hence the force required to remove this area also increases which forces the machine tool to consume

more power. The surface roughness also increases with increase in feed. It is quite obvious because for a given tool nose radius the theoretical surface roughness is a function of feed (Shaw, 1984). This situation can be explained as the increase in feed leads to vibration and more heat generation and therefore contributes to higher surface roughness (Sarıkaya and Güllü, 2014). In actual practice, build-up edge formation and vibration (chatter) are the major factors affecting surface quality. An increase in cutting speed reduces the possibility of built-up edge formation and hence improves the surface quality. This results support the argument that high cutting speeds reduce cutting forces together with the effect of natural frequency and vibration, giving better surface finish. The better surface quality with least power consumption can be achieved at lower feed and depth of cut.

6.7.2 Comparative benefit between proposed model and literature models

This chapter optimizes surface roughness and power consumption simultaneously during a turning operation on AISI 1045 steel. There is one research paper (Hanafi et al., 2012) which provides simultaneous optimization of power and surface roughness during turning operation but on a composite material. Hanafi et al. (2012) used GRA and Taguchi optimization methodology to optimize power consumption and surface roughness for poly-etheretherkeytone material and the results revealed that depth of cut is the most influential parameter and feed is the least influential parameter. However, the current research shows that feed rate is the most significant factor and cutting speed is least significant. This difference may be because of difference in the workpiece materials. Moreover, theoretically as well as experimentally it is well known that feed has the maximum influence on surface roughness during the machining of metals. The proposed model does not assume the weights of the two factors, viz. power consumption and surface roughness, but determines the weights of the factors using principal component analysis. Hanafi et al.

(2012) have assumed the weights of the two factors. The RSM technique used in this paper can model the response in terms of significant parameters, their interactions and square terms. 3D surfaces generated by RSM can help in visualizing the effect of parameters on response in the entire range specified whereas Taguchi's technique used by Emami et al. (2014), Camposeco-Negrete (2013), Hanafi et al. (2012), etc gives the average value of response at given level of parameters. In this research the mean relative error between the experimental and predicted data is 4.79% and is well in agreement with the results from literature. The mathematical model developed using RSM by the Sarıkaya and Güllü (2014) shows that the percentage deviation between the experimental data and predicted data between 2.72% and 7.14%.

6.8 Conclusions

This chapter presents a multi-objective predictive model for the minimization of surface roughness and power consumption simultaneously during the machining of AISI 1045 steel. It has been found that the predictive model provides optimum machining parameters. The results of the proposed model provide an improvement of 6.59% reduction in power consumption and 2.65% improvement in surface roughness over the best experimental run. It has been observed that the feed is the main influencing machining parameter for the minimization of power consumption and surface roughness simultaneously followed by the depth of cut and the cutting speed. The 3D surface and contour plots constructed during the study can be used for choosing the optimal machining parameters to obtain particular values of power consumption and surface roughness or vice-versa these can be used by the machine tool manufacturers to provide the range of cutting speeds, feed and depth of cut for a particular application. This work can be further extended to analyze the effect of different cutting conditions and cutting tools on power consumption and surface roughness during machining.

References

Camposeco-Negrete, C., 2013. Optimization of cutting parameters for minimizing energy consumption in turning of AISI 6061 T6 using Taguchi methodology and ANOVA. J. Clean. Prod. 53, 195–203.

Deng Julong, 1989. Introduction to Grey System Theory. J. Grey Syst. 1, 1–24.

Emami, M., Sadeghi, M.H., Sarhan, A.A.D., Hasani, F., 2014. Investigating the Minimum Quantity Lubrication in grinding of Al2O3 engineering ceramic. J. Clean. Prod. 66, 632–643.

Fung, C.-P., Kang, P.-C., 2005. Multi-response optimization in friction properties of PBT composites using Taguchi method and principle component analysis. J. Mater. Process. Technol. 170, 602–610.

Hanafi, I., Khamlichi, A., Cabrera, F.M., Almansa, E., Jabbouri, A., 2012. Optimization of cutting conditions for sustainable machining of PEEK-CF30 using TiN tools. J. Clean. Prod. 33, 1–9.

He, Y., Liu, B., Zhang, X., Gao, H., Liu, X., 2012. A modeling method of task-oriented energy consumption for machining manufacturing system. J. Clean. Prod. 23, 167–174.

Jolliffe, I.T., 2002. Principal Component Analysis, Second. ed. Springer, New York.

Kaiser, H.F., 1960. The Application of Electronic Computers to Factor Analysis. Educ. Psychol. Meas. 20, 141–151.

Li, W., Zein, A., Kara, S., Herrmann, C., 2011. An Investigation into Fixed Energy Consumption of Machine Tools, in: Hesselbach, J., Herrmann, C. (Eds.), Glocalized Solutions for Sustainability in Manufacturing: Proceedings of the 18th CIRP International Conference on Life Cycle Engineering. Springer Berlin Heidelberg, Berlin, Heidelberg, pp. 268–275.

Liu, S., Lin, Y., 2010. Grey Systems Theory and Applications. Springer Verlag, Berlin Heidelberg.

Lu, H.S., Chang, C.K., Hwang, N.C., Chung, C.T., 2009. Grey relational analysis coupled with principal component analysis for optimization design of the cutting parameters in high-speed end milling. J. Mater. Process. Technol. 209, 3808–3817.

Pradhan, M.K., 2013. Estimating the effect of process parameters on MRR, TWR and radial overcut of EDMed AISI D2 tool steel by RSM and GRA coupled with PCA. Int. J. Adv. Manuf. Technol. 68, 591–605.

Pusavec, F., Krajnik, P., Kopac, J., 2010. Transitioning to sustainable production – Part I: application on machining technologies. J. Clean. Prod. 18, 174–184.

Sanguansat, P., 2012. Principle Component Analysis. InTech, Crotia.

Sarıkaya, M., Güllü, A., 2014. Taguchi design and response surface methodology based analysis of machining parameters in CNC turning under MQL. J. Clean. Prod. 65, 604–616.

Shaw, M.., 1984. Metal Cutting Principles. Oxford University Press, Oxford, New York.

Tzeng, C.-J., Lin, Y.-H., Yang, Y.-K., Jeng, M.-C., 2009. Optimization of turning operations with multiple performance characteristics using the Taguchi method and Grey relational analysis. J. Mater. Process. Technol. 209, 2753–2759.

Van Luttervelt, C.A., Childs, T.H.C., Jawahir, I.S., Klocke, F., Venuvinod, P.K., Altintas, Y., Armarego, E., Dornfeld, D., Grabec, I., Leopold, J., Lindstrom, B., Lucca, D., Obikawa, T., Sato, H., 1998. Present Situation and Future Trends in Modelling of Machining Operations Progress Report of the CIRP Working Group "Modelling of Machining Operations." CIRP Ann. - Manuf. Technol. 47, 587–626.

Chapter 7

Conclusions

This study presents predictive and optimization models for the prediction and optimization of machining parameters leading to least power consumption and surface roughness during turning of AISI 1045 steel using tungsten carbide tools. Experimental set up and plan was developed to select the machine tool, cutting tool, workpiece material, machining parameters and their levels, and experiments were conducted using well known Taguchi's orthogonal array to acquire the power consumption and surface roughness data. The developed predictive and optimization models based on experimental data, assist not only in analyzing the influence of the different process parameters on the two most dominant machining criteria, but are also useful for the optimality search of the various parametric combinations for achieving the maximum fulfillment of the objective requirements.

In chapter 2, a review of 72 research papers from year 2000 onwards in terms of machining process involved, work piece material, cutting tool material, machining parameters, machining performance, predictive technique, and optimization technique has been presented. The literature review reveals that researchers have focused on various predictive modelling and optimization techniques to determine optimal or near-optimal cutting conditions. Statistical regression analysis and artificial neural networks have been widely used modelling techniques in development of predictive models for machining. However, RSM is most widely used as it offers enormous information from even small number of experiment and even it is possible to analyze the influence of independent parameters on performance characteristics. The various authors have used Taguchi method, RSM, genetic algorithm, grey relation analysis, *etc*. as optimization

techniques. The most widely machining performances considered by the researchers are surface roughness followed by machining/production cost and material removal rate. It has been observed that most of the researchers have used steel as workpiece material. The few works available for optimization of power consumption for different materials show contrasting results – few authors observed that cutting speed is the most significant factor followed by depth of cut to reduce the power consumption. Other authors observed that depth of cut is the significant factor followed by cutting speed to reduce the power consumption. Some authors observed that feed rate is the significant factor followed by depth of cut to reduce the power consumption. The review revealed that a generalized relationship between the cutting parameters and the process performance is hard to model accurately mainly due to the nature of the complicated stochastic process mechanisms in machining. Therefore, more studies need to be carried out to observe the influence of machining parameters on performance characteristics. Simultaneous optimization of surface finish and power consumption is also required so that product quality and sustainability are optimized simultaneously.

In chapter 3, experimental setup and plan is developed to select the machine tool, cutting tool, workpiece and cutting tool material, machining parameters and their levels, and performance characteristics (power consumption and surface roughness). Experiments were designed using full factorial L_{27} orthogonal array through well known Taguchi method. Experiments have been conducted for the 27 combinations of orthogonal array to get the power consumption and surface roughness data.

In chapter 4, predictive and optimization models have been presented to determine the machining parameters leading to minimum surface roughness. Three empirical models for prediction of surface roughness have been developed using RSM, SVR and ANN.

The optimization models have been developed using RSM and GA to find the values of machining parameters leading to minimum surface roughness. Further the confirmation experiments are carried out to validate that the developed predictive and optimization models match with the experimental results for machining of AISI 1045 steel.

The results reveal that the developed predictive model using RSM predicts prediction of surface roughness within 7.64% error. Feed rate is the main influencing factor on the surface roughness with 89.22% contribution, followed by the cutting speed with 1.57% contribution in the total variability of model. The depth of cut, quadratic and interaction effects of machining parameters do not have statistical significance on surface roughness. The 3D surface plots can be used for estimating the surface roughness values for any combination of the machining parameters within the suitable range. This is very useful in practice for the operator or the part programmer. These plots can also be used by the machine tool designers during the design of machine tools to estimate the suitable range of parameters to be provided. SVR is capable of accurately predicting the surface roughness during turning operations. The mean relative error between the predicted and experimental values was found to be 5.17%. The predictive model developed using the ANN shows that the surface roughness values could be obtained with the selected ANN parameters. ANN has provided a close relation between the predicted values and the experimental values. The mean relative error between the predicted and the experimental values using ANN is 3.07%. It has been found that the model developed using ANN is capable of predicting accurately using a small number of training samples.

The developed predictive models are compared using relative error and validated using hypothesis testing. It has been found that ANN and SVR models are better than RSM for

predicting surface roughness. The mean relative errors for ANN and RSM models are 3.07% and 7.64% respectively. Also, among ANN and SVR, ANN performs better as compared to SVR. Low feed rate and high cutting speed were found to provide better surface finish within the specific test range using the desirability function analysis and genetic algorithms. Moreover, desirability function analysis and GA provided similar results. Confirmations experiments carried out using the optimum machining parameters show that the developed predictive and optimization model can be used for turning of AISI-1045 steel within 4.67% error.

In chapter 5, predictive and optimization models have been presented to determine the machining parameters leading to minimum power consumption during machining. Three empirical models for prediction of power consumption have been developed using RSM, SVR and ANN. The optimization models have been developed using RSM and GA to find the values of machining parameters leading to minimum power consumption. Further, the confirmation experiments were carried out to show that the developed predictive and optimization models can be used for machining of AISI 1045 steel.

The results reveal that the predictive model developed using RSM allows prediction of power consumption with a 95% confidence interval. Depth of cut is the main influencing factor for the power consumption with 61.71% contribution, followed by the cutting speed with 16.41% contribution and feed rate with 12.85% contribution in the total variability of model. The quadratic effects of machining parameters do not have statistical significance on power consumption. The interactions [($v \times f$), ($v \times d$) and ($f \times d$)] have 1.36%, 2.87% and 2.36% contributions on power consumption respectively. The 3D surface plots can be used for estimating the power consumption values for any combination of the machining parameters within the suitable range. This is very useful in

practice for the operator or the part programmer. These plots can also be used by the machine tool designer to estimate the suitable range of parameters during the design of machine tools. SVR is capable of accurately predicting the power consumption during turning operations. The mean relative error between the predicted and experimental values was found to be 2.14%.

The predictive model developed using the ANN shows that the power consumption values could be obtained with the selected ANN parameters. ANN model has provided a close relation between the predicted values and the experimental values. The mean relative error between the predicted and the experimental values is 3%. It has been found that the model developed using ANN is capable of predicting power consumption accurately using a small number of training samples.

The developed predictive models have been compared using relative error and validated using hypothesis testing. It has been found that ANN and SVR models are better than RSM for predicting power consumption because they generally offer the ability to model more complex non-linearities and interaction. The mean relative errors for ANN and RSM models are 3% and 5.1% respectively. The mean relative error for SVR is 2.14%. Mean relative error illustrates that the SVR performs slightly better as compared to ANN. The minimum power consumption of 0.529 kW is found at cutting speed of 118.95 m/min, feed rate of 0.12 mm/rev and depth of cut as 0.5 mm using RSM and GA. Confirmation experiments carried out at the optimum machining parameters shows that the developed predictive and optimization models can be used for turning of AISI 1045 steel within 3.29% error.

In chapter 6, a multi-objective predictive model for the minimization of surface roughness and power consumption simultaneously during the machining of AISI 1045

steel has been presented. The results of the proposed model provide an improvement of 6.59% reduction in power consumption and 2.65% improvement in surface roughness over the best experimental run. It has been observed that the feed is the main influencing machining parameter for the minimization of power consumption and surface roughness simultaneously followed by the depth of cut and the cutting speed. The 3D surface and contour plots constructed during the study can be used for choosing the optimal machining parameters to obtain particular values of power consumption and surface roughness or vice-versa these can be used by the machine tool manufacturers to provide the range of cutting speeds, feed and depth of cut for a particular application.

Major Contributions of the Thesis

- Experimental investigations on the influence of machining parameters on surface roughness and power consumption.
- Development of RSM, SVR and ANN models for the prediction of surface roughness and power consumption.
- Development of RSM and GA models for the optimization of surface roughness and power consumption.
- Development of a multi-objective predictive model for the minimization of surface roughness and power consumption simultaneously using RSM coupled with GRA and PCA.
- Development of 3D contour and surface plot to provide a range of near-optimal solutions for the power consumption and surface finish. These can be used by the part programmers and the operators for selecting the machining parameters from the available range on the machine tools.

Limitations and Future Scope of the Research

Predictive modelling and optimization is a complex and re-emerging field of research. The scope of the research work is endless due to large number of variables involved in machining of materials. The effect of machining parameters like tool geometry, tool coatings, coolants, *etc*. on the surface roughness and power consumption has not been studied. Further, the effect of machining parameters on material removal rate can be analyzed. This work can be extended to include the advanced materials like titanium alloys and composites materials.

This study has optimized the power consumption and surface finish simultaneously. However, in practice surface roughness is not taken as a variable of the machining process but a fixed parameter (predefined range by designers). Therefore, future research can be directed at mapping of optimum machining parameters for minimum energy consumption for a range of expected surface finish. The results can also be analyzed using other optimization techniques such as particle swarm optimization, simulated annealing, artificial bee colony, *etc*., and the effectiveness of various optimization techniques can be compared.

List of Publications

International Journals

[1] Kant, G., Sangwan, K.S., 2014. Prediction and optimization of machining parameters for minimizing power consumption and surface roughness in machining. Journal of Cleaner Production 83, 151–164.

[2] Kant, G., Sangwan, K.S., 2015. Predictive modelling for power consumption in machining using artificial intelligence techniques. Procedia CIRP 26, 403–407.

[3] Kant, G., Sangwan, K.S., 2015. Predictive modelling and optimization of machining parameters to minimize surface roughness using artificial neural network coupled with genetic algorithm. Procedia CIRP 31, 448-453.

[4] Kant, G., Sangwan, K.S., 2015. Predictive modelling for energy consumption in machining using artificial neural network. Procedia CIRP 37, 205–210.

[5] Sangwan, K.S., Saxena, S., Kant, G., 2015. Optimization of machining parameters to minimize surface roughness using integrated ANN-GA approach. Procedia CIRP 29, 305-310.

[6] Kant, G., Rao V, V., Sangwan, K.S., 2013. Predictive modelling of turning operations using response surface methodology. Applied Mechanics and Materials 307, 170–173.

[7] Sangwan, K.S., Kant, G., Deshpande, A., Sharma, P., 2013. Modelling of stresses and temperature in turning using finite element method. Appllied Mechanics and Materials 307, 174–177.

[8] Kant, G., Sangwan, K.S., 2011. Modelling and Simulation of Metal Cutting Processes. International Journal of Mechanical Engineering Research 1, 129–138.

International Conferences

[1] Kant, G., Rao V, V., Sangwan, K.S., 2013. Development of predictive models for forces in machining using regression analysis, response surface methodology, artificial neural network and support vector regression, in: 3rd International Conference on Production and Industrial Engineering CPIE-2013. NIT, Jalandhar, Punjab, India.

[2] Kant, G., Rao V, V., Lakshminarayana, Sangwan, K.S., 2013. The influence of machining parameters on surface roughness during turning of AISI 1045 Steel, in: 8th International Conference on Advances in Metrology (AdMet-2013). CSIR-National Physical Laboratory & Metrology Society of India (MSI), New Delhi, India

[3] Kant, G., Rao V, V., Rajput, P., Sangwan, K.S., 2013. Temperature and cutting force measurement during machining of AISI 1045 steel, in: 8th International Conference on Advances in Metrology (AdMet-2013). CSIR-National Physical Laboratory & Metrology Society of India (MSI), New Delhi, India.

[4] Kant, G., Khanna, N., Sangwan, K.S., 2009. The influence of cutting speed on work piece temperature and effective stress during machining of AISI 1045 Steel, in: International Conference on Simulation Modeling and Analysis (COSMA). NIT, Calicut, Kerala, India.

[5] Kant, G., Khanna, N., Sangwan, K.S., 2010. Modelling and simulation of orthogonal metal cutting process using finite element method, in: International Conference on Advances in Mechanical Engineering. SVNIT, Surat, Gujrat, India.

[6] Kant, G., Gupta, N., Sangwan, K.S., 2013. Measurement of tool chip interface temperature in machining : A comprehensive review, in: 3rd International Conference on Production and Industrial Engineering CPIE-2013. NIT, Jalandhar, Punjab, India.

Brief Biography of the Candidate

Mr. Girish Kant did his B.E. in Production Engineering from Marathwada Institute of Technology (MIT), Aurangabad (MH) and M.Tech. in Manufacturing Systems Engineering from Sant Longowal Institute of Engineering and Technology (SLIET), Longowal (PB). He is presently pursuing PhD at Birla Institute of Technology & Science, Pilani (BITS, Pilani) and working as a Lecturer with Department of Mechanical Engineering, BITS-Pilani, Pilani Campus. He has thirteen years of teaching experience at under graduate and postgraduate levels. His teaching and research interstes are in the manufacturing engineering, computer aided manufacturing and modelling and optimization of machining operations, *etc*.

Brief Biography of the Supervisor

Dr Kuldip Singh Sangwan is a Professor in the Department of Mechanical Engineering at Birla Institute of Technology and Science, Pilani, Rajasthan. He did his B.E. and M.E. from Punjab Engineering College, Chandigarh, and PhD from BITS Pilani. He has more than 22 years of experience in academic and research. He is an active researcher in the field of metal cutting, green manufacturing, reverse logistics, lean manufacturing, sustainable manufacturing, green supply chain management, and cellular manufacturing systems. He has guided 6 PhD students and 8 students are registered under him. He has published more than 50 reserach papers since 2011 alone in reputed international journals like IJPR, PPC, IJOPM, IJPEM, J. of Engineering Manufacture, J. of cleaner production, *etc*. He has developed curriculum for the post graduate and undergaraduate graduate programmes of engineering technology, manufacturing management, manufacturing engineering, engineering management, automotive engineering, *etc*. for the working professionals. He has developed collaboration with TU Braunschweig, Germany and Mondragon University, Mondragon, Spain. He has sponsored research projects from German Academic Exchange Programme (DAAD), UGC, Volkswagen, and DST. He has been a member of the prestigious International Scientific Committees of CIRP International conferences. Dr. Sangwan has also worked as trainer/consultant to industries like Batliboi Machine Tools Ltd., Surat; Satyam Technologies Ltd., Hyderabad; Bhilai Steel Plant, Bhilai; and Modern Insulators, Abu Road. He has a rich experience of nine years in academic administration and has worked as Assistant Dean of Engineering Services Division, Chief of Central Workshop and Head of Mechanical Engineering Department. Professor Sangwan is a Fellow of Institution of Engineers (India).